December, 2020

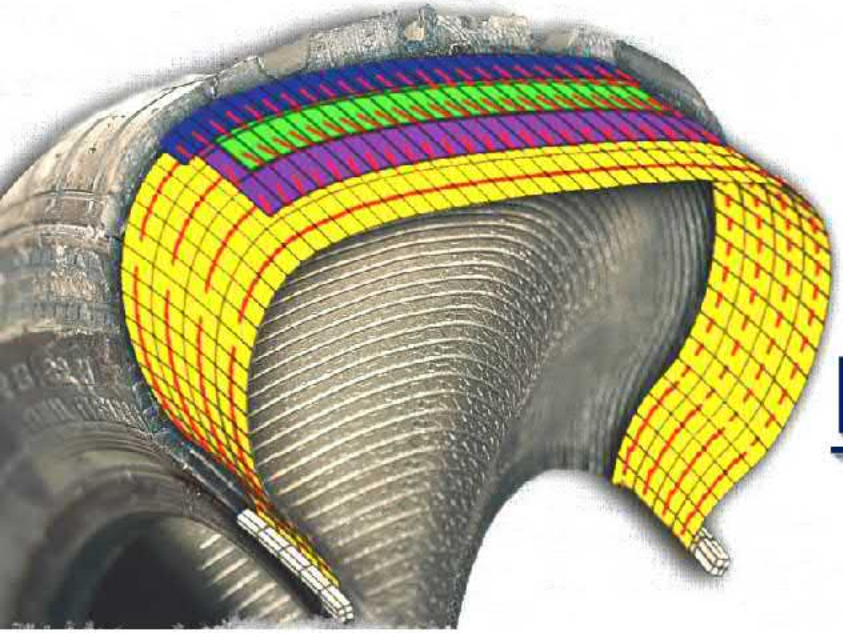

Experiments and Computational Modelling of Tires

Textbooks for university students

Assoc. Prof. Ing. Jan KRMELA, Ph.D.

ISBN 978-80-270-9020-4

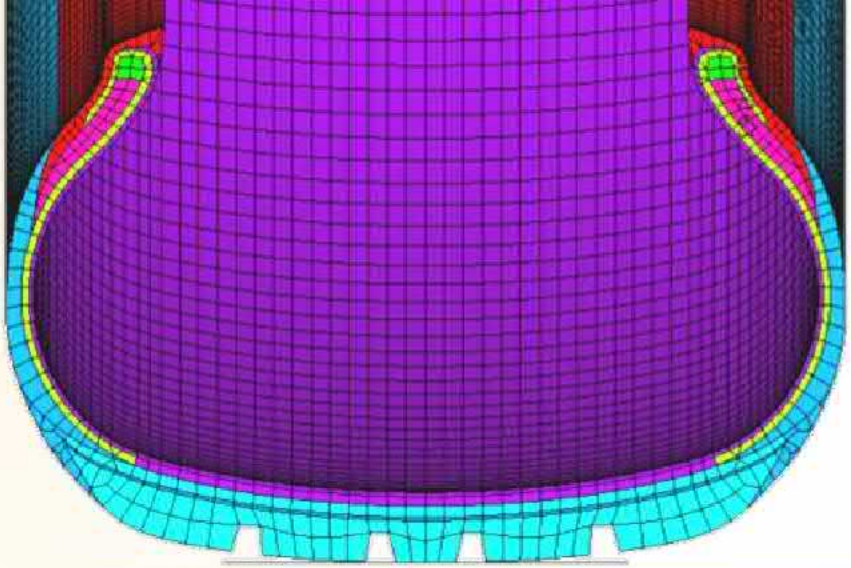

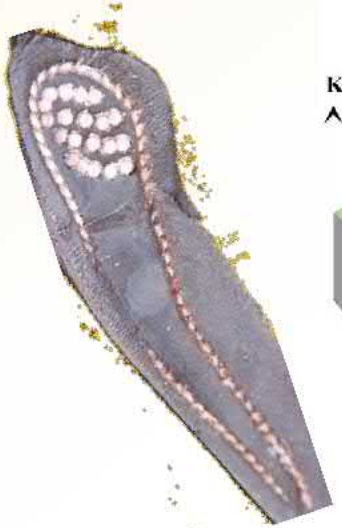

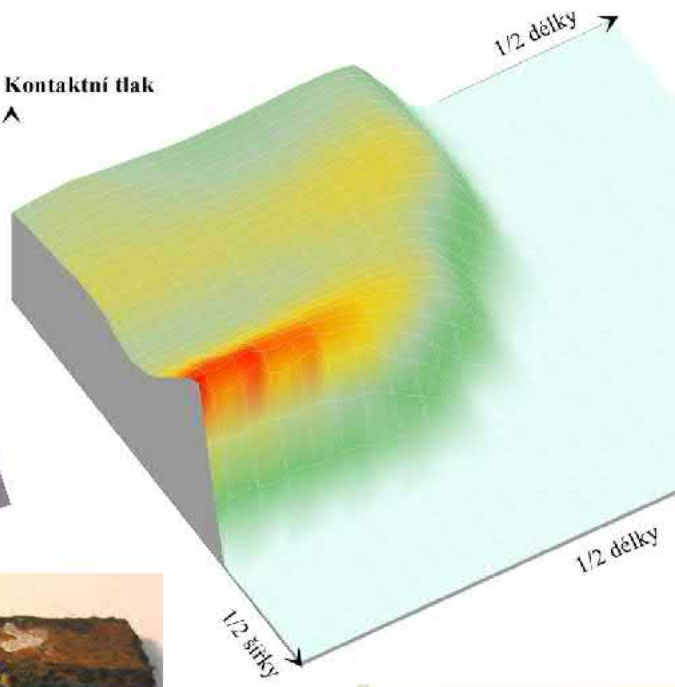
Kontaktní tlak
1/2 délky
1/2 délky
1/2 šířky

SEQV (AVG)
DMX =4.742

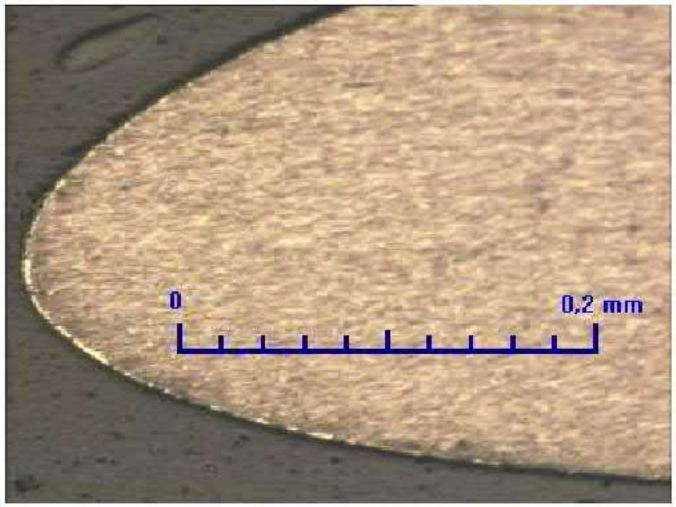
0
0,2 mm

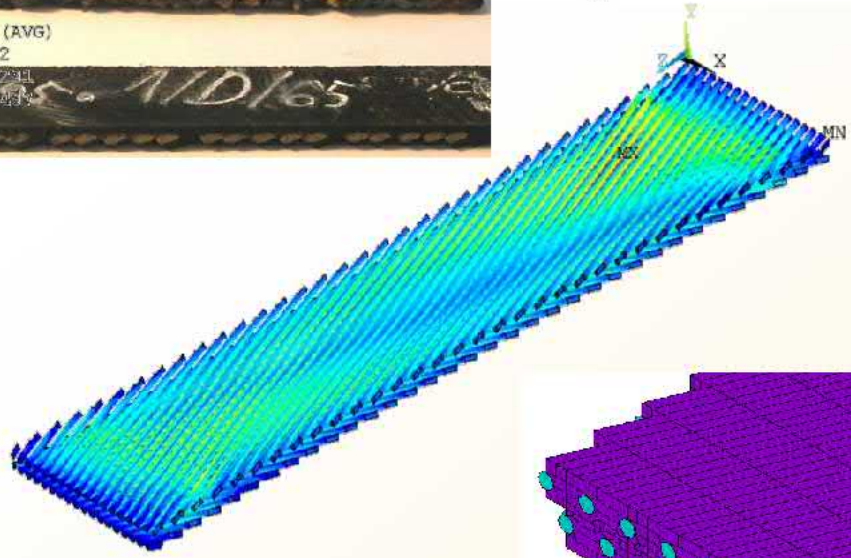
MN

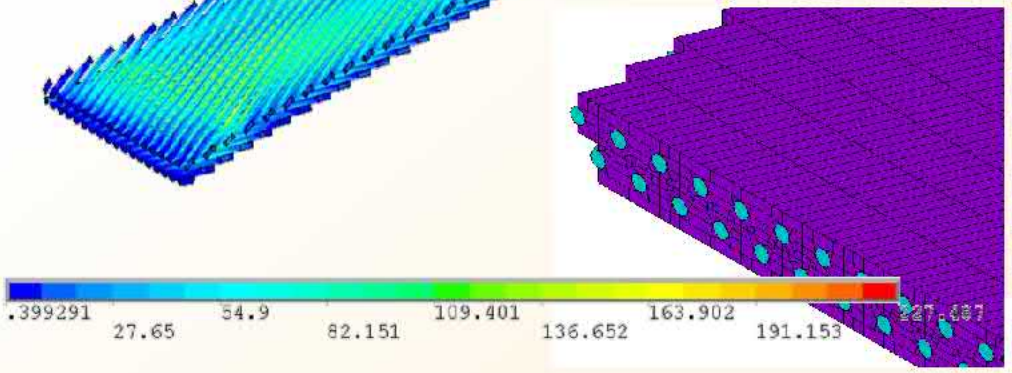
.399291
27.65
54.9
82.151
109.401
136.652
163.902
191.153

Jan Krmela

Experiments and Computational Modelling of Tires

Textbooks for university students

2020, December

9 788027 090204

Author: Associate Professor (doc.) Ing. Jan KRMELA, Ph.D.
Author's workplace: **Faculty of Industrial Technologies, Alexander Dubček University of Trenčín**, I. Krasku 491/30, 020 01 Púchov, Slovak Republic, fpt.tnuni.sk www.tnuni.sk
Author's e-mails: jan2.krmela@post.cz jan.krmela@tnuni.sk

Title: **Experiments and Computational Modelling of Tires : Textbooks for university students**
Book type: Textbook for university students **(VŠ učebnice)**
Language: English
First edition. Published in December 2020
Page size: 254 x 190.5 mm, 370 pages, pdf format, electronic version
Publisher: Jan Krmela, Zborov 32, 78901 Zábřeh
Country of publisher: Czech Republic
Number of author's sheets: **3.90**, number of standard pages: 78.0

This textbook has not been checked and corrected for spelling errors.

Reviewers:

Prof. Dr. Ing. Libor BENEŠ (Jan Evangelista Purkyně University in Ústí nad Labem, Ústi and Labem, Czech Republic)

Assoc. Prof. Artem ARTYUKHOV, PhD. (Sumy State University, Sumy, Ukraine)

Assoc. Prof. Andrej KASPEROVICH, PhD. (Belarusian State Technological University, Minsk, Belarus)

© Jan Krmela, 2020
This publication can be used as study material for university students.

ISBN 978-80-270-9020-4

About the Author

Since 2013, assoc. professor Jan Krmela (1978) has been the Head of the Department of numerical methods and computational modeling at the Faculty of Industrial Technologies in Púchov at Alexander Dubček University in Trenčín, Slovakia. He received his Ing. degree with honors in the field of study Transport Means – Road Vehicles at Jan Perner Transport Faculty at the University of Pardubice, Czech Republic and a Ph.D. in Transport Means and Infrastructure at the same institution. He habilitated in Transport Means and Infrastructure (the habilitation work "The computational modeling of automobile tires") at the same university in 2010. He is a member of the Association of Mechanical Engineers (A.S.I.), the Czech Society for Mechanics and the Scientific Council at the Faculty of Industrial Technologies in Púchov. In 2006, he received a special award for science and research activities by the Rector of the University of Jan Evangelista Purkyně in Ústí nad Labem, Czech Republic. In 2016, he was awarded the Bronze Medal of Maximilián Hell for the development of the Faculty of Industrial Technologies in Púchov, science and education. At 2020, he received Awards for the development and support of science, research and education, Alexander Dubček University of Trenčín.

He has been gaining experience in the FEM program ANSYS since 2000. He co-operated with the Fraunhofer Institut für Techno- und Wirtschaftsmathematik ITWM, Kaiserslautern, Germany and the Kompetenzzentrum - Das Virtuelle Fahrzeug Forschungsgesellschaft mbH, Graz, Austria (long-term stays by programs Erasmus+, DAAD and others stays). In 2016, he delivered lectures at the Belarusian State Technological University in Minsk, Belarus. He has been a supervisor of dissertation thesis; five Ph.D. students successfully finished under his guidance. He received financed projects GAČR, FRVS, KEGA and Erasmus+. He gives lectures, lessons and organizes seminars on technical subjects. The results of his work have been presented at conferences and in technical papers in journals, monographs and chapters of books. Jan Krmela authored over 270 publications in the following research areas:

- Computational modeling and tests of composites with a rubber (an elastomer) matrix such as tire casings, especially with focus on strain-stress states and modal analysis and computational modeling of composites after the degradation processes, tire-road interaction and vehicle parts;
- Tests of tires on static and dynamic test machines with the pressure footprint analyses of contact footprints between tires and a plane road or a bump and also prediction of radial stiffness of tires;
- Low cyclic loading tests of composites with textiles on a test machine with a video extensometer and static tests of composites with planning of tests with a design of geometric parameters of test samples and test conditions for testing of tire casing parts;
- Determination of material parameters that can be used as input data into computational models;
- Microscopic observation of interface bonds between steel and textile cords and an elastomer;
- 3D printing of technical objects.

LinkedIn and Research Gate: see at the website **http://krmela.wz.cz/contact.html**

Acknowledgments

This research work and this textbook had been financially supported by the Cultural and Educational Grant Agency of the Slovak Republic (KEGA), grant No. **KEGA 002TnUAD-4/2019 "The influence of temperature and other parameters on the tensile properties of polymer composites and polymers under the uniaxial and biaxial cyclic loading".**

CONTENTS of Textbook

Preface 14

1. Tire Introduction 17
2. Tire Tests 48
3. Outputs from Experiments 84
4. Experiments of Tire Parts 157
5. Degradation Processes 200
6. Computational Modelling of Tire 236
7. Creation of Computational Models 266
8. Outputs from Simulations 287
9. Interest Information 315
10. Conclusion 357

References 369

Emails: jan.krmela@tnuni.cz jan2.krmela@post.cz

Web **krmela.wz.cz**

Linkedin

https://www.linkedin.com/in/jan-krmela-117b50b5_

(English and Czech profiles)

ResearchGate:

http://www.researchgate.net/profile/Jan_Krmela_

RESEARCH AREA

- **Experiments of tires**;
- Experiments **of structure parts of tires**;
- **Microstructure of interfaces** between reinforcement cords and non-linear matrixes inside composites such as steel-cord belts and their computational modeling after **degradation processes**;
- **Computational modeling of tires**;
- Computational modeling **of structure parts of tires**.

Author deals with:

The complex approach to experiments and computation of tires from macrostructure and microstructure too. Namely computational modelling of strain-stress states of the composite structures of tire-casing and the tire-road interaction and experimental modelling of tires too. Also computational modelling of parts and structural parts of vehicle, computation and experiments of composites with non-linear matrixes, microscopy observation of bond between cord reinforcement and rubber matrixes, degradation processes of tires and composite structures with rubber.

- For TIRE COMPUTATIONAL MODELING (analyses: stress- strain, modal, temperature field, combine, dynamic)
- by FEA tires models in programs: ANSYS (over 16 years)

VERIFICATION APPROACH TO COMPUTATIONAL MODEL OF RADIAL TIRE

- EXPERIMENTS FOR OBTAIN MATERIAL PARAMETERS
- EXPERIMENTS OF TIRES ON „ADHESOR“
- PRESSURE FOOTPRINT ANALYSES

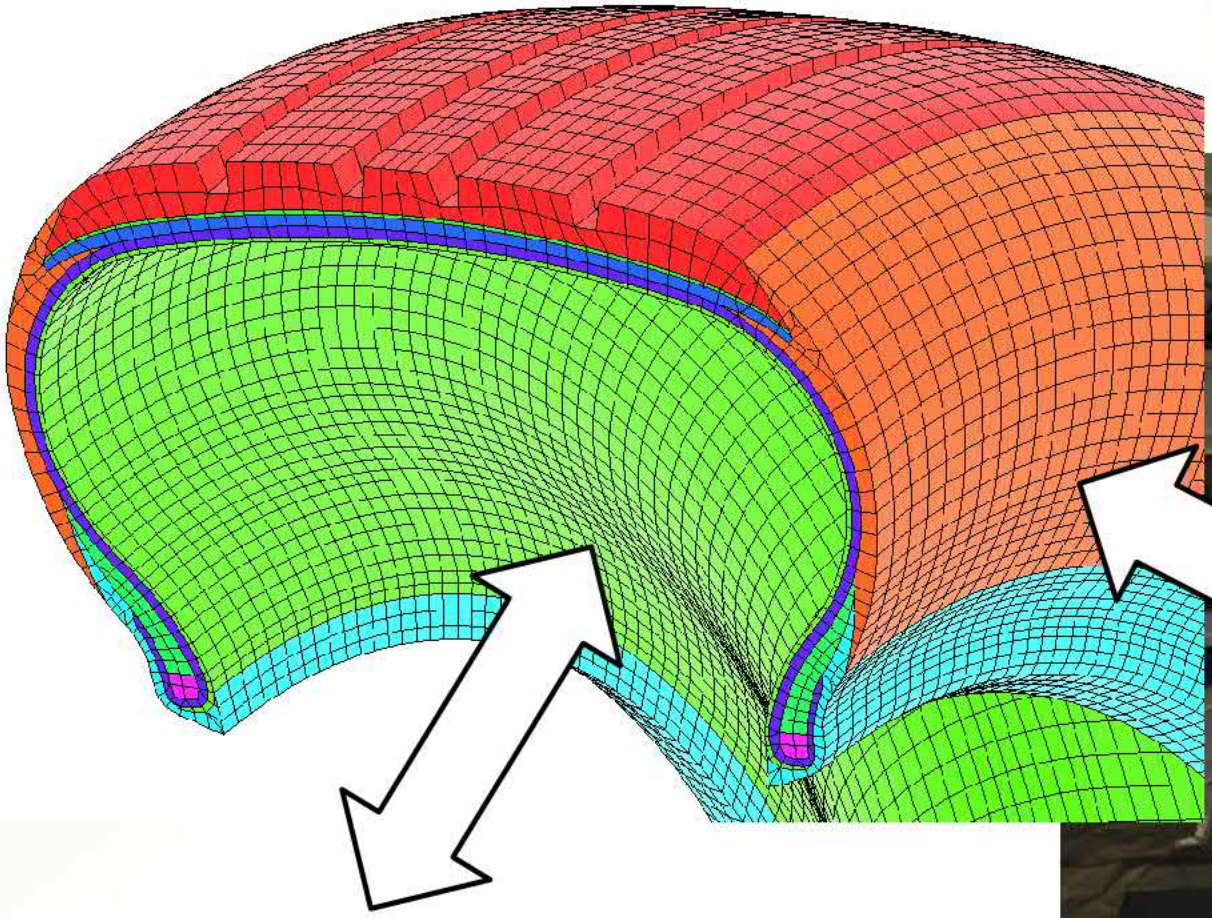

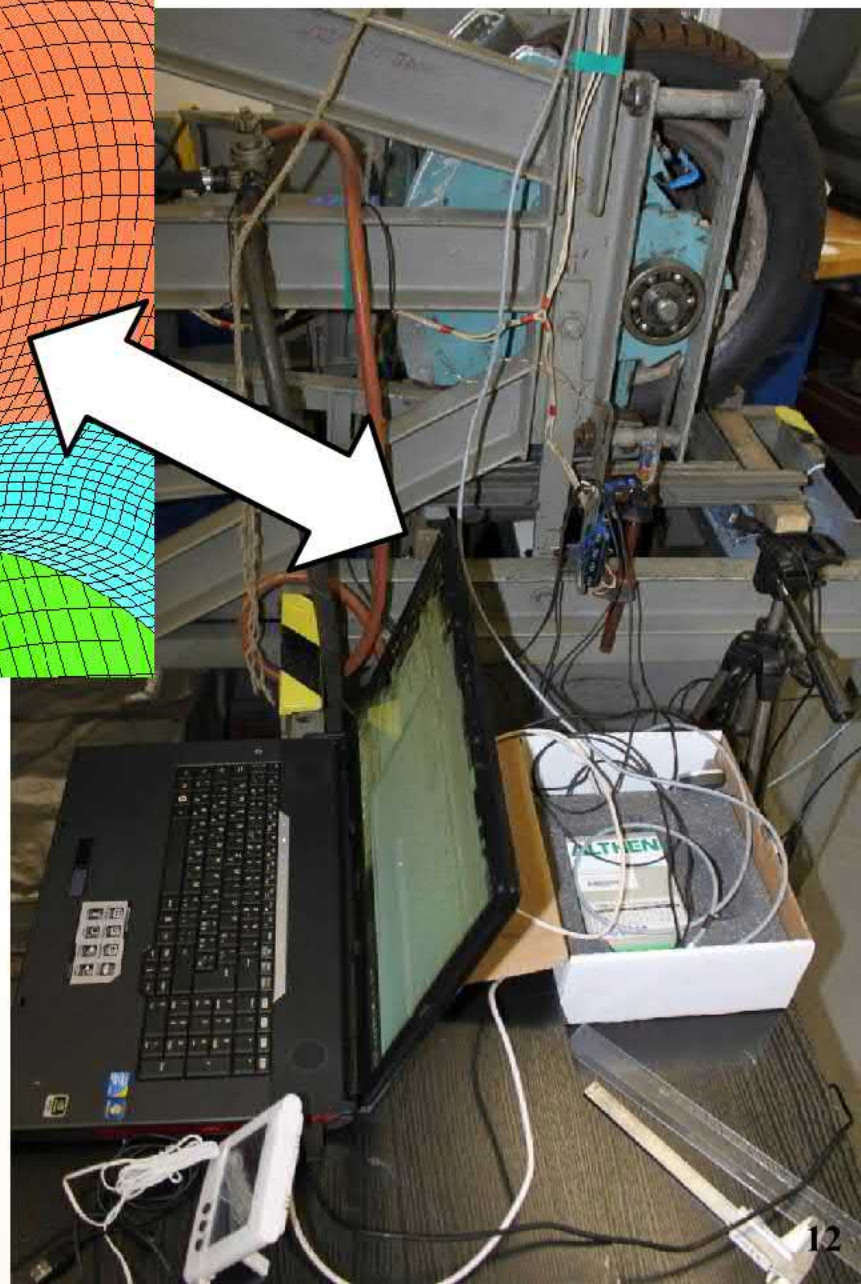

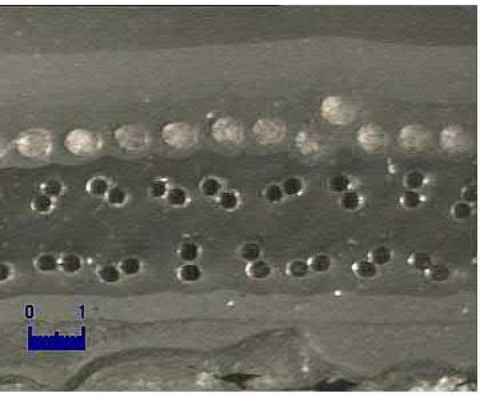

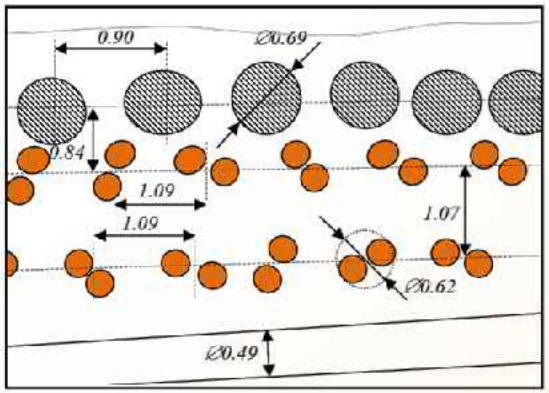
0.90
Ø0.69
0.84
1.09
1.09
1.07
Ø0.62
Ø0.49

Experiments and Computational Modelling of TIRES

The university textbook has an international significance. It can be used by students of universities / faculties in Minsk Belarus, Sumy Ukraine, Graz Austria, Katowice Poland, Pardubice Czech Republic, with which the author collaborates, but also students who are interested in the issue of tires.

Preface

This special textbook deals with experiments and computational modelling of tires as complex specific long fiber composites. The textbook is focused on the radial tires for passenger cars namely. Students gain knowledge about structure of tire, about the inputs parameters to the tire calculation, abut evaluation the results of the calculations and experiments etc.:

1. *Tire introduction*: Definitions, Composite, Structure of cross section of tire, Type of tire casing.
2. *Tire tests*: Planned experiments, Static adhesor, Dynamic adhesor, Deformation characteristics, Radial stiffness – calculation.
3. *Output from experiments*: Load conditions of tires, Contact patch, Contact pressure, Pressure footprint analyses, Comparison winter with summer tires, Special graphs from dynamic tests, Static test of bicycle tire.
4. *Experiments of tire parts*: Preparation of test samples, Tensile load, Bend load, Character of deformation, Outputs from tests.

5. *Degradation processes*: Degradation, Limit state, Corrosive test, Outputs from tensile tests, Microscopic evaluation of interaction of the cord – rubber (elastomer).
6. *Computational modelling of tire*: FEA by program ANSYS, Parts of tire, Elastomer, Determination of Mooney-Rivlin parameters, Comparison of experiment results with simulation results of tire parts.
7. *Creation of computational models*: Geometrical parameters, Material parameters (characteristics) as input for computational model, Replacement of belt structure for FEA of tire.
8. *Outputs from simulations:* Strain-stress analysis, Verification criteria, Simulation of tire-road interactions, Outputs from plane surfaces and obstacles, Dynamic loading, Modal analysis.
9. *Interest information*: Optimalization of computational time, Material parameters and their sensitivity to the precision of results, Structure of truck tire, Freeware (CADEC) for compute of composite material parameters.
10. *Conclusion*: Recycling of tires, Future tire design – advantage and disadvantage, Search study about computational modeling of tire noise.

I believe that this textbook will help university students to better understand the interdependencies between material parameters, experiments and tire calculations, and the information contained in it will contribute to broadering of knowledge of the wider professional public and will be used by students anywhere in the World.

Jan Krmela, the author

Part 1 – TIRE INTRODUCTION

Definitions, Composite, Structure of cross section of tire, Type of tire casing, Tire production

Definitions

Tire

ČSN 641001: tire casing + rim + inflation pressure.

Tire casing

ČSN 641001: only part of tire = „elastic “ part = interaction with road and rim.

TIRE

- Bike
- Motorcycle
- Bath chair
- Passenger car
- Truck
- Autobus
- Trailer
- Semitrailer
- Tractor

VEHICLE

- Road
- Off-road
- Universal
- Agricultural
- Military
- Sports
- Amphibian
- Special

AIRPLANE

- Civil
- Agricultural
- Military
- Space shuttle

OTHER

- Agricultural machinery and tractor
- Coal mechanism
- Handling machine
- Dredger, excavator
- Special mechanism

TYPE OF VEHICLE

TYPE OF TIRE-CASING

- RADIAL
- DIAGONAL
- BIAS BELTED
- SPECIAL

RADIAL

in agreement with tire tread pattern
- Summer
- Winter
- Universal
- Special
- Tractor, aj.

DIAGONAL

in agreement with application
- On road
- Off-road
- Universal
- Special (e.g. steel works, sports)

BIAS BELTED

in agreement with materials into reinforcing plies
- All textile
- Steel cord
- Combined
- Modern materials

SPECIAL

- Tactical
- High-profile
- Arched
- Cylindrical

- TUBULESS
- TUBE-TYPE

One construction of tire is used for passenger cars, other constructions for trucks, off-highway cars and sports cars. The tires for air transportation, agricultural vehicle, mining machine and other vehicles have got complicated structured in comparison radial tires for passenger cars.

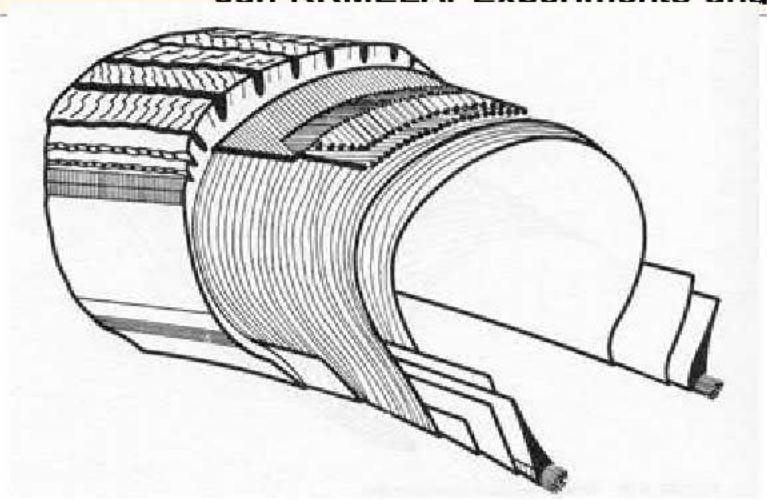

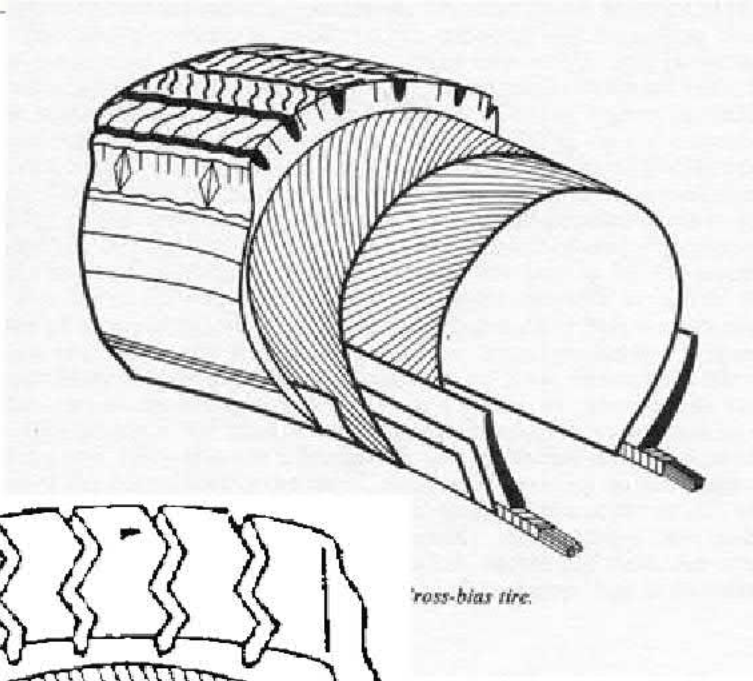

'ross-bias tire.

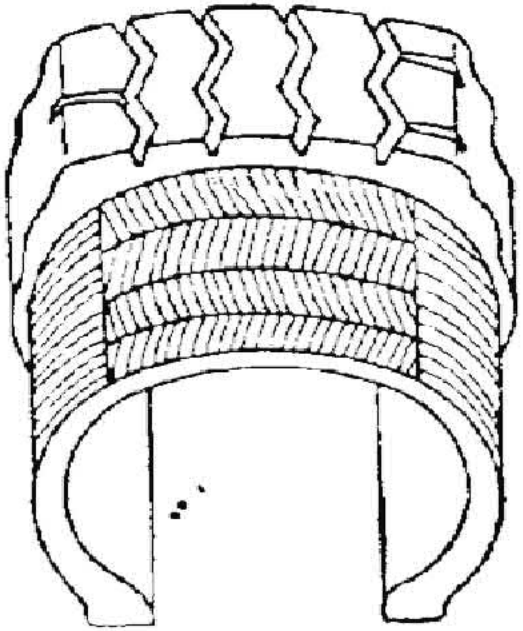

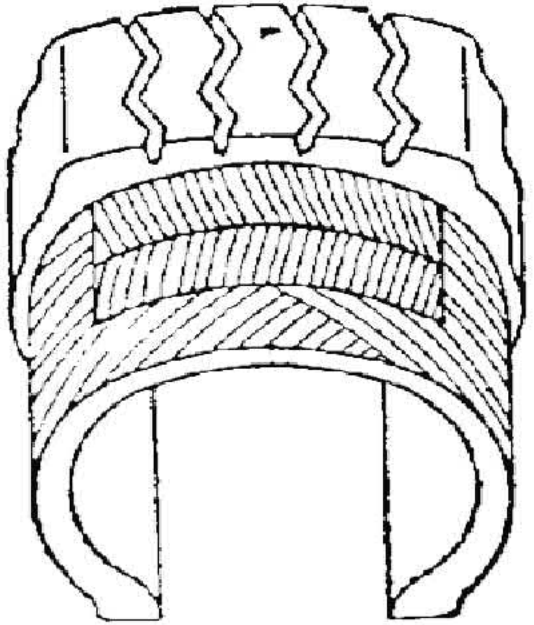

Bias-ply tires have plies that cross at **35-45°** angles

Radial tire – plies carcass - angle 90°

TIRE FOR VEHICLE

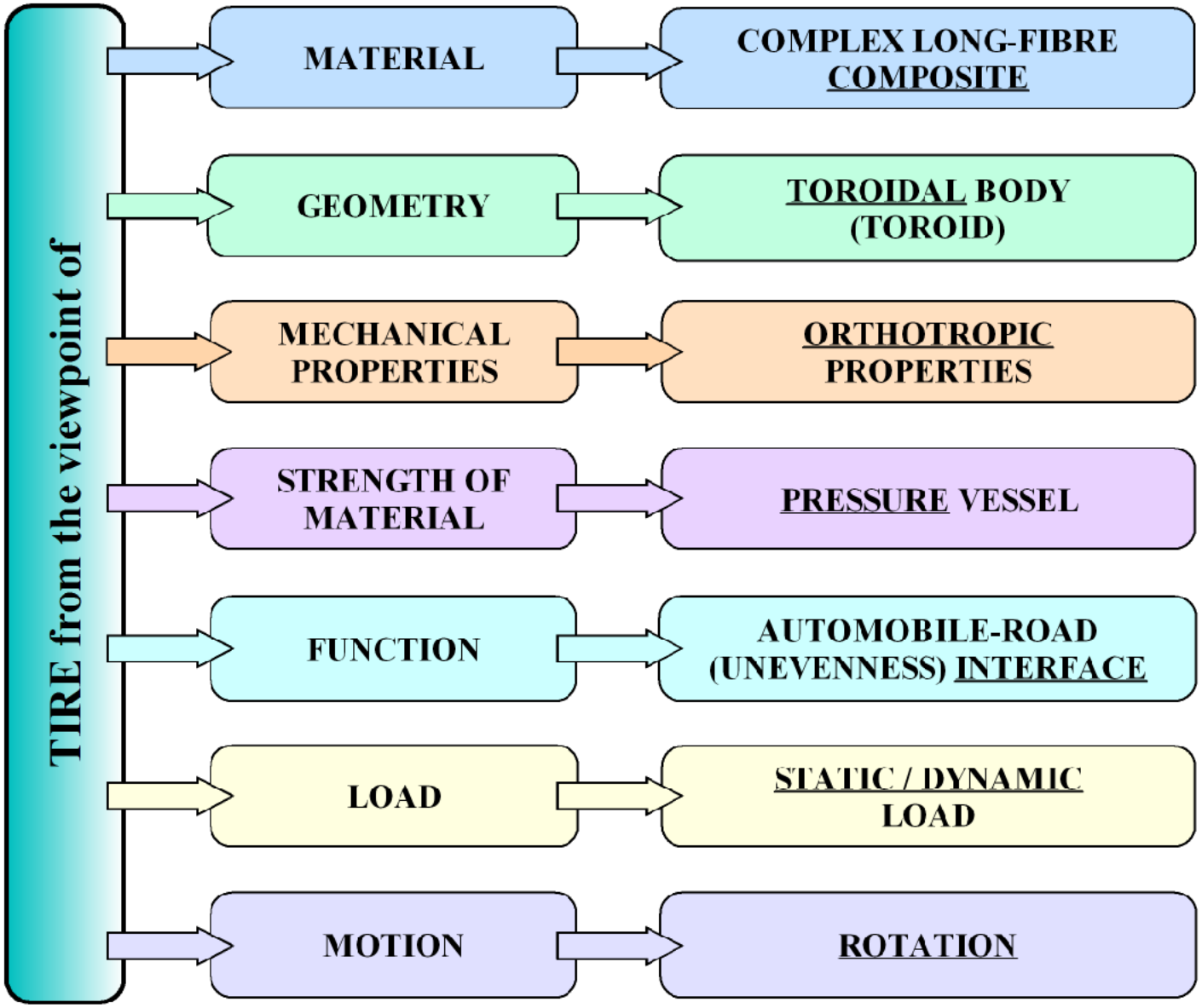

Tire = as polycomponent composite with a rubber matrix reinforced with textile and steel cords.

COMPOSITE - definition

Consist of min. 2 phases (namely called matrix + fibre).

Phases must be different in mechanical or physical or chemical properties.

Min. 5% fibre in matrix.

Composite must be material with better material parameters than matrix and fibre themselves.

Tire has **specific behavior** by complex structure ⇒ **requirements**

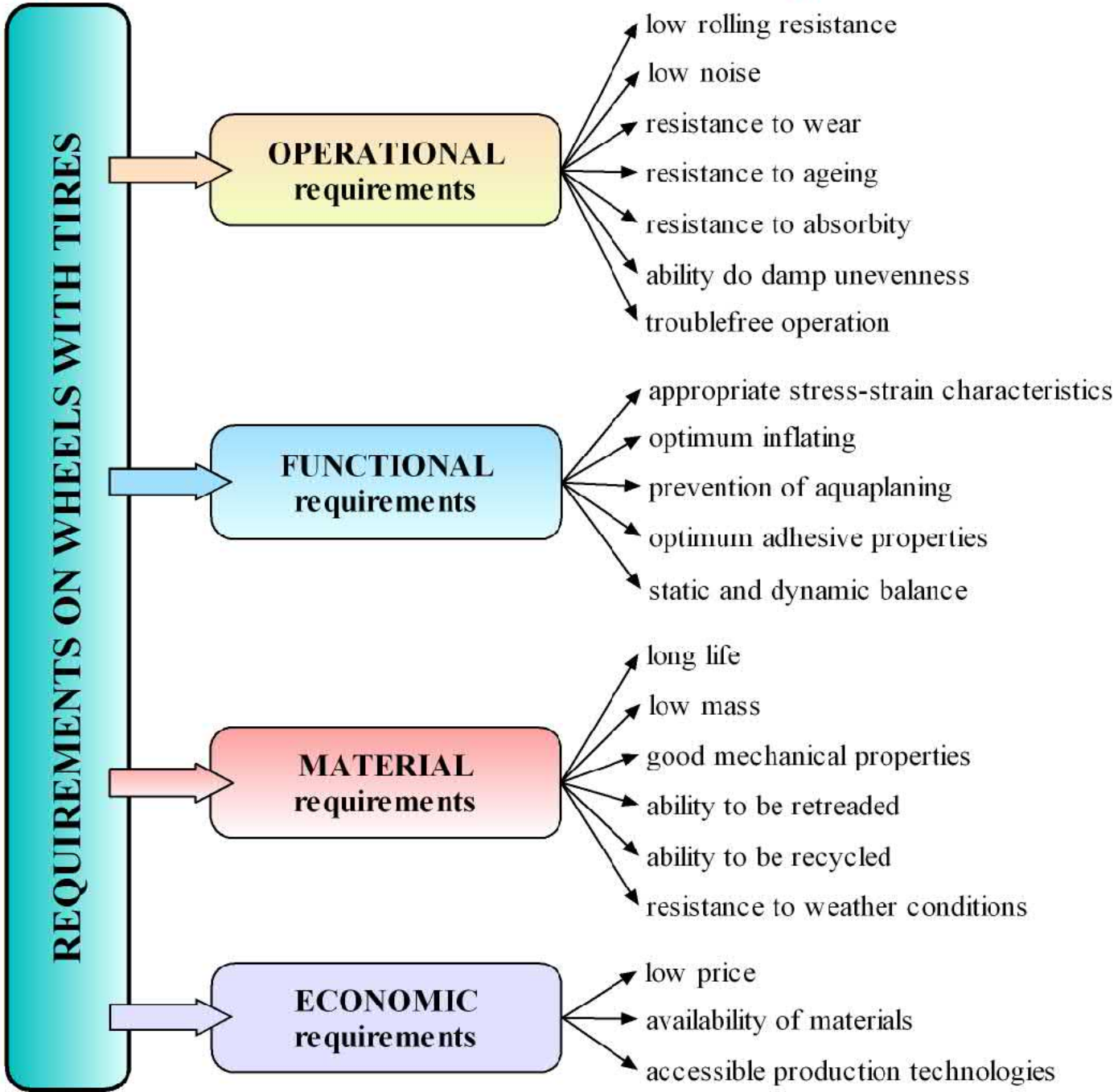

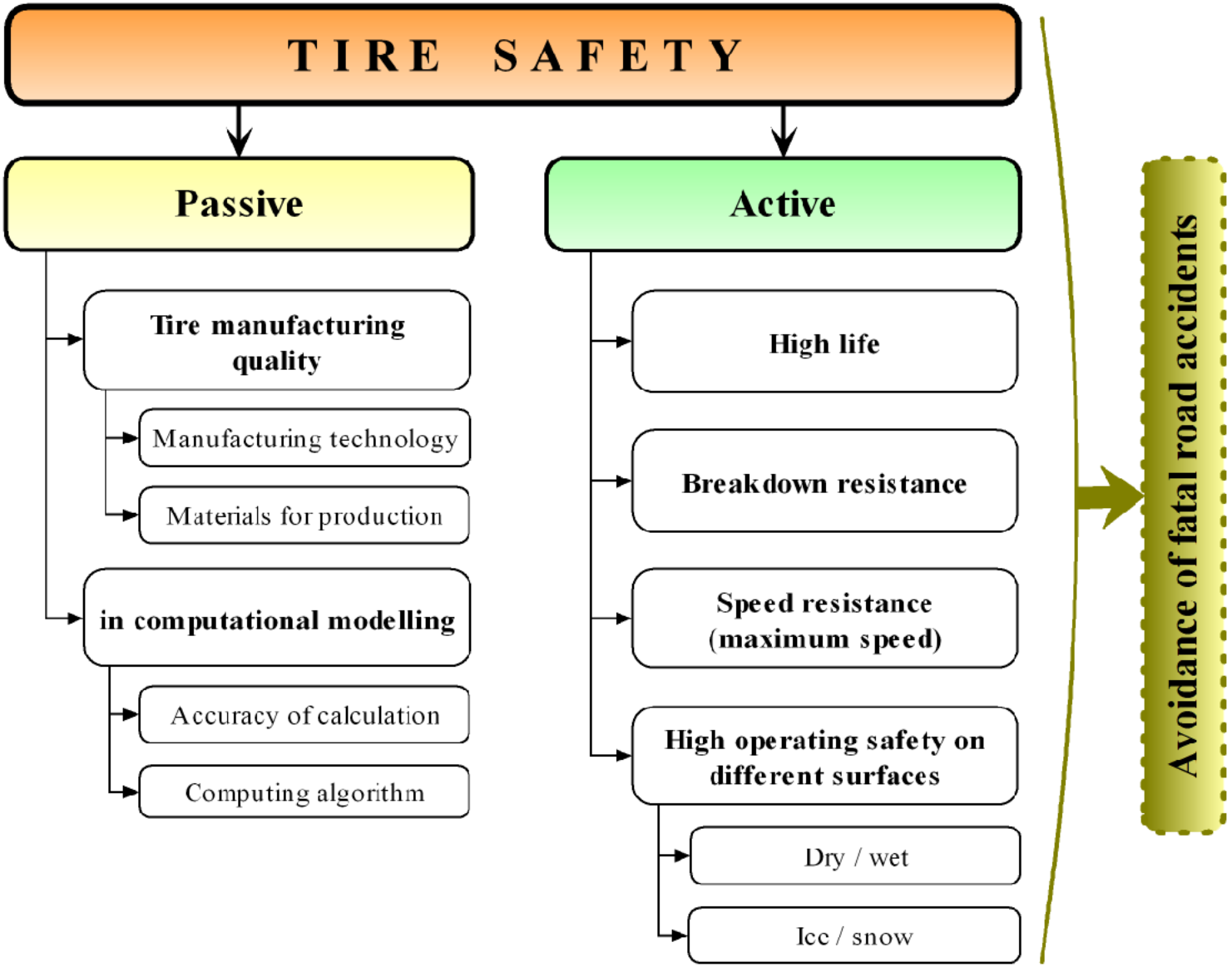
TIRE SAFETY
Passive
Active
Tire manufacturing quality
Manufacturing technology
Materials for production
in computational modelling
Accuracy of calculation
Computing algorithm
High life
Breakdown resistance
Speed resistance (maximum speed)
High operating safety on different surfaces
Dry / wet
Icc / snow
Avoidance of fatal road accidents

STRUCTURE

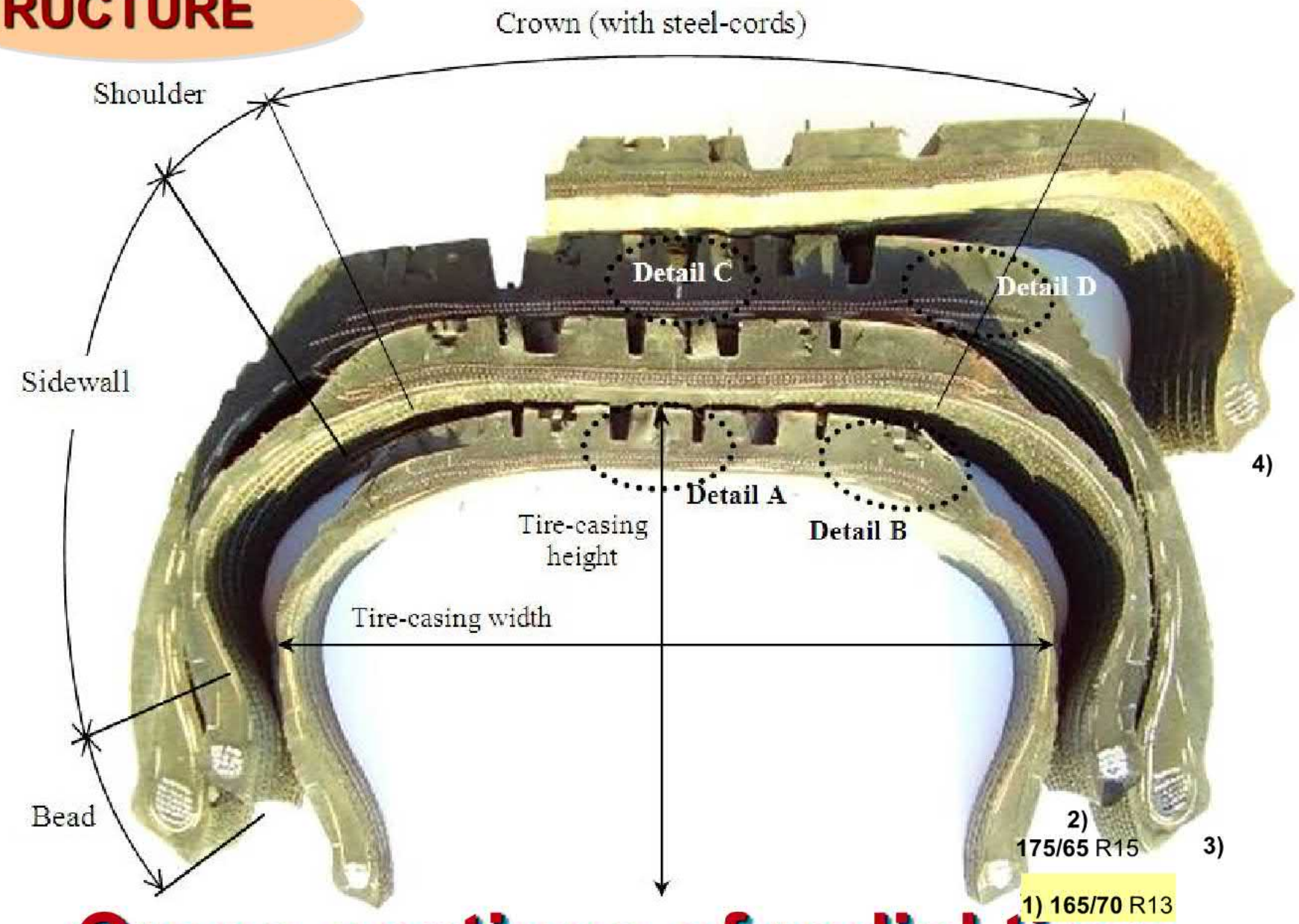

Cross-sections of radial tires

The vehicle tire can be generally understood as long-fiber composite material where there is an interaction with the elastomeric matrix with metallic as well as non-metallic reinforcements. The composite structures used in tire with the different cord-angle, material of cords, numbers of layer (single-layer or multi-layer) are:

- textile tire carcass;
- overlap textile belt;
- steel cord belt.

The standard automobile radial tire consists of elastomer parts and parts with textile-cords and steel-cords in tire tread as reinforcements. The sidewall of tire for passenger cars consists of one polyester ply and into tread are namely four plies: one polyester-, two steel- and one polyamide- ply. The textile carcass density (it is number of ends per one meter width, marked as EPM) is from 700 to 1 150 m^{-1}. The EPM of textile cap ply is 1 100÷1 200 m^{-1}. Tests of specific long-fibre composite materials with elastomer are not standardized. Therefore, for tests of cyclic loading the shape of specimens of single-layer with textile cords and elastomer must be designed.

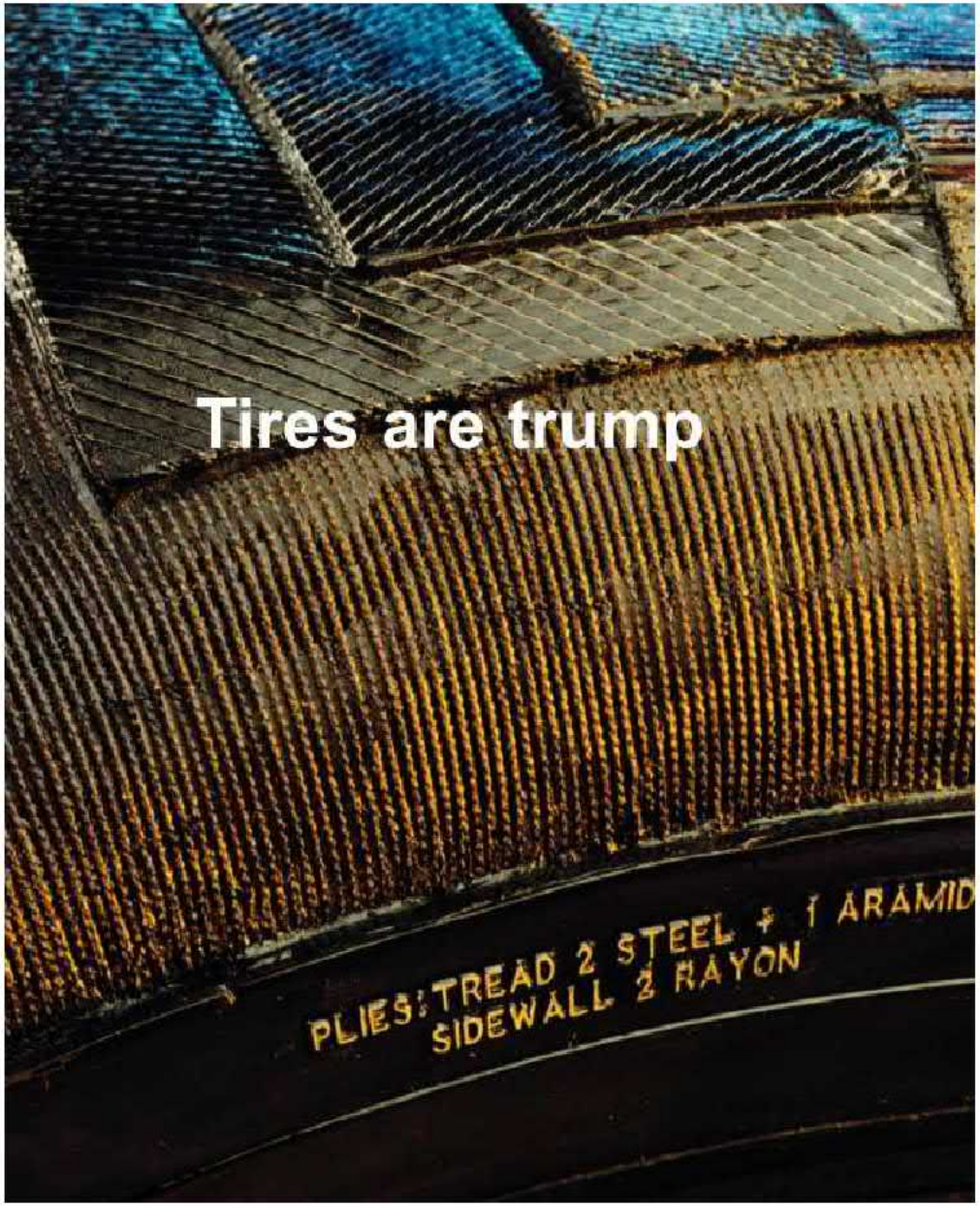
Tires are trump
PLIES: TREAD 2 STEEL + 1 ARAMID
SIDEWALL 2 RAYON

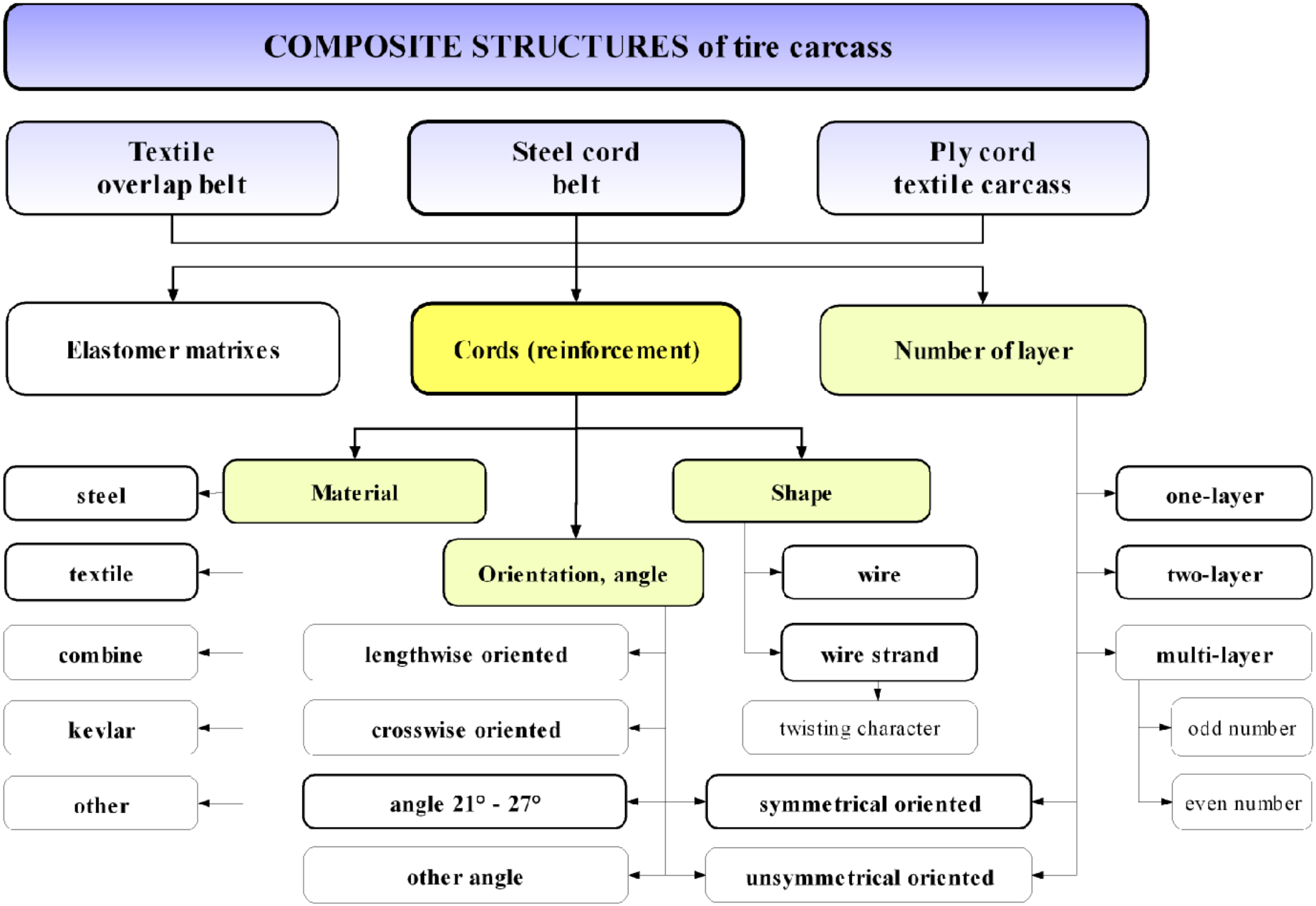
COMPOSITE STRUCTURES of tire carcass
Textile overlap belt
Steel cord belt
Ply cord textile carcass
Elastomer matrixes
Cords (reinforcement)
Number of layer
Material
Shape
steel
textile
combine
kevlar
other
Orientation, angle
lengthwise oriented
crosswise oriented
angle 21° - 27°
other angle
wire
wire strand
twisting character
symmetrical oriented
unsymmetrical oriented
one-layer
two-layer
multi-layer
odd number
even number

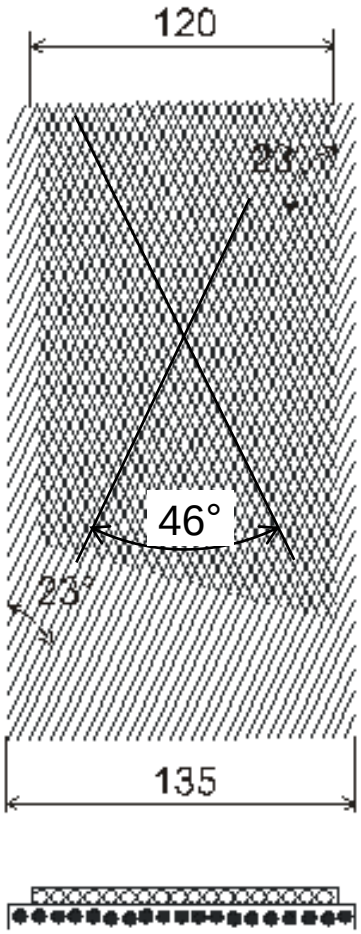

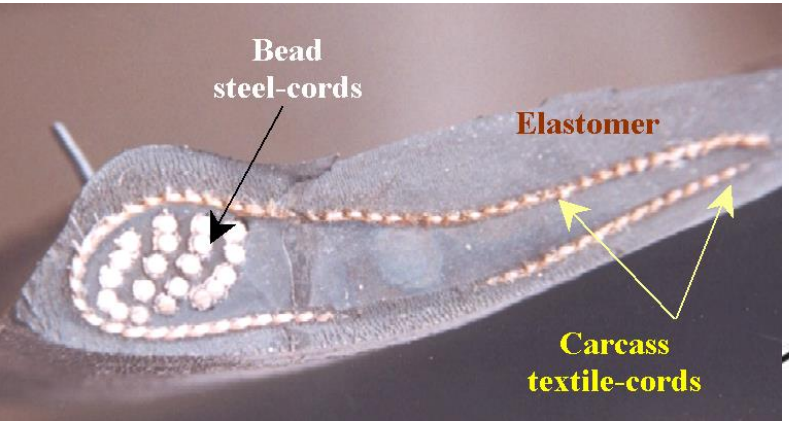

A) 165/70 R13 **Matador**

EPM = texture 961 (number of steel-cord over meter width of belt). The cord angle is ± 23°

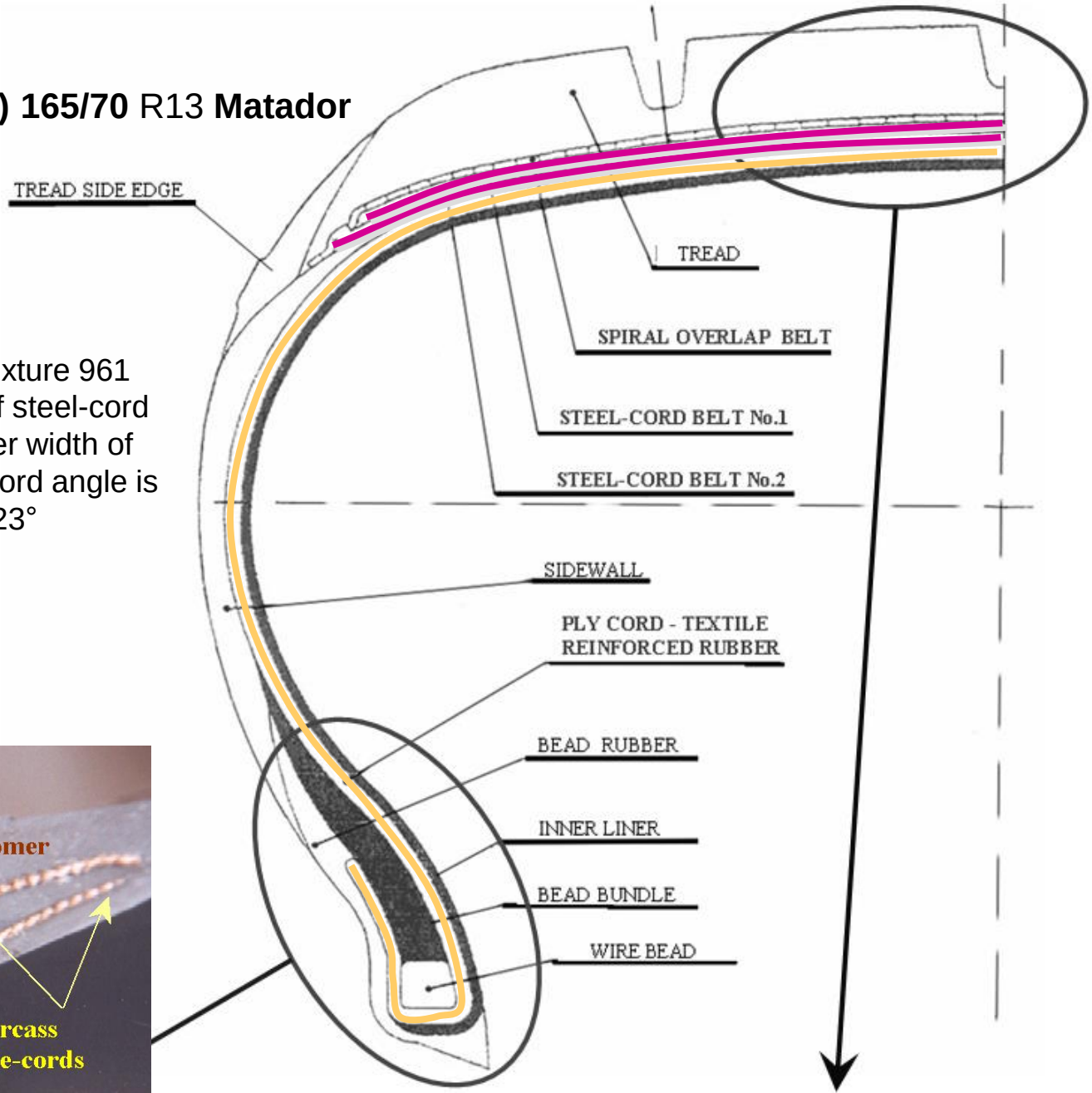

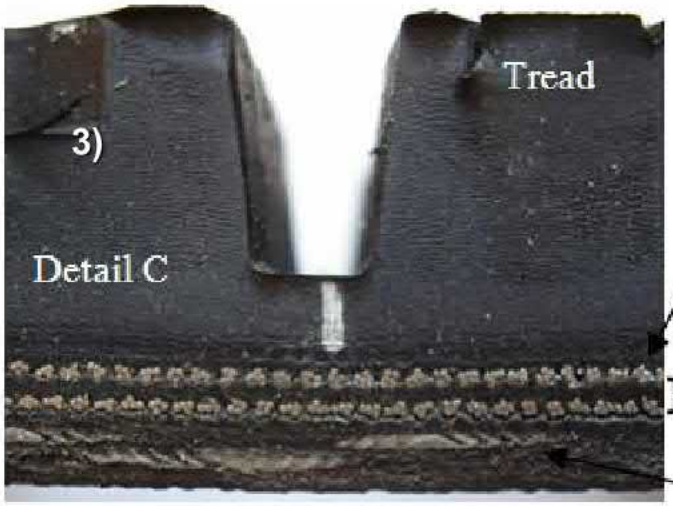

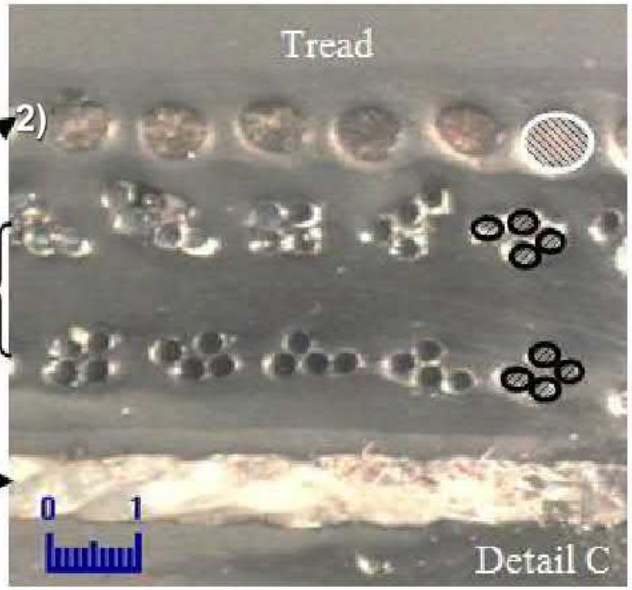

Structure in the middle of tire crown

Steel-cord 2+2x0.28 mm

Steel-cord and elastomer interface

of different radial tires (1 and 2)

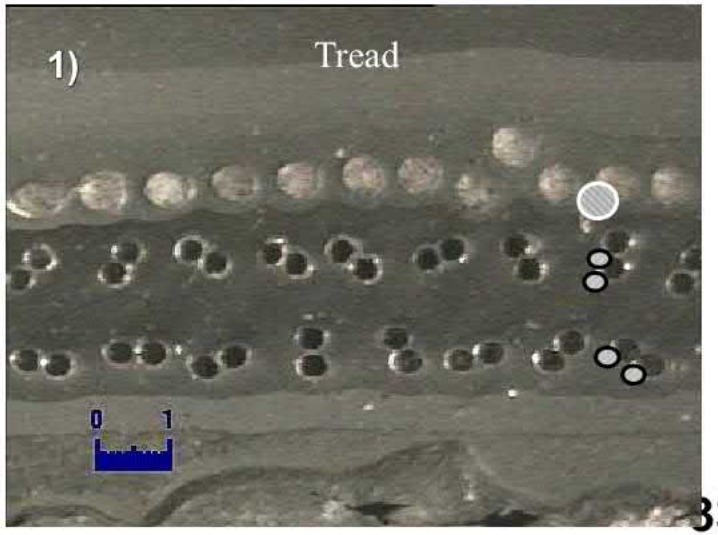

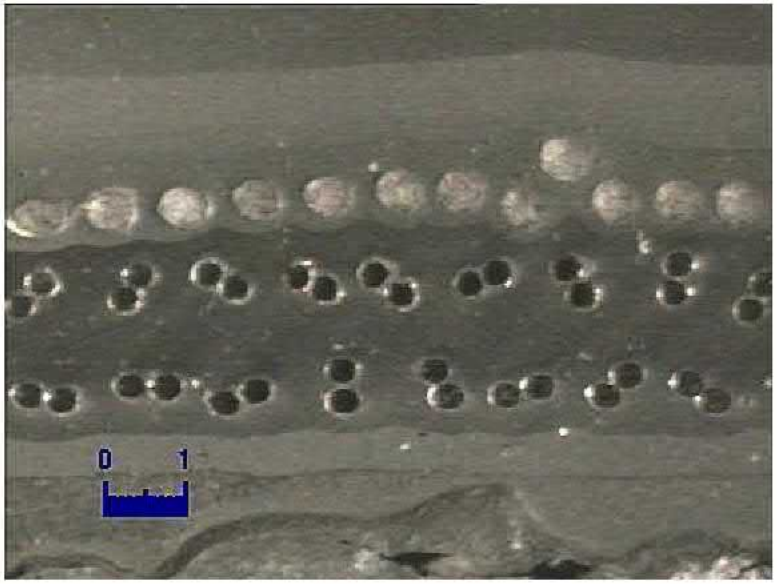
0 1

0 1

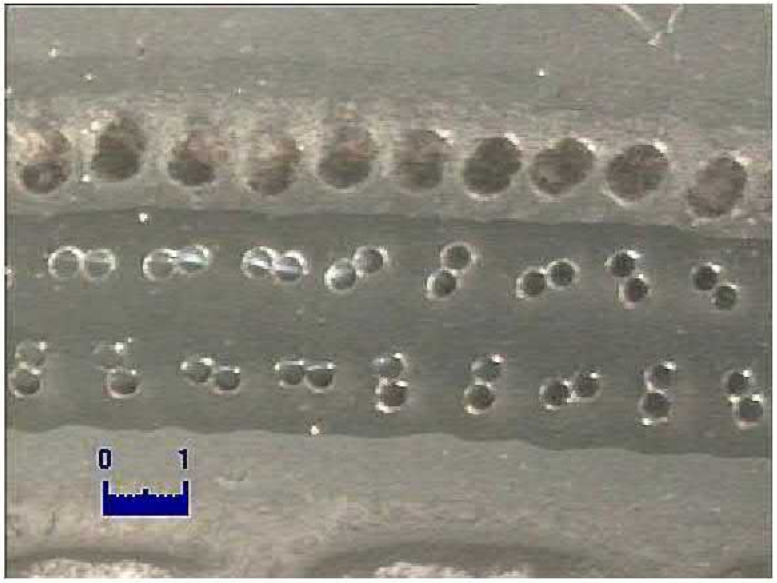
0 1

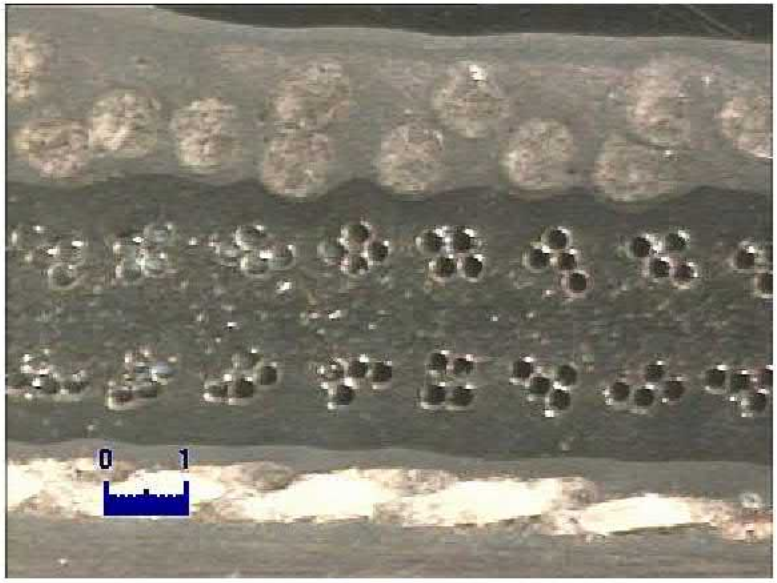
0 1

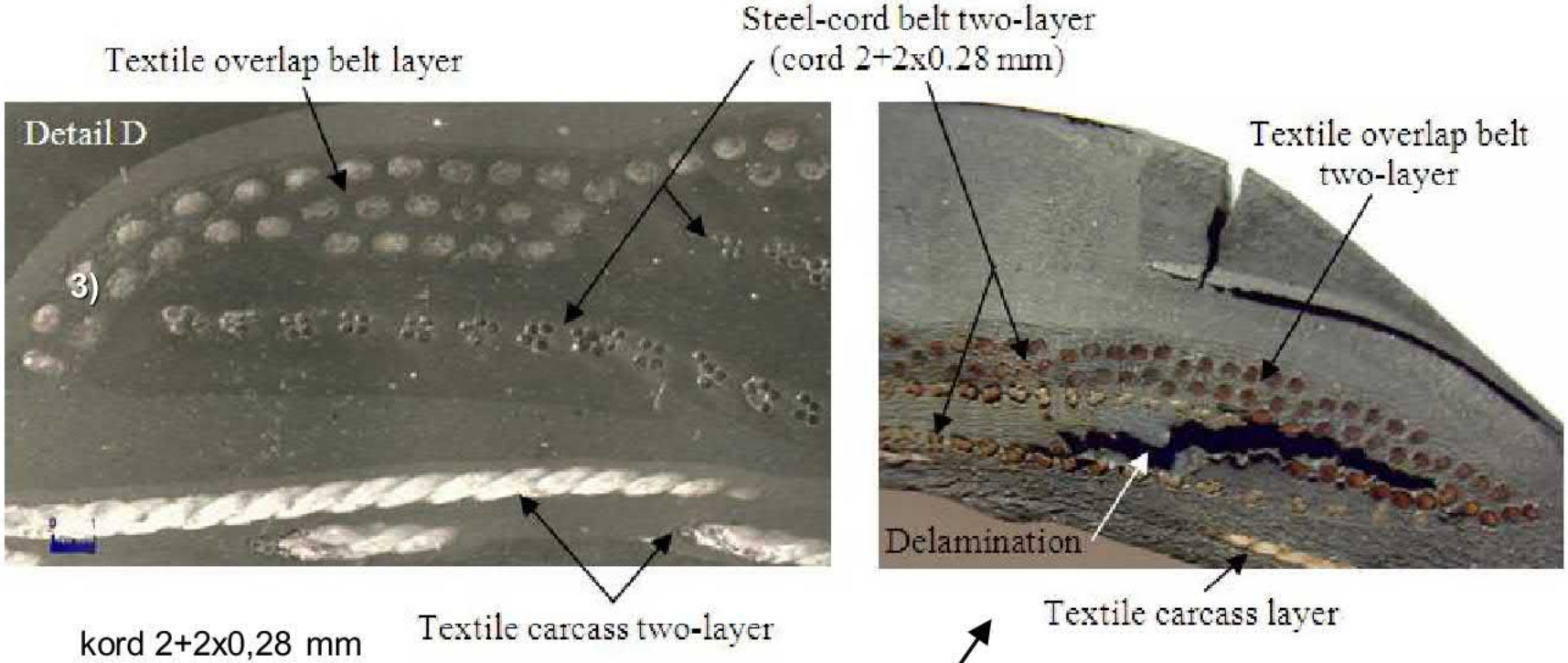

Structure at the end of the belt layers

Delamination (separation) between steel-cord belt layers

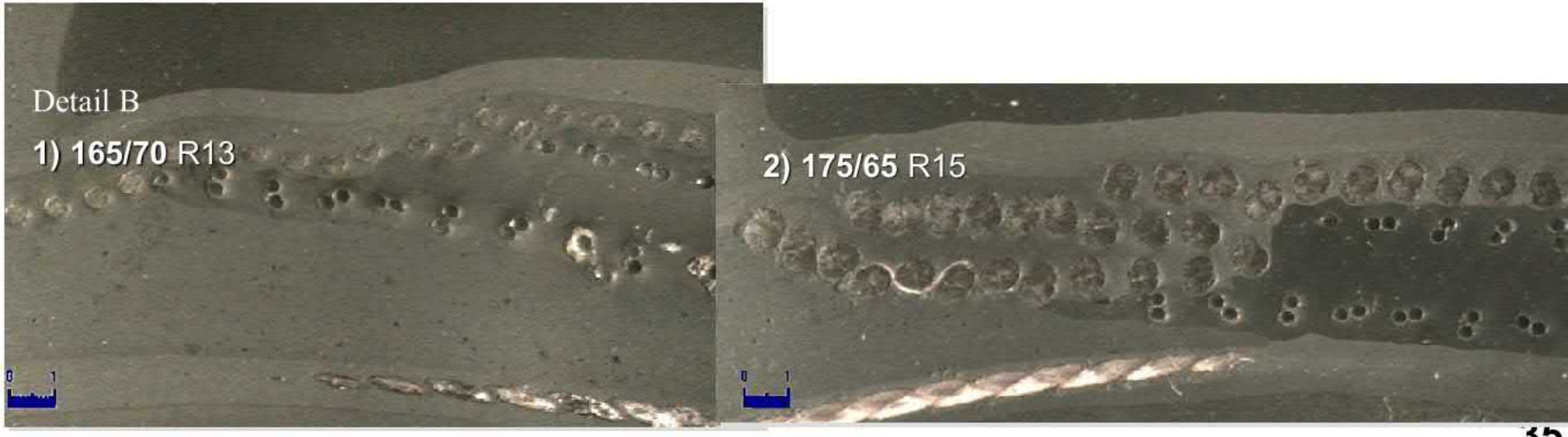

0
1

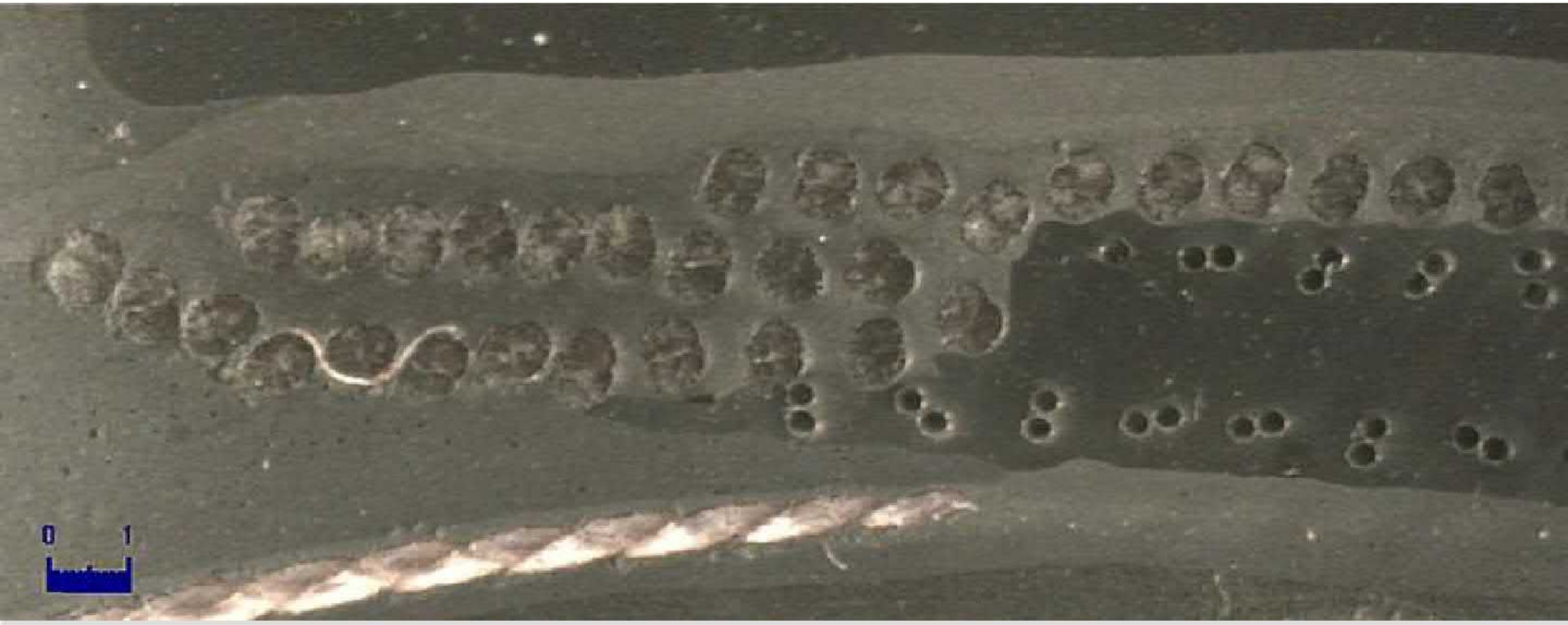
0
1

These structures of tire have got:

- **Different cord-angle** (e.g. for steel belt applied angle 21-27° into radial tire for passenger car);
- **Material** of cords (steel, textile, Kevlar, combine);
- Shape and **construction** of cord (wire, wire strand);
- **Numbers of layer** (single-layer or multi-layer).

$\Rightarrow$

So tire has got **characteristic specific deformation properties**

Steel-cords

Steel-cords can be in form of thin wire or wire strand with different constructions

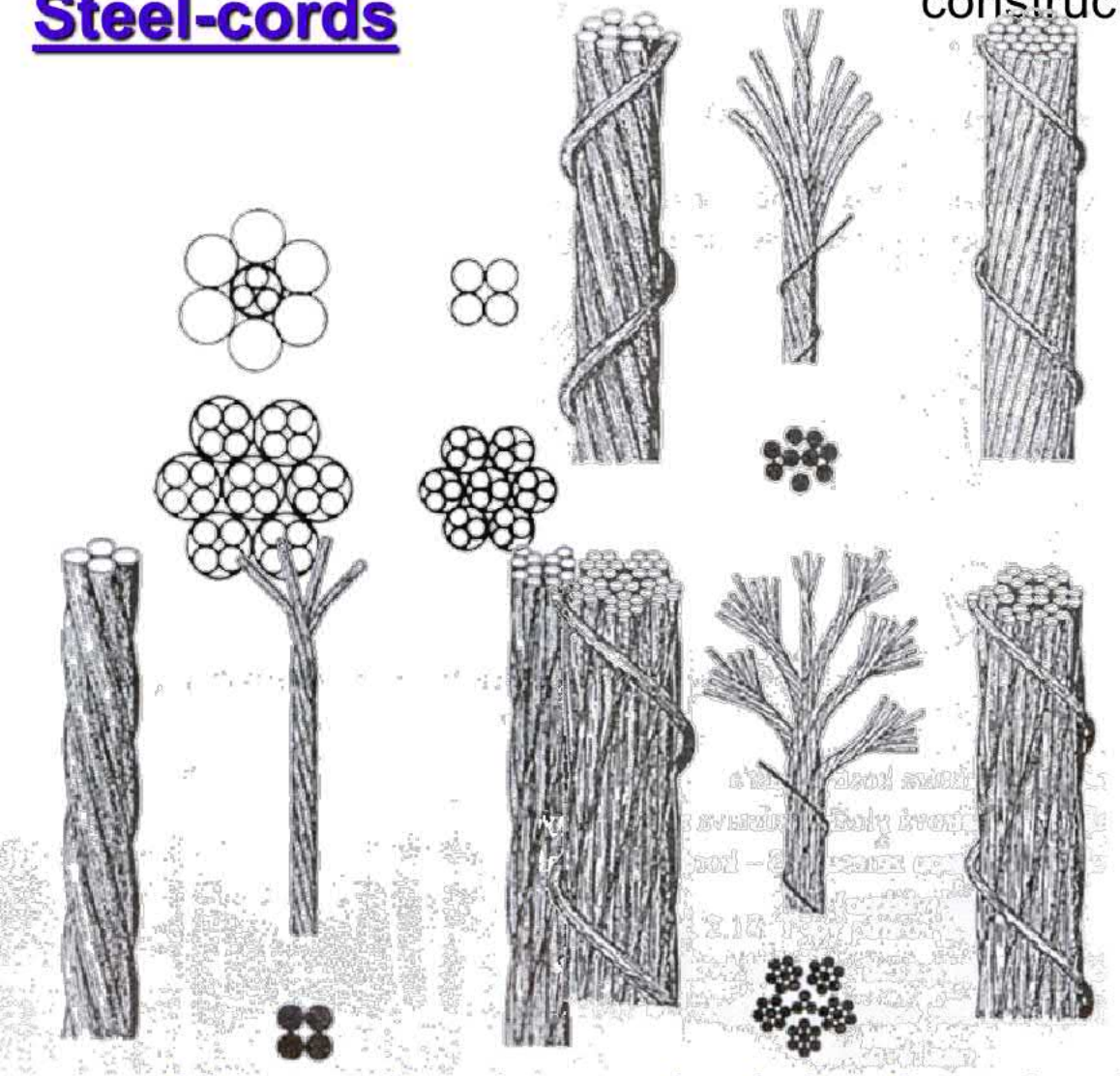

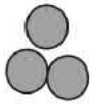

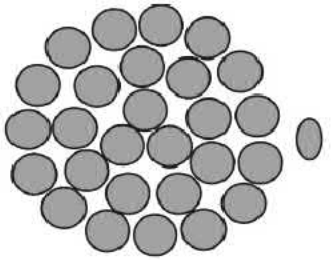

Tire for passenger car

Truck tire

High-strength steels are used exclusively for steel-cord production and good adhesive bond between rubber and cords required. Steel-cord surfaces are modified by chemical-thermal treatment - braze or copperier (cooper 63,5 % and brass 3 ÷ 7 g/kg steel), to achieve the best adhesive bond of a steel cord and rubber and get it corrosion resistant

Construction of steel-cords

Construction	*Diameter of cord* D_c [mm]	*Maximum load* [N]
2×0,30 HT	0,60	405
4×0,28	0,66	600
3×0,15 + 6×0,27	0,85	960
3×0,20 + 6×0,35	1,13	1 550
3×0,20 + 6×0,35 HT	1,13	1 770
3+9×0,22+0,15	1,17	1 210
12×0,22+0,15	1,18	1 210
3×7×0,22 HE	1,52	1 720
27×0,22+0,15	1,58	2 600
3+9+15×0,22+0,15	1,60	2 600
7×4×0,22+0,15	1,81	2 725

Tire cord types (by MATADOR Púchov and producer e.g. DRÔTOVŇA Hlohovec, BEKAERT):

- HT high tensile,
- NT normal tensile,
- **HE HIGH ELONGATION CORD = e.g. 3x7x0,22 HE** (= 3x7x0,22 **SS**) – overlap belt with angle 0°. **Elongation up to 7.5 %.** Expensive production. **.**

Modern cords: hybrid with polymer inside, carbon C 0,60-1,15%, manganate Mn 0,10-1,10%, silicon Si max. 0,90% + Cr, Ni, Cu, Co, V.

TEXTILE cords

Textile	labelling	appplication
Polyester	PES 144×1×2 PES 167×1×3	Tire casing
Polyamid 6	PA 6 94×1×2 PA 6 94x1	Overlap belt
Polyamid 6.6 (nylon)	PA 66 140×1×2	Overlap belt
Viskóza (rayon)	VS 184×1×2 VS S3 184×1×3 VS 244/1x2	Tire casing
Aramid	Aramid 110×1×2	Sport

For tire carcass **rayon** and **polyamid** (**nylon** PA 66):

- High strength,
- Elastic property.

Aramid (tire casing for sport) high strength (to 2 750 MPa), low module of elasticity, low elongation and dimensional stability.

EPDM 70 ÷ 115 (numer of cord for 10 cm width).

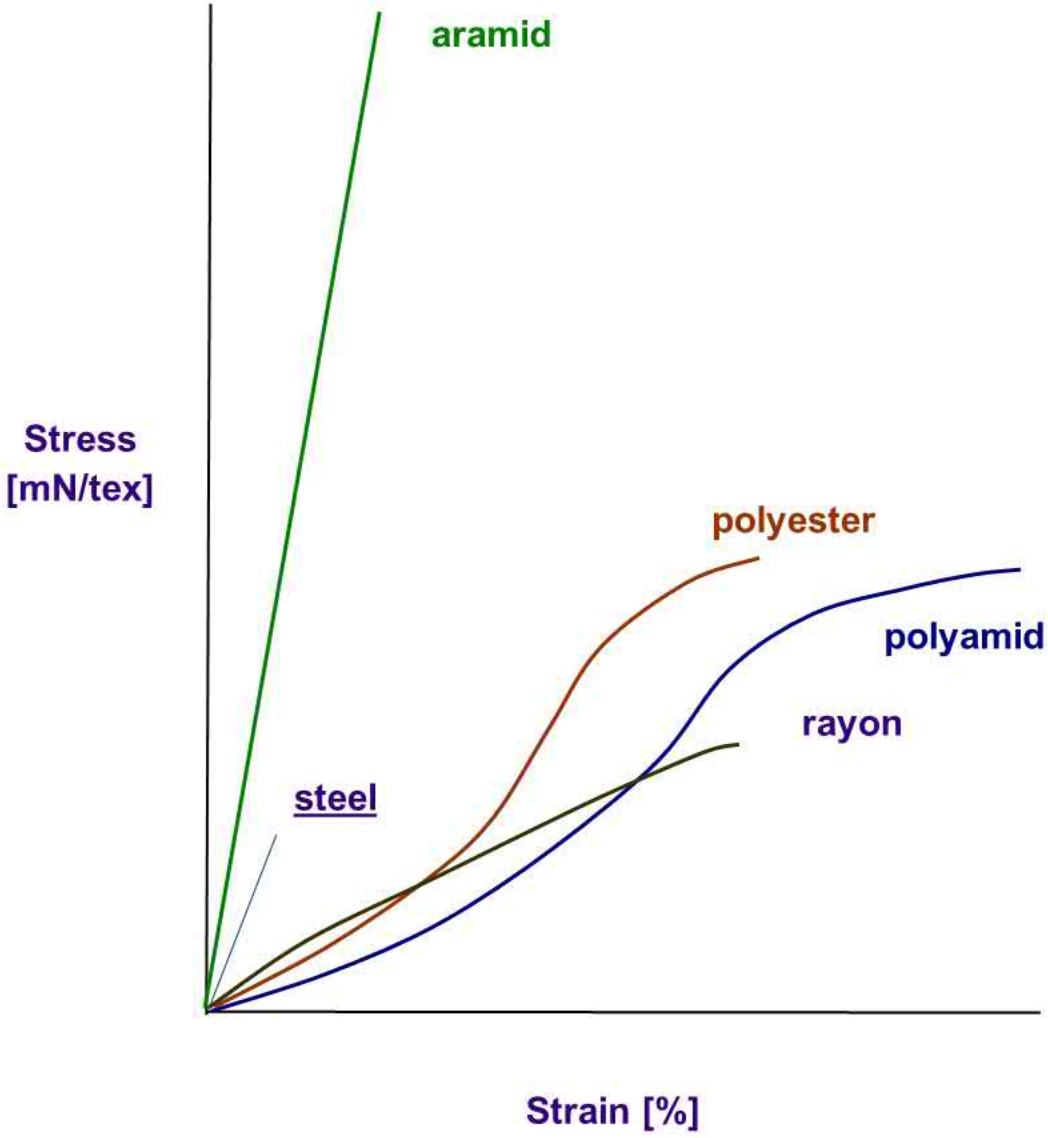
aramid
Stress
[mN/tex]
polyester
polyamid
rayon
steel
Strain [%]

- ***Modulus of elasticity***

  (from producer or experiment modulus for ε = 5 % = name of modulus is LASE – Load At Specific Elongation 5 %;

  Or modulus as stress necessary on elongation 100 %, extrapolation for elongation 2 %)

- ***Poisson ratio*** **=** no constant, dependence on deformation

⇒ **standard strength (N/dtex) and elongation (%).**

After vulcanization process – modulus can be change **(influence heat).**

material	***modulus*** E_t [MPa]	***Poiss. ration*** ν_t [1]
Nylon *(PA 66; overlap belt PA 94x1)*	**1 600 ÷ 2 000** (900 ÷ **3 450**; 9 ÷ **50** cN/dtex)	**0,32 ÷ 0,45**
Rayon *(carcass PES 144x1x2)*	**1 200 ÷ 1 400** (600 ÷ **11 000**; 8 ÷ **120** cN/dtex)	0,38

⇒ ***Temperature 20°C*** **and humidity** ***65 %***
length **500 mm**

⇒ ***unit of E***

cN/dtex

Part 2 – TIRE TESTS:

Planned experiments, Static adhesor, Dynamic adhesor, Deformation characteristics, Radial stiffness – calculation

Planned experiments of tire

- Why experiments?
- Knowledge? Can I test?? If yes, than continue/ If no, I must study of problem !
- Which test? Static / dynamic ?? Why?
- Which tire? Passenger car, truck, ….
- Why test (purpose)? Stiffness, contact area, ….??
- Which standards? ČSN, …
- Which test machine? Have I them? If yes, than ….

  If no, I have done because I can not do experiments.
- Barriers? Time, finance, software, … If no barriers, than no problems, I can start with experiments……..
- Experiment conditions? Given or must be design
- Parameters of test? Loading by ? speed, …
- Verification analyse of results? By literature?
- Outputs from experiments?
- Outputs for computational modelling?

TEST OF TIRE

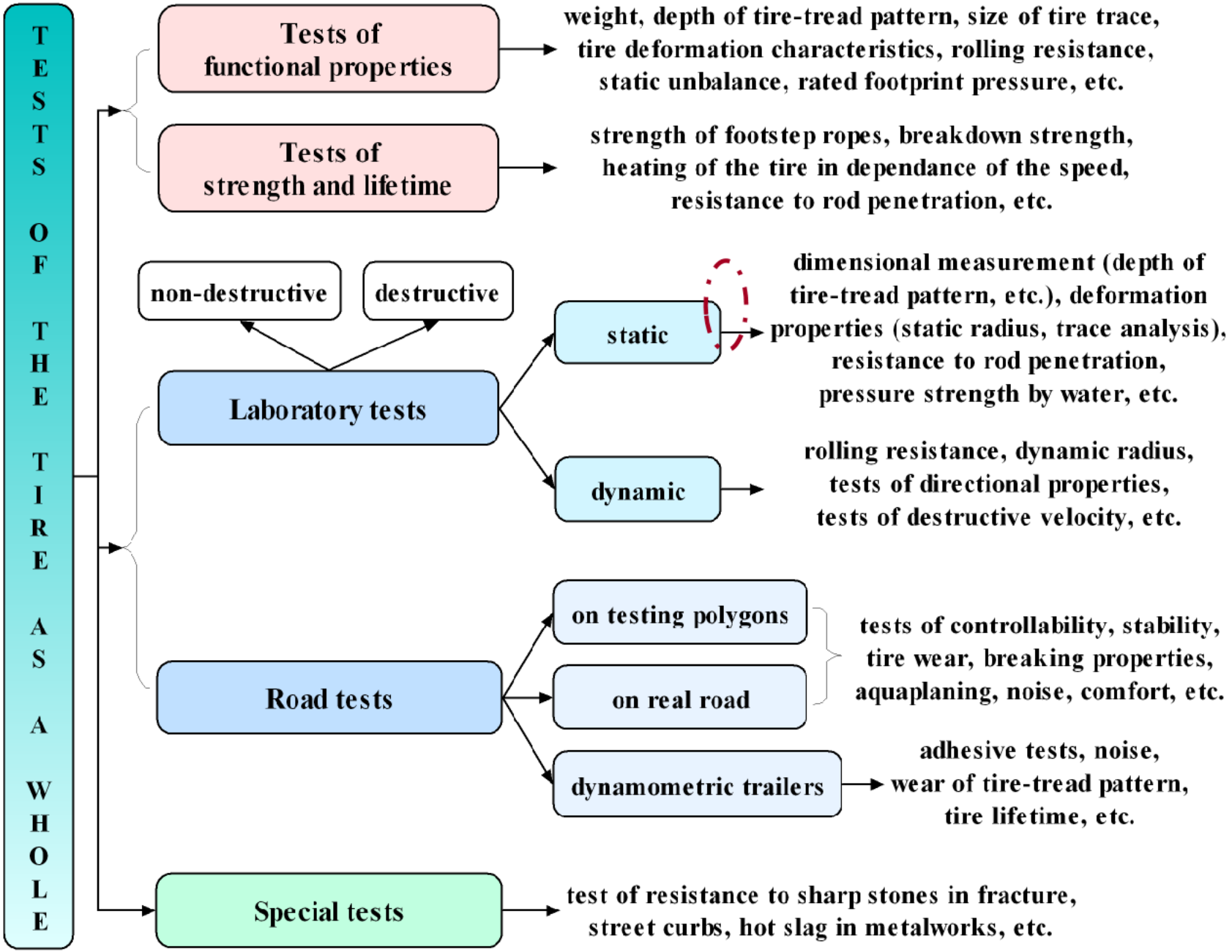
TESTS OF THE TIRE AS A WHOLE
Tests of functional properties
weight, depth of tire-tread pattern, size of tire trace, tire deformation characteristics, rolling resistance, static unbalance, rated footprint pressure, etc.
Tests of strength and lifetime
strength of footstep ropes, breakdown strength, heating of the tire in dependance of the speed, resistance to rod penetration, etc.
non-destructive
destructive
Laboratory tests
static
dimensional measurement (depth of tire-tread pattern, etc.), deformation properties (static radius, trace analysis), resistance to rod penetration, pressure strength by water, etc.
dynamic
rolling resistance, dynamic radius, tests of directional properties, tests of destructive velocity, etc.
Road tests
on testing polygons
on real road
tests of controllability, stability, tire wear, breaking properties, aquaplaning, noise, comfort, etc.
dynamometric trailers
adhesive tests, noise, wear of tire-tread pattern, tire lifetime, etc.
Special tests
test of resistance to sharp stones in fracture, street curbs, hot slag in metalworks, etc.

ČSN 63 1001-4 – Standard: Terminology of tyres. Testing, 1980 (in Czech and English)

ČSN 63 1502 – Standard: Tyre testing. Introduction for the preparation of tyres for laboratory tests, 1988 (in Czech)

ČSN 63 1554 – Standard: Tyre testing. Determination of tyre / ground contact pressure, 1983 (in Czech)

ČSN 63 1509 – Standard: Determination of force variation at radial stress, 1985 (in Czech)

ČSN 63 1511 – Standard: Testing of tyres. Determination of static radial stiffness and static tyre radius, 1983 (in Czech)

- ***Load index***

  Maximum static radial load.

- ***Static loaded radius***

  Non-rotation tire

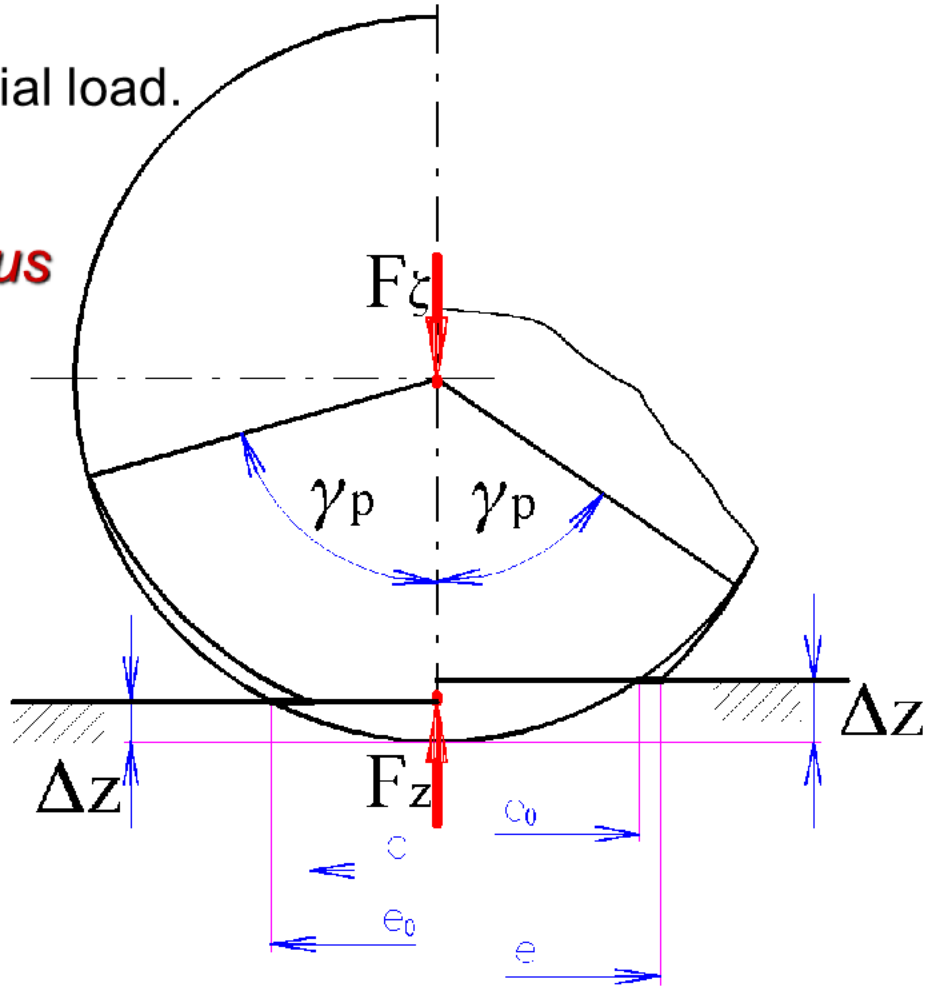

Deflection of tire

diagonal **radial**

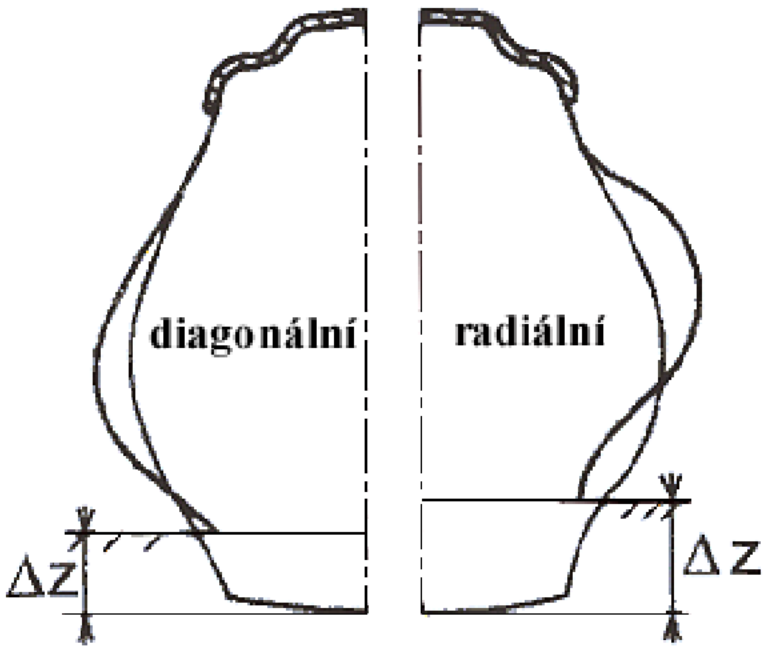

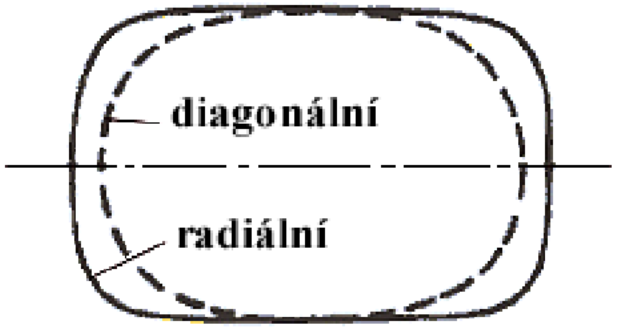

Contact area of radial tire is greather than diagonal tire.

Contact area dependences on:

- Radial loading;
- Inflation pressure;
- velocity.

Deformation characteristics of tire

(load-deflection curves)

Radial

Torsion

Lateral

Radial deflection (vertical deformation) characteristic

of tire - dependence between radial load (tire normal force) and radial deflection.

Full radial deformation characteristic = loading up and loading down.

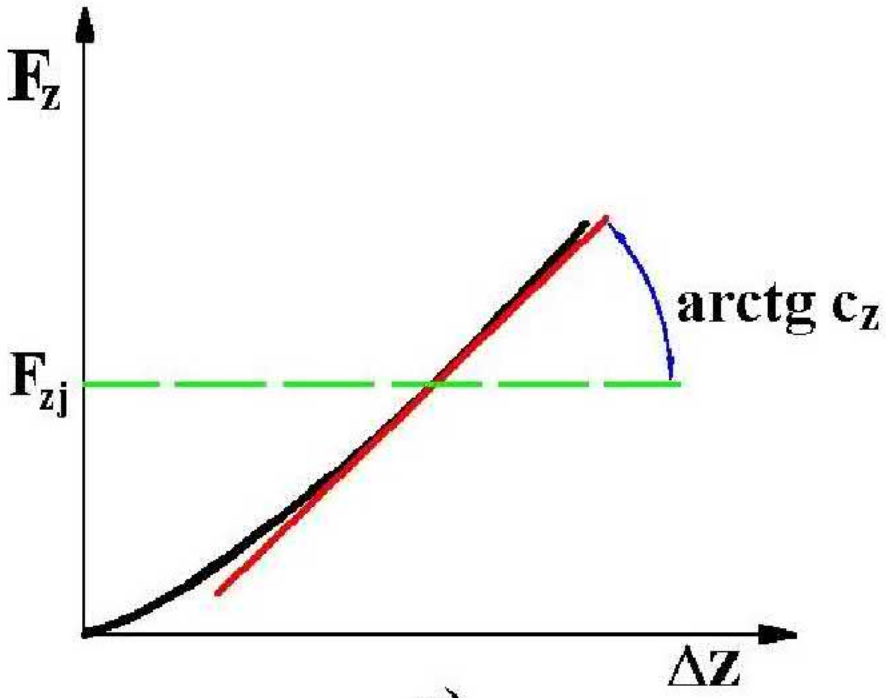

a)

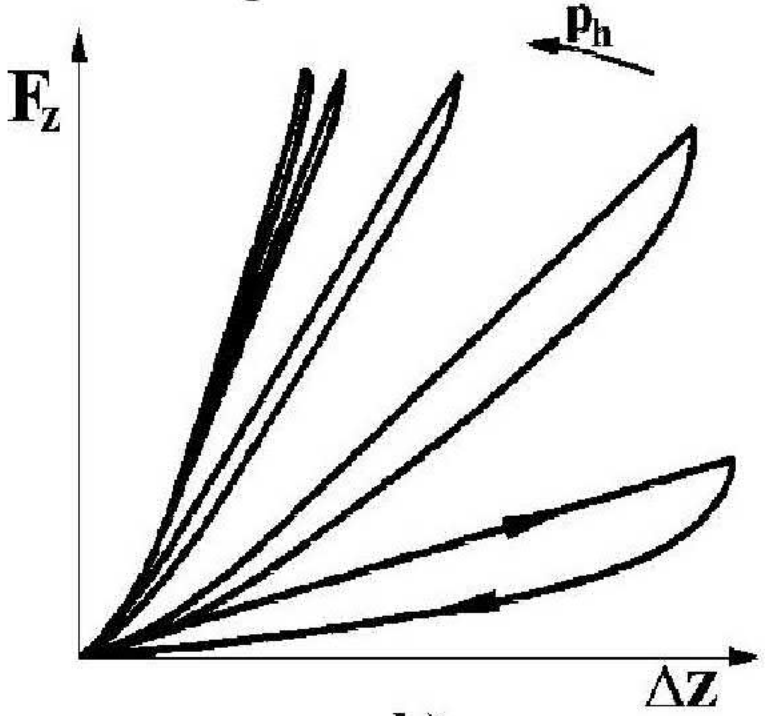

b)

Dependence on shape of obstacle (convex = decrease, concave = increase)

Radial stiffness

The radial stiffness, which is obtained from the radial deformation characteristic by calculation, is an important parameter entering the calculation of entire cars, because the stiffness parameter replaces the whole tire.

The standard ČSN 63 1511 defines the radial stiffness from the radial deformation characteristic by using a computational relationship, which is determined by points corresponding to 75% and 125% of LI (load index).

Radial stiffness

The radial stiffness dependences on inflation pressure of tire.

$$S = \frac{F_{125\%load} - F_{75\%load}}{x_{125\%load} - x_{75\%load}} \text{ [N/mm]}$$

Where:

S [N/mm]	radial stiffness;
$F_{125\%load}$ [N]	vertical force for 125% load;
$F_{75\%load}$ [N]	vertical force for 75% load;
$x_{125\%load}$ [mm]	radial deformation for 125% load ($F_{125\%load}$);
$x_{75\%load}$ [mm]	radial deformation for 75% load ($F_{75\%load}$).

load index (LI)

The radial stiffness can be obtained by calculation relating to the static radial deformation characteristics from two points of deformations corresponding to forces for 75 and 125 % of tire load capacity (marked as LI) by the standard ČSN 63 1511.

Stiffness is an important parameter in relation to the calculation of tires as the integral car system because the stiffness value replaces the tire including its geometry, structure, material parameters, influence reinforcements and inflation pressure.

Tire Matador 165 / 65 R13 MP16 77 T Stella 2) for passenger cars (on steel wheel rim 5Jx13) by the help of two test machines for static and dynamic experiments. The tire has maximum load capacity of 412 kg (load index LI is 77) and the maximum inflation pressure of the tire is 300 kPa.

Maximum velocity of tire is 190 km/h (the speed index is T).

The tire carcass consists of one layer of polyester and the tread consists of two layers of steel-cord belt and two layers of polyamide belt. The density of the steel-cord belt is 96.1 ends per decimeter.

The inflation pressures of the tire used for static experiments were 160 kPa (underinflated tire) and 240 kPa (current inflation pressure of tire for given passenger car). Different pressures were used for the comparison of their influence on the static radial deformation characteristics.

The maximum circumference of the tire is 1713 mm for maximum inflation pressure.

Tire 165 / 65 R13 for experimental testing

From the technical data of the tire-casing in the catalogue of the producer can be seen that the static loaded radius of the new tire-casing for the maximum load capacity and the given inflation pressure (probably 250 kPa) is 248.0 mm. The static loaded radius is the distance from wheel axle centerline to supporting tread surface at a given radial load and inflation pressure in a static condition.

By recalculation (from the diameter of new tire) the preliminary value of the radial deformation of the tire-casing in contact with the ground can be obtained for maximum load capacity of the tire. In this case the radial deformation is 24.0 mm. The static radial stiffness (for the given inflation pressure, which is related to the value of the radial deformation) can be estimated, using a simple equation, as the ratio of the maximum load capacity in N and radial deformation in mm according to equation (1):

$$S = \frac{F_{100\,\%\text{ of LI}}}{x_{100\,\%\text{ of LI}}} = \frac{412 \cdot 9.81\,[\text{N}]}{24.0\,[\text{mm}]} = 168.4\,[\text{N/mm}]$$

Where: S [N/mm] or [kN/m] – static radial stiffness of tire (for the given inflation pressure 250 kPa),
$F_{100\,\%\text{ of LI}}$ [N] – vertical force for maximum load capacity of tire (LI),
$x_{100\,\%\text{ of LI}}$ [mm] – radial deformation of tire-casing for LI.

The static radial stiffness for the given inflation pressure 250 kPa is 168.4 N/mm. It is only a preliminary value from equation

Radial stiffness in N/mm

High profile number (70 – 82) stiffness

200 N/mm.

Low profile number (45 – 40) stiffness 280-300 N/mm (R16- R18)

Standard stiffness values for modern tire for passenger cars are 200-320 N/mm.

The radial stiffness depends on the inflation pressure of tire. It is a fact that with the increasing inflation pressure, the radial stiffness increases. Moreover, the radial stiffness depends on the composition and the construction of the tire-casing. Tires with high profile number from 70 to 82 have static radial stiffness 200 N/mm, tires with profile number 50 have stiffness e.g. 240 N/mm. Tires with low profile number 45 – 40 and radiuses from R16 to R18 have stiffness approx. 260 – 320 N/mm. In general, the static radial stiffness values of radial tires for passenger cars are in range 200 – 320 N/mm.

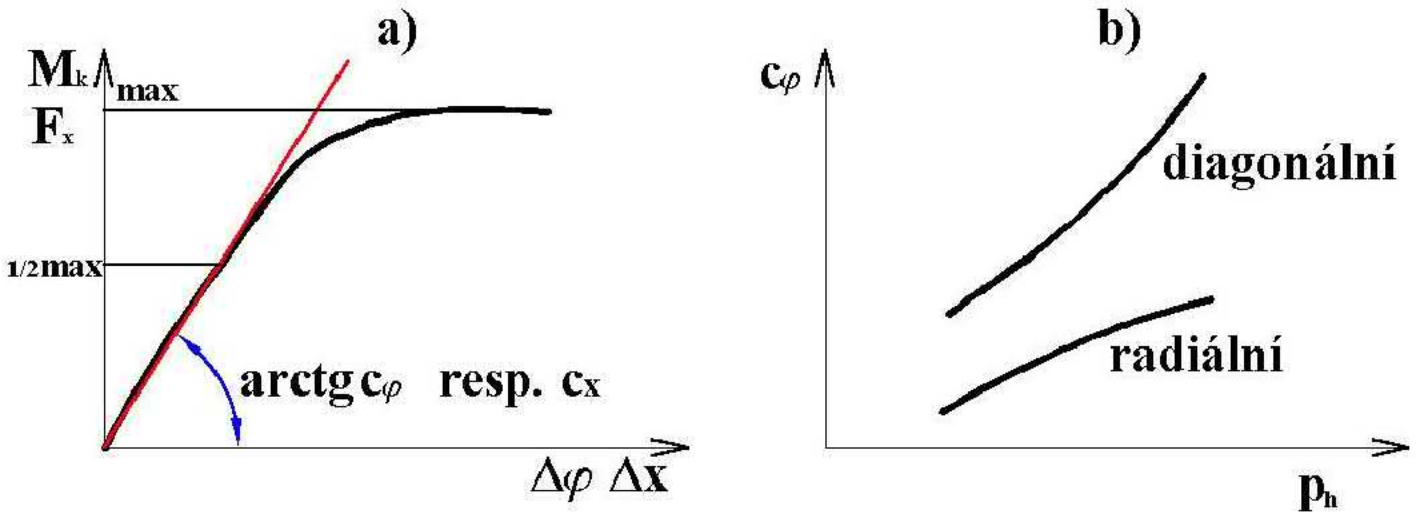

Torsional deformation characteristic

Torsional deformation characteristic

Dependence between torsion moment M_k and angle rim-casing $\Delta\varphi$.

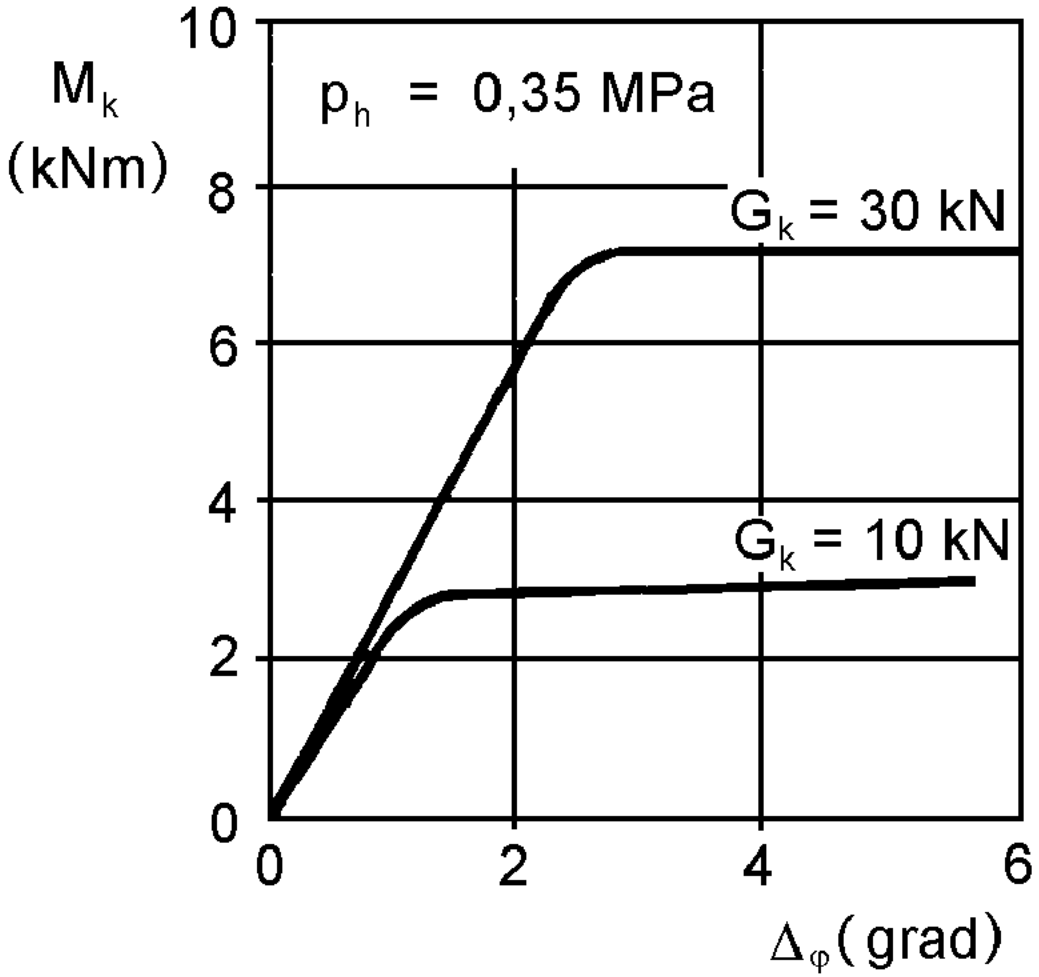
M_k
(kNm)
10
8
6
4
2
0
p_h = 0,35 MPa
G_k = 30 kN
G_k = 10 kN
0
2
4
6
Δ_φ (grad)

Lateral deformation characteristic

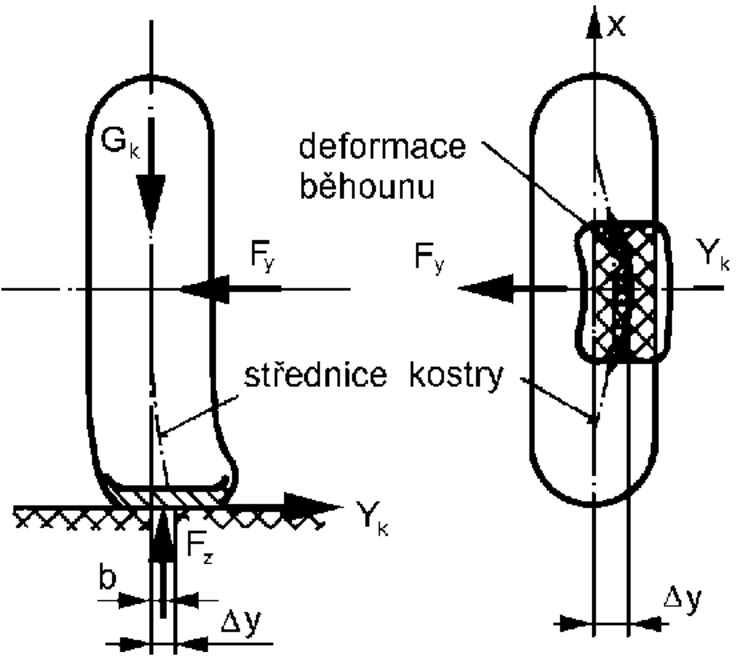

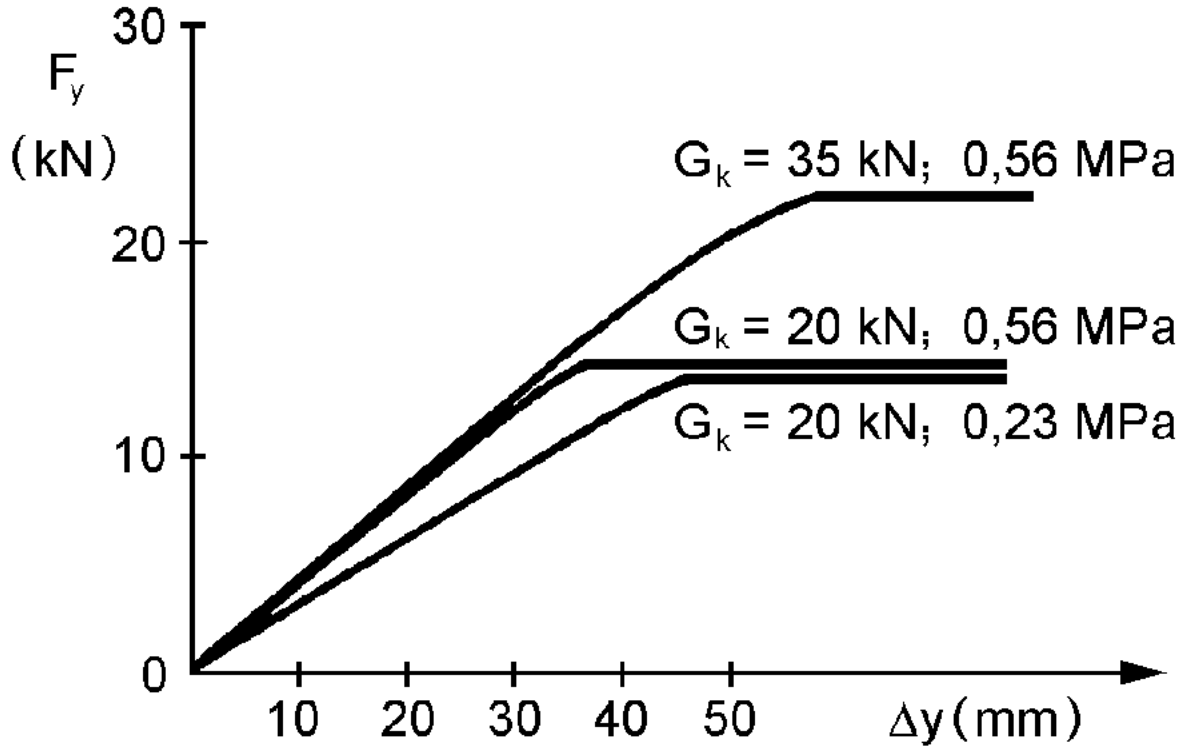

ROLLING RESISTANCE

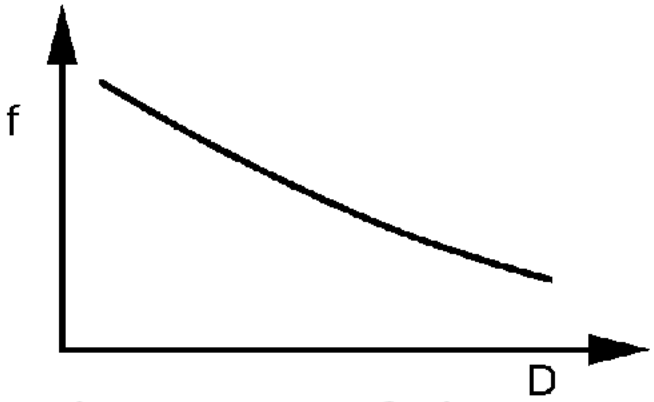

Diameter of tire

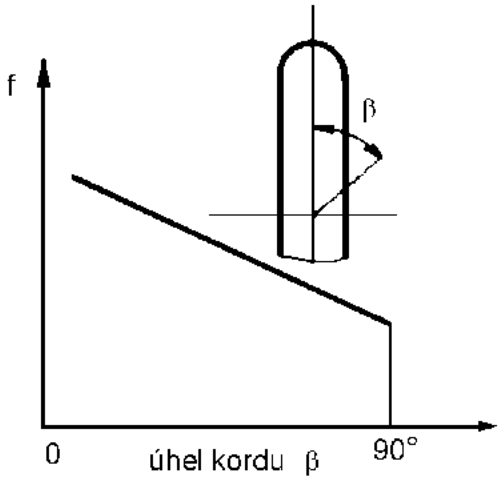

Cord angle

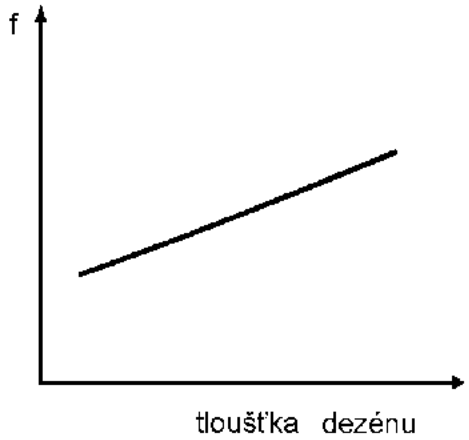

Thickness tread

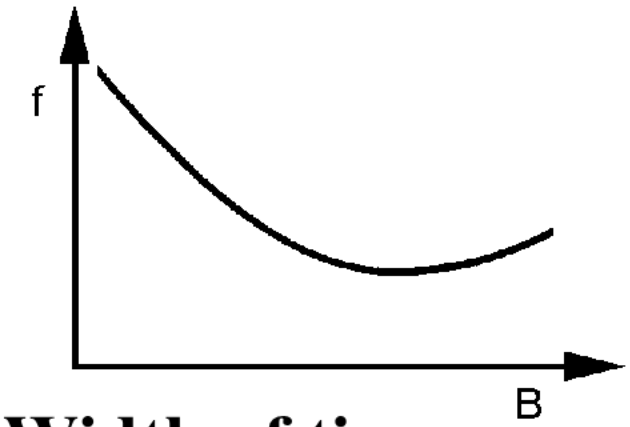

Width of tire

Radial tire casing

expensive, accuracy of manufacture in comparison with diagonal

- *economic*: low rolling resistance $\Rightarrow$ **low fuel consumption**
  slower tread wear $\Rightarrow$ **higher lifetime in km**
- *safeness*: bigger contact area $\Rightarrow$ **shorter braking distance**
  good cornering stability
- *comfort*: elasticity sidewall $\Rightarrow$ **vibration of road surface bumps = less than diagonal**

TIRE TREAD PATTERN

Winter comparison with summer tire:

- tread profile
- rubber mixture with silica.

winter ↗ SILICA, supplanting black = goog elasticity under 7° C to **-30 °C** ⇒

M+S („mud and snow“).

- Profile number
- LI, GSY, PR (equivalent of number of plies)
- TWI
- Wear (progresive ↑ with *speed* and *temperature*)
- REGLOOWABLE
- Inflation pressure
- Radius r static, r dynamic
- … ….

Load index

Load index	Max. load (kg)	Load index	Max. load (kg)	Load index	Max. load (kg)	Load index	Max. load (kg)
50	190	68	315	86	530	104	900
51	195	69	325	87	545	105	925
52	200	70	335	88	560	106	950
53	206	71	345	89	580	107	975
54	212	72	355	90	600	108	1000
55	218	73	365	91	615	109	1030
56	224	74	375	92	630	110	1060
57	230	75	387	93	650	111	1090
58	236	76	400	94	670	112	1120
59	243	77	412	95	690	113	1150
60	250	78	425	96	710	114	1180
61	257	79	437	97	730	115	1215
62	265	80	450	98	750	116	1250
63	272	81	462	99	775	117	1285
64	280	82	475	100	800	118	1320
65	290	83	487	101	825	119	1360
66	300	84	500	102	850	120	1400
67	307	85	515	103	875	---	---

EXPERIMENTS OF TIRES ON „STATIC ADHESOR“

- Static loading max **2 t** with **hydraulic hand jack (1 t with manual)**
- Tire casing from **R13 to R19**
- Tire width max **240 mm**

STATIC ADHESOR

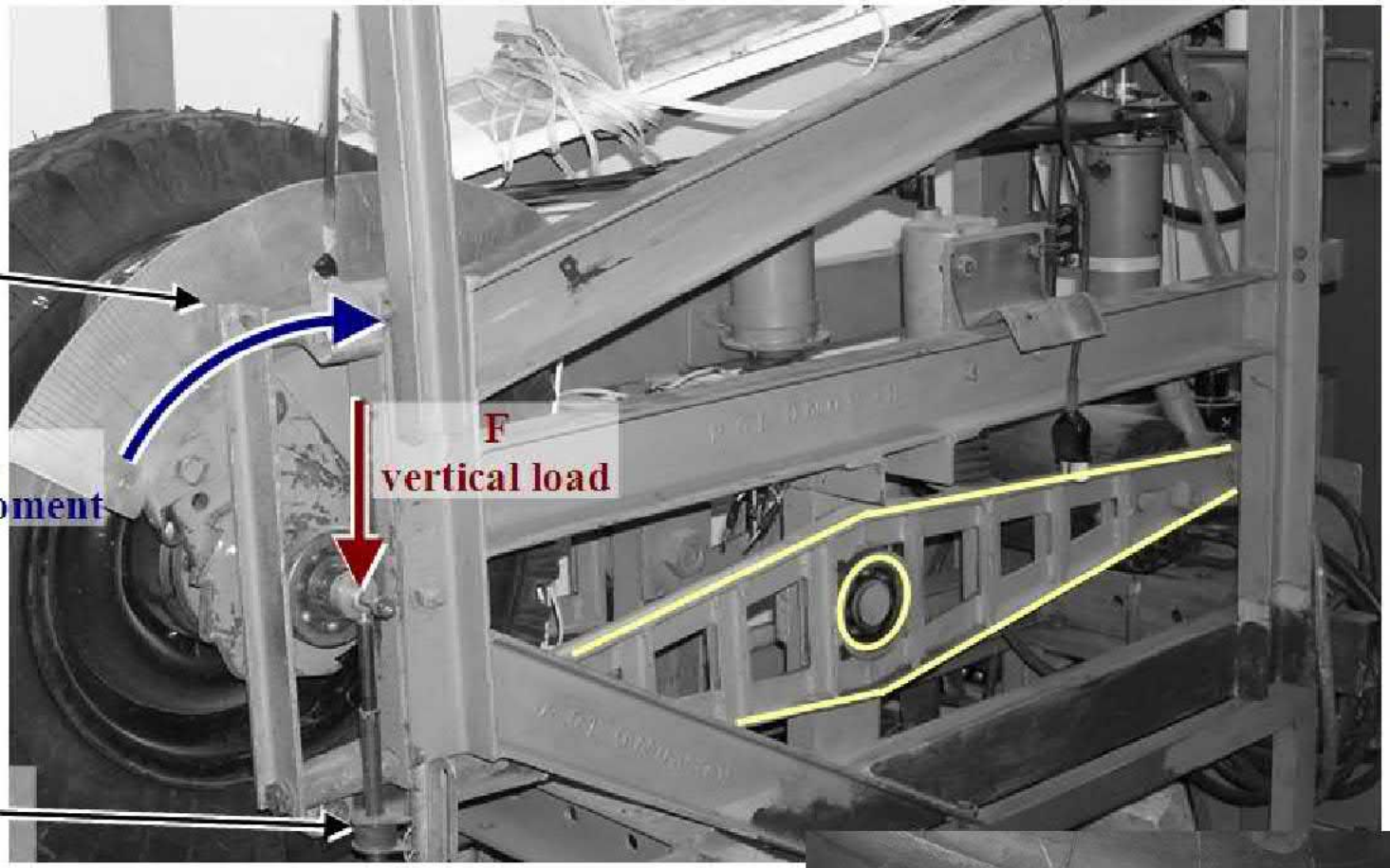

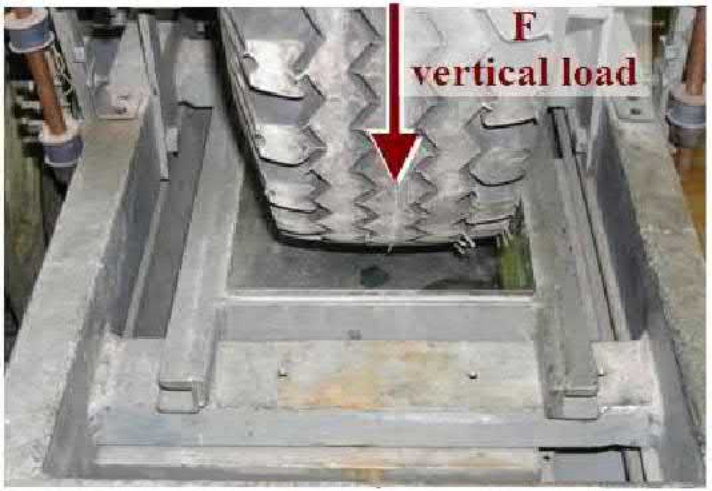

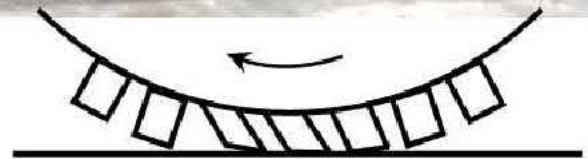

detail of contact patch

STATIC ADHESOR

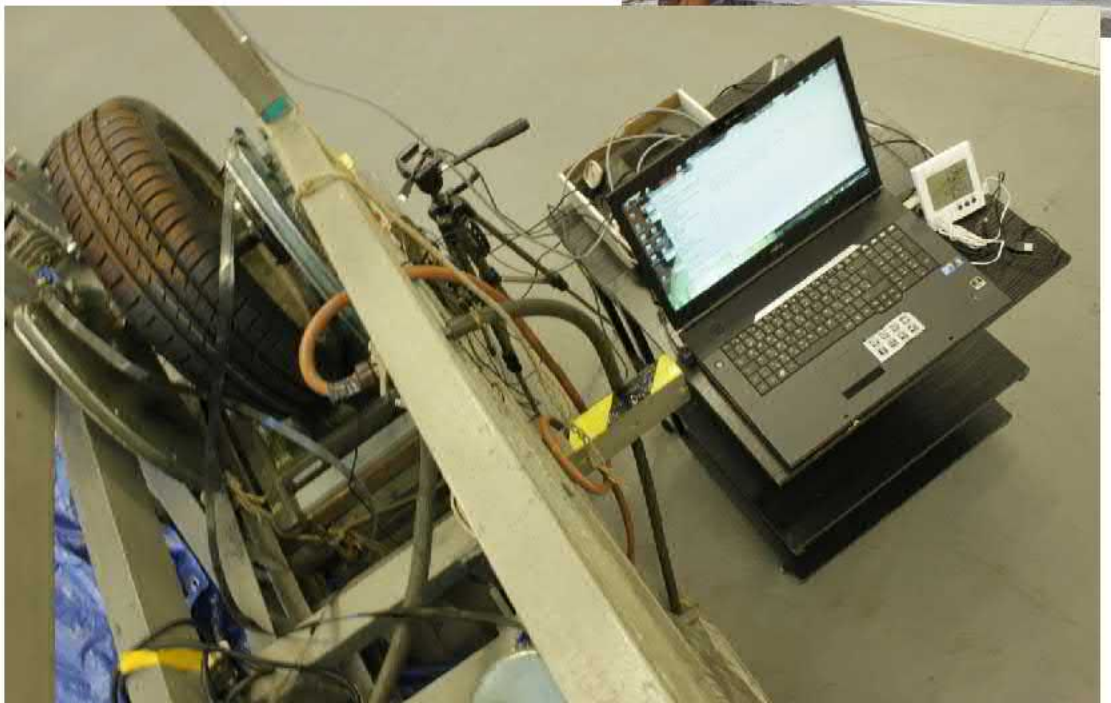

On the statical adhesor is possible to tests the tires from the radius of tire R13 to R18 and maximum width of tire-casing c. 245 mm.

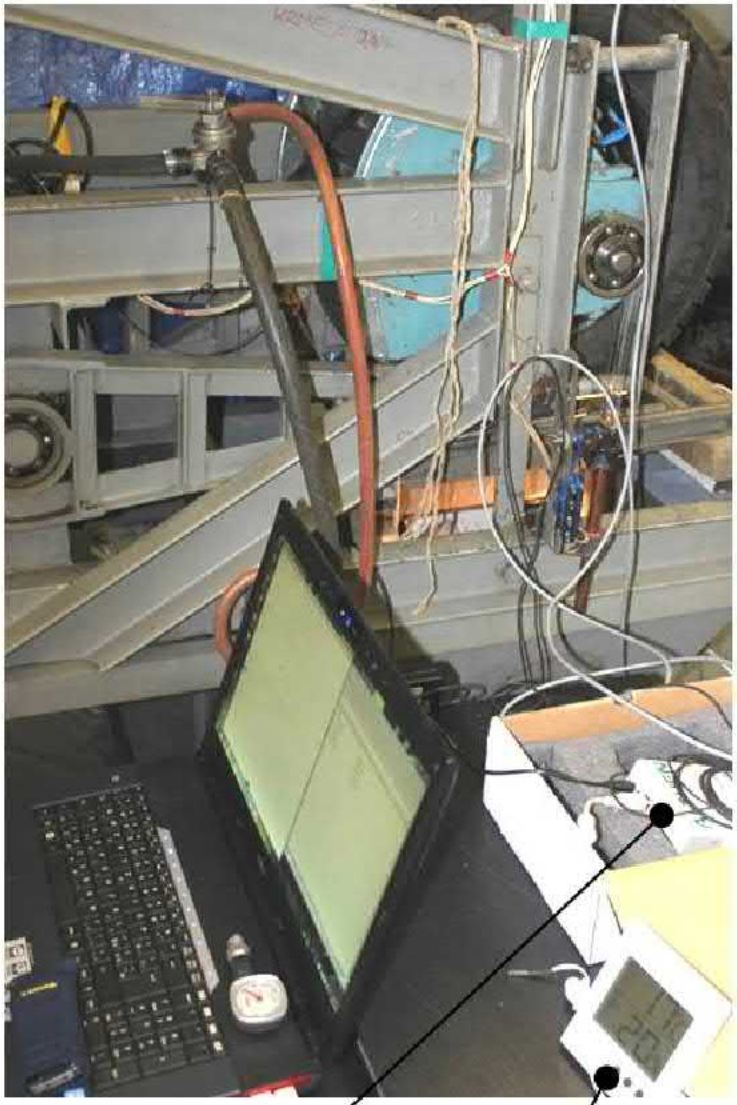

Data logger

Sensor for humidity and temperature

Force tensiometer sensors

Linear potentiometer

SENSORS ON STATIC ADHESOR FOR MEASUREMENTS:

Force:

Three force tensiometer (strain-gauge) sensors EMSYST EMS40 2.0kN

Deformation:

Linear potentiometer

and three Position inductive sensors with X-Y Recorder for orientation of force-deformation dependence

Data logger:

Data Logger System dataq DI-718B-US with three Strain Gage Input Modules DI-8B38 and one Potentiometer Input Modules DI-8B360

Software WinDaq/Lite for on-line data record on notebook.

Force accuracy: c. 100 N on 10 000 N

Position accuracy: c. 0.1 mm on 100 mm

Photo documentary by Canon EOS 600 D with objective and tripod

It is possible to obtain outputs as:

- **Statical radius** of tire;
- **Radial deformation characteristic** (dependence between radial force loading of tire and radial deformation);
- **Radial stiffness** (in radial force loading / radial deformation) in N/mm;
- **Torsion (longitudinal) deformation characteristic** (slip curve by twist moment);
- **Torsion stiffness** (in twist moment / rim angle) in Nm/° or longitudinal stiffness (in tangential force / tangential deformation) in N/mm;
- **Contact patch - footprint shape and size with contact pressure colour distribution** in contact patch by special pressure FUJIFILM Fuji Prescale® indicating film (Ultra Low film LLLW, pressure range 2-6 kg/cm^2);

  At following main conditions:
  - **Loading** (radial force, twist moment);
  - **Size of radial deformation**;
  - **Inflation pressure** (under-inflation, overinflated tire, specified and practiced pressure);
  - **Unevenness (shape, surface roughness, material)** etc.

Data on the tyre:

- ✓ radial deformation characteristics
- ✓ size and shape of contact surface
- ✓ distribution of contact pressure in contact surface

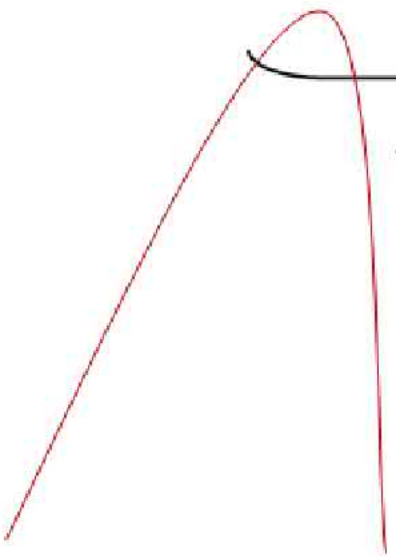

based on specified measurement conditions:

- shape of the obstacles
- loading
- inflation pressure
- size of radial deformation
- ambient temperature.

STATIC

ADHESOR

They are possible other measurements on static adhesor:

- contact pressure analyze by pressure FUJIFILM indicating film (distribution of contact pressure in contact area)
- statical torsion (longitudinal) stiffness with torsion deformation characteristic etc.

EXPERIMENTS OF TIRES ON „DYNAMIC ADHESOR“

Drum testing machine

A smooth surfaced, rotating drum with a diameter of 1705 mm is turned by an engine at the desired speed. The testing machine can simulate contact between the tire and the road with specified velocity.

The conditions relating to the use of the dynamic test machine:

- radial load of the tires up to the value of 500 kg,
- maximum speed is 180 km/h,
- test of the tires from the radius of R13 to R17 tire.

Part 3 – OUTPUT FROM EXPERIMENTS:

Load conditions of tires, Contact patch, Contact pressure, Pressure footprint analyses, Comparison winter with summer tires,

Special graphs from dynamic tests, Static test of bicycle tire

RADIAL STATIC STIFFNESS

The new formula takes into account more real operating conditions during the loading of tires.

$$S = \frac{F_{(1.25 \cdot 0.75 \cdot LI)} - F_{(0.75 \cdot 0.75 \cdot LI)}}{x_{(1.25 \cdot 0.75 \cdot LI)} - x_{(0.75 \cdot 0.75 \cdot LI)}} \text{ [N/mm]}$$

Where: S [N/mm] – radial stiffness;

$F_{(1.25.0.75.LI)}$ [N] – vertical force for 125% of 0.75·maximum load;

$F_{(0.75.0.75.LI)}$ [N] – vertical force for 75% of 0.75·maximum load;

$x_{(1.25.0.75.LI)}$ [mm] – radial deformation for 125% of 0.75·maximum load ($F_{(1.25.0.75.LI)}$);

$x_{(0.75.0.75.LI)}$ [mm] – radial deformation for 75% of 0.75·maximum load ($F_{(0.75.0.75.LI)}$).

Tires are loading approximately 75% of LI.

RADIAL STATIC STIFFNESS

The **FINAL equation** for calculation of the values of radial stiffness from the experimental data was designed, which corresponds to operating conditions. The two points corresponding to 60 % and 100 % of LI (it is 0.8 multiple of load by the standard ČSN 63 1511) are used for obtain of stiffness by equation (1):

$$S = \frac{F_{(0.8\cdot 125)} - F_{(0.8\cdot 75)}}{x_{(0.8\cdot 125)} - x_{(0.8\cdot 75)}} = \frac{F_{100} - F_{60}}{x_{100} - x_{60}}$$

where

S [N/mm] = radial stiffness for the given inflation pressure,

F_{100} [N] = vertical force for 100 % of LI,

F_{60} [N] = vertical force for 60 % of LI,

x_{100} [mm] = radial deformation for 100 % of LI,

x_{60} [mm] = radial deformation for 60 % of LI.

Sample of radial deformation characteristic

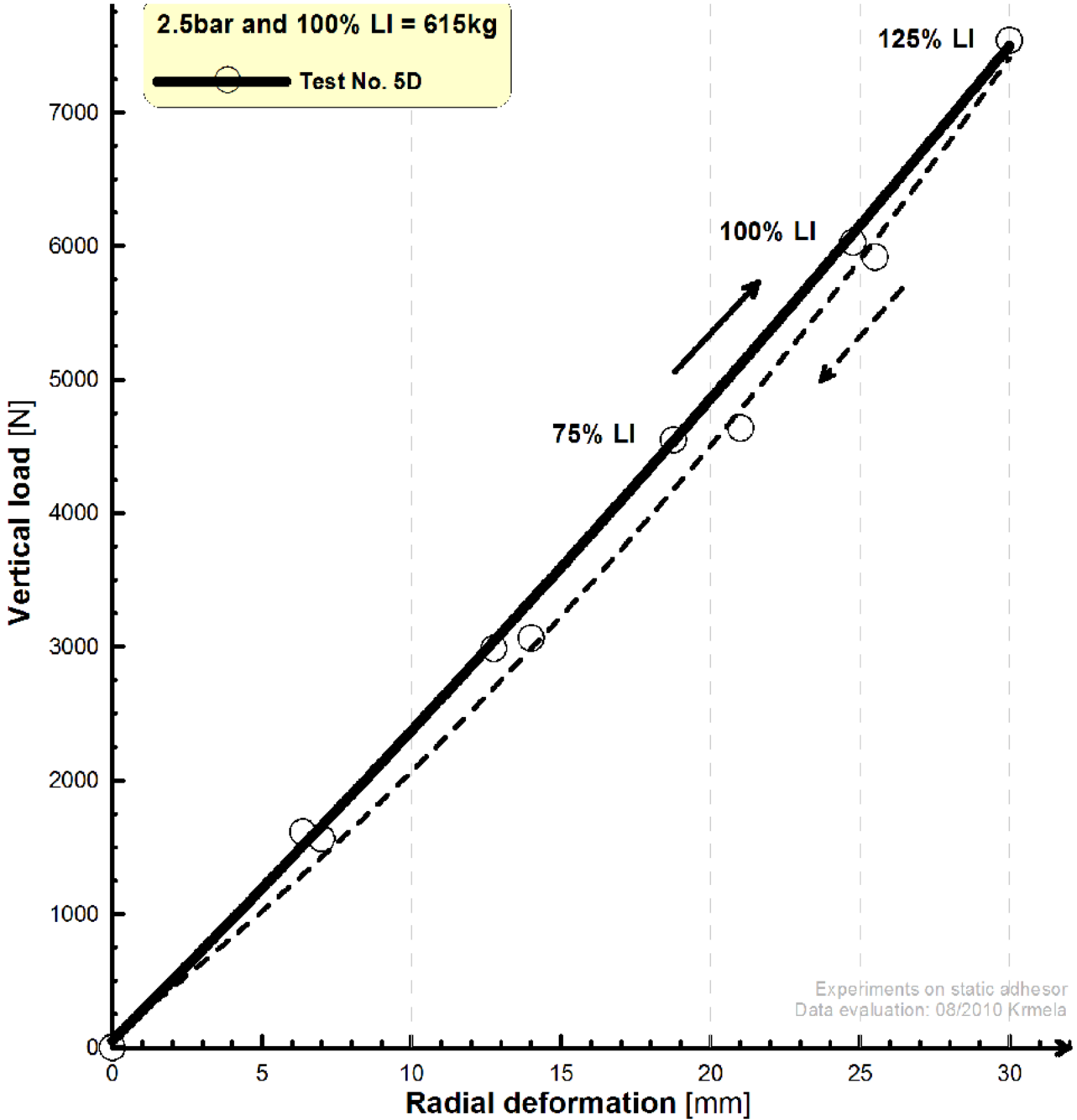

Light truck tire

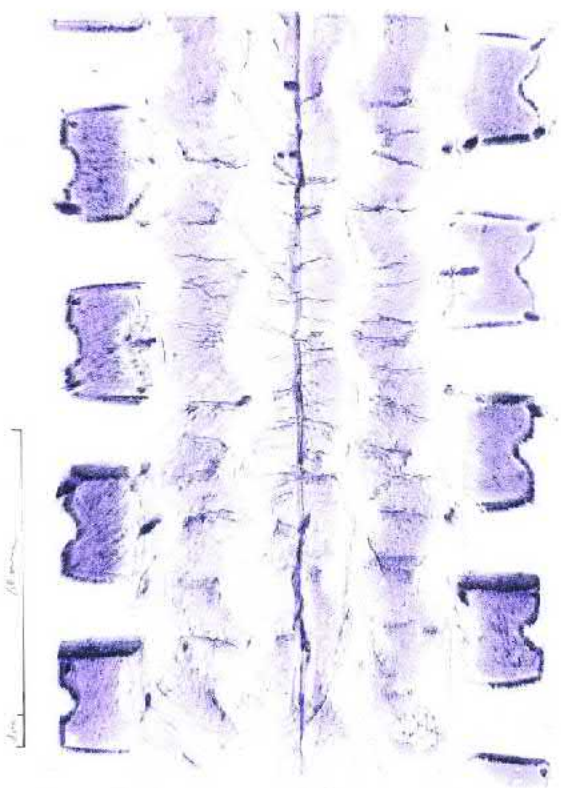

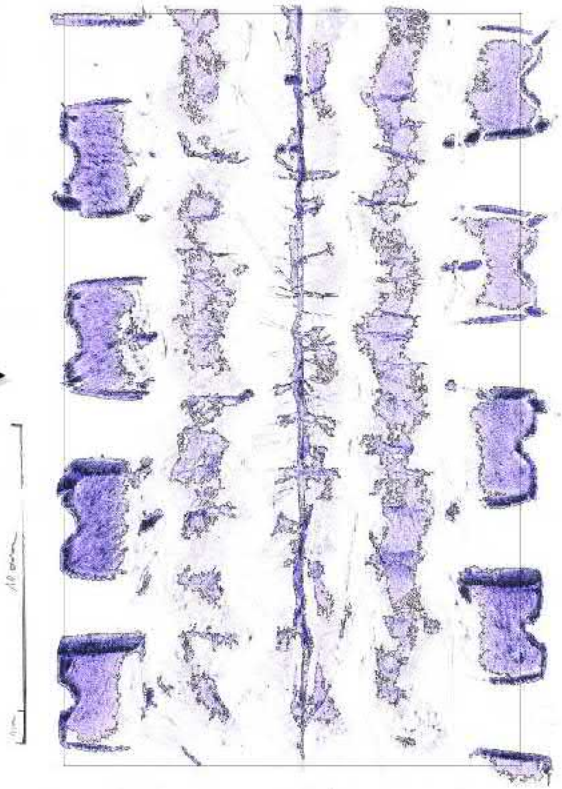

Sample of contact area analyses:
Area size 97,7 cm^2
Area in per cent from rectangle 37%

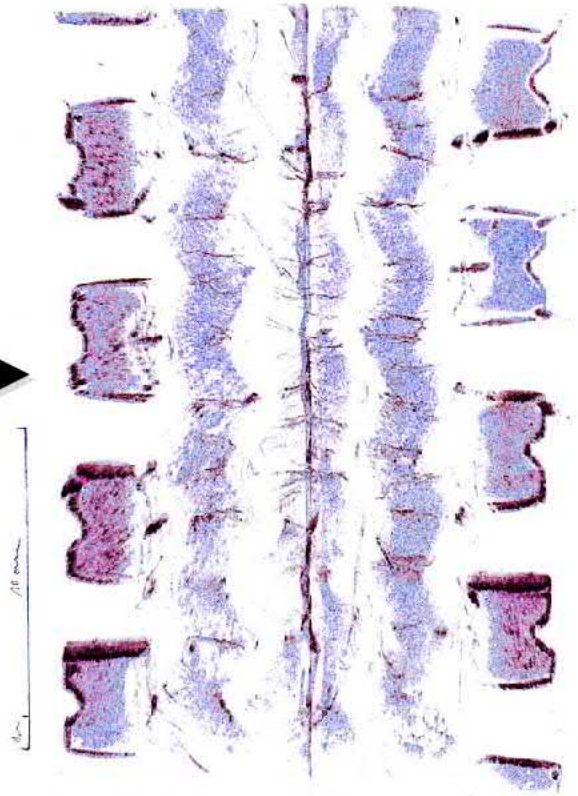

Sample of contact pressure analyses:
Gradation of colours
Red = maximum
(green, yellow)
Blue = minimum

Non pressurex film
only **blue carbon paper**

The software FPD-8010E by FUJIFILM (Fujifilm Pressure Distribution Mapping System for Prescale) for contact pressure analyses by FUJI Prescale® indicating film

Software 4000 Eur (film patch ⇒ scan ⇒ analyses).

Film only 300 Eur.

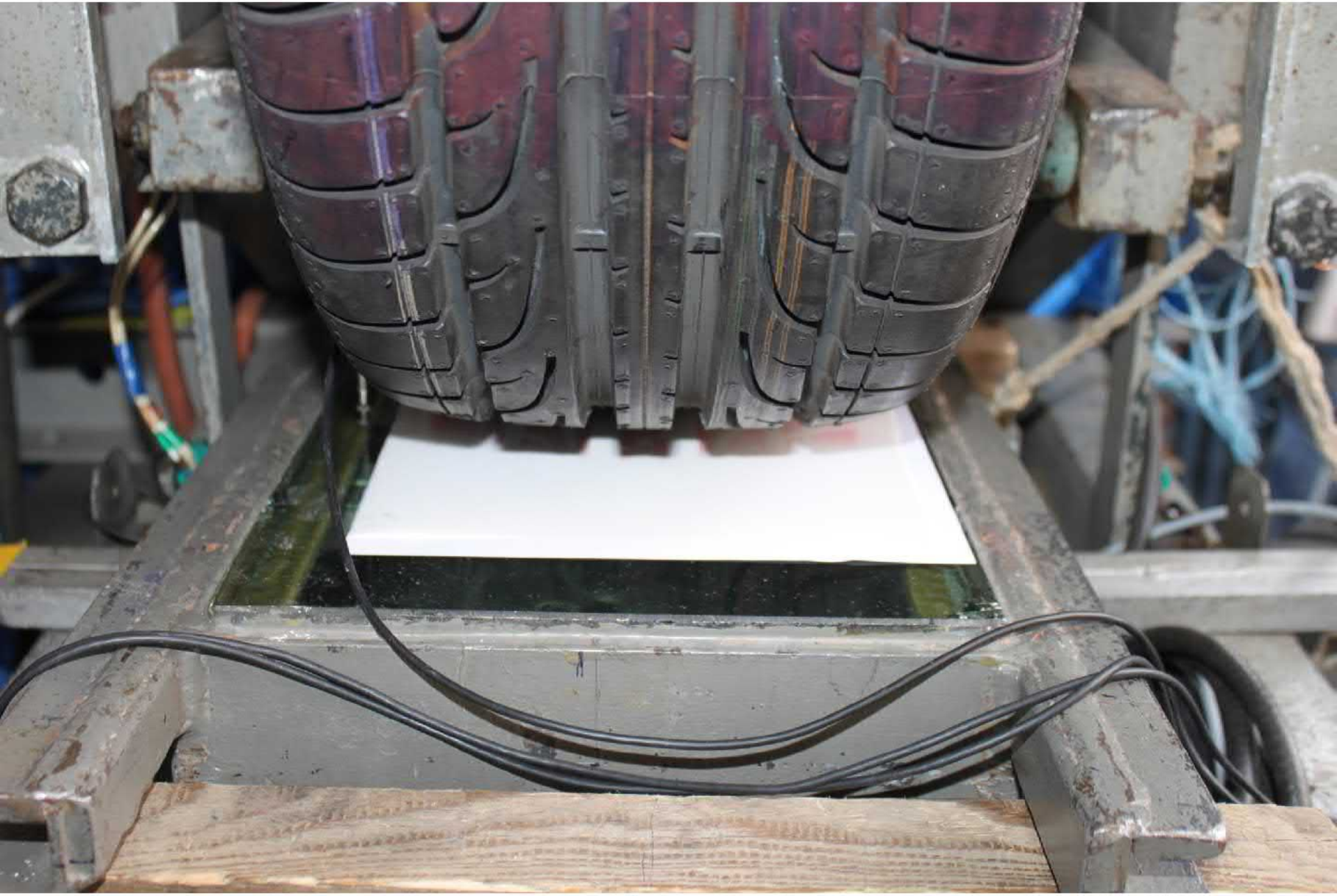

Sample: winter tire 165 R13 (= 165 / 82 R13)

Deformation of tire-casing of winter tire for 2.3 bar and load 530 kg

Extended pressure measurements - With extended pressure method, applied pressure is increased gradually up to the given level, and it will be maintained continuosly at that level. In order to get the best and accurate results (and where it is possible and applicable), prefereably pressure should be applied gradually up to its highest value by a 2 minutes time basis, and it should be maintained at the highest level for other 2 minutes.

Momentary pressure measurements - If necessary *Prescale Film* could be also used for impact pressure measurements, with application time depending from application itself. When possible (and where applicable) prefereably pressure should be applied gradually up to its highest magnitudo by a 5 seconds time basis, and it should be maintained at the highest level for other 5 seconds.

Determining the pressure level and distribution

As explained, with pressure applied, *Prescale Film* turn into a several level of magenta color, whose intensity (density), is directly proportional

The Ultra Low Film Fuji Prescale® with exposure time 2 minutes and 30 seconds wa

standard used for contact patch with contact pressure distribution.

1. Film type used (PSI of kg/cm^2): 28-85 PSI (2-6 kg/cm^2)

Ultra Low Film from roll

2. Approximate exposure time: 2 minutes and 30 seconds

3. Approximate temperature: c. 16°C

4. Approximate humidity: c. ≤ 20%

5. Experiment date:

6. Radial force loading 530 kg;
Tire inflating pressure 2.3 bar (c. 33.4 PSI).

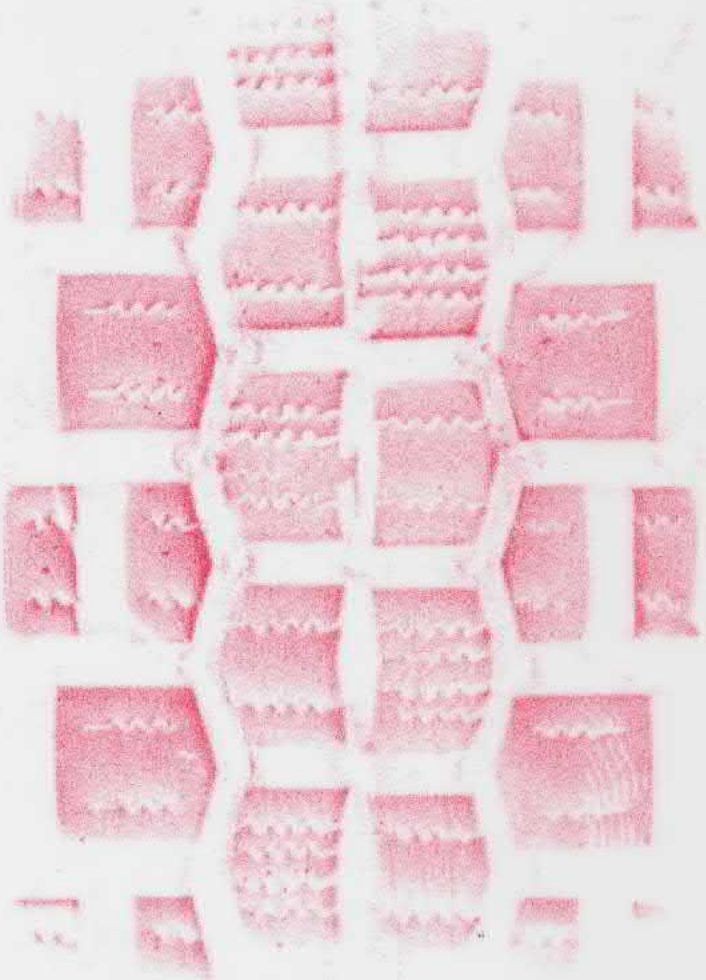

VRANIK, 2,3bar, 100%LI = 475kg
11.5.2011 23°C, 37%, 2min

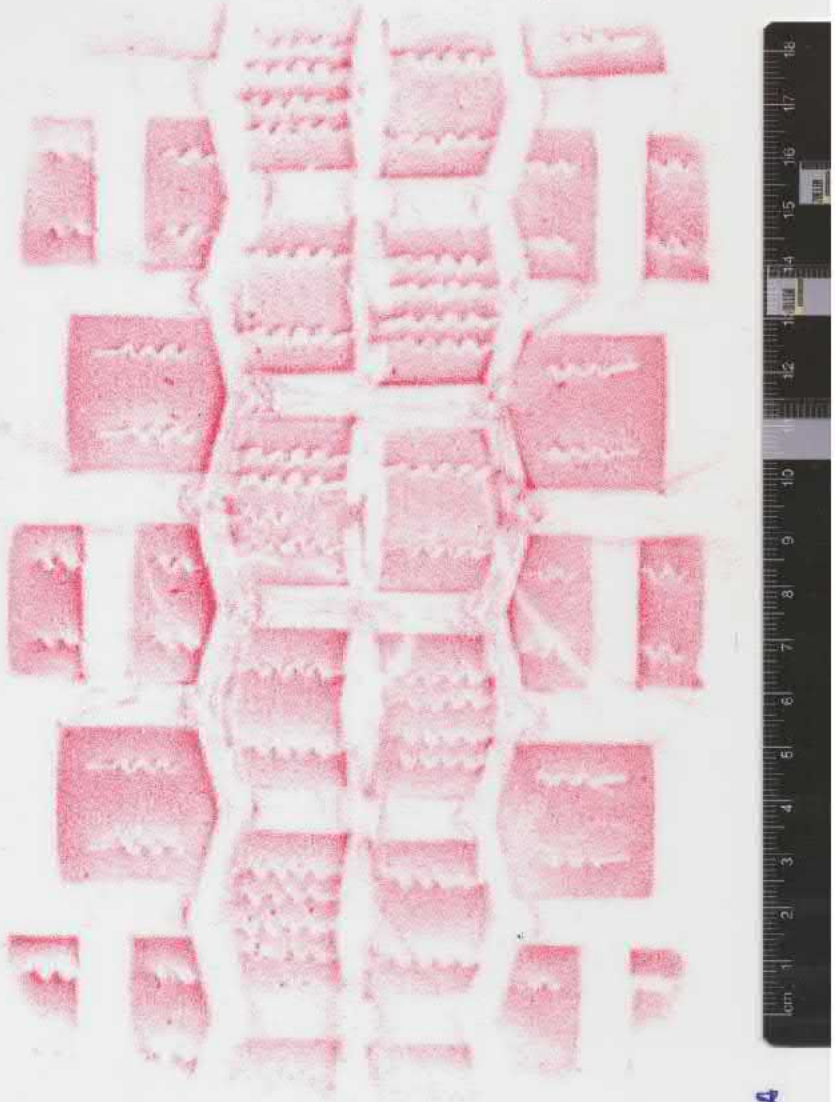

VRANIK, 1.8bar, 100%LI = 475kg
11.5.2011, 23°C, 37%, 2min

4 KRMELA

PRESSURE FOOTPRINT ANALYSES

The contact patch and contact pressure by FUJI film

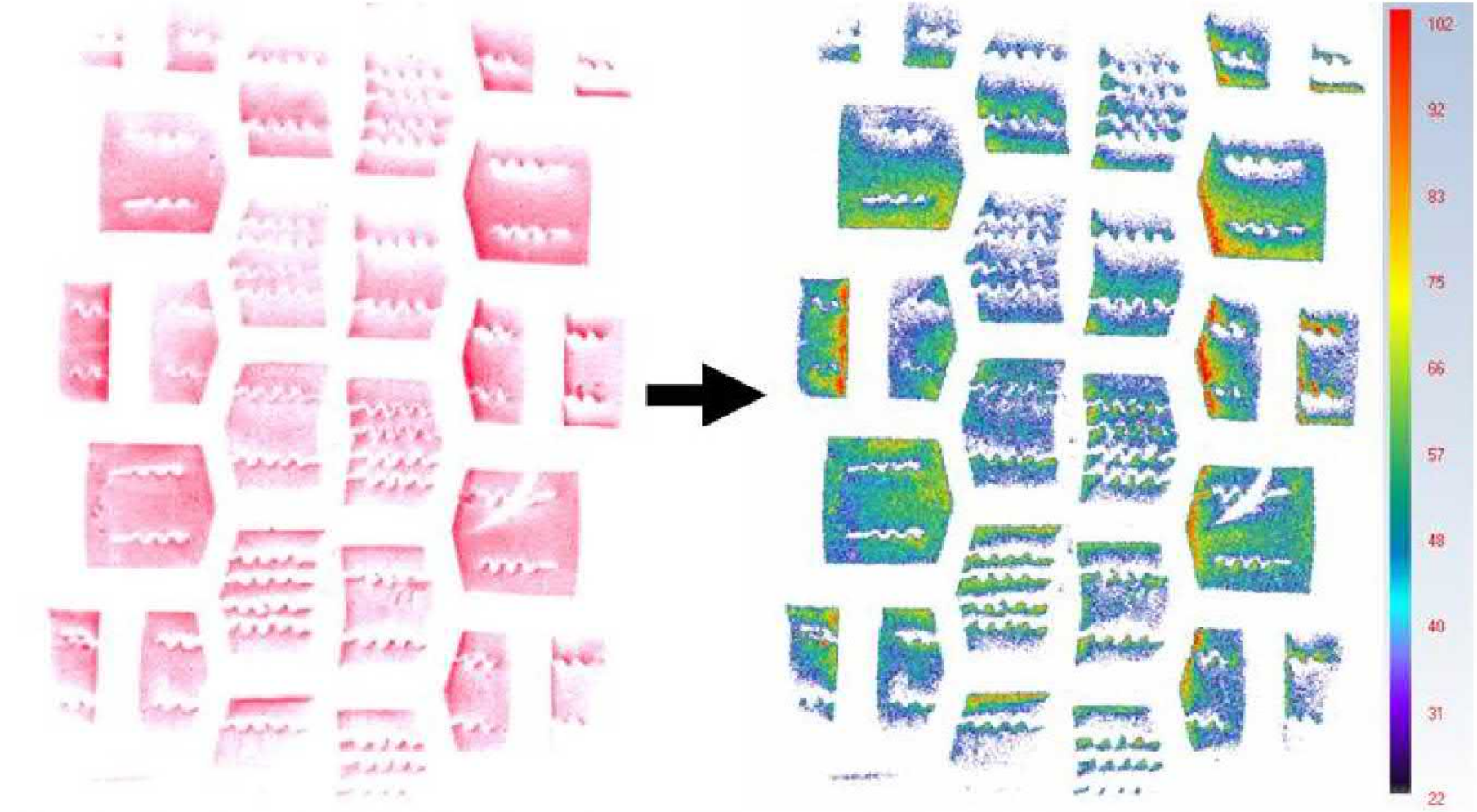

Contact patch after measurement (left) and color "map" of contact pressure distribution after special analysis with color indicates precise PSI value (right)

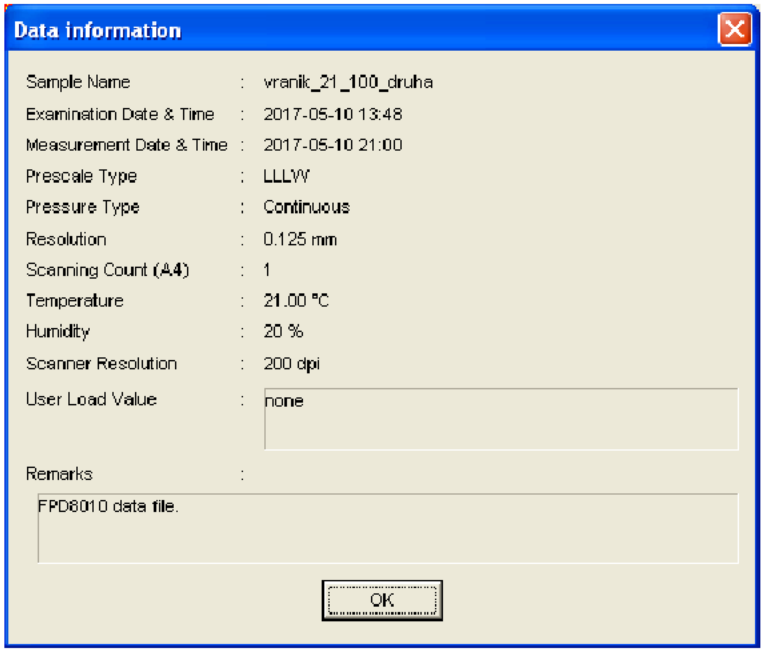
Data information
Sample Name : vranik_21_100_druha
Examination Date & Time : 2017-05-10 13:48
Measurement Date & Time : 2017-05-10 21:00
Prescale Type : LLLW
Pressure Type : Continuous
Resolution : 0.125 mm
Scanning Count (A4) : 1
Temperature : 21.00 °C
Humidity : 20 %
Scanner Resolution : 200 dpi
User Load Value : none
Remarks :
FPD8010 data file.
OK

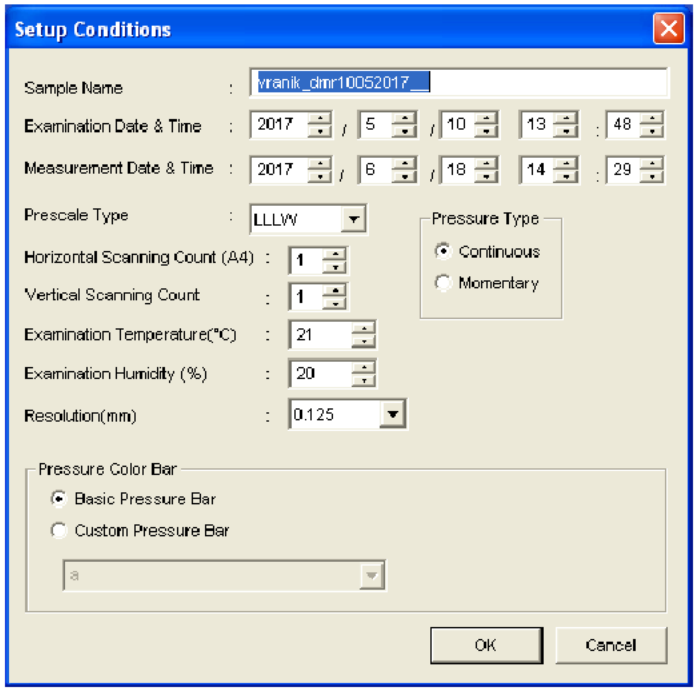
Setup Conditions
Sample Name : vranik_dmr10052017
Examination Date & Time : 2017 / 5 / 10 13 : 48
Measurement Date & Time : 2017 / 6 / 18 14 : 29
Prescale Type : LLLW
Horizontal Scanning Count (A4) : 1
Vertical Scanning Count : 1
Examination Temperature(°C) : 21
Examination Humidity (%) : 20
Resolution(mm) : 0.125
Pressure Type
Continuous
Momentary
Pressure Color Bar
Basic Pressure Bar
Custom Pressure Bar
OK
Cancel

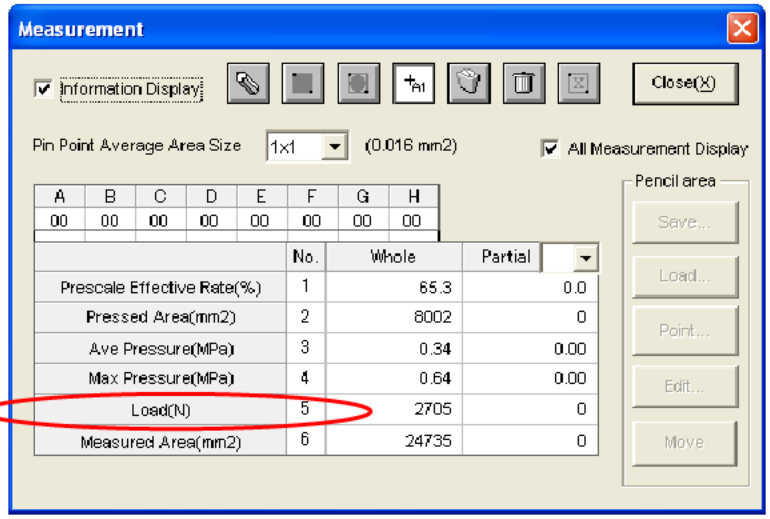
Measurement
Information Display
Close(X)
Pin Point Average Area Size 1x1 (0.016 mm2)
All Measurement Display
Pencil area
Save...
Load...
Point...
Edit...
Move
A B C D E F G H
00 00 00 00 00 00 00 00
No. Whole Partial
Prescale Effective Rate(%) 1 65.3 0.0
Pressed Area(mm2) 2 8002 0
Ave Pressure(MPa) 3 0.34 0.00
Max Pressure(MPa) 4 0.64 0.00
Load(N) 5 2705 0
Measured Area(mm2) 6 24735 0

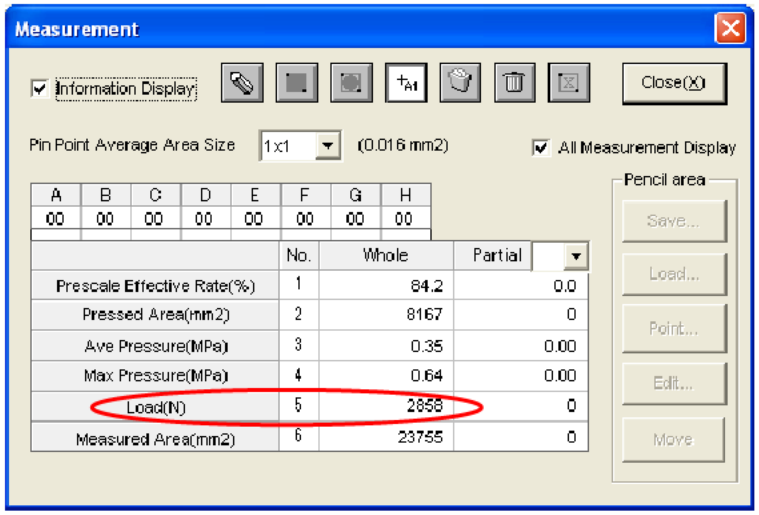
Measurement
Information Display
Close(X)
Pin Point Average Area Size 1x1 (0.016 mm2)
All Measurement Display
Pencil area
Save...
Load...
Point...
Edit...
Move
A B C D E F G H
00 00 00 00 00 00 00 00
No. Whole Partial
Prescale Effective Rate(%) 1 84.2 0.0
Pressed Area(mm2) 2 8167 0
Ave Pressure(MPa) 3 0.35 0.00
Max Pressure(MPa) 4 0.64 0.00
Load(N) 5 2858 0
Measured Area(mm2) 6 23755 0

THE RADIAL DEFORMATION CHARACTERISTICS

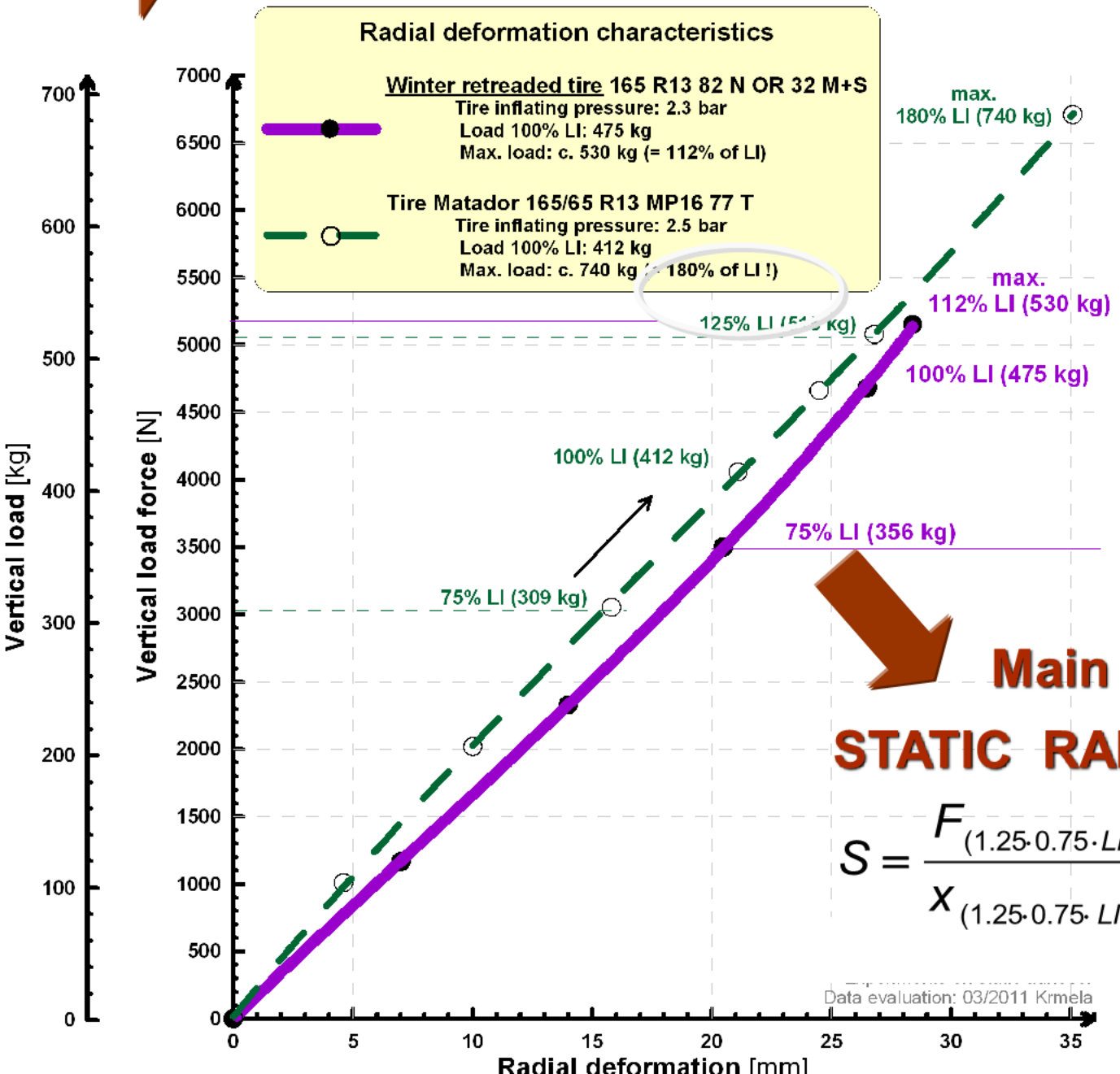

Main output:

STATIC RADIAL STIFFNESS

$$S = \frac{F_{(1.25 \cdot 0.75 \cdot LI)} - F_{(0.75 \cdot 0.75 \cdot LI)}}{x_{(1.25 \cdot 0.75 \cdot LI)} - x_{(0.75 \cdot 0.75 \cdot LI)}} \text{ [N/mm]}$$

190.5 N/mm

0% loading

25% loading

50% loading

75% loading

100% loading = 475 kg

125% loading

150% loading

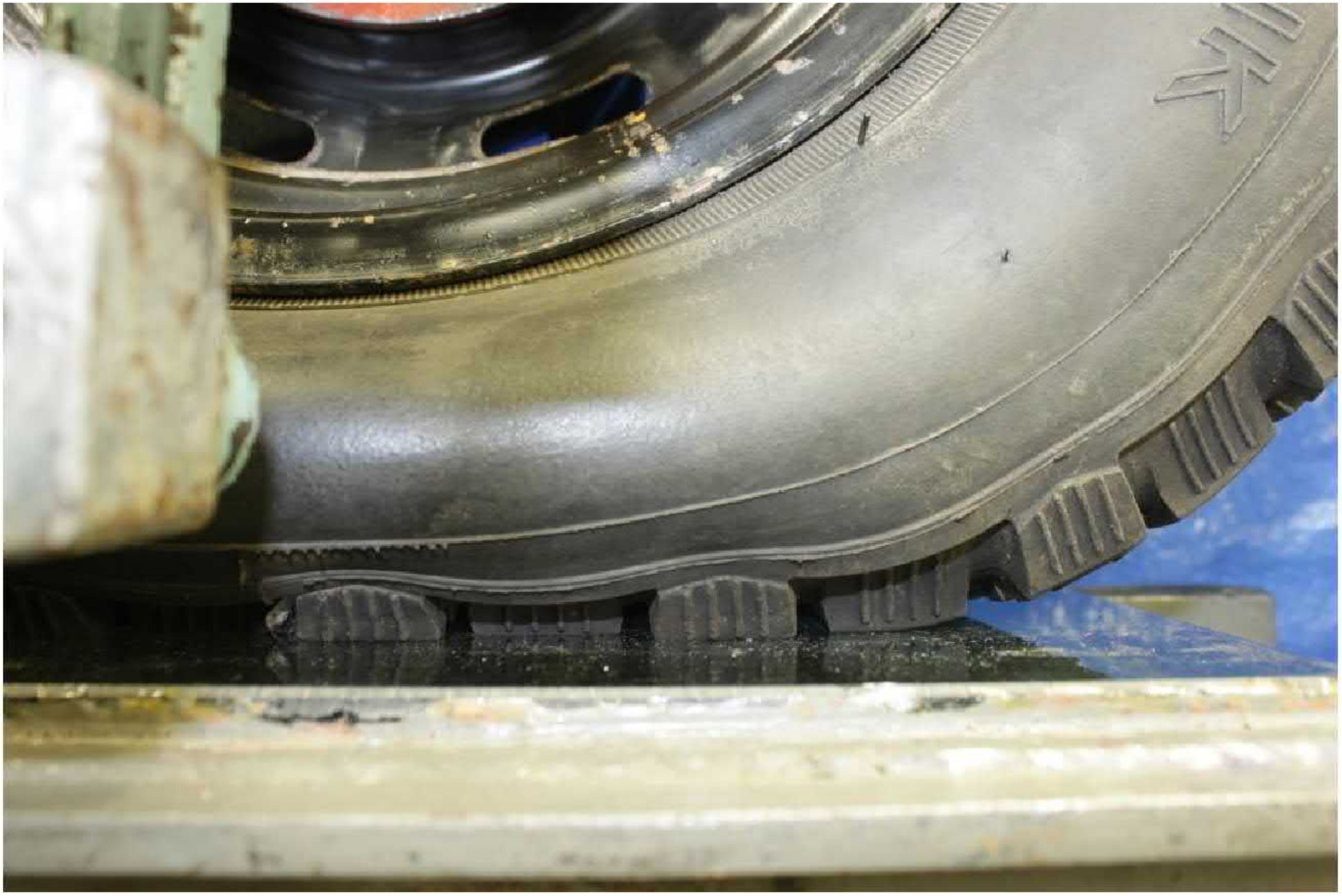

170% loading = cca 810 kg !!!! = very overloaded tire

Tire Matador 165 / 65 R13

2.1 bar and radial force 412 kg equal 100% load

0%

25% (103 kg)

50% (206 kg)

75% (309 kg)

100% (412 kg)

125% (515 kg)

Output data / Inflation pressure	1.8 bar	2.5 bar
Radial deformation for 100% LI = 412 kg [mm]	27.0	22.5
Value of radial stiffness [N/mm]	153	185
Size of contact patch [mm^2]	11 820	10 125

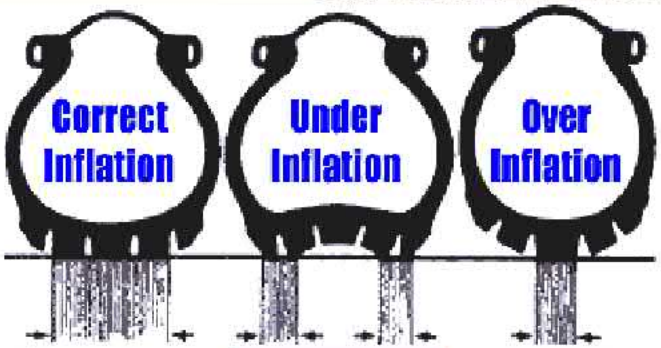

250 kPa

180 kPa

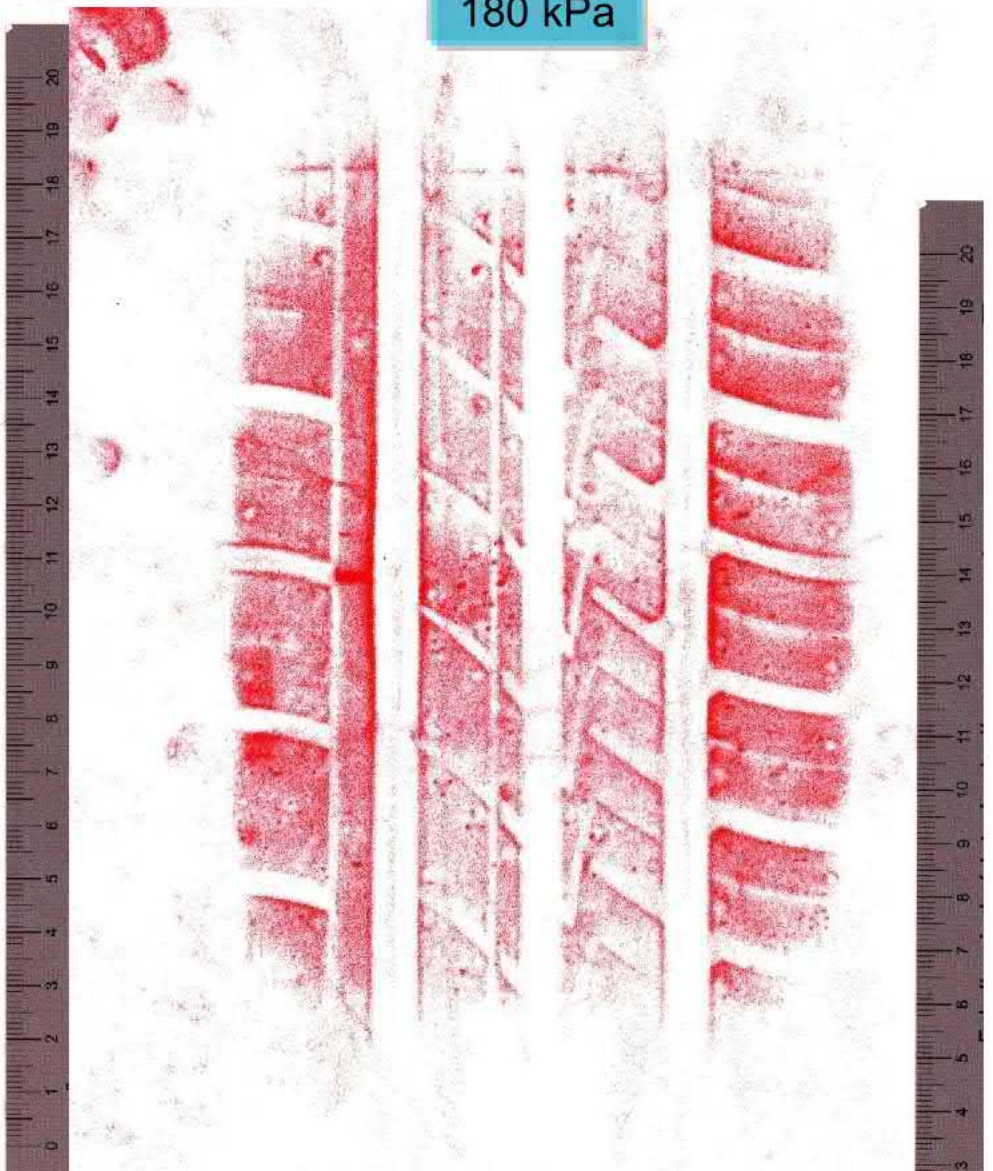

The contact patch and contact pressure by FUJI film

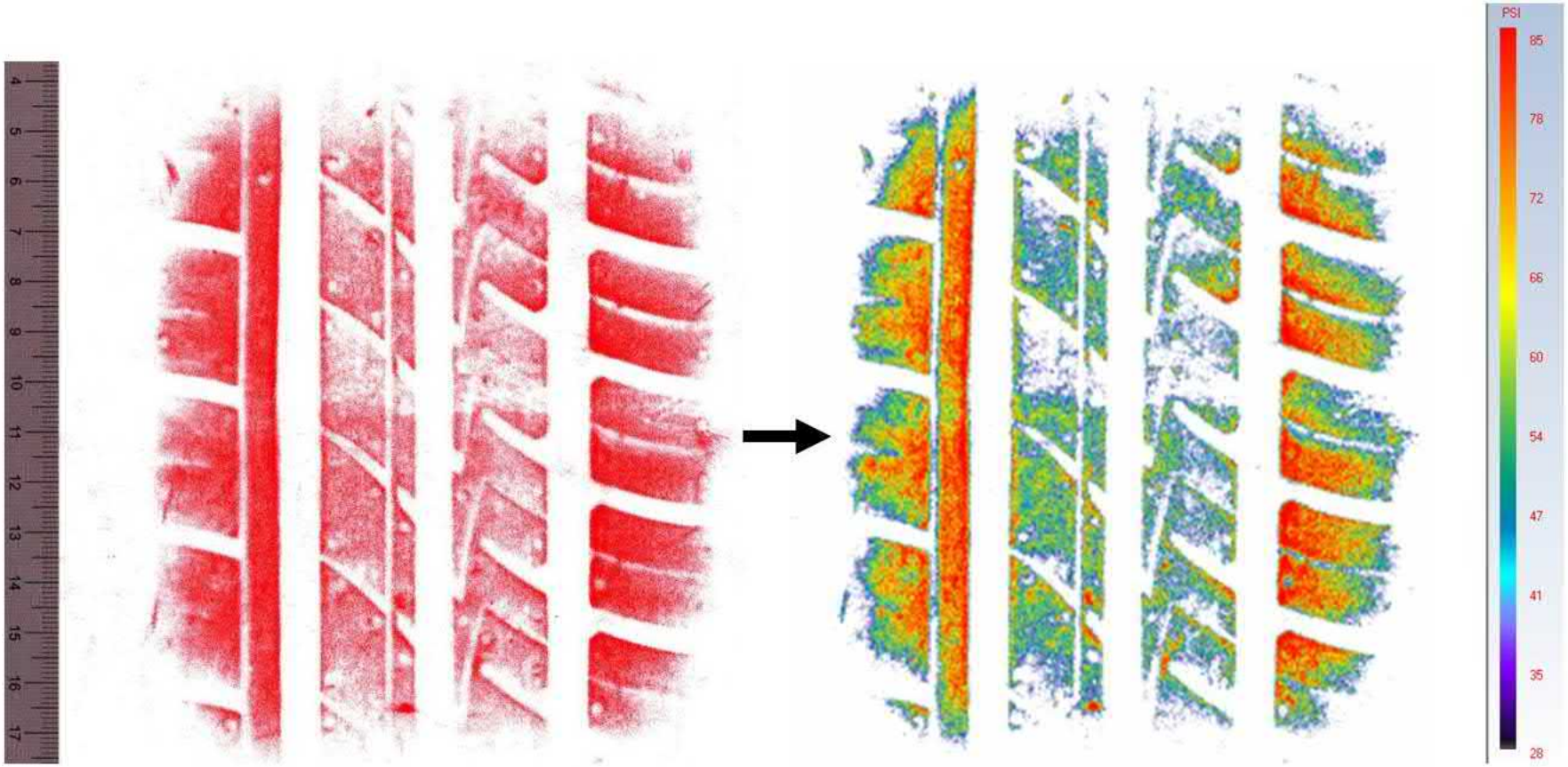

Contact patch after measurement for 2.5 bar (left) and colour "map" of contact pressure distribution after special analyse with colour indicates precise PSI value (right)

Experiments of tire 245/40 R18 on test machine. EXTRA LOAD !!!!!!

The tire has maximum tire pressure 3.5 bar and maximum load 730 kg (signs on tire-casing). But tire is necessary inflation pressure for concrete car e.g. requirement is 2.6 bar which is only c. 75% of maxima tire pressure. The maximum load is not 730 kg for this pressure but only 670 kg as load index (LI marking) by technical databook. Next e.g. for 2.9 bar maximum load is 730 kg. History of deformation process of tire near contact patch during loading for inner pressure 2.6 bar is on the Fig.

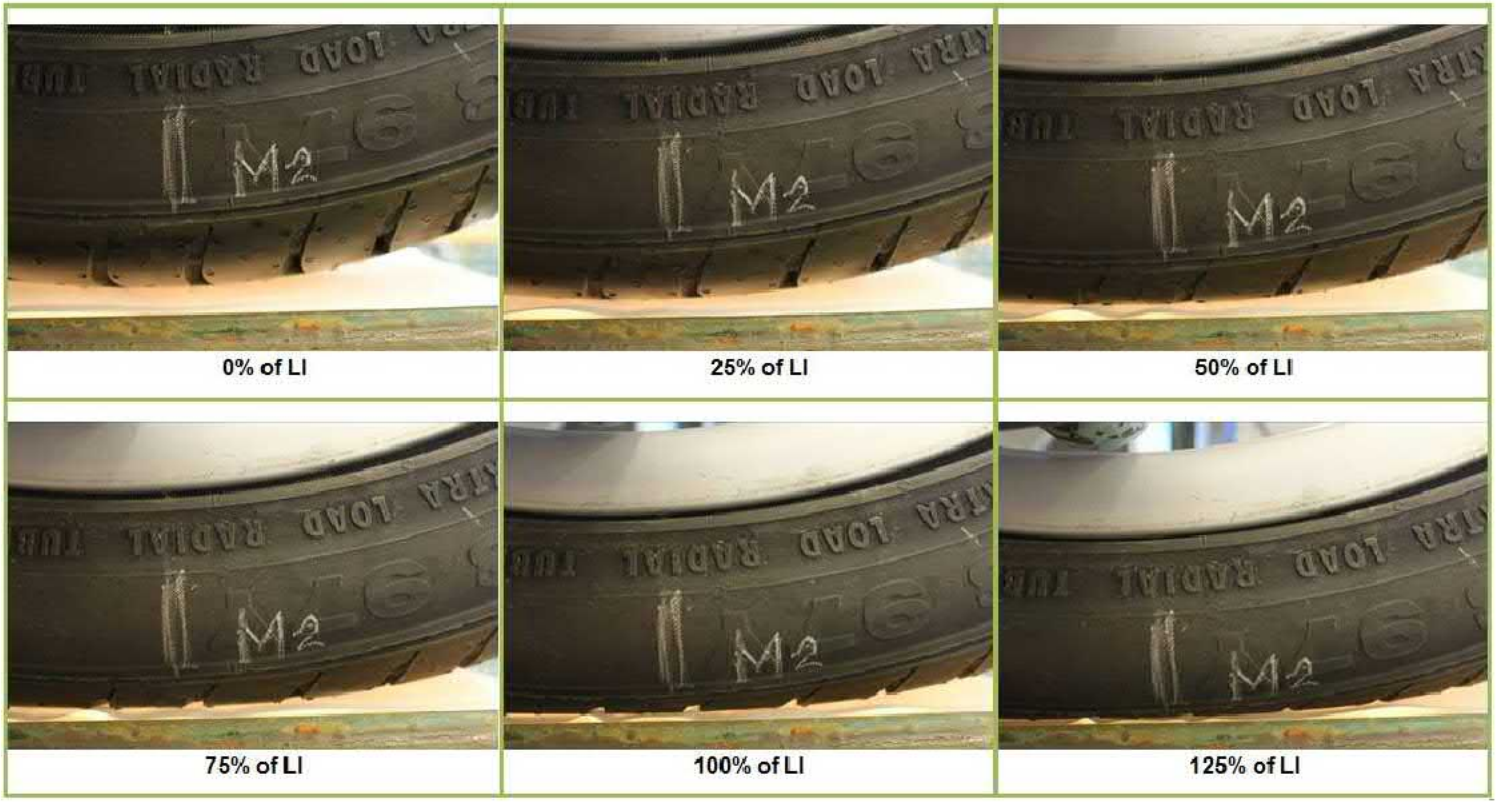

125% of LI	100% of LI
Load: 836 kg Radial deformation: 28.3 mm Tire pressure: 2.6 bar Contact area: c. 17950 mm^2	Load: 673 kg Radial deformation: 22.6 mm Tire pressure: 2.6 bar Contact area: c. 14800-15800 mm^2
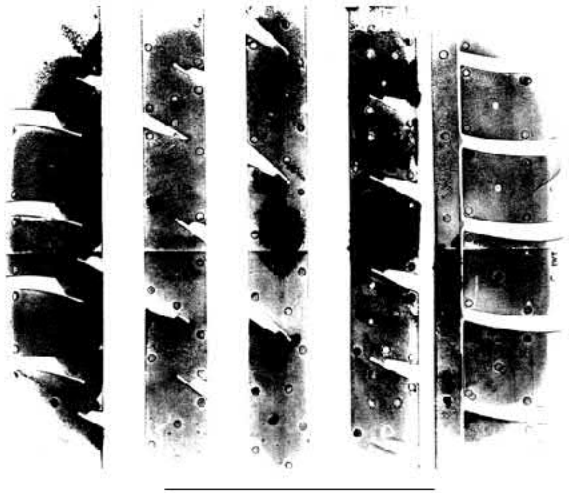 100 mm	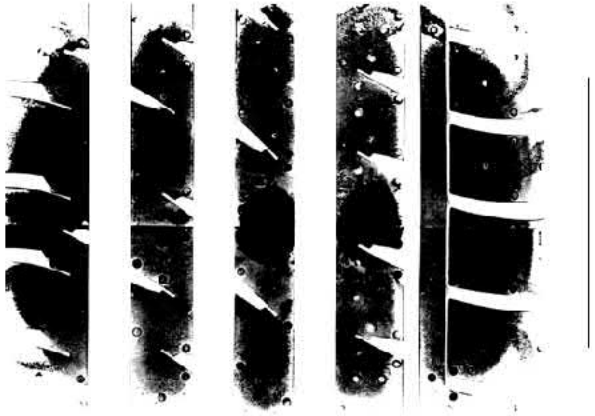 100 mm

The radial stiffness by Eq. (standard) is 280 N/mm and by Eq. (new) is 270 N/mm that is better for description of real state of tire loading.

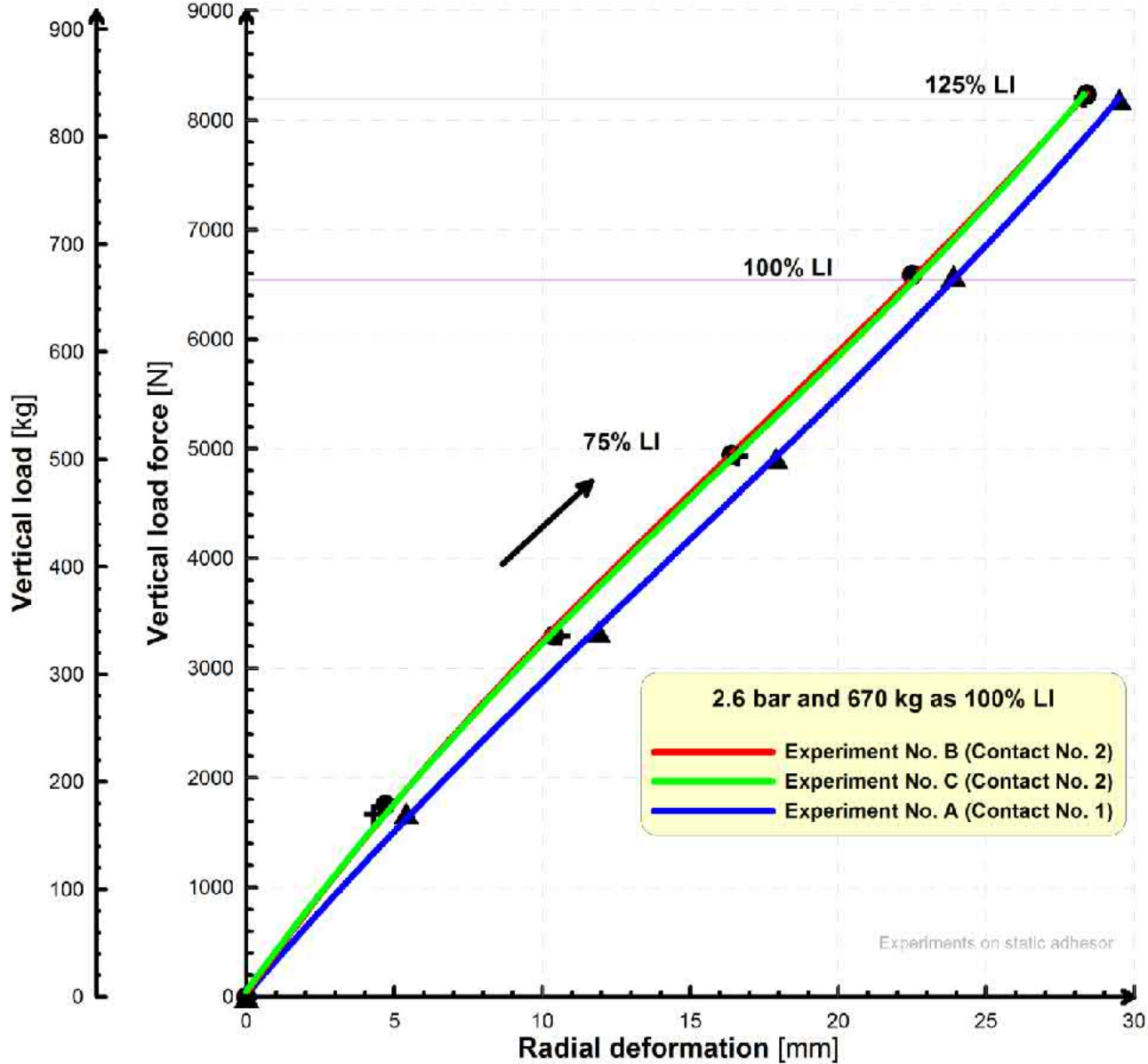

Continental 225/50 R17

Matador 165/70 R13

Bridgestone 205/55 R16

comparison

Character of deformation

Deformation of the tire-casing 165/70 R13 in contact with the surface plate was recorded during the experiment.
The deformation of tire-casing for 100% of LI is c. 21.5 mm.

Deformation of the tire-casing 205/55 R16 for 100% of LI is 26.5 mm.

The tire 225/50 R17 has deformation equal c. 25.0 mm for 100% of LI.

Deformation of the tire casing 205/55 R16

0% of LI

75% of LI

100% of LI

125% of LI

Deformation of the tire casing 225/50 R17

0% of LI

75% of LI

100% of LI

125% of LI

0 % of LI
Start of experiment

75 % of LI
Deformation is 16.4 mm

100 % of LI
Deformation is 22.5 mm

125 % of LI
Deformation is 27.5 mm

165 / 65 R13 Deformations of the tire-casing for 240 kPa by static experiment

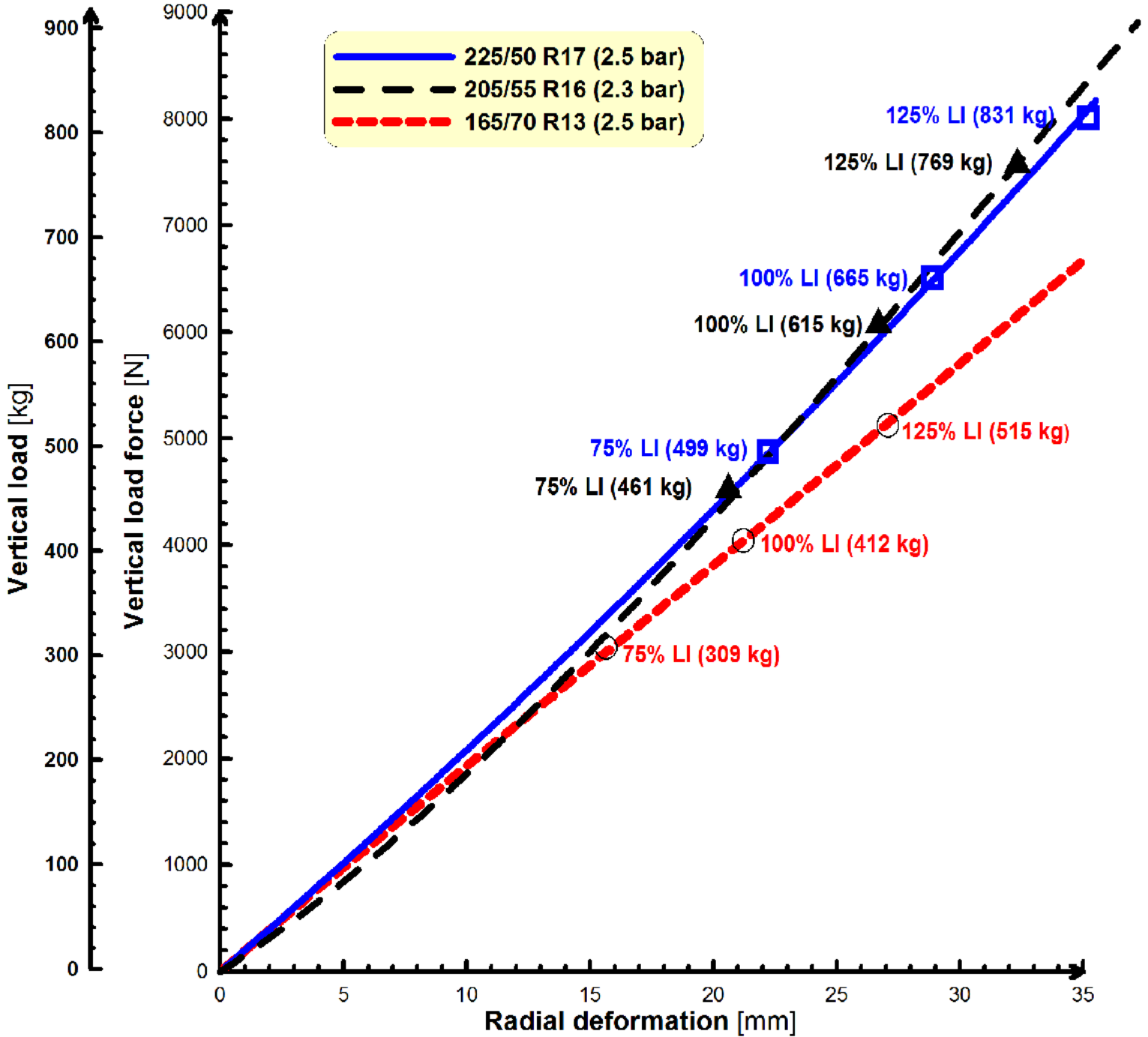
225/50 R17 (2.5 bar)
205/55 R16 (2.3 bar)
165/70 R13 (2.5 bar)
125% LI (831 kg)
125% LI (769 kg)
100% LI (665 kg)
100% LI (615 kg)
75% LI (499 kg)
75% LI (461 kg)
125% LI (515 kg)
100% LI (412 kg)
75% LI (309 kg)
Vertical load [kg]
Vertical load force [N]
Radial deformation [mm]
0
100
200
300
400
500
600
700
800
900
1000
2000
3000
4000
5000
6000
7000
8000
9000
5
10
15
20
25
30
35

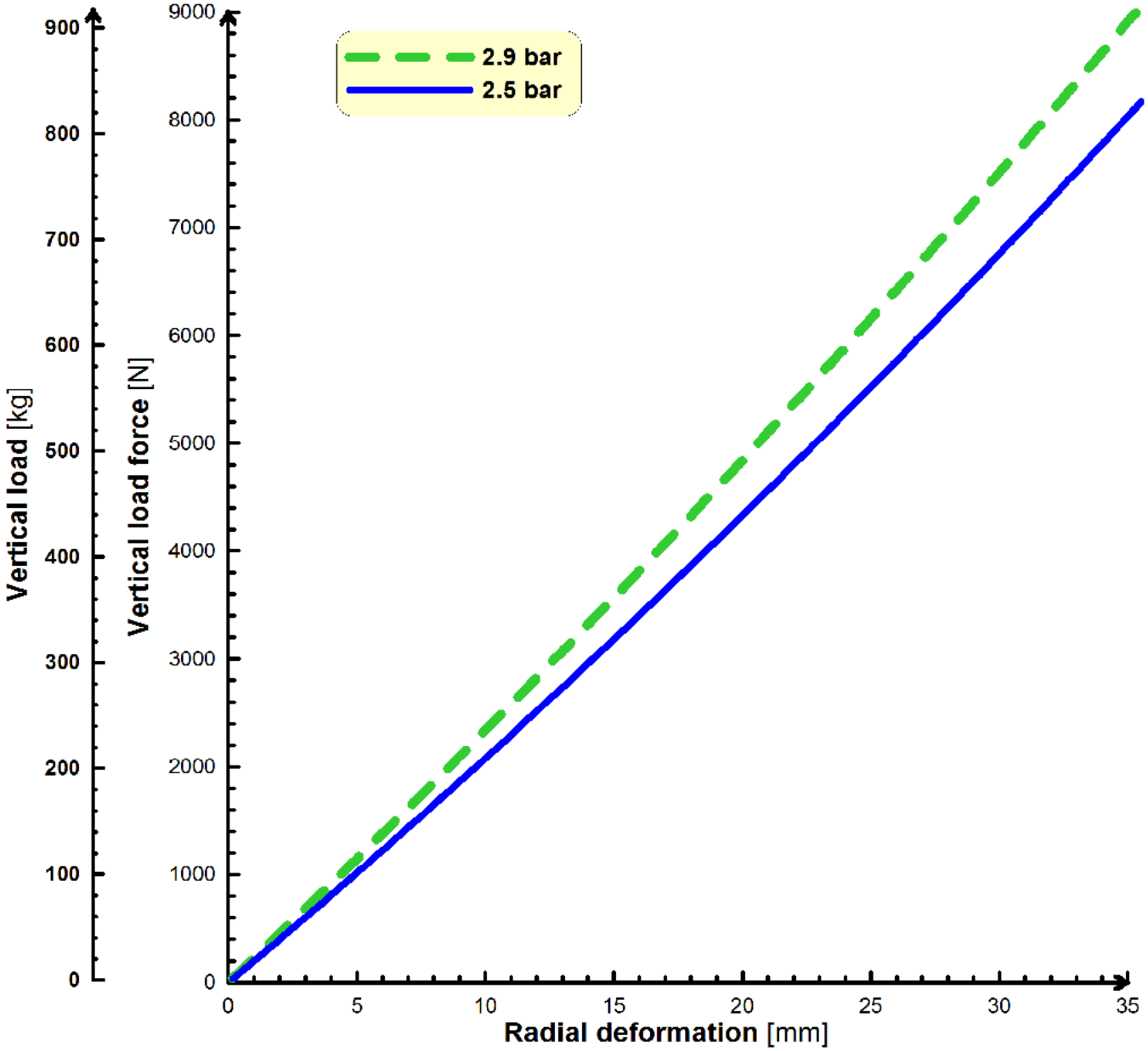

Radial deformation characteristics of 225/50 R17 for different pressures

The radial stiffness of tire 165/70 R13 is c. 185 N/mm.
The value of the stiffness for tire 205/55 R16 is 251 N/mm.
The tire 225/50 R17 has stiffness c. 240 N/mm.

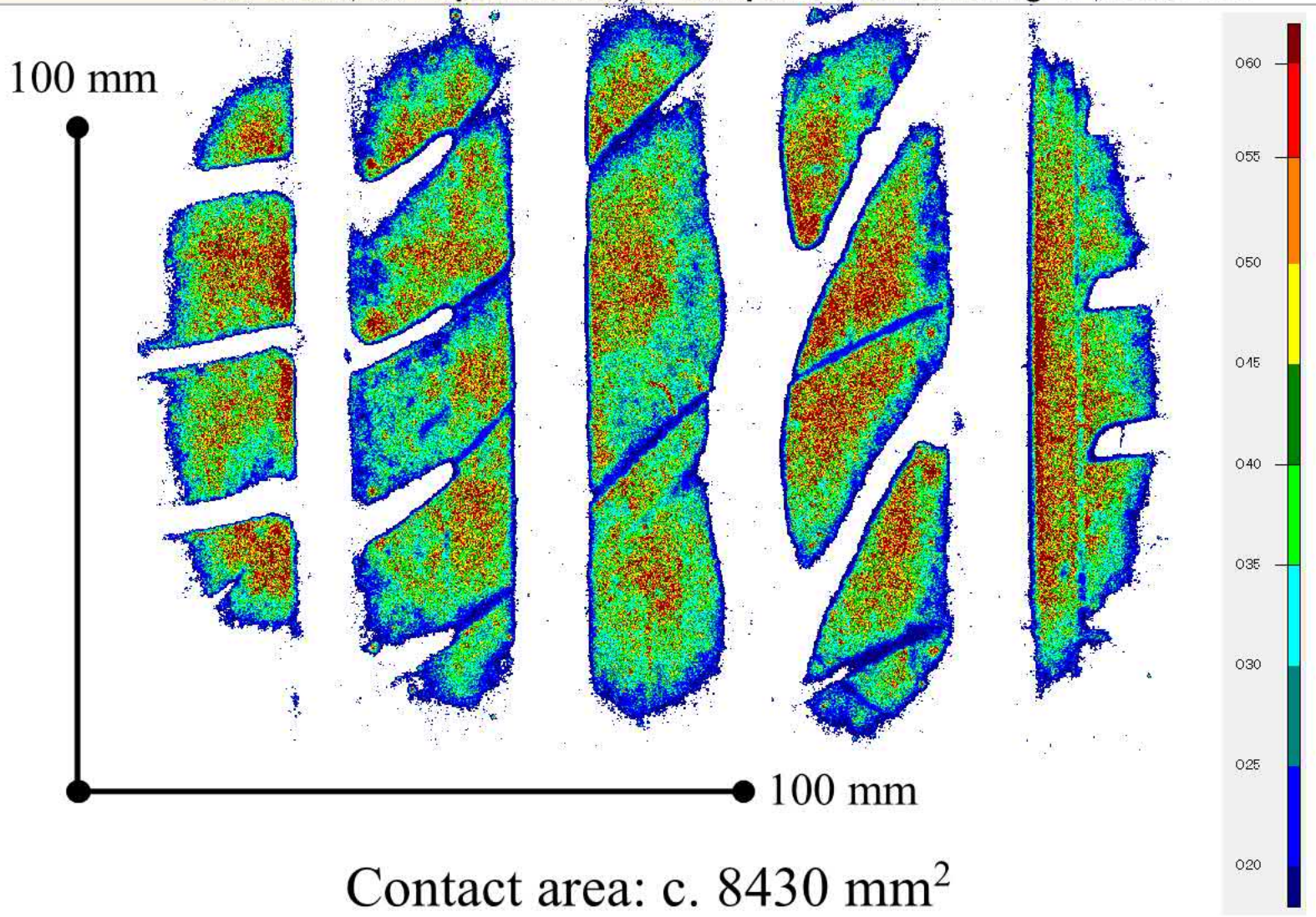

Contact area: c. 8430 mm^2

Contact pressure [kPa]

Contact patch with distribution of contact pressure by indicating film analysis for tire 205/55 R16 for 50% of LI and 2.3 bar

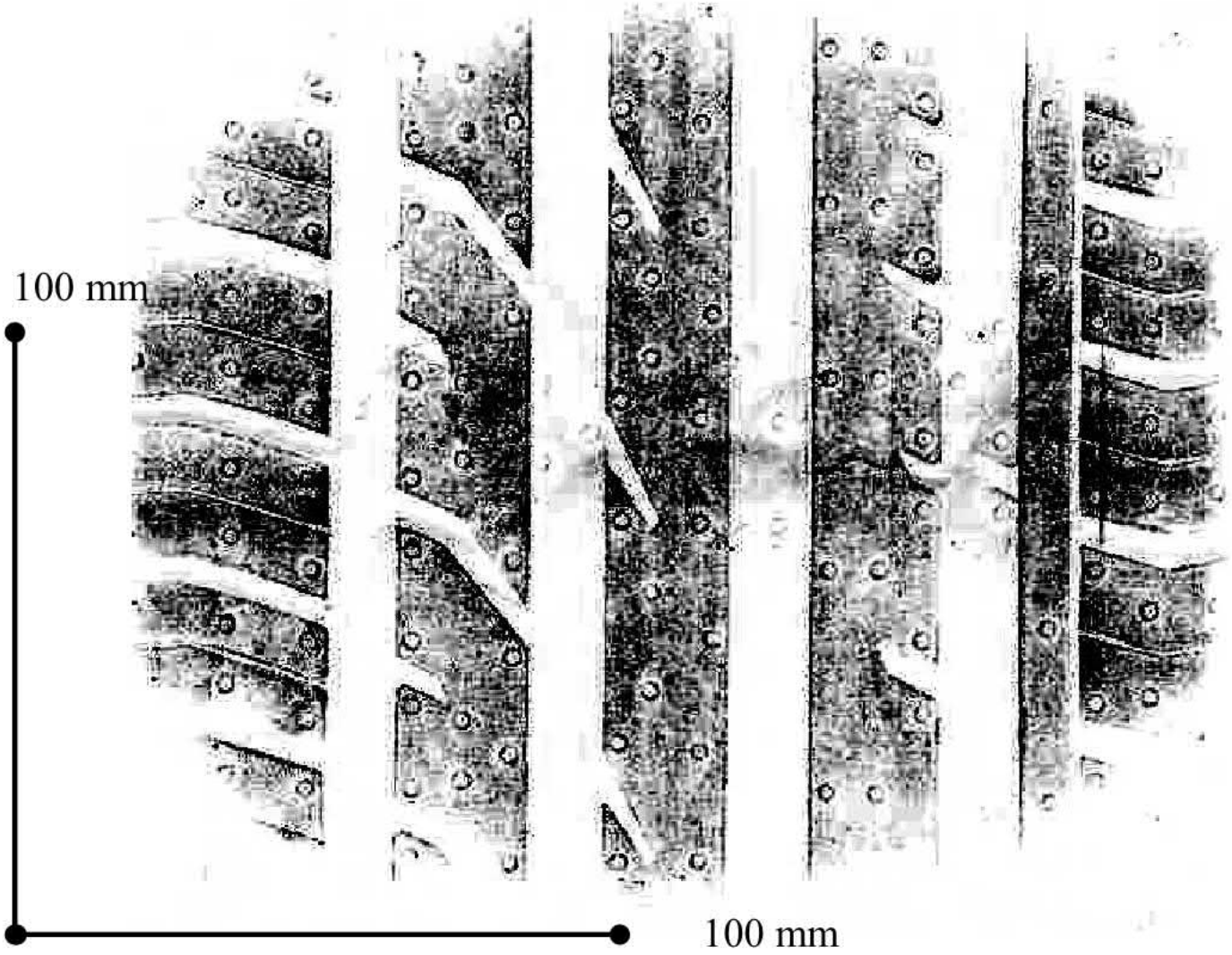

Contact area: c. 12850 mm^2

Contact patch by "ink print" method for tire 225/50 R17 for 100% of LI and 2.5 bar

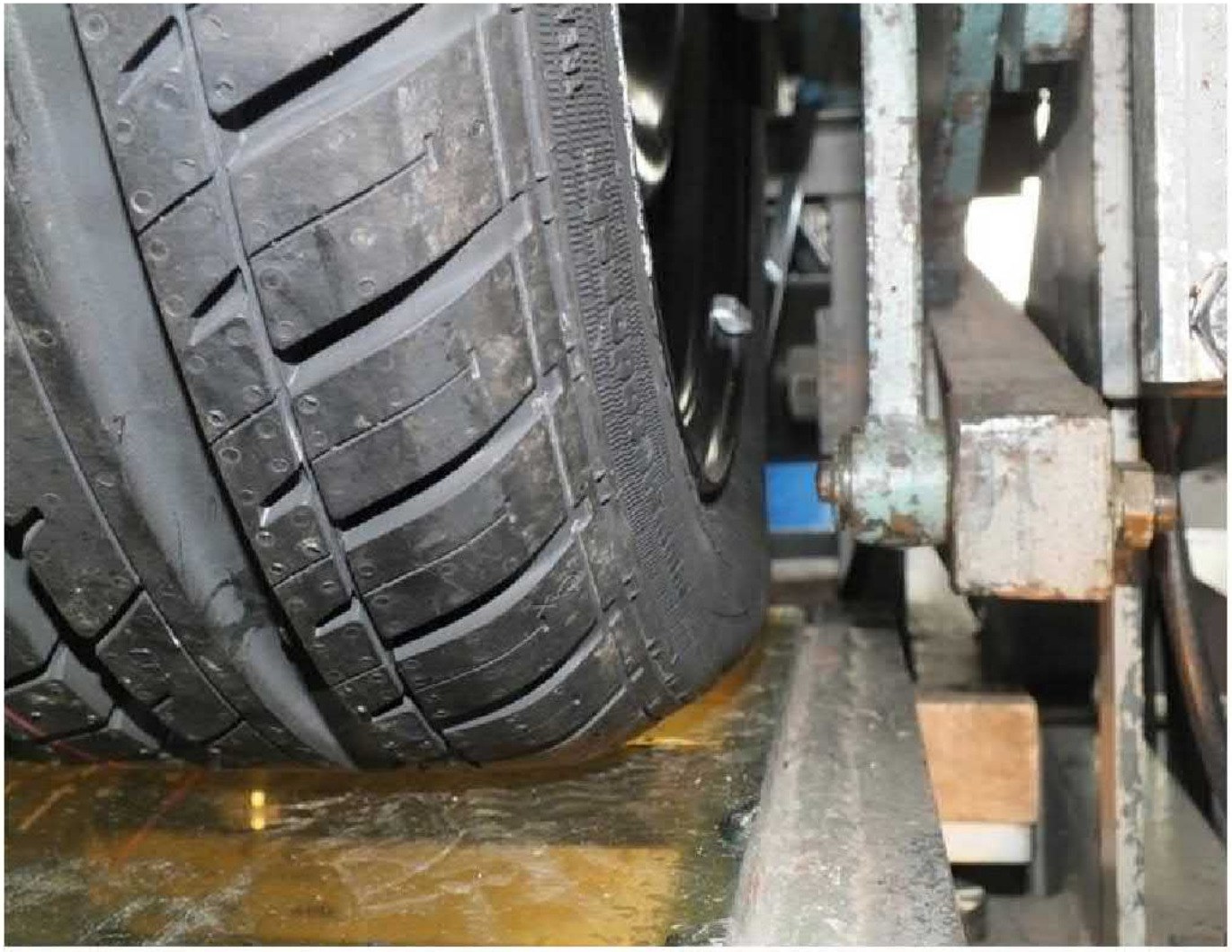

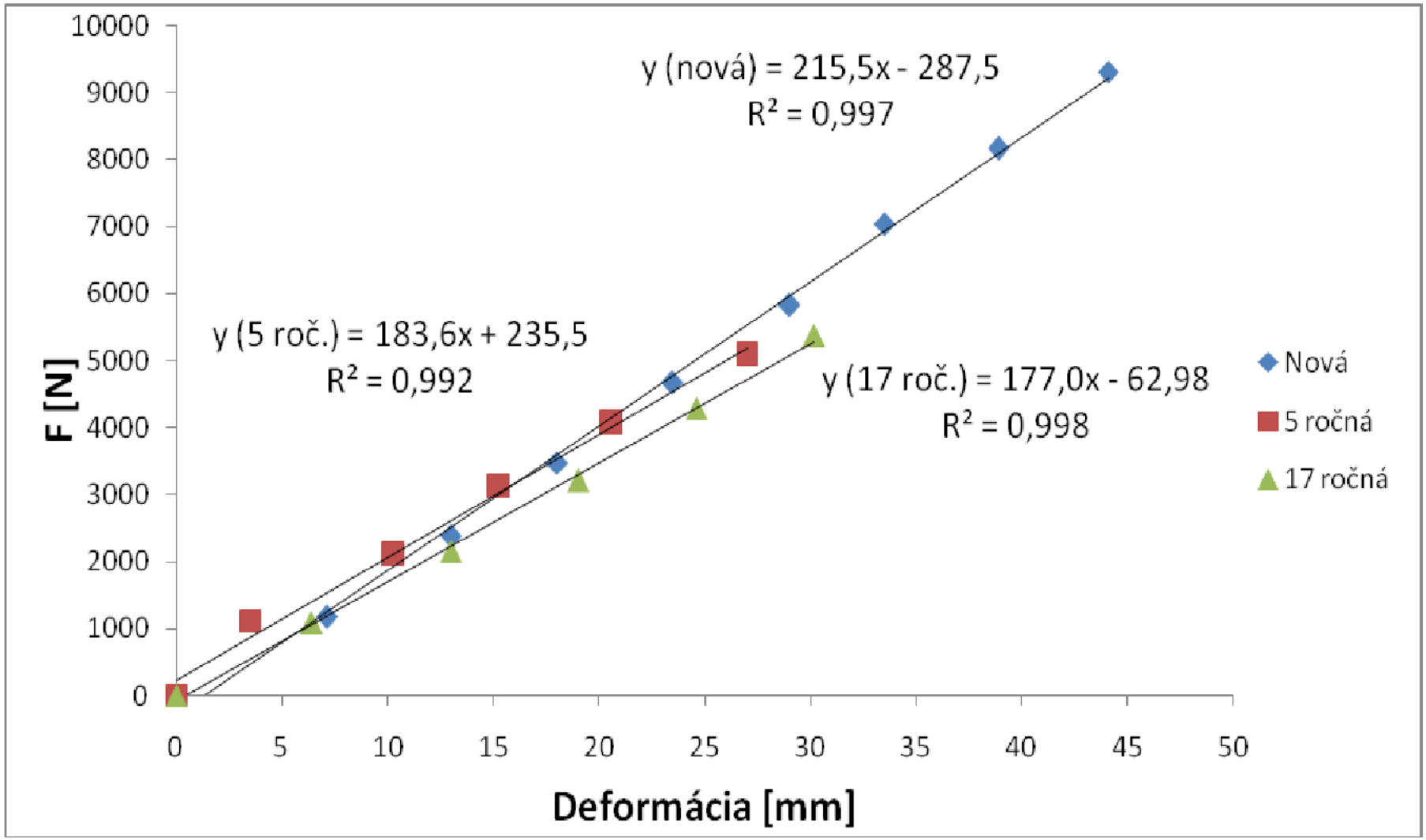
y (nová) = 215,5x - 287,5
R² = 0,997
y (5 roč.) = 183,6x + 235,5
R² = 0,992
y (17 roč.) = 177,0x - 62,98
R² = 0,998
Nová
5 ročná
17 ročná
F [N]
Deformácia [mm]
10000
9000
8000
7000
6000
5000
4000
3000
2000
1000
0
0
5
10
15
20
25
30
35
40
45
50

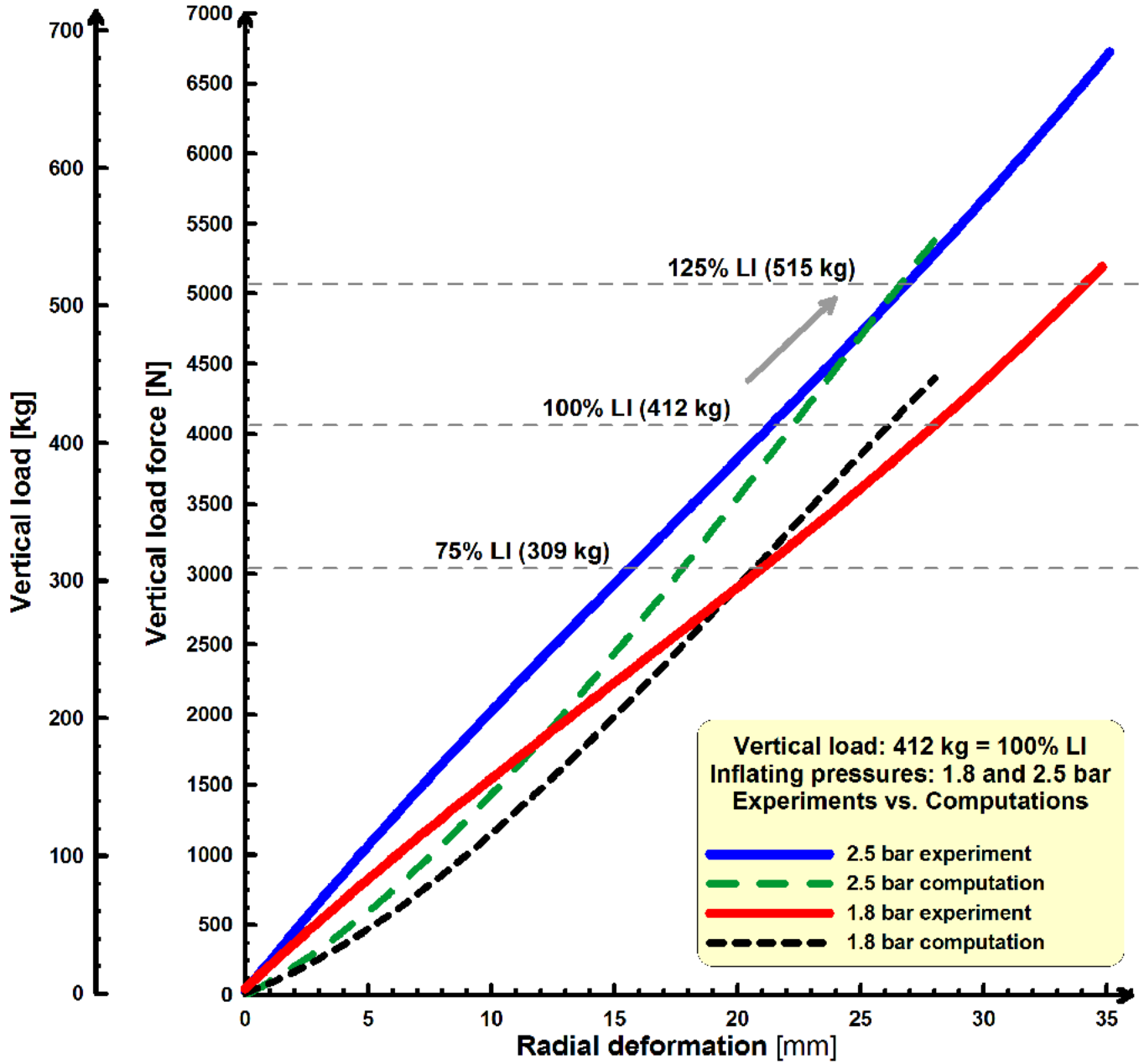

Radial deformation characteristics for different inflation pressures – verification analyses between computations and experiments

Thank you

The laboratory with **statical adhesor** for measurement of tires **is complexly laboratory** at Slovak university which enabling on-line measurements and evaluation all outputs from experiments of tires **for passenger cars**.

In future in contemplation test machine will next **innovation in special pressure system and construction design of adhesor for quasi-dynamically tests of tires** (only low velocity).

Maximum of vertical loading on the static adhesor is c. 2 000 kg. Some tires with low load index (e.g. tire 165/70 R13 where maximum load LI is only 412 kg) are possible to test from 0 to 240% of LI and those tires for small car can be overloaded with great deformation. Low-profile tires with maximum load index c. 102 are possible to test on the static adhesor.

The knowledge about contact patches and contact pressures is necessary for verification analyses between experiments and computations of tires by Finite Element Analyses.

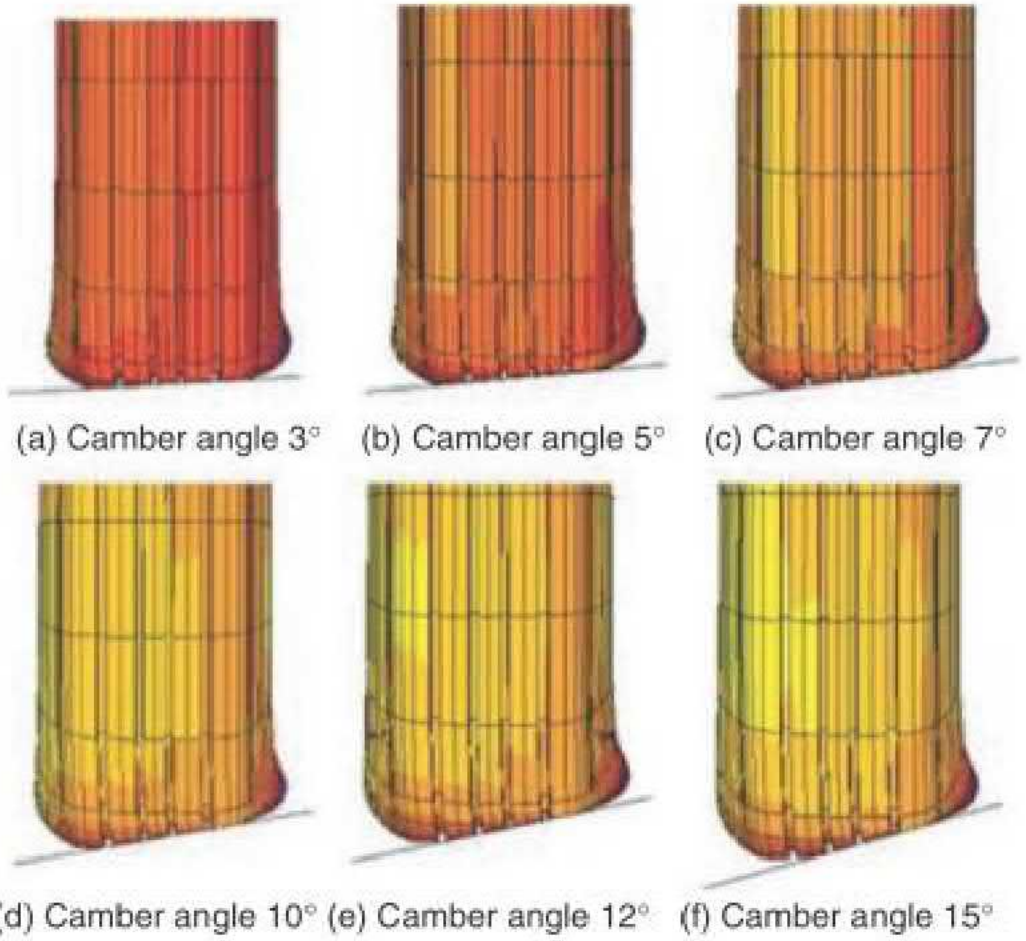

Figure 11. *Tire camber deformation under different camber angles (the inflation pressure is 0.25 MPa, and the vertical load is 5194 N).*

BICYCLE TIRE

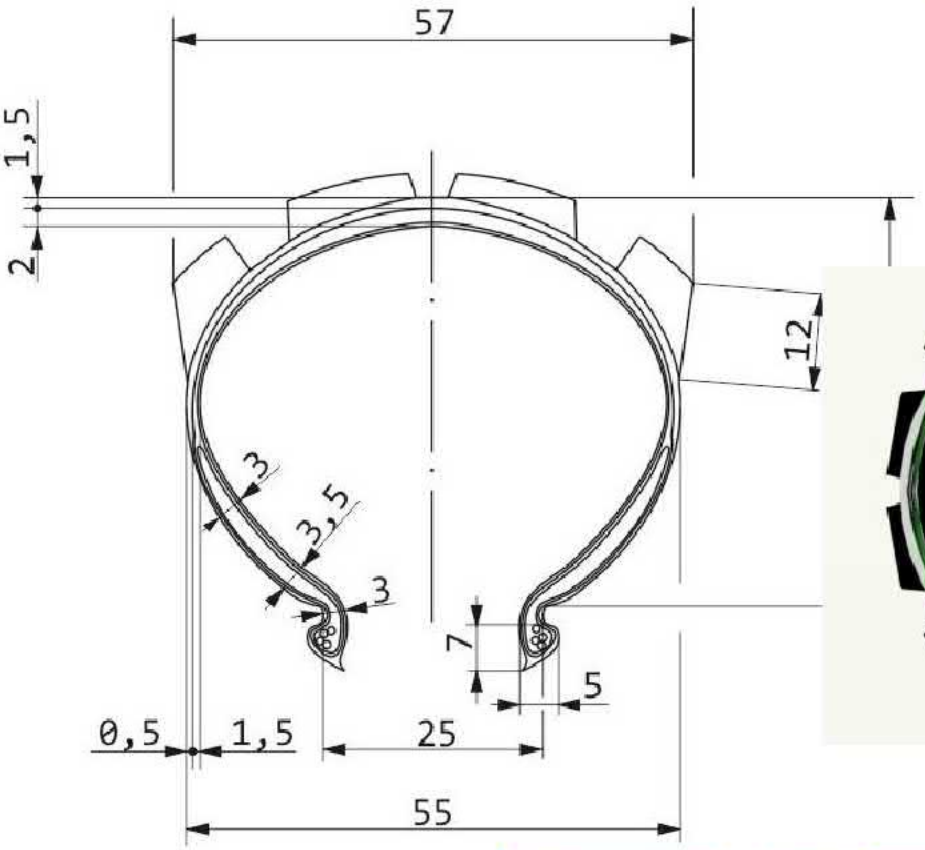
57
1,5
2
12
3
3,5
3
7
5
0,5
1,5
25
55

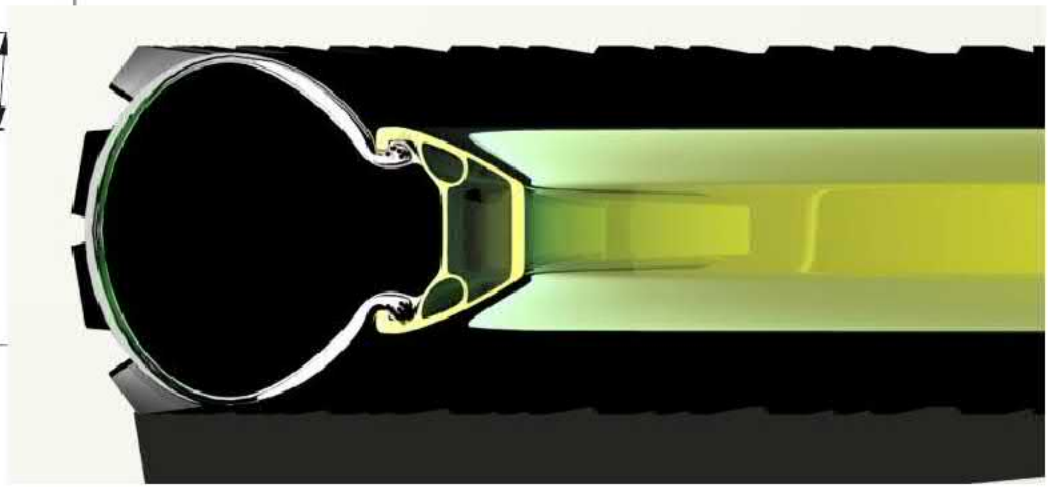

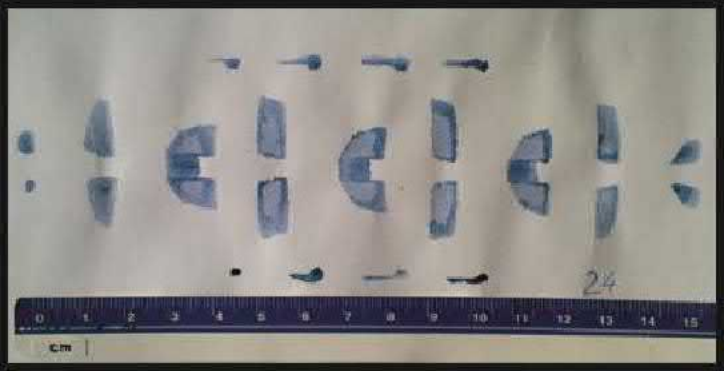

(24) Maxxis High Roller 26x2,50

Určenie- zjazd
Dezén- jednosmerný, 90% stav
Mat. pätky- oceľ
Mat. textilnej výstuže- Nylon
Prevádzkový tlak- 250 - 450 kPa
Max. zaťaženie- neznáme
Krajina pôvodu- Taiwan
TPI- 60
Poznámka- zmes gumy Super Tacky, butylová výstuž bočnice

Atramentový odtlačok

Tlak- 180 kPa
Zaťaženie- 70 kg

Bicycle tires was tested at three different inflation pressures **180. 280 and 380 kPa**

Load: 200 kg

Inflation pressure: 180 kPa

Deformation: 27.8 mm

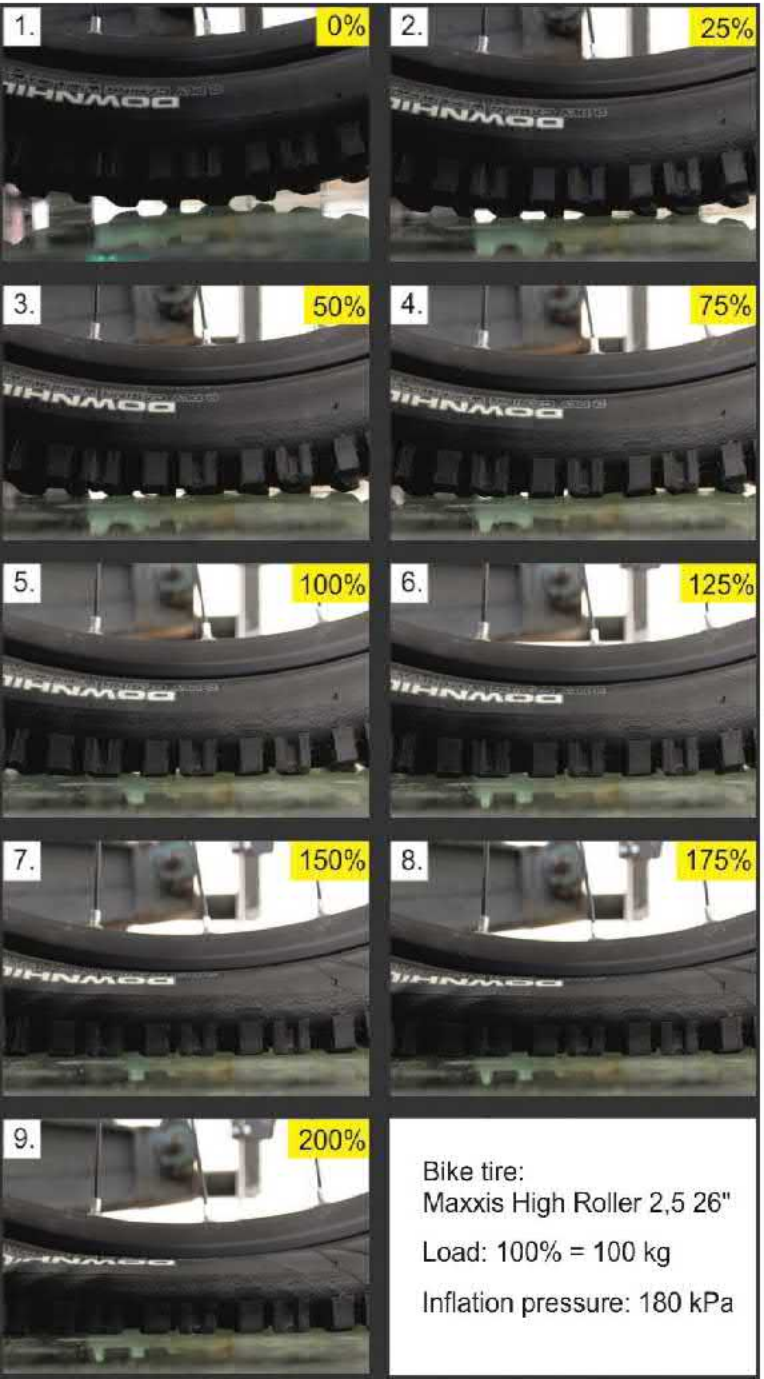

Bike tire:
Maxxis High Roller 2,5 26"

Load: 100% = 100 kg

Inflation pressure: 180 kPa

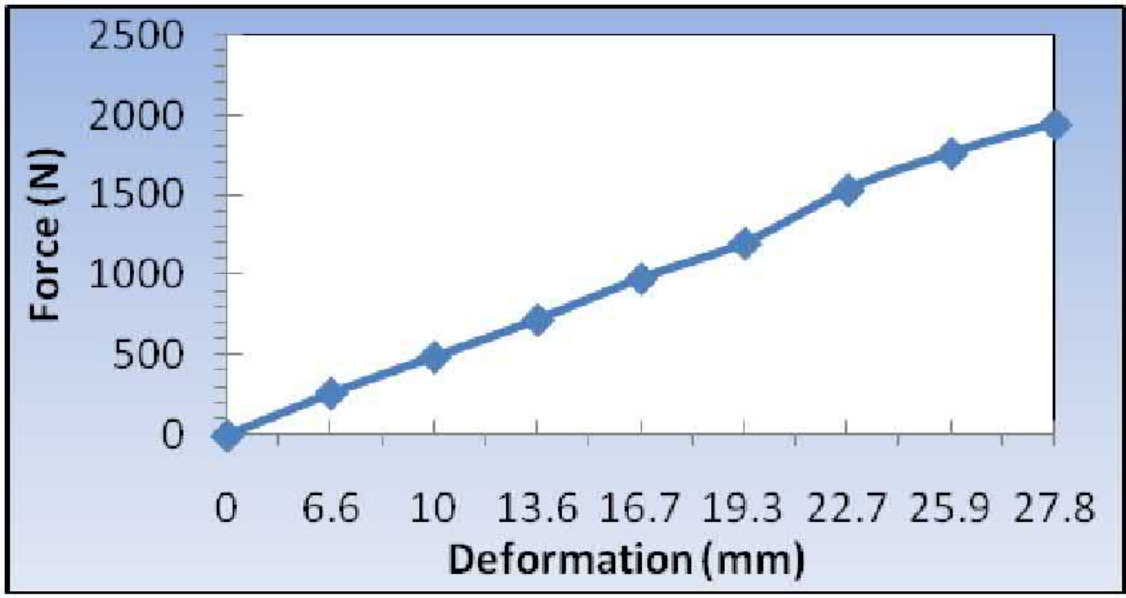

The radial deformation characteristic
(dependency radial deformation of tire out of the radial load) at inflation pressure 180 kPa

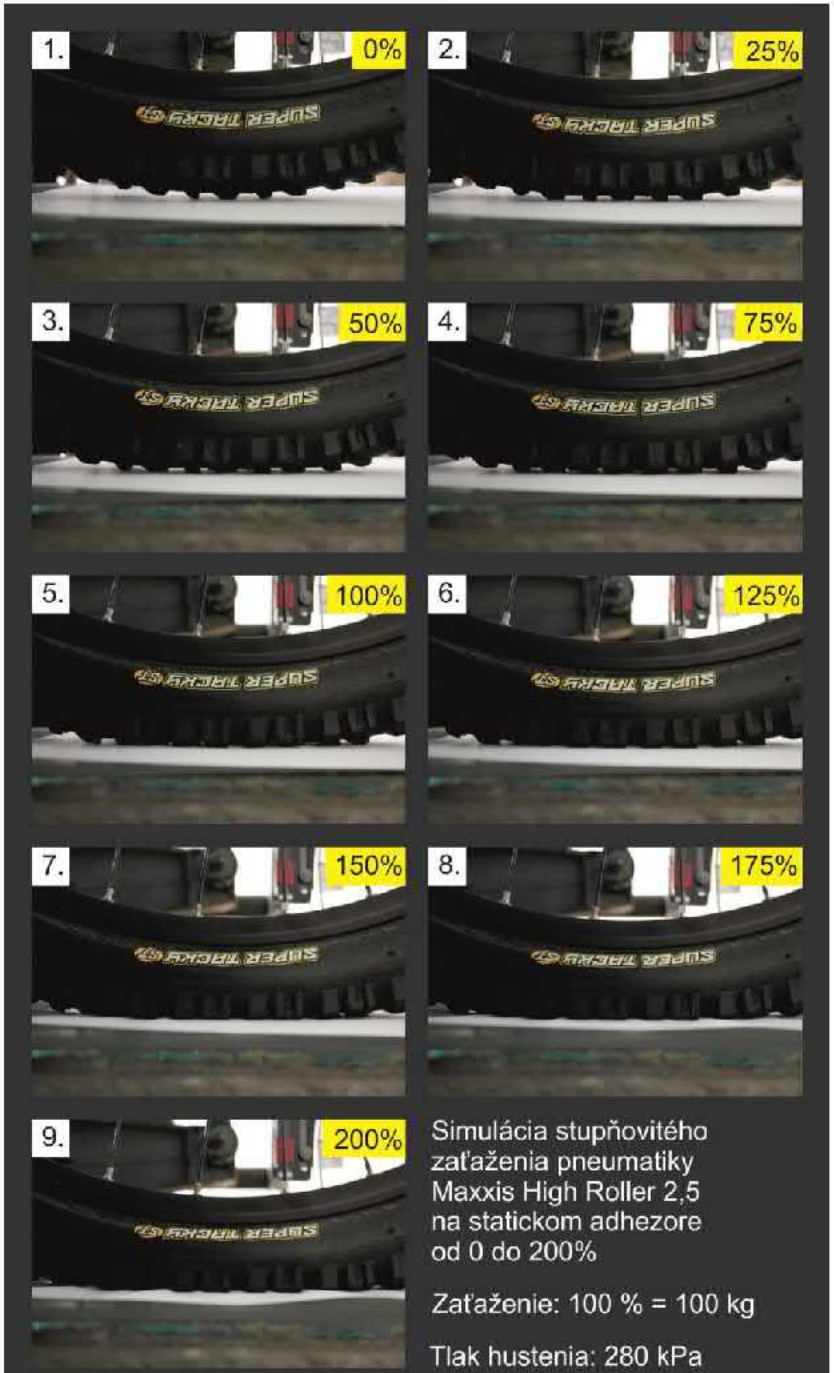
1.
0%
2.
25%
3.
50%
4.
75%
5.
100%
6.
125%
7.
150%
8.
175%
9.
200%
Simulácia stupňovitého zaťaženia pneumatiky Maxxis High Roller 2,5 na statickom adhezore od 0 do 200%
Zaťaženie: 100 % = 100 kg
Tlak hustenia: 280 kPa

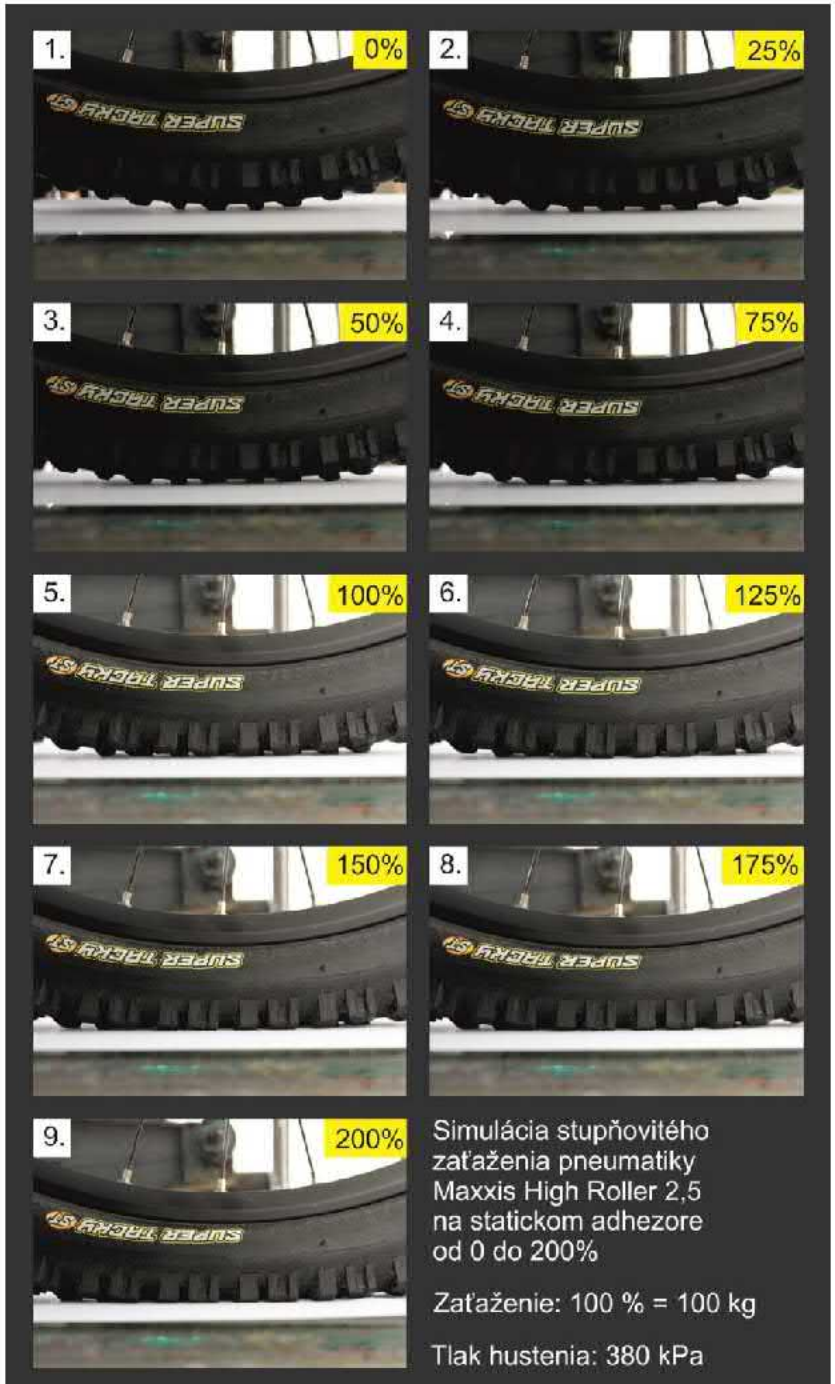
1.
0%
2.
25%
3.
50%
4.
75%
5.
100%
6.
125%
7.
150%
8.
175%
9.
200%
Simulácia stupňovitého zaťaženia pneumatiky Maxxis High Roller 2,5 na statickom adhezore od 0 do 200%
Zaťaženie: 100 % = 100 kg
Tlak hustenia: 380 kPa

The radial stiffness of bicycle tire for given inflation pressures

Pressure (kPa)	Radial stiffness (N/mm)
180	84.0
280	96.5
380	120.0

The determined values of the radial stiffness of the tire very depending on inflation pressure of tire.

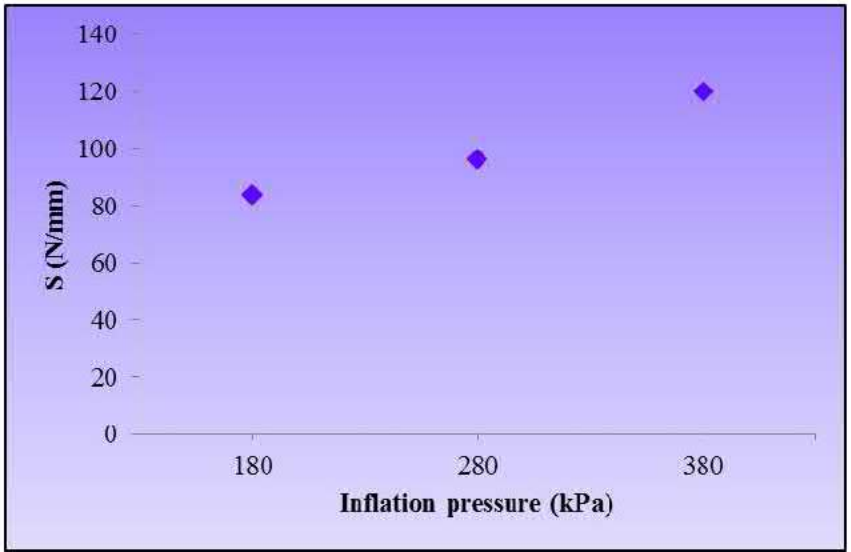

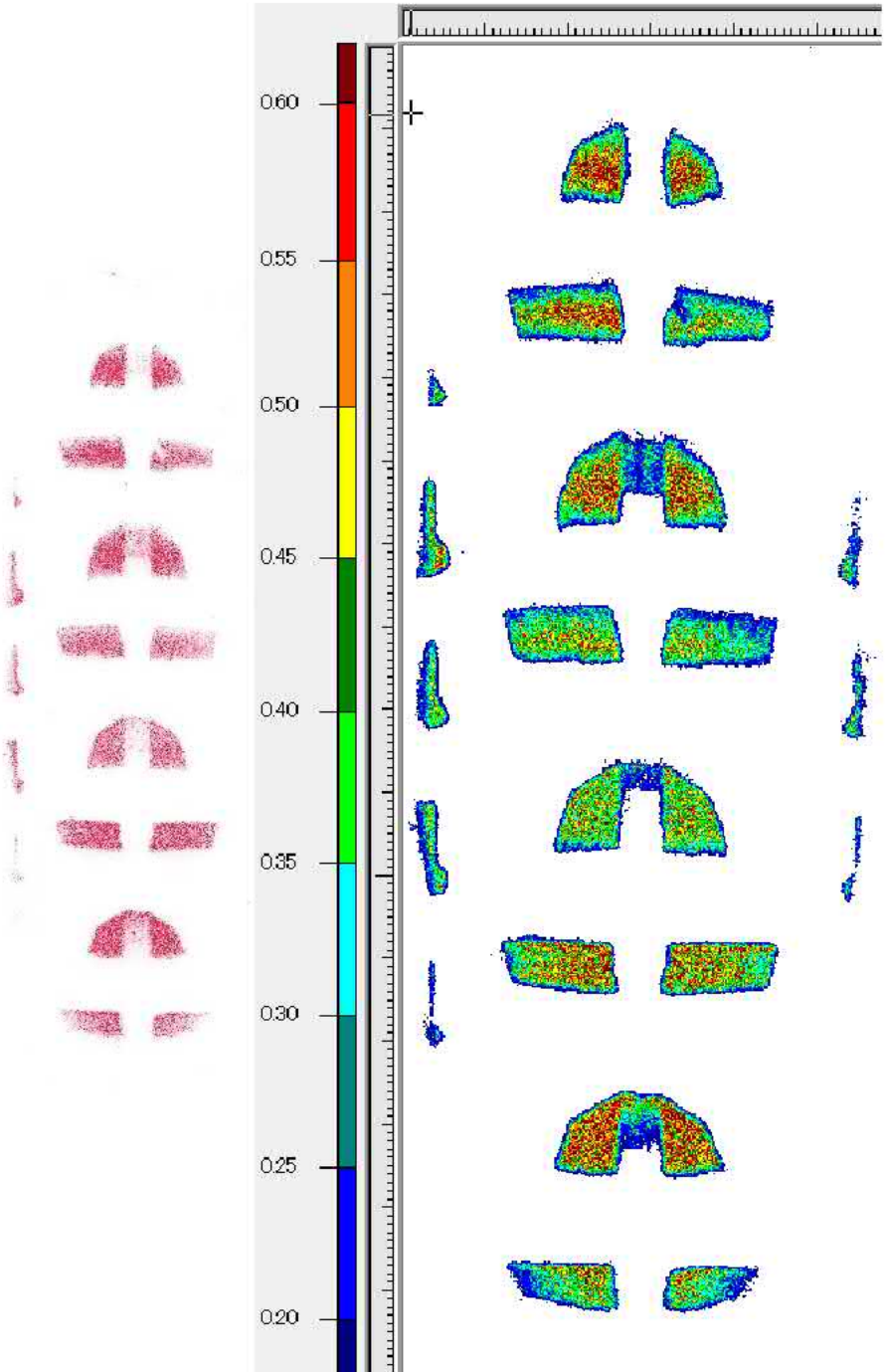

With the application of a pressure - sensitive film is able to analyze the contact pressure distribution, which is in color spectrum

Distribution of contact pressure
in the contact patch by inflation pressure 180 kPa and load 100 kg

EXPERIMENTS OF TIRES ON „DYNAMIC ADHESOR“

- Radial loading max **0.5 t**
- Maximum **velocity 180 km/h**

The tire inflation pressures used for dynamic experimental testing at different velocities of 0, 30, 60, 90 and 120 km/h were 160 kPa (underinflated tire), 180, 205, 215, 230, 240, 250, 260, 280 kPa, and the maximum inflation pressure 300 kPa.

RADIAL DEFORMATION CHARACTERISTICS

for velocity 0 km/h for different inflation pressures

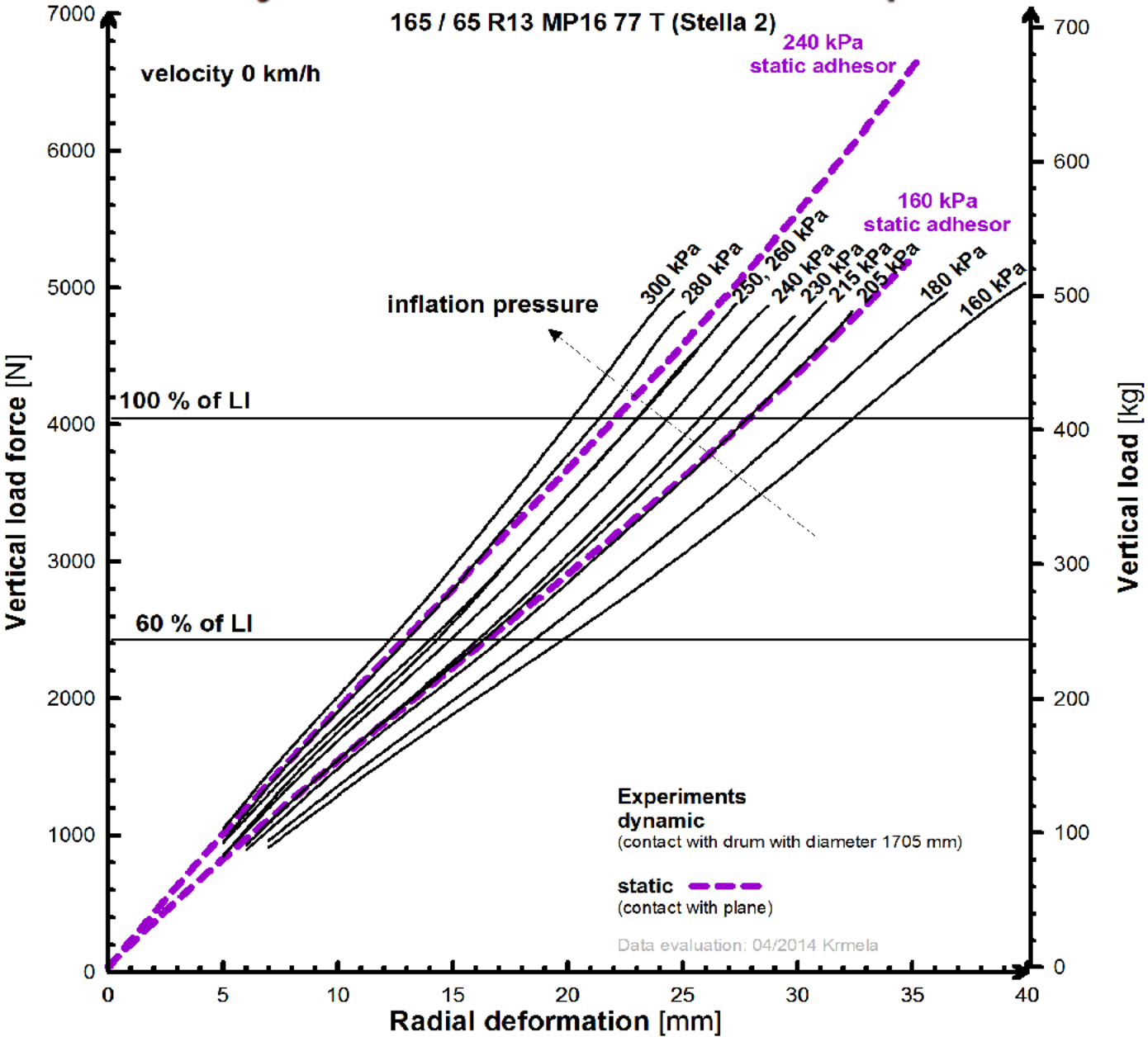

radial deformation characteristics WITH LINES OF CONSTANT DEFORMATION for different inflation pressures

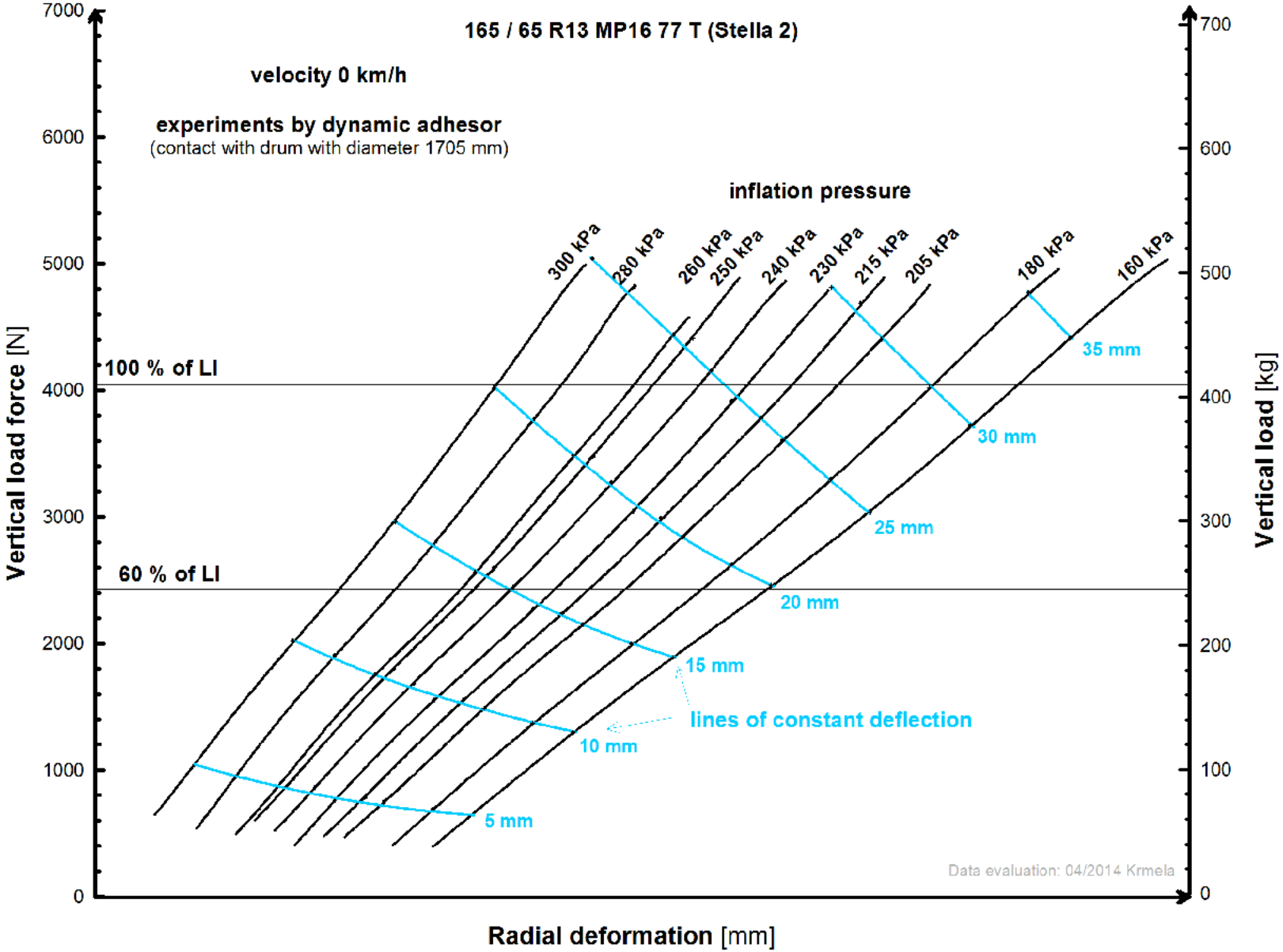

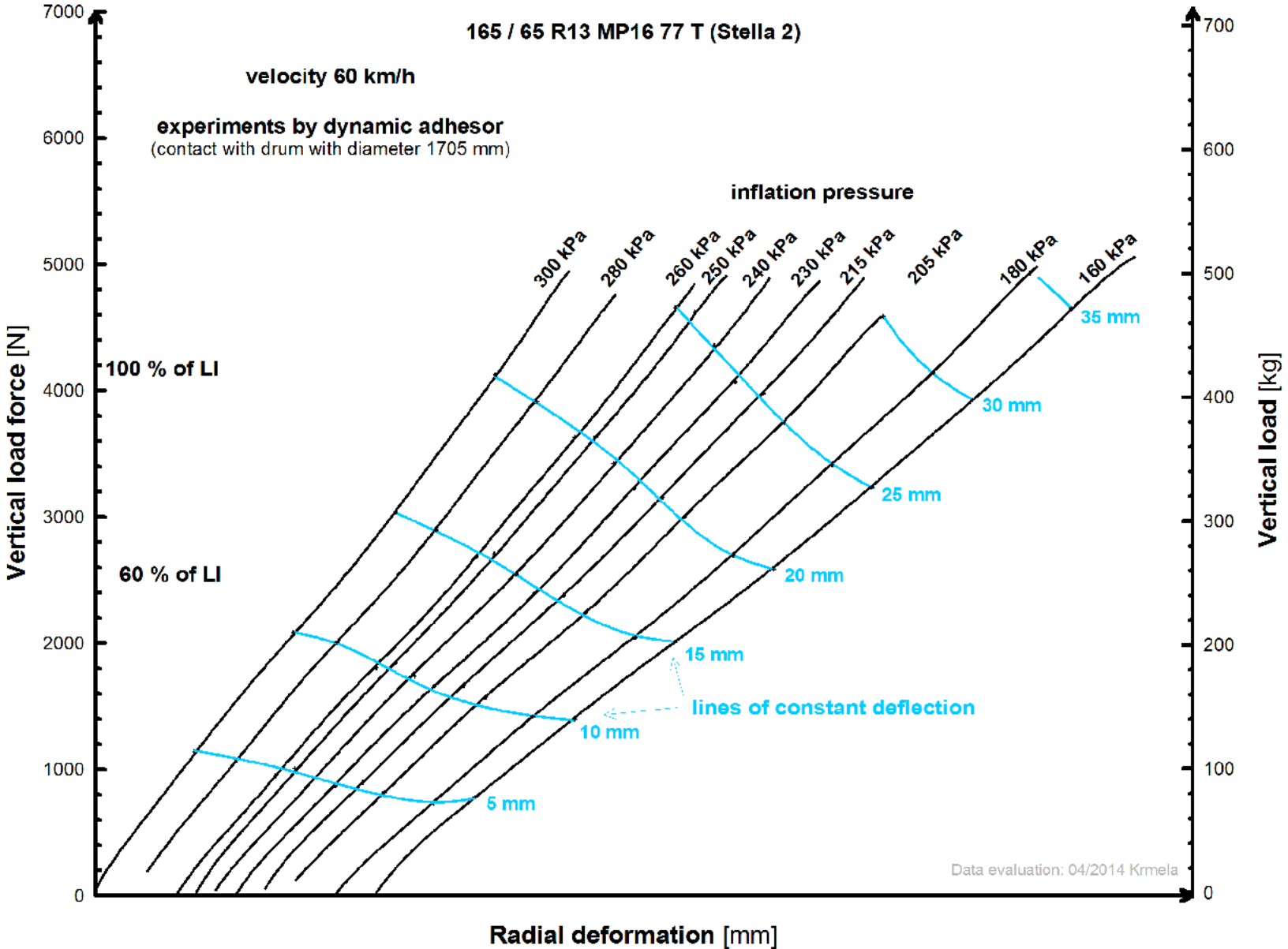
165 / 65 R13 MP16 77 T (Stella 2)
velocity 60 km/h
experiments by dynamic adhesor
(contact with drum with diameter 1705 mm)
inflation pressure
300 kPa
280 kPa
260 kPa
250 kPa
240 kPa
230 kPa
215 kPa
205 kPa
180 kPa
160 kPa
100 % of LI
60 % of LI
35 mm
30 mm
25 mm
20 mm
15 mm
10 mm
5 mm
lines of constant deflection
Data evaluation: 04/2014 Krmela
Vertical load force [N]
Vertical load [kg]
Radial deformation [mm]
0
1000
2000
3000
4000
5000
6000
7000
0
100
200
300
400
500
600
700

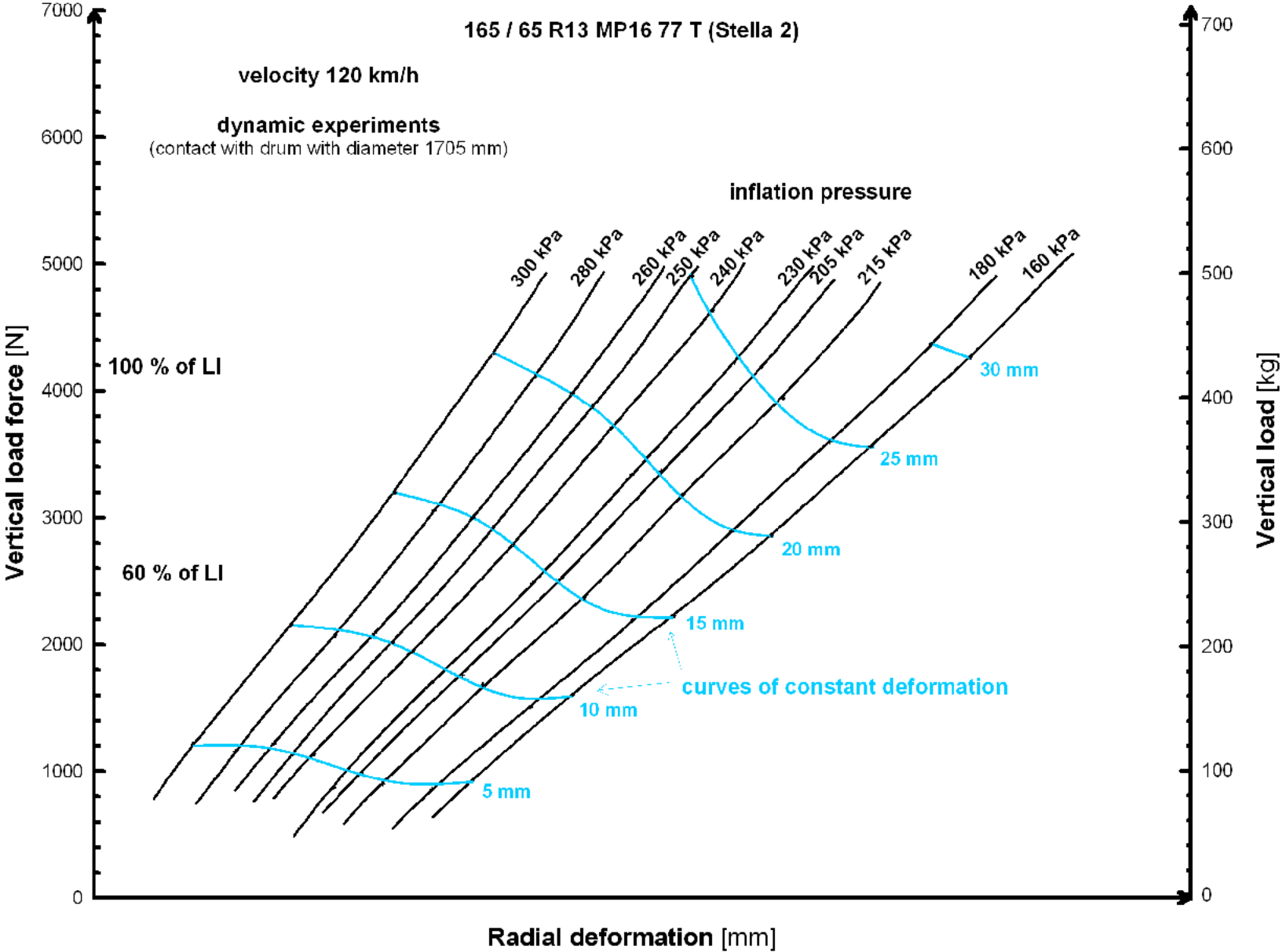
165 / 65 R13 MP16 77 T (Stella 2)
velocity 120 km/h
dynamic experiments
(contact with drum with diameter 1705 mm)
inflation pressure
300 kPa
280 kPa
260 kPa
250 kPa
240 kPa
230 kPa
205 kPa
215 kPa
180 kPa
160 kPa
100 % of LI
60 % of LI
30 mm
25 mm
20 mm
15 mm
10 mm
5 mm
curves of constant deformation
Vertical load force [N]
Vertical load [kg]
Radial deformation [mm]
7000
6000
5000
4000
3000
2000
1000
0
700
600
500
400
300
200
100
0

radial deformation characteristics: COMPARISON BETWEEN STATIC AND DYNAMIC EXPERIMENTAL DATA

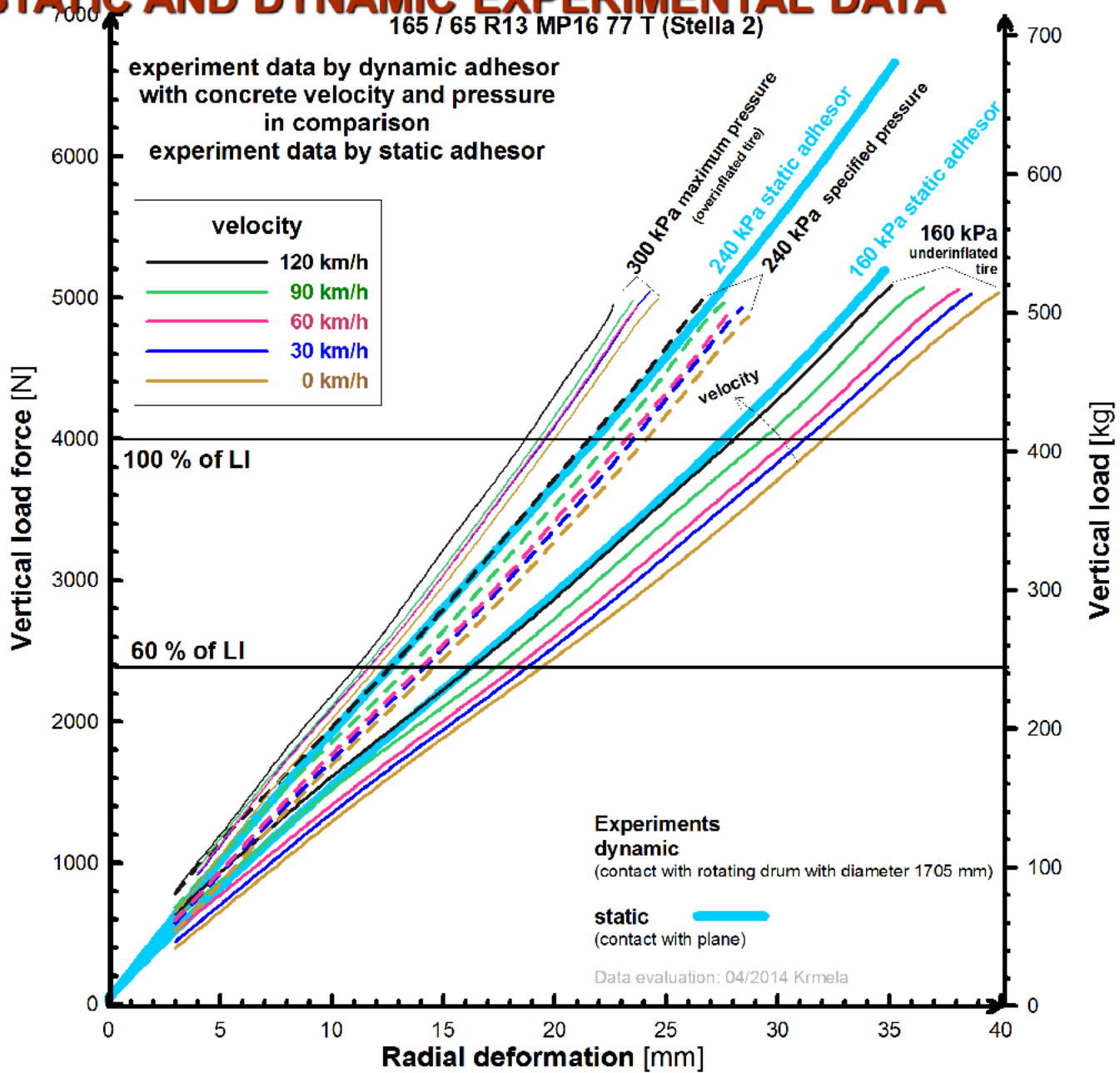

radial deformation characteristics: COMPARISON BETWEEN STATIC AND DYNAMIC EXPERIMENTAL DATA

The radial deformation characteristic for inflation pressure of 160 kPa and velocity of 120 km/h from the dynamic adhesor is conformable to the radial deformation characteristic for the same inflation pressure from the static adhesor. In addition, the radial deformation characteristic for inflation pressure of 240 kPa and velocity of 120 km/h from the dynamic adhesor is conformable to the characteristic for the same inflation pressure of 240 kPa from the static adhesor.

Values of radial stiffness for different velocities and inflation pressures of tire

Radial stiffness [N/mm]		Velocity [km/h]					
		0	30	60	90	120	S0*
Inflation pressure [kPa]	160	128.0	130.7	132.2	135.1	136.5	142.1
	180	139.2	140.0	141.0	143.5	144.2	
	205	150.6	153.6	155.0	155.8	158.6	
	215	157.9	160.6	160.8	163.6	164.1	
	230	166.6	168.8	169.9	170.8	171.8	
	240	171.4	173.1	175.3	176.6	182.3	177.5
	250	179.9	181.6	185.9	188.4	190.4	
	260	185.4	188.2	190.5	193.6	195.4	
	280	191.9	197.6	199.3	201.5	204.6	
	300	205.5	206.8	207.5	207.6	212.3	

* S0 - static adhesor (velocity 0 km/h), only for pressures 160 and 240 kPa

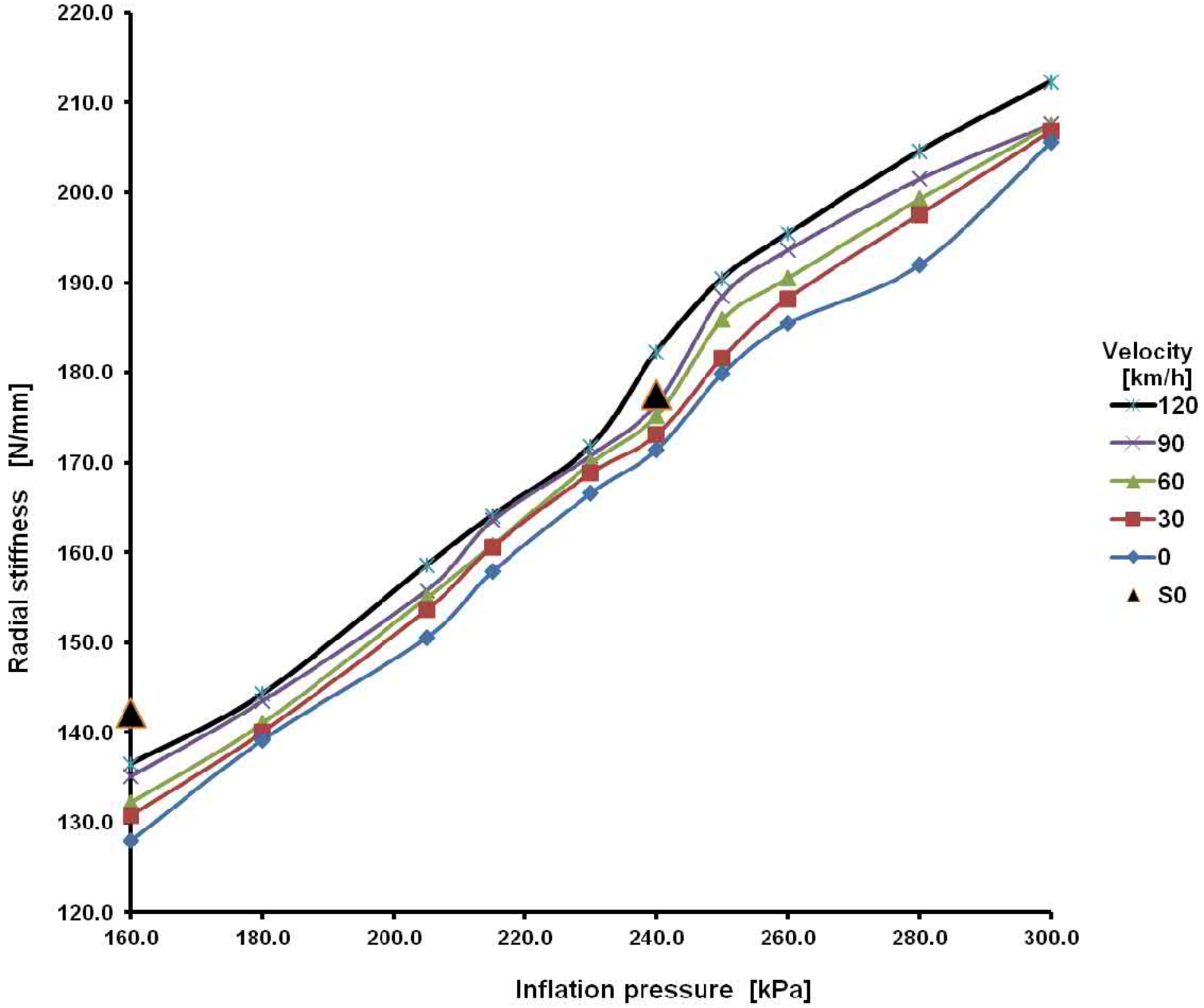

Dependence of radial stiffness on inflation pressure of tire for different velocities

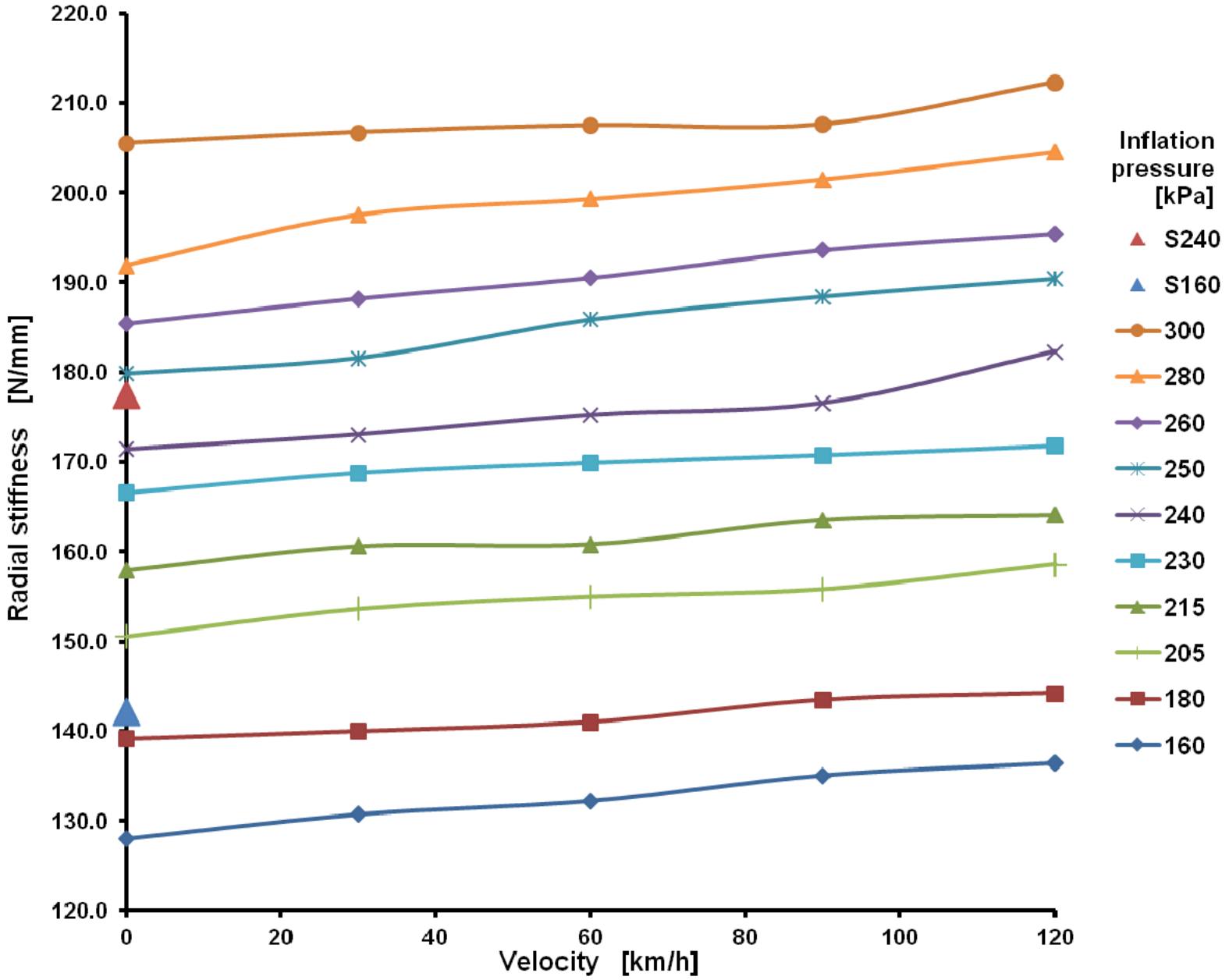

Dependence of radial stiffness on velocities for different inflation pressure of tire

Main output:

STIFFNESS for different velocities and inflation pressures

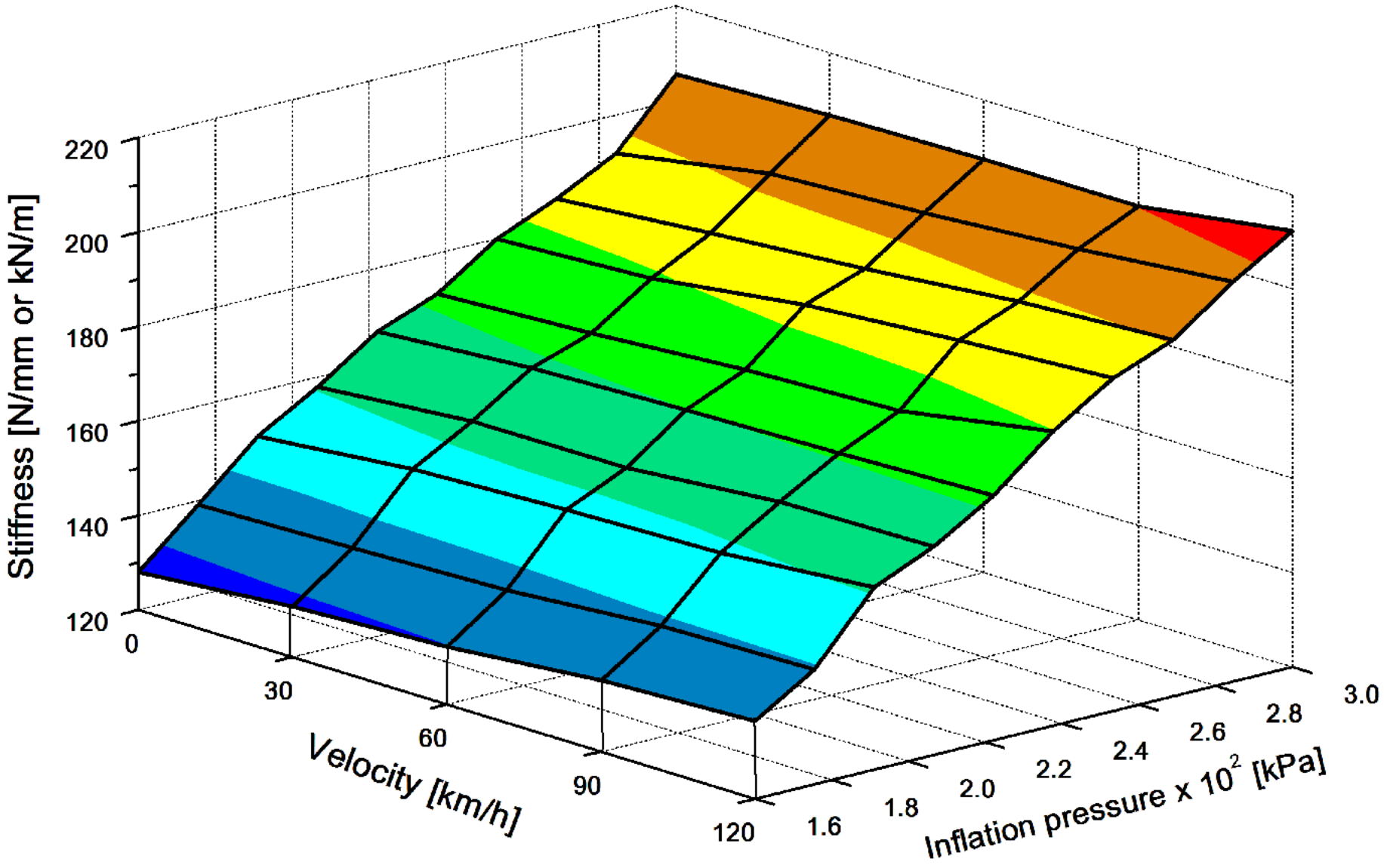

Prediction of radial stiffness

The radial stiffness can be predicted on the basic of results of radial stiffness obtained from experiments. The radial deformation characteristics can be transformed into the dependences of vertical force parameter on radial deformation The vertical force parameter is calculated by equation:

$$y = \frac{100 \cdot F}{p + \mathrm{A} \cdot p_r} \,[\mathrm{N/kPa}]$$

Where:

y [N/kPa] – vertical force parameter,

F [N] – vertical load force,

p [kPa] – inflation pressure of tire,

A [1] – constant depended on specified velocity,

p_r [kPa] – rated (current) inflation pressure of tire and for tested tire, p_r is 240 kPa.

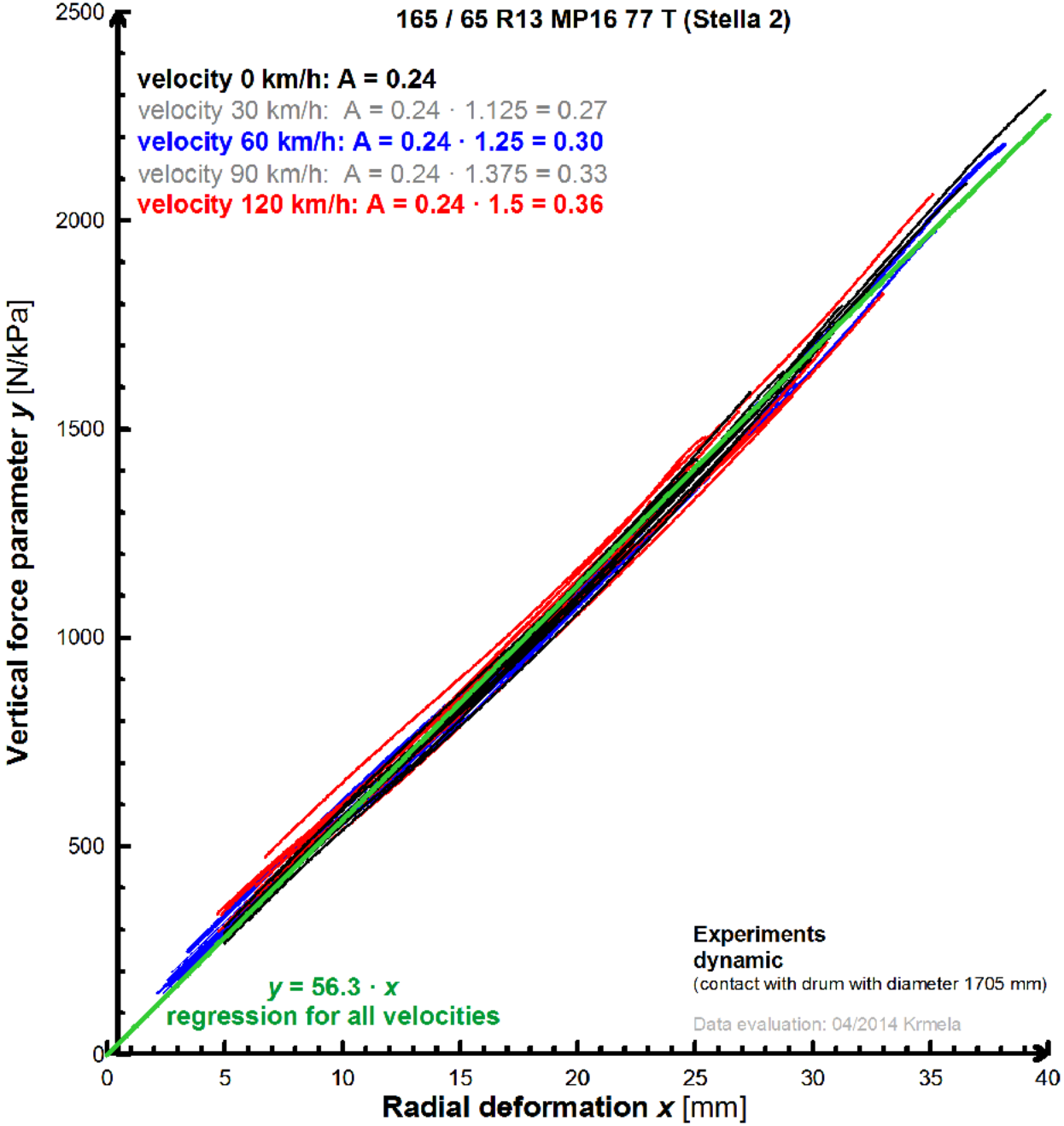
165 / 65 R13 MP16 77 T (Stella 2)
velocity 0 km/h: A = 0.24
velocity 30 km/h: A = 0.24 · 1.125 = 0.27
velocity 60 km/h: A = 0.24 · 1.25 = 0.30
velocity 90 km/h: A = 0.24 · 1.375 = 0.33
velocity 120 km/h: A = 0.24 · 1.5 = 0.36
Vertical force parameter y [N/kPa]
Radial deformation x [mm]
y = 56.3 · x
regression for all velocities
Experiments
dynamic
(contact with drum with diameter 1705 mm)
Data evaluation: 04/2014 Krmela

The A constant is 0.24 for tire 165 / 65 R13 and velocity is 0 km/h. The A constants for velocities of 30, 60, 90 and 120 km/h are shown in figure. The linear regression has been calculated for the vertical force parameter and radial deformation for specified tire:

$$y = 56.3 \cdot x \ [\mathrm{N/kPa}]$$

Where:

x [mm] – radial deformation.

Then, the values of radial stiffness can be predicted for given velocity and inflation pressure by equation:

$$S_{pv} = 56.3 \cdot \left(p + \mathrm{A} \cdot p_r \right) \cdot 100 \ \ [\mathrm{N/mm}]$$

Where:

S_{pv} [N/mm] – predicted static radial stiffness for the different velocities and the inflation pressures.

If velocity increases about one km/h that constant A increases about one thousandth, e.g. for velocity 100 km/h the constant A is 0.24 plus 0.1, therefore this constant A is 0.34. Similarly, constant A is 0.42 for velocity 180 km/h etc.

The values of radial stiffness calculated are shown in Table. The average error of the values of radial stiffness from experiments in comparison to the values of predicted radial stiffness is less than 1.9 %. The maximum error is 4.7 %.

Values of predicted radial stiffness for different velocities and inflation pressures of tire

Radial stiffness [N/mm]	Velocity [km/h]				
Inflation pressure [kPa]	0	30	60	90	120
160	122.7	126.8	130.8	134.9	138.9
180	134.0	138.0	142.1	146.1	150.2
205	148.1	152.1	156.2	160.2	164.3
215	153.7	157.8	161.8	165.9	169.9
230	162.2	166.2	170.3	174.3	178.4
240	167.8	171.9	175.9	180.0	184.0
250	173.4	177.5	181.6	185.6	189.7
260	179.1	183.1	187.2	191.3	195.3
280	190.4	194.4	198.5	202.5	206.6
300	201.6	205.7	209.8	213.8	217.9

The inflation pressure has much more influence on the change of radial stiffness in comparison to the velocity. When the tire is in a rolling motion, the radial stiffness of the tire is higher in comparison to the tire which is in the stationary position (dynamic experiments for velocity of 0 km/h).

Then estimate of predicted stiffness is possible for other velocities (e.g. stiffness value is 192.2 N/mm for velocity 180 km/h and pressure 240 kPa) and other pressures (e.g. stiffness value is 201.0 N/mm for pressure 270 kPa and velocity 120 km/h).

Some of experiments with utilization of the dynamic adhesor with drum can be replaced by experiments with utilization of the static adhesor on the plane surface or some of experiments with utilization of the static adhesor can be replaced by experiments with utilization of the dynamic adhesor.

The laboratory with **statical adhesor** for measurement of tires **is complexly laboratory** which enabling on-line measurements and evaluation all outputs from experiments of tires **for bicycle and passenger cars**.

Experiment on adhesor: Stiffness – FINAL FORMULA

$$S = \frac{F_{(0.8\cdot 125)\,\%\,\text{of LI}} - F_{(0.8\cdot 75)\,\%\,\text{of LI}}}{x_{(0.8\cdot 125)\,\%\,\text{of LI}} - x_{(0.8\cdot 75)\,\%\,\text{of LI}}} = \frac{F_{100\,\%\,\text{of LI}} - F_{60\,\%\,\text{of LI}}}{x_{100\,\%\,\text{of LI}} - x_{60\,\%\,\text{of LI}}} \; [\text{N/mm}]$$

Part 4 – EXPERIMENTS OF TIRE PARTS: Preparation of test samples, Tensile load, Bend load, Character of deformation, Outputs from tests

PLAN OF EXPERIMENTS				
Activity name / time - year	**2007**	**2008**	**2009**	**2010**
Study literature, information	x			
Test specimen's preparation for experiments	x	x x	x x	x
Tests of specific statically characteristics of whole tires - deformation characteristics and pressure measurement	x	x x	x x	x
The corrosion tests in a corrosion chamber	x	x x	x x	x
The statically tests of structure parts of tires - tensile tests - tests under combined loading states	x	x x	x x x	x
Hardness tests according to SHORE A method	x	x x	x x	x
Tests of resistance to aggressive surroundings and wear tests	x	x x	x x	x x
The microscopy observation of - the interfaces between steel-cord and elastomer - the interfaces after failure after corrosion test	x	x x x x	x x x x	x x x
The computational modelling of strain-stress analyses of - tires - parts of tires	x	x x x x	x x x x	x x
The evaluation and analysis of obtained results from experiments	x	x x	x x	x x
The verification analysis and confrontations of outputs from computations	x	x x	x x	x x
The confrontations of outputs from microscopy observation	x	x x	x x	x x
The publishing of obtained results	x	x x	x x	x x

Planned experiments

- **Which test? tensile/bend/…**
- **Why test (purpose)? E, stress-strain, force-deformation**
- **Which standards? ASTM, ISO, …**
- **Which test machine? universal test machine, ….**
- **Geometry parameters of specimens (by standard or must be design)? Width, lengh, shape, …**
- **Number of specimens?**
- **Parameters of test? loading speed, …**
- **Outputs from experiments for computational modelling?**

Elastomer

Standards: ČSN 640605 or ISO 37 (2005)

ISO 527-1 and ISO 527-2, or ASTM D638

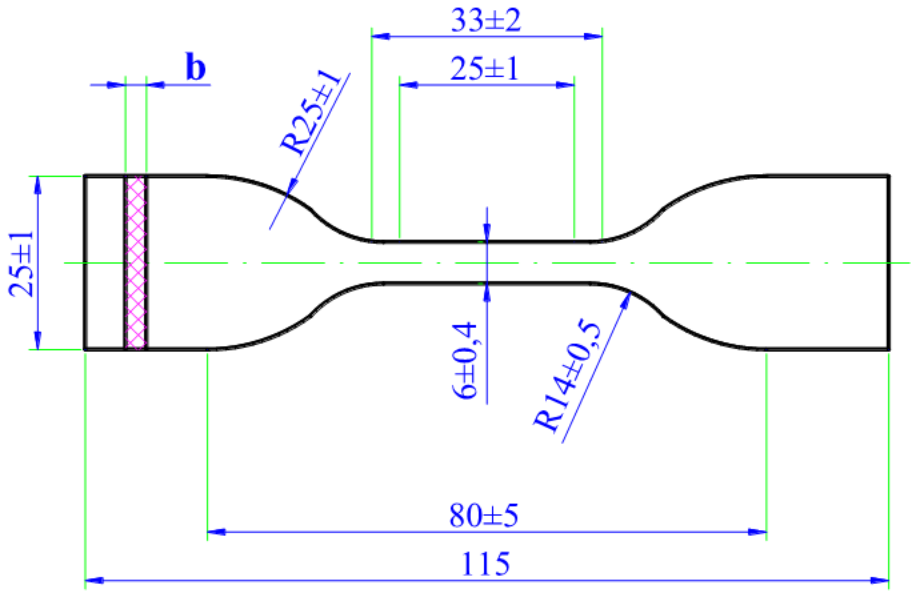

Elastomer – type tests / standard	ASTM (American Society for Testing and Materials – USA normy)	ISO
Clash-Berg Modulus	ASTM D1043	ISO 815
Compression Set	ASTM D395	ISO 37
Elongation at Break	ASTM D412	--
Elongation at Yield	ASTM D412	--
Elongation Set After Break	ASTM D412	--
Tear Strength	ASTM D624	ISO 34-1
Tear Strength, Split	ASTM D412	--
Tensile Set	**ASTM D412**	**--**
Tensile Strength at Break	**ASTM D412**	**ISO 37**
Tensile Strength at Yield	ASTM D412	ISO 37
Tensile Stress at 100%	ASTM D412	ISO 37
Tensile Stress at 200%	ASTM D412	ISO 37
Tensile Stress at 300% (E 300 %)	**ASTM D412**	**ISO 37**
Tensile Stress at 50%	ASTM D412	--

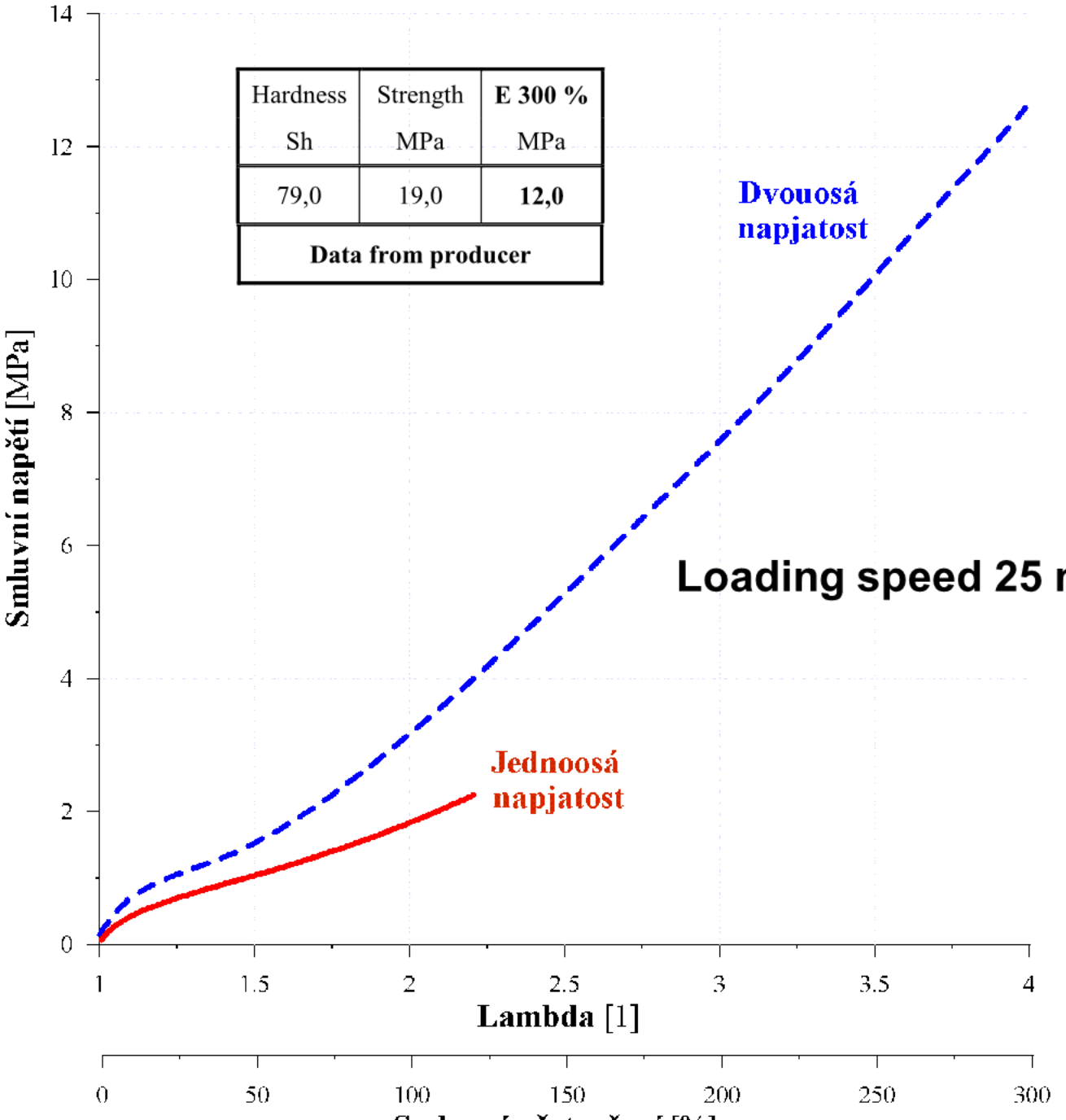
Hardness Sh
Strength MPa
E 300 % MPa
79,0
19,0
12,0
Data from producer
Dvouosá napjatost
Jednoosá napjatost
Loading speed 25 mm/min
Smluvní napětí [MPa]
Lambda [1]
0
2
4
6
8
10
12
14
1
1.5
2
2.5
3
3.5
4
0
50
100
150
200
250
300

Composites

Elastomer – typ zkoušky / Norma	ASTM
Mass per unit area of prepregs	BS EN ISO 10352: 1997
Resin flow of pre-impregnates	ISO 15034
Analysis of uncured sample by DSC	BS EN ISO 11357
Degree of cure by DSC	BS EN ISO 11357
Gel time	ISO 15040
Test panel manufacture	ISO 1268: 1974
Test and conditioning atmospheres	BS EN ISO 291: 1997
Tensile - unidirectional	**BS EN ISO 527-5: 1997**
Tensile - **multidirectional**	BS EN ISO 527-**4**: 1997
Compression - unidirectional	**ISO 14126**
Compression - multidirectional	ISO 14126
Shear : 45 degree tension	BS EN ISO 14129: 1998
Shear modulus : plate twist	ISO 15310
ILSS : through thickness	BS EN ISO 14130: 1998
Flexure	BS EN ISO 14125: 1998
Mode I fracture toughness	ISO 15024
Fatigue	ISO 13003
Creep testing	ISO 899
Moisture uptake/conditioning	ISO 62
Effect of water/moisture	ISO 62/175
Effect of chemicals	ISO 175
Effect of heat ageing	IEC 60216

Laminate

Tensile Test Methods	
ASTM D 3039	Tensile Properties of Polymer Matrix Composite Materials Specimen Type: Rectangular, with tabs
ASTM D 638	Tensile Properties of Plastics Specimen Type: Dumbbell
ISO 3268	Plastics - Glass-Reinforced Materials - Determination of Tensile Properties Specimen Type: Type I Dumbbell Type II Rectangular, no tabs Type III Rectangular, with tabs
SACMA SRM 4	Tensile Properties of Oriented Fiber-Resin Composites Specimen Type: Rectangular, with tabs
SACMA SRM 9	Tensile Properties of Oriented Cross-Plied Fiber-Resin Composites Specimen Type: Rectangular, with tabs

steel cord belt ply of tire

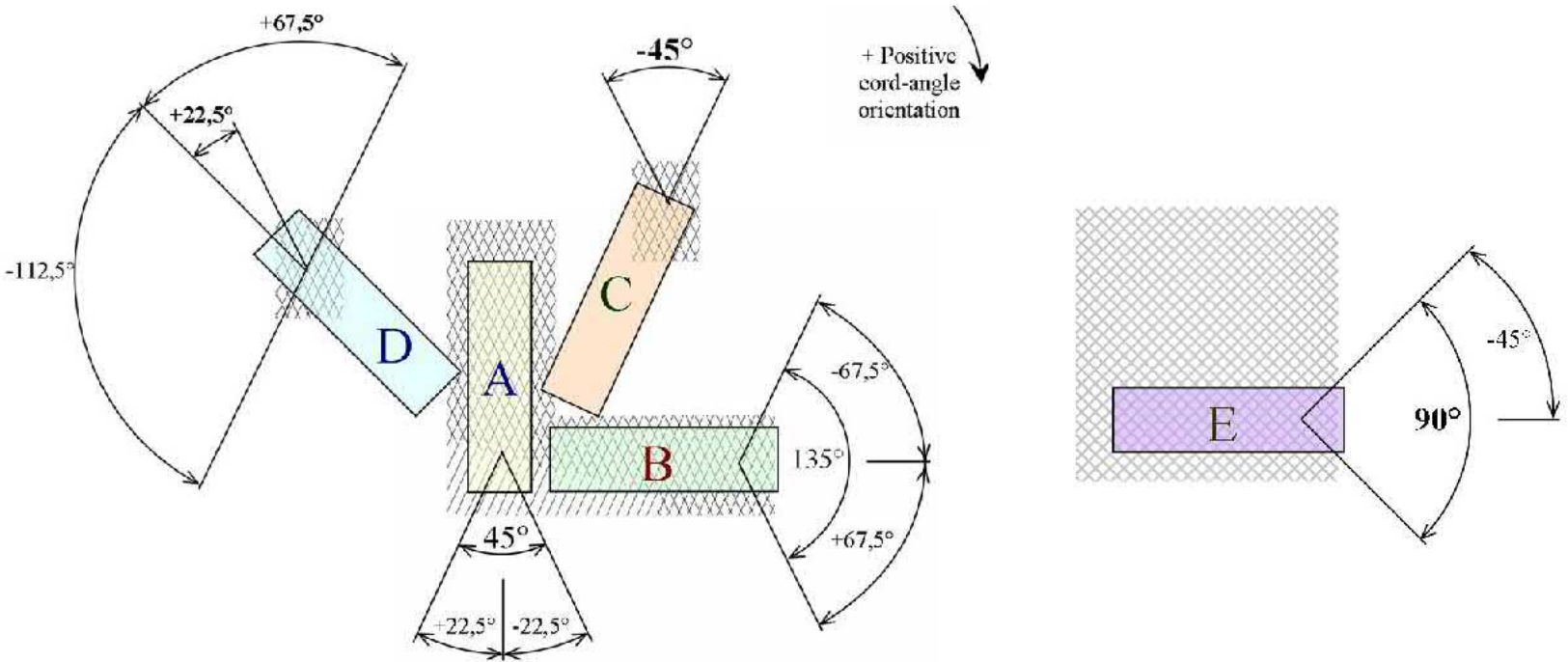

The samples must have different:

- **Angle** of cord (with respect of the direction of loading – not only longitudinal and transverse orientated samples);
- **Material** of cord (surface treatment);
- **Form** of cord (wire, thin wire);
- **Number of layers** (single-layer, two-layer, multi-layer);
- Specimen **width, shape** etc.

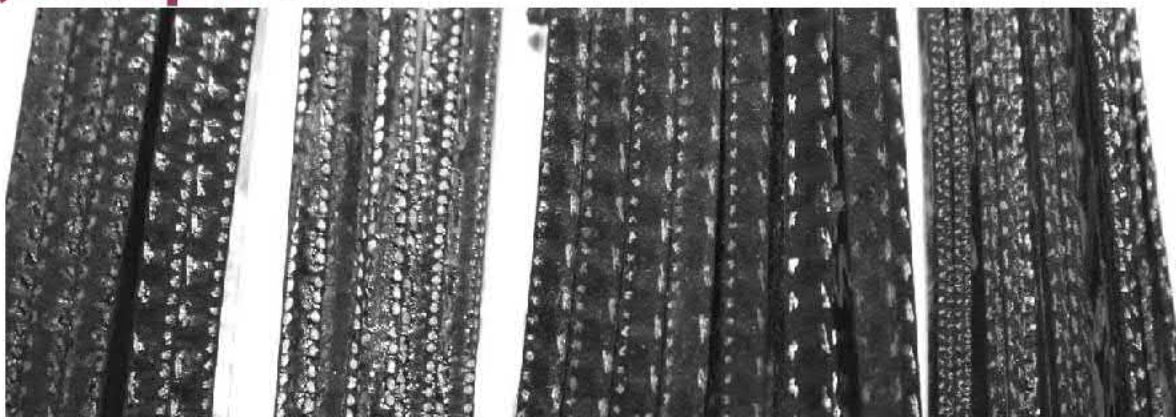

designed multi-layer test samples with different wide 10, 15 and 25 mm and of length 120 mm. The cord-angle orientations in single-layer specimens are 0°, 22.5°, 45°, 67.5° and 90°. Two-layer specimens are symmetrically orientated between top/bottom layer ±22.5°, ±67.5°, ±45° and asymmetrically orientated with cord-angles +0°/-45° and +67.5°/+22.5° (it is +22.5°/-112.5°, specimen D) with thickness 4 mm.

cutting machine with abrasive water jet (AWJ) technology

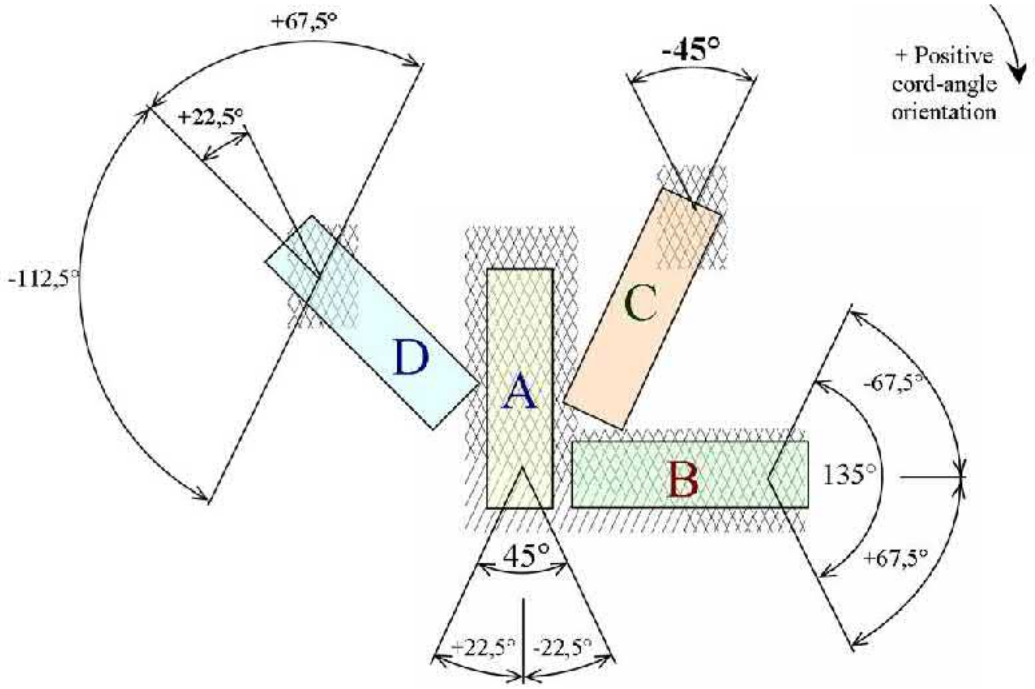

Geometrical parameters of sample

length …. 120 mm

wide ….. 10, 15 and 25 mm.

Also must be determined conditions for individual type of tests:

- **Statically tensile** tests (uniaxial and biaxial);
- **Statically bend** tests;
- Statically tests of composites under **combined loading** states (combinations tensile with bend) - that are to be approximated tire real state during tire operational loading (predicate about real deformation behaviors of steel-cord belt plies);
- **Corrosion tests** in a corrosion chamber (exposition time);
- **Dynamically test** etc.

Test condictions

Tensile

- Initial length between the jaws of the testing machine is 92 mm;
- Elongation measured on the same length and also measured on 50 (or 25 mm) in centre of specimens;
- Rate of test is 10 or 25 mm/min.

Bend

- tree-point;
- distance between end points 50 mm.

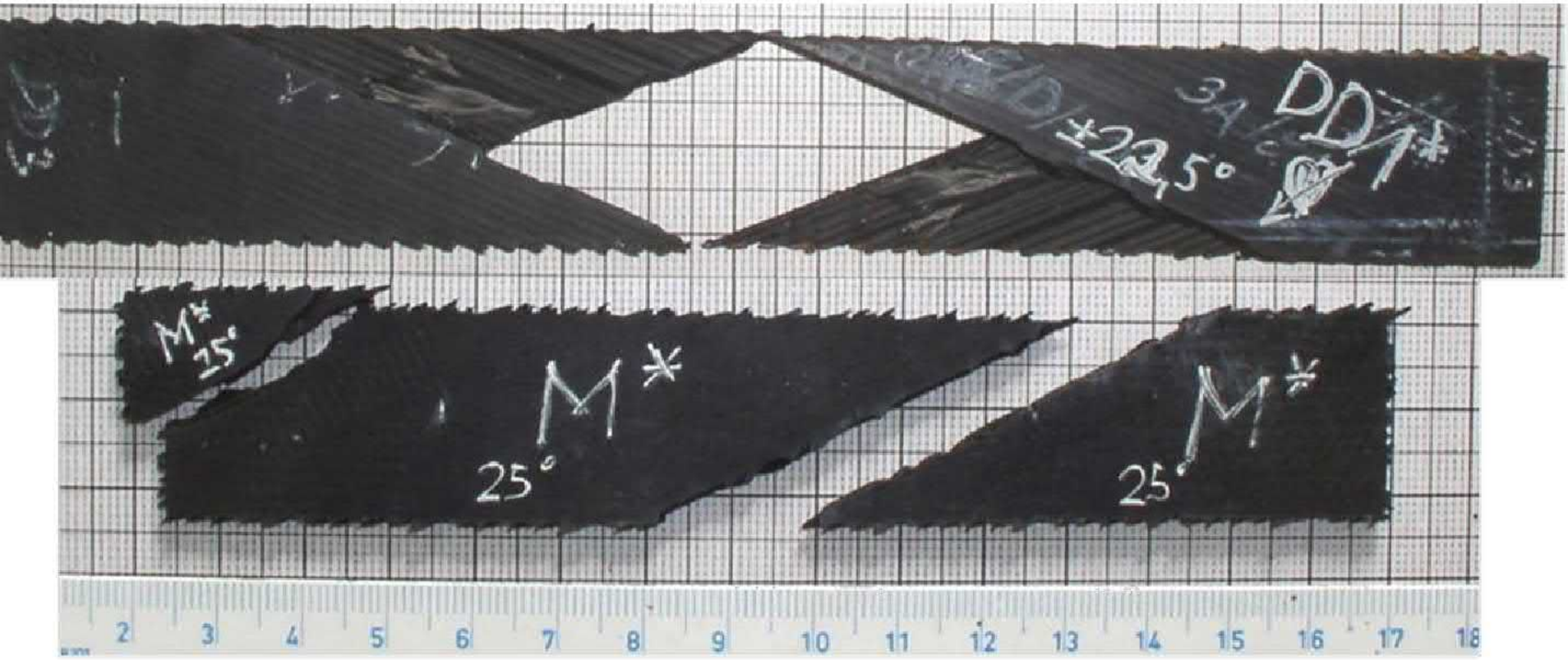

One layer versus two layers

symetrical

Asymmetrical

Failure of two-layer symmetrical ±22.5° and asymmetrical specimens +67.5°/+22.5° (right) after tensile test

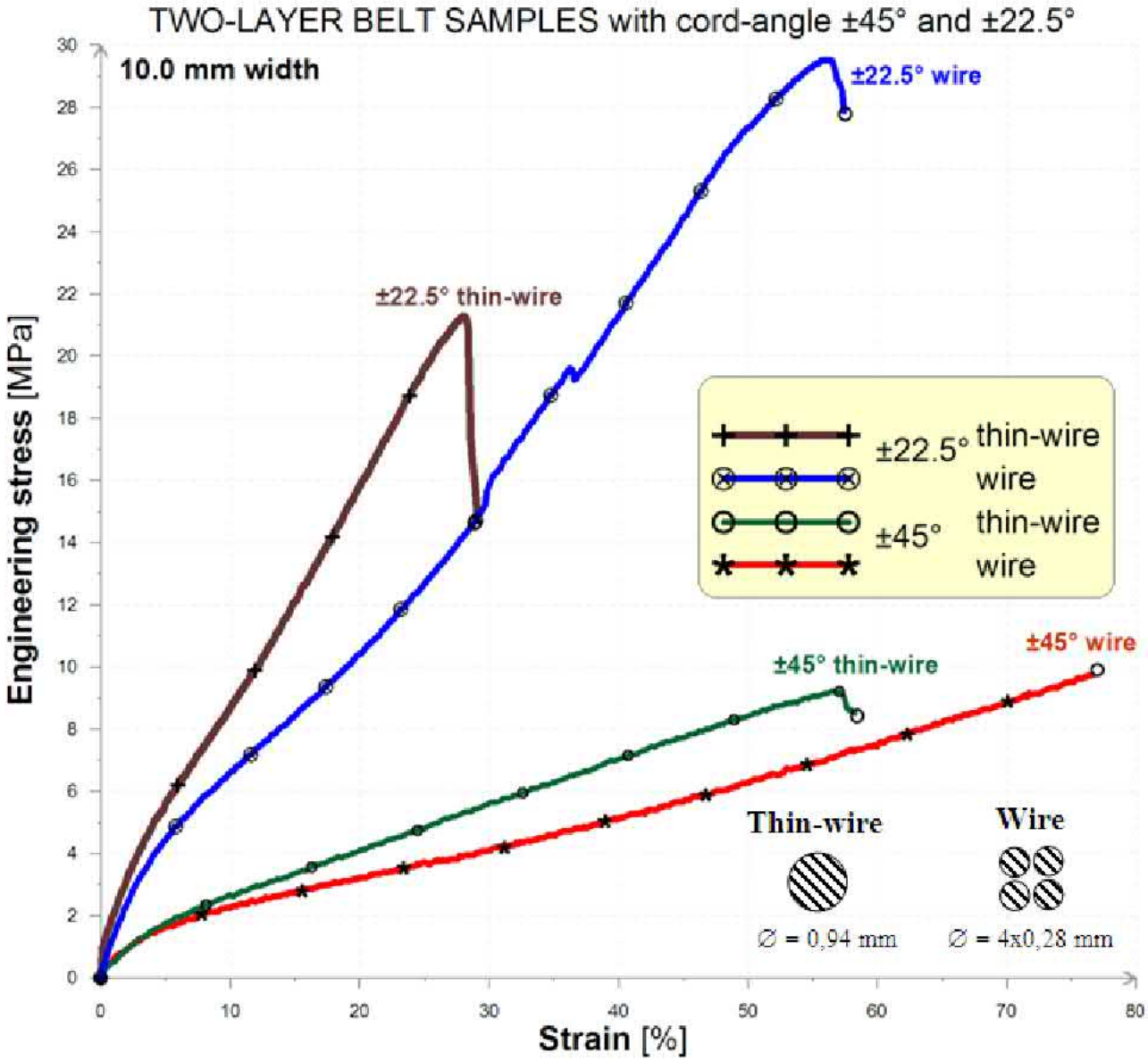

Outputs from tensile test of steel-cord belt samples – stress-strain dependences

Test of steel-cord belt

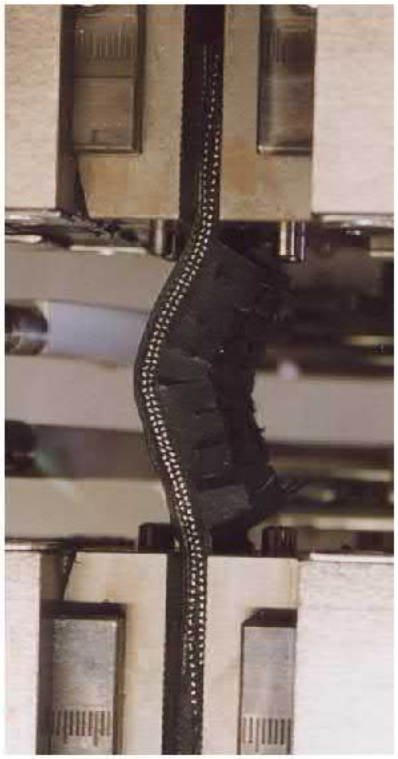

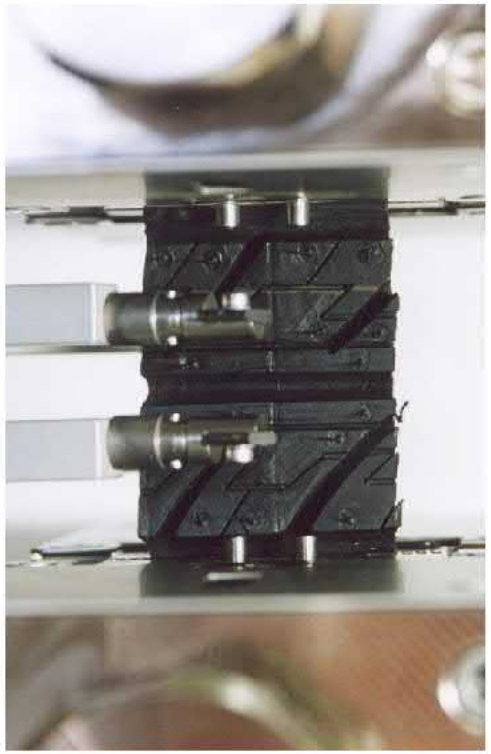

Tensile test.

SIMPLE TYPES OF LOADING

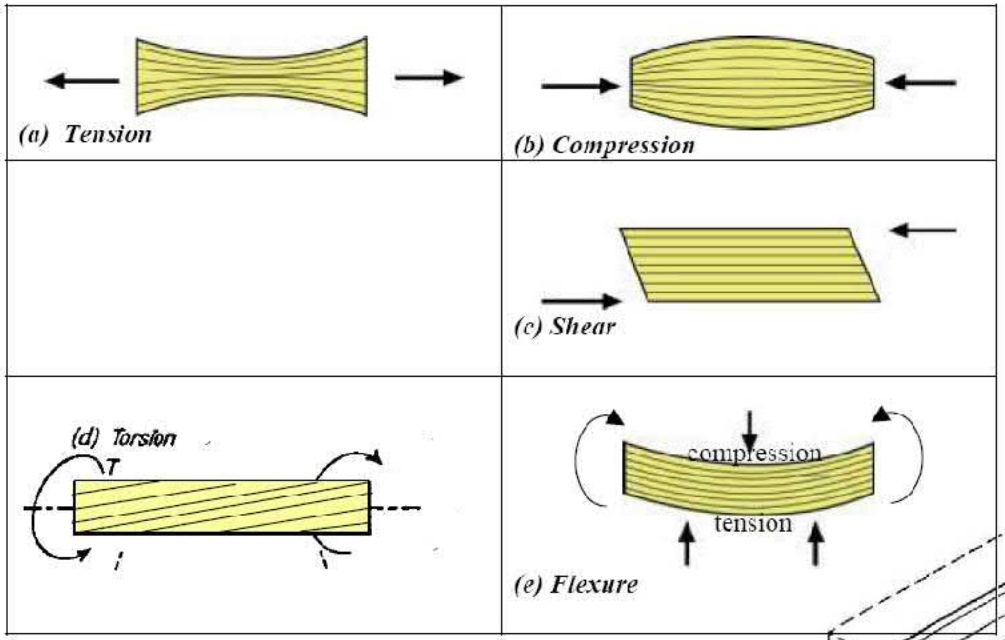

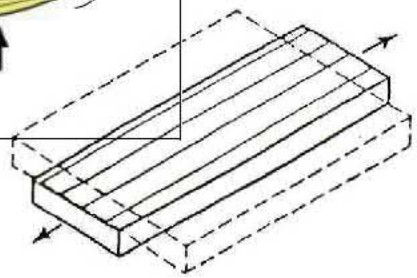

a Orthotropic Lamina

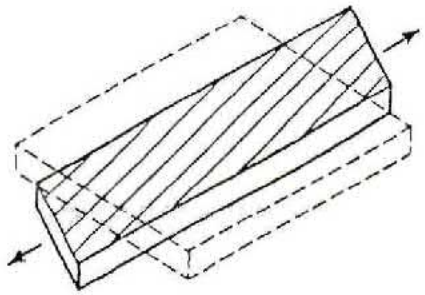

b Tension–Shear Coupling

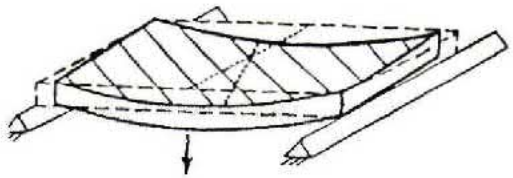

c Bending–Twisting Shear Coupling

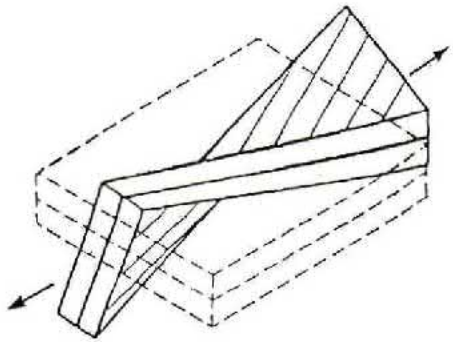

d Tension–Twisting Coupling

Illustration of tension/shear/bending coupling effects which are observed in cord/rubber laminates.

EXPERIMENTS OF PART OF TIRE CASING

The tire casing was cut by water jet cutter in longitudinal and transverse direction in order to obtain the specimens from the whole under-tread reinforcing area of the casing. The specimens were prepared with different width and it was 10, 15 and 20 mm.

The static tensile tests and bend tests were performed for the specimens in an agreement with standard specifications and it was with the aim to obtain modulus of elasticity for different directions of configuration of specimens.

Specimens - cuttings in longitudinal direction (up) and transverse direction (down) with different width, prepared for performance of the tensile and bend tests

The main purpose of the research was to determine the required materials parameters for the reinforcing layers in relation to selected casing which is designated as 245/40 R18 type. The chosen tire casing was cut by water jet cutter in longitudinal and transverse direction in order to obtain the specimens from the whole under-tread reinforcing area of the casing. The specimens were prepared with different width and it was 10, 15 and 20 mm. The static tensile tests and bend tests were performed for the specimens in an agreement with standard specifications and it was with the aim to obtain modulus of elasticity for different directions of configuration of specimens.

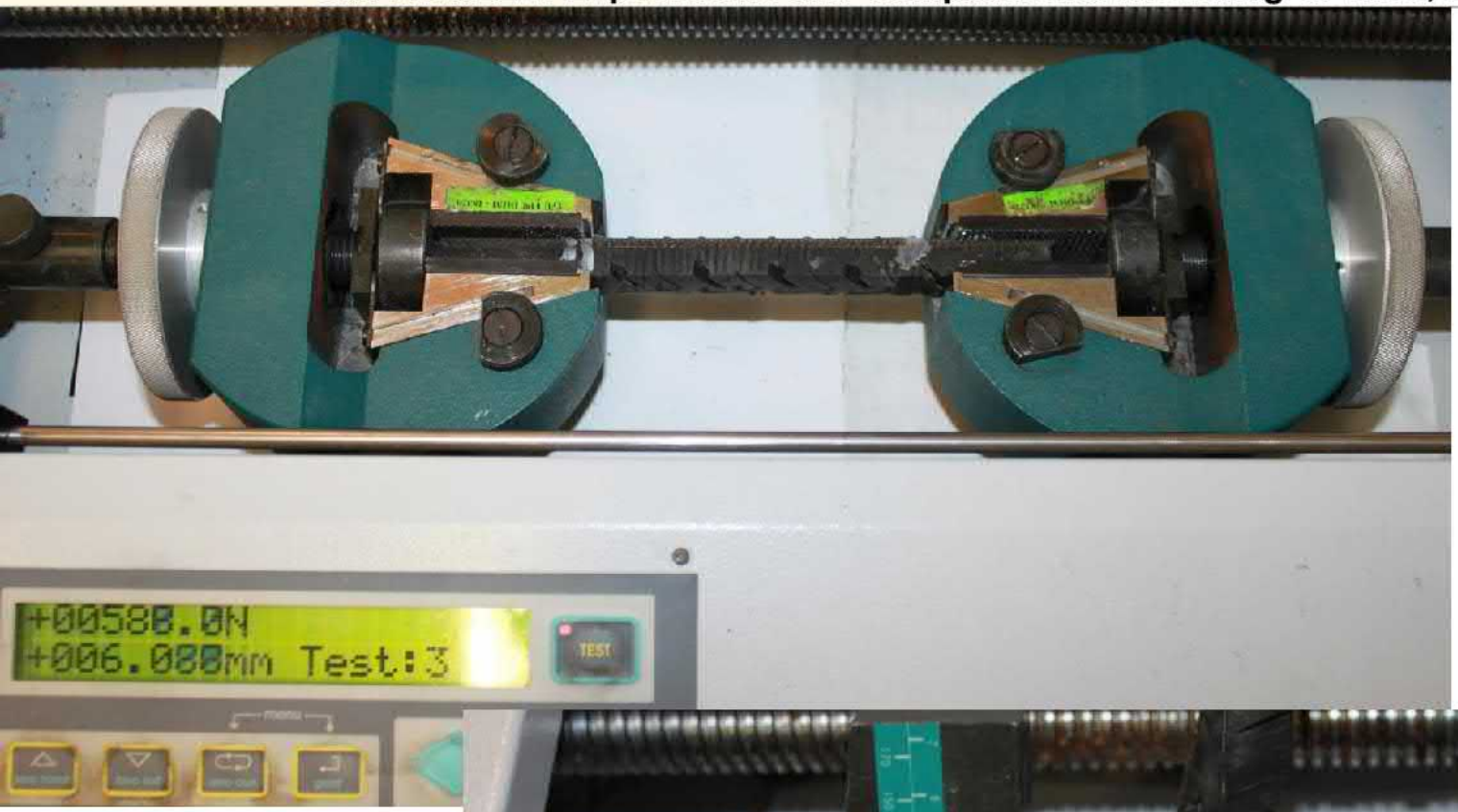
+00588.0N
+006.088mm Test:3
TEST

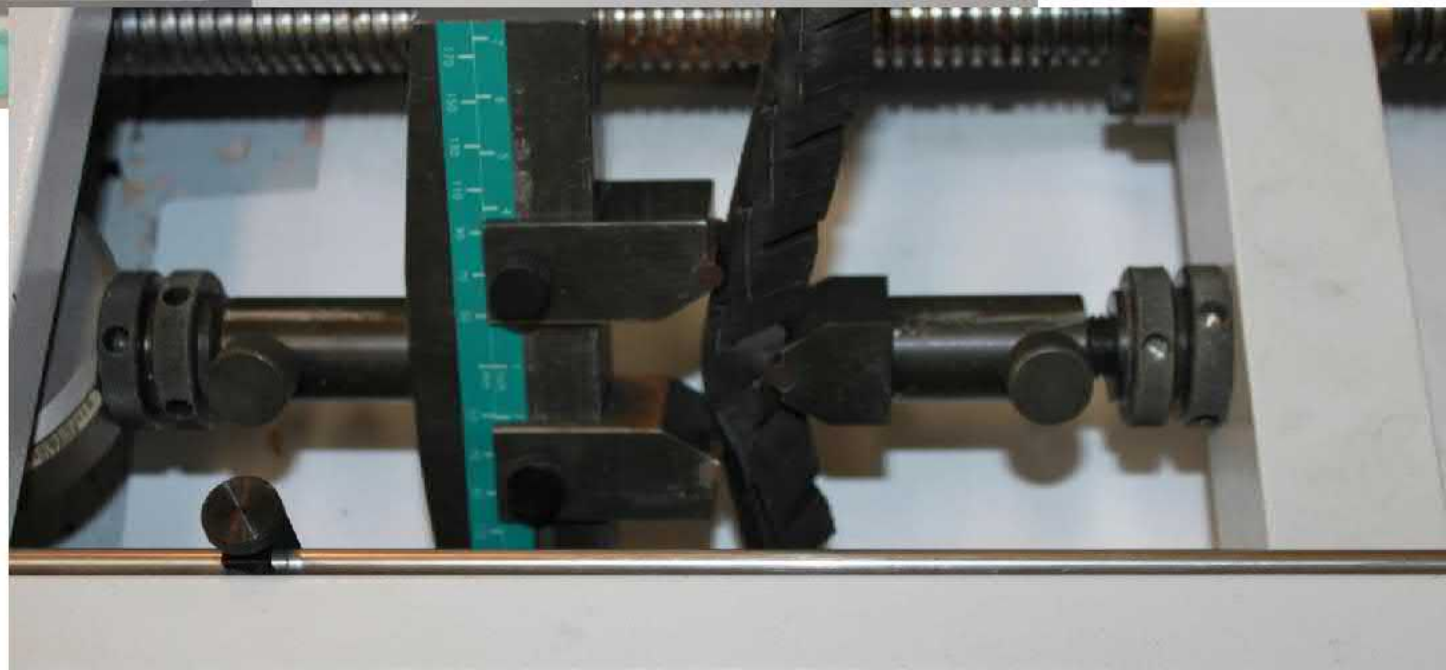

The conditions of the tensile tests were:

- **Starting value of length between clamps of test machine was 100 mm;**
- **Elongation measured on the same length;**
- **Loading speed was 10 mm/min.**

The conditions of the bend tests were:

- **The value of distance between outside points was 50 mm;**
- **The loading speed was 5 mm/min**

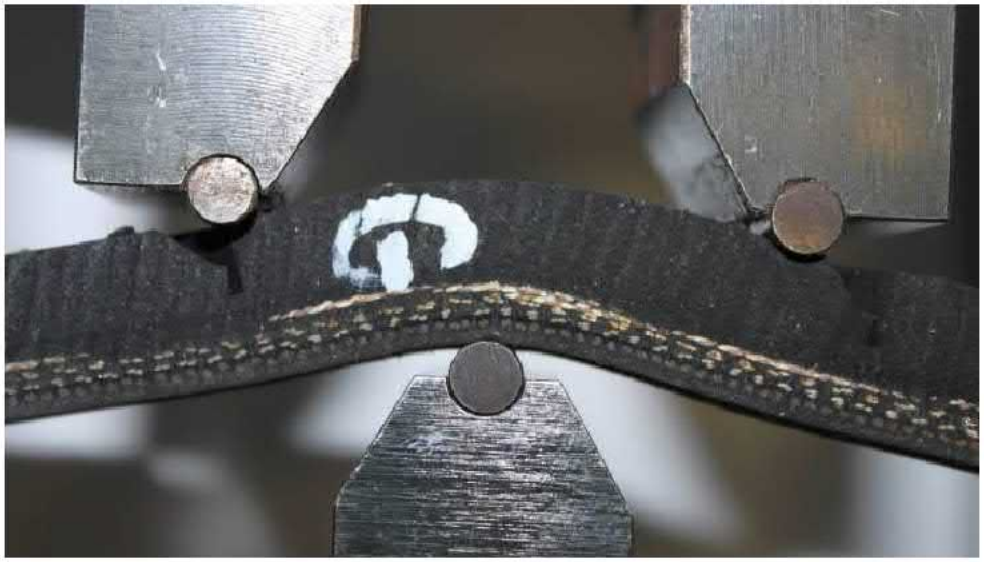

Specimens in radial direction with and without tread after bending loading

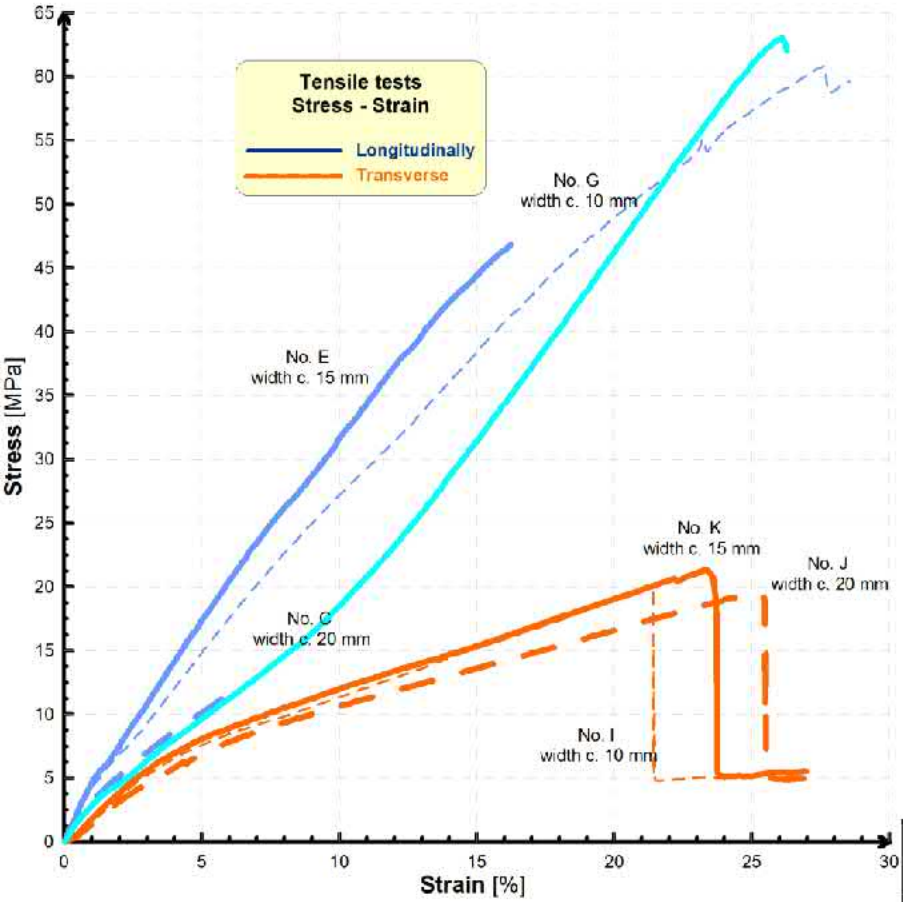

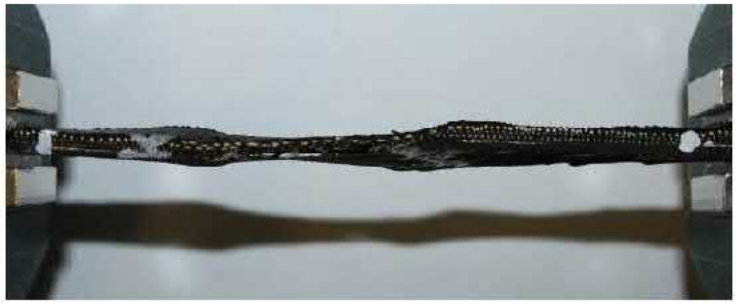

MODULES OF ELASTICITY

STRESS-STRAIN DEPENDENCES

Modulus of elasticity [MPa]		Specimen width 10 mm	15 mm	20 mm
Loading in direction	Longitudinally [1]	380	400	285
	Transverse [1]	200	205	185
	Radial [2]	90-110 for longitudinally specimens		

[1] modules of elasticity from tensile tests

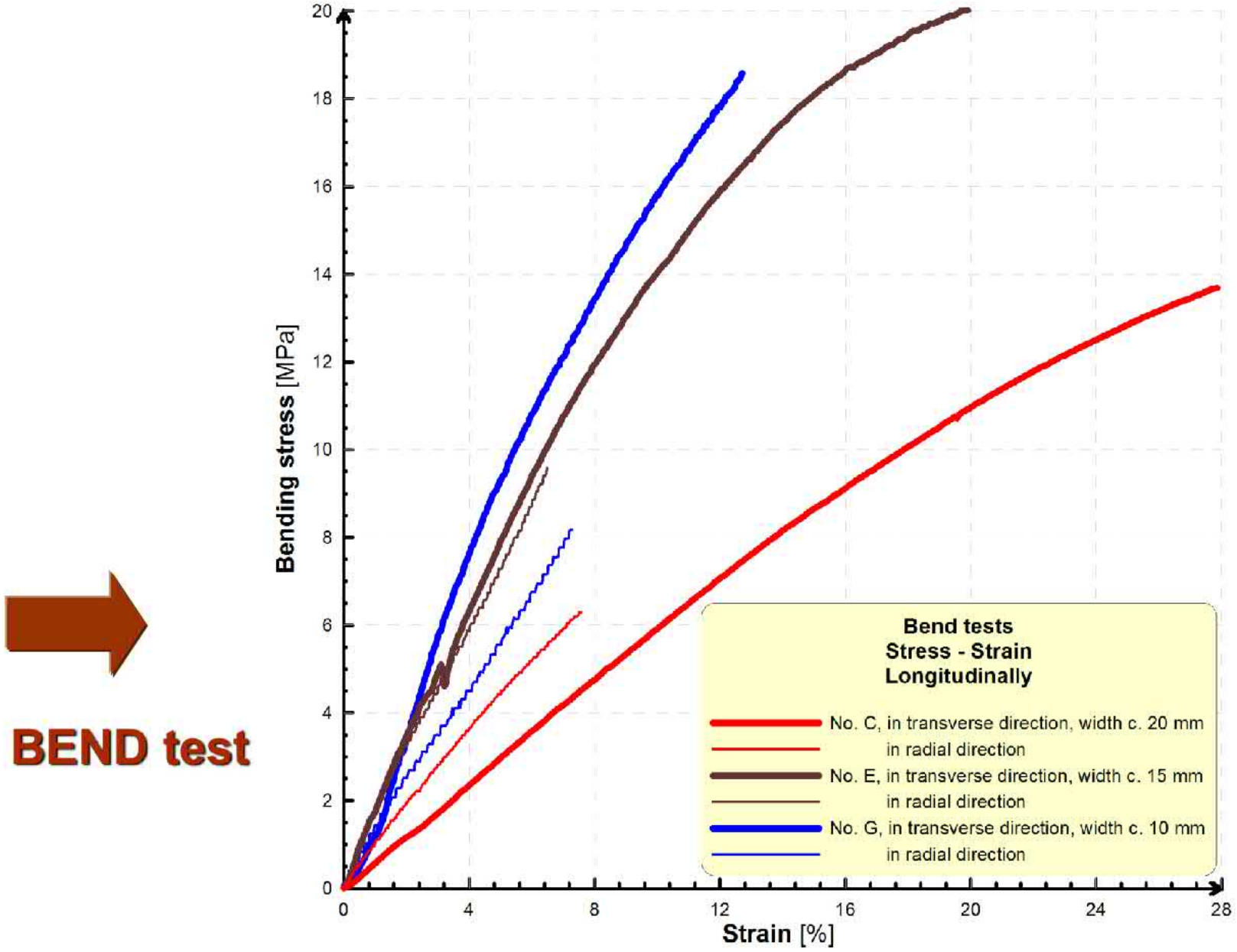
Bending stress [MPa]
Strain [%]
0
2
4
6
8
10
12
14
16
18
20
0
4
8
12
16
20
24
28
Bend tests
Stress - Strain
Longitudinally
No. C, in transverse direction, width c. 20 mm
in radial direction
No. E, in transverse direction, width c. 15 mm
in radial direction
No. G, in transverse direction, width c. 10 mm
in radial direction

BEND test

Specimen No.	**Steel –cord belt** accordant with the tire	**Cord-angle** [°]	**Specimen geometry** width x thickness [mm]
1	165 R13	±23°	14.3 x 2.4
2	235/65 R17	±32°	14.0 x 1.0
3	MATADOR unspecified	±23°	14.0 x 1.5
4*	not from real tire	±23°	14.3. x 4.5
5	BARUM unspecified	±31°	14.0. x 1.0

The concrete initial conditions which were used – speed of loading is 10 mm/min and initial length of specimen between brackets of tensile test machine is 80 mm.

No. 1

No. 2

No. 3

No. 4

No. 5

Specimens after tensile tests

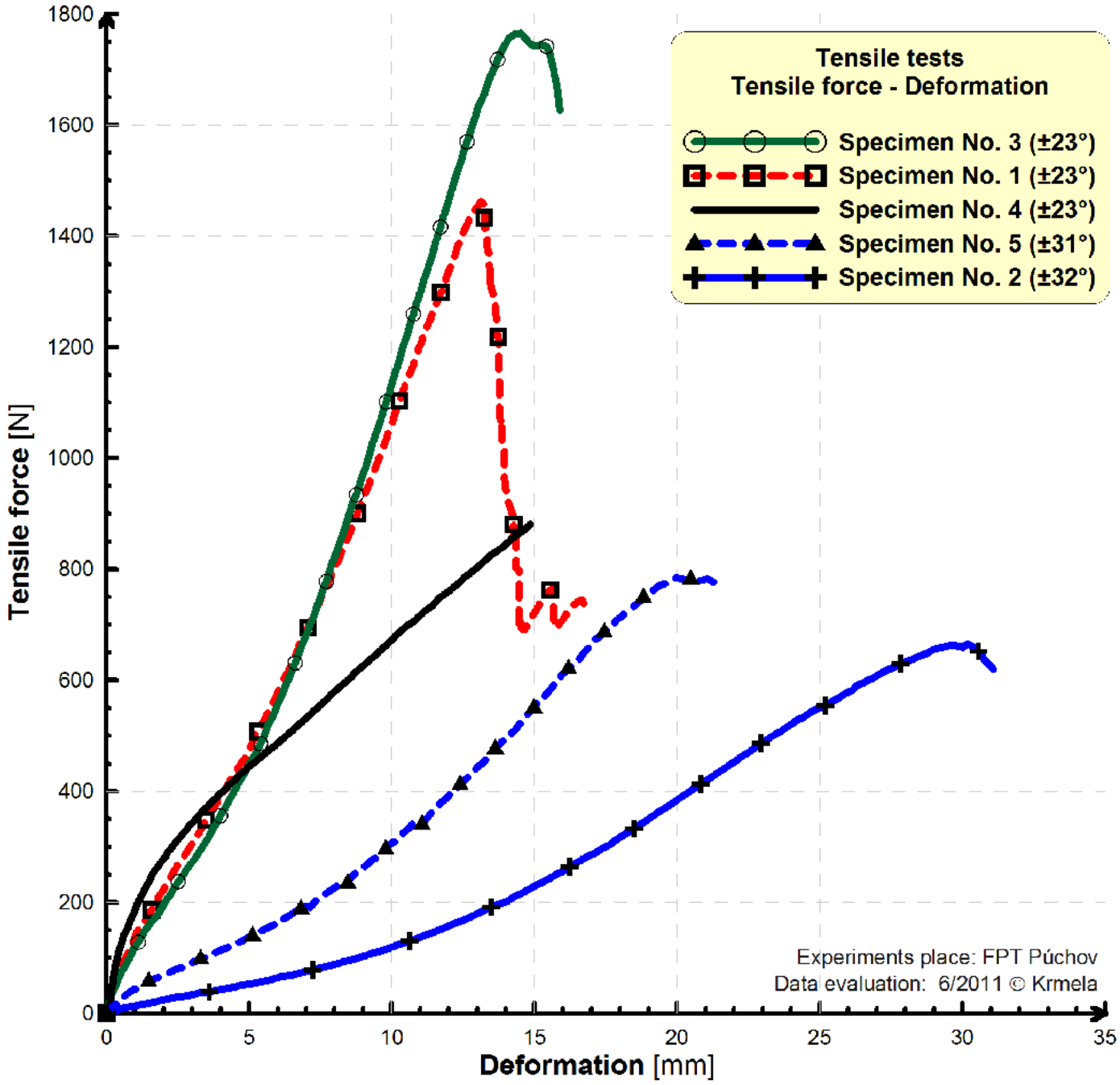
Tensile tests
Tensile force - Deformation
Specimen No. 3 (±23°)
Specimen No. 1 (±23°)
Specimen No. 4 (±23°)
Specimen No. 5 (±31°)
Specimen No. 2 (±32°)
Tensile force [N]
Deformation [mm]
0
200
400
600
800
1000
1200
1400
1600
1800
0
5
10
15
20
25
30
35
Experiments place: FPT Púchov
Data evaluation: 6/2011 © Krmela

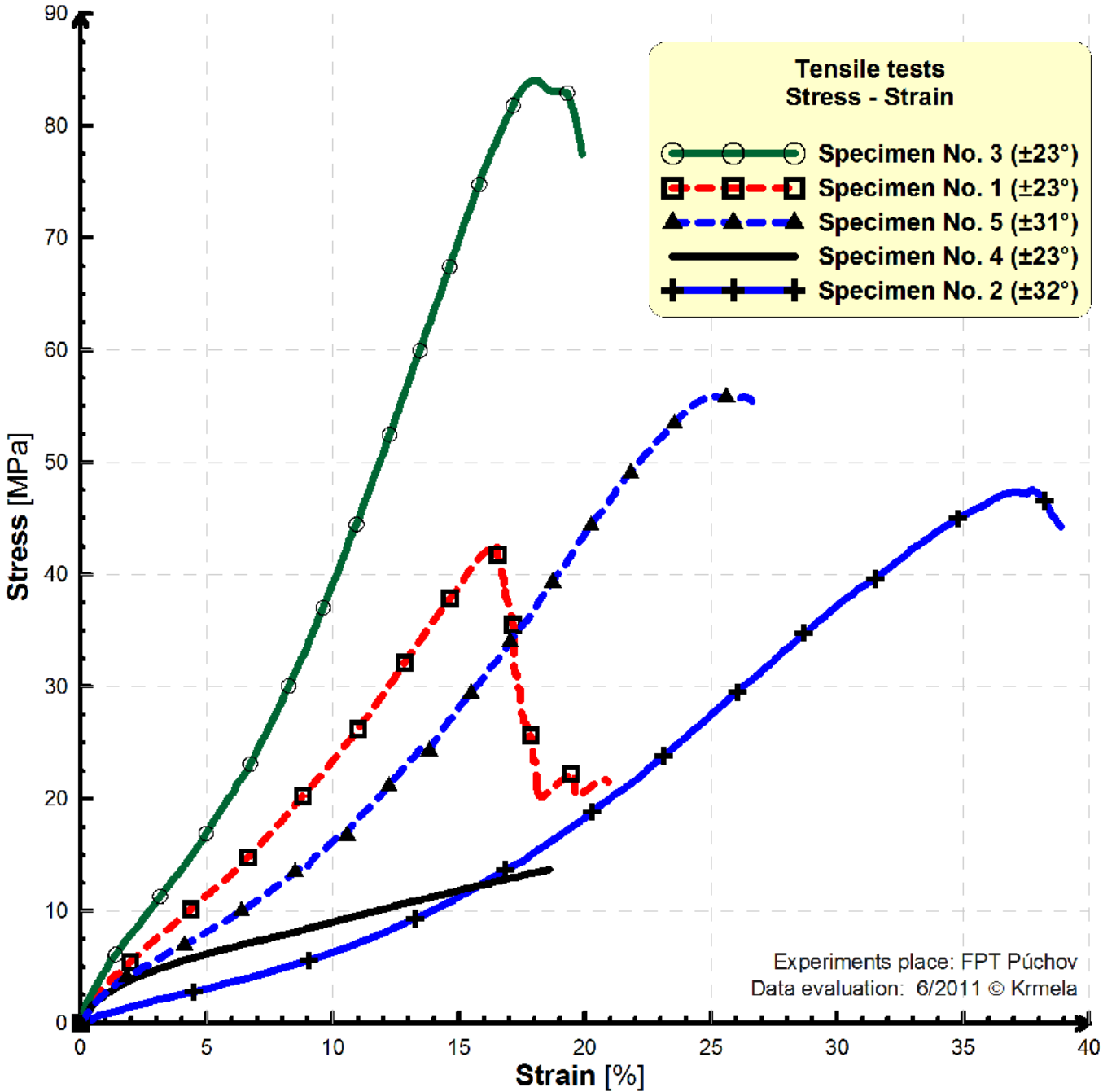
Tensile tests
Stress - Strain
Specimen No. 3 (±23°)
Specimen No. 1 (±23°)
Specimen No. 5 (±31°)
Specimen No. 4 (±23°)
Specimen No. 2 (±32°)
Stress [MPa]
Strain [%]
0
10
20
30
40
50
60
70
80
90
0
5
10
15
20
25
30
35
40
Experiments place: FPT Púchov
Data evaluation: 6/2011 © Krmela

METHODS FOR DETERMINATION OF MODULUS OF ELASTICITY

As the first method we have selected a method based on 0-8% strain. Principle of the method consists in calculating the value of 8% strain of the specimens. From intersection of the graph we read the values for applied force for given strain and these values insert into the equation for calculating modulus of elasticity.

Other methods are similar, but we change the values of the strain of 4-8%, 0-10% and 4-10%. The last method is based on reading values of strain of linear part of graphs. The strain into tires is moving between 0-10%. By reason of the most accurate determination of modulus of elasticity we suggested just these computing methods.

$$E = tg\alpha = \frac{\sigma}{\varepsilon} = \frac{F \cdot l}{\Delta l \cdot S} = \frac{\left(F_n - F_0\right) \cdot l}{\left(l_n - l_0\right) \cdot S} \ [\text{MPa}]$$

Where:

E [MPa] ..... the modulus of elasticity;

σ [MPa] ..... the stress;

ε [%] ..... the strain;

F [N] ..... the tensile force applied to the specimen;

l [mm] ..... the initial length of the specimen between brackets of tensile test machine;

S [mm^2] ..... the initial cross-section area of specimen;

Δl [mm] ..... the length through which the specimen is elongated amount;

F_n [N] ..... ending tensile force for concrete method;

F_o [N] ..... starting tensile force for concrete method;

l_n [mm] ..... ending elongation for concrete method;

l_o [mm] ..... starting elongation for concrete method.

Final modulus of elasticity for specific tire composite structure specimens

Specimen No.	**Methods** start – end of strain [%]	**E** [MPa]
1	0 – 8%	225.8
	4 – 8%	**218.5**
	0 – 10%	223.1
	4 – 10%	233.1
	linear part	265.4
2	0 – 8%	55.4
	4 – 8%	**53.6**
	0 – 10%	58.6
	4 – 10%	59.5
	linear part	200.0
3	0– 8%	357.1
	4 – 8%	**380.9**
	0 – 10%	380.9
	4-10%	412.6
	linear part	1 023.1

4	0– 8%	109.2
	4 – 8%	**65.5**
	0 – 10%	101.3
	4-10%	67.0
	linear part	64.0
5	0– 8%	106.7
	4 – 8%	**151.7**
	0 – 10%	160.7
	4-10%	154.7
	linear part	295.2

From the results was the task as precisely as possible the method for determination of the modulus of elasticity, which is suitable for other specimens of steel-cord belt configurations.

Because of nonlinear character given depending, force-deformation dependences, we have identified several methods that we consider most appropriate for determination of modulus of elasticity. The comparing of the results of modulus of elasticity obtained by individual methods between the specimens, we concluded that the most appropriate method to calculate of modulus of elasticity of steel-cord belts is a method based on determination of the modulus of elasticity of 4-8% elongation.

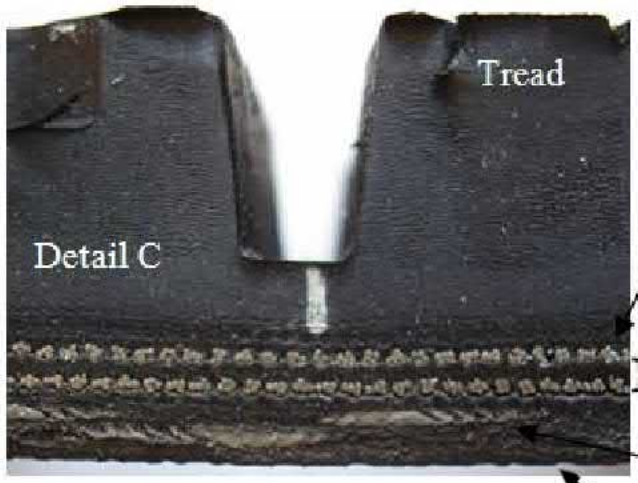

Textile overlap belt layer

Steel-cord belt two-layer
(cord 2+2x0.28 mm)

Textile carcass two-layer

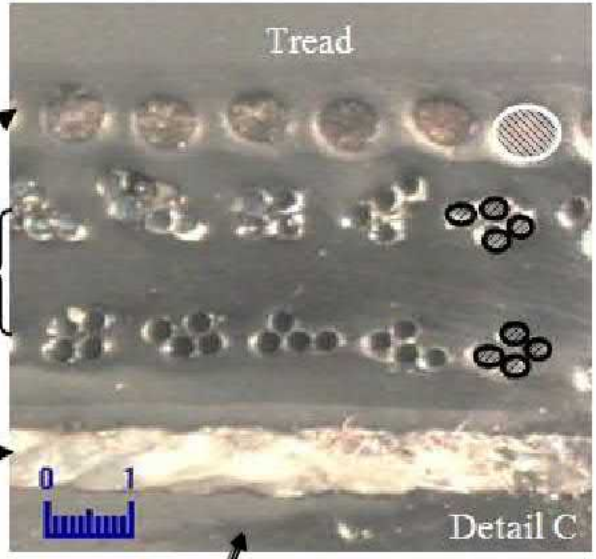

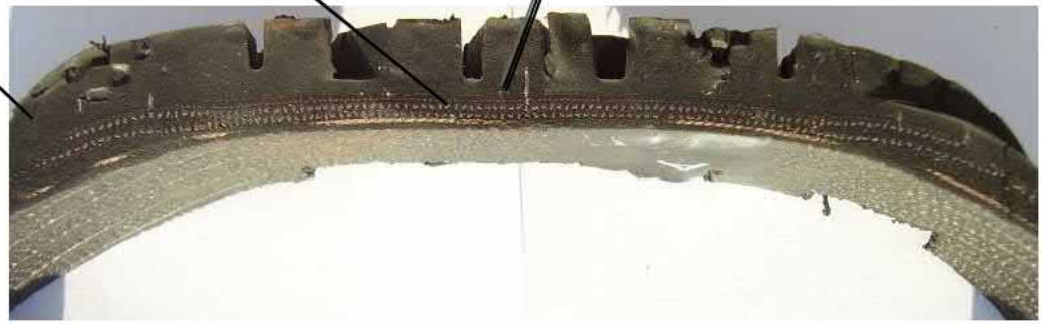

The photographic documentation showing the geometric configuration of reinforcing cords in steel cord belts and tire-crown was supplied in order to obtain accurate geometric data which were needful for computational modeling of the given steel cord belt.

The software IMPOR 5.0 with plug-in ObjectMeasuring is used for image analysis.

The geometric parameters of the reinforcements of tlre-casing 245/40 R18 in place end of steel-cord belts are showed on the Figure 6 on the left and schematic structure in the center of the tread is on the right. The EPM of textile cap ply is 800÷900 m^{-1}.

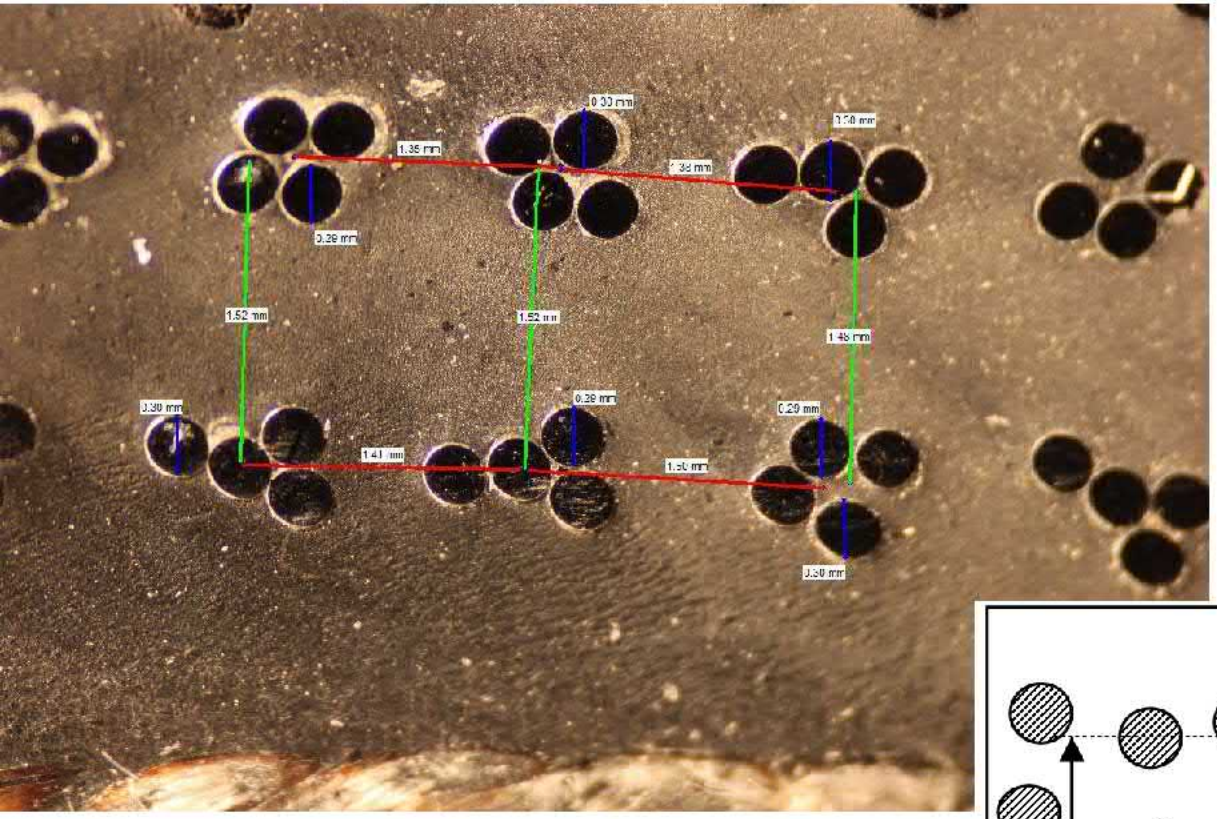

PHOTOGRAPHS ANALYSES

Thickness of layers *t* [mm]
Diameter of cords *D* [mm]
Construction of steel-cords
Number of steel-cords per decimeter width of one steel-cord belt layer (plumb on cords) [10cm^{-1}] (EPDM) ……

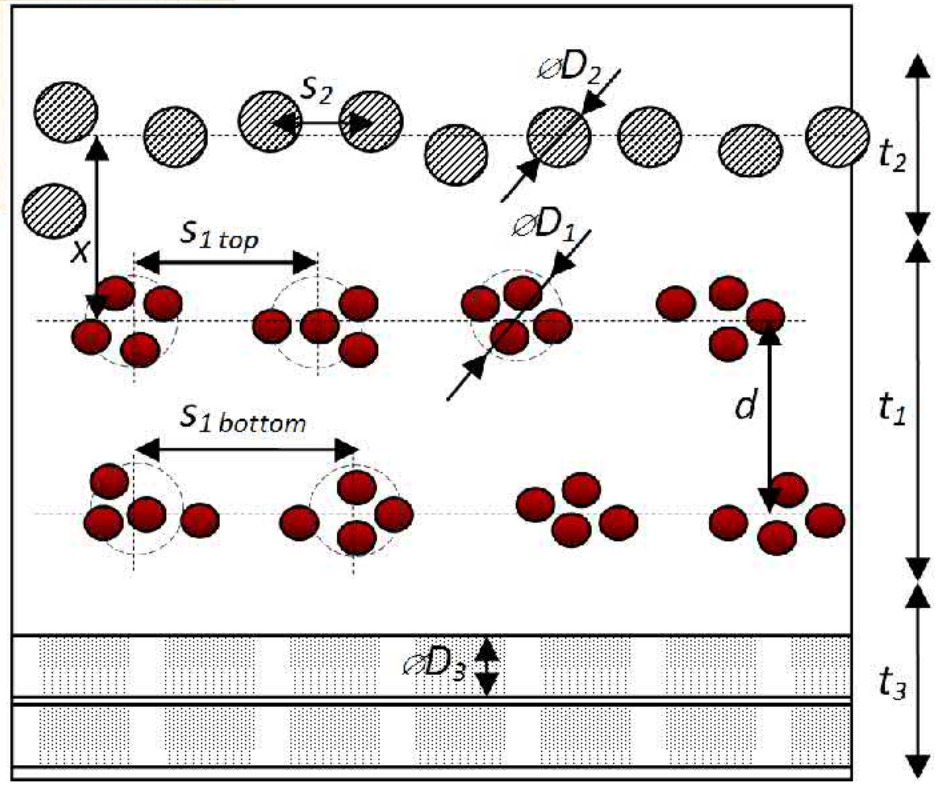

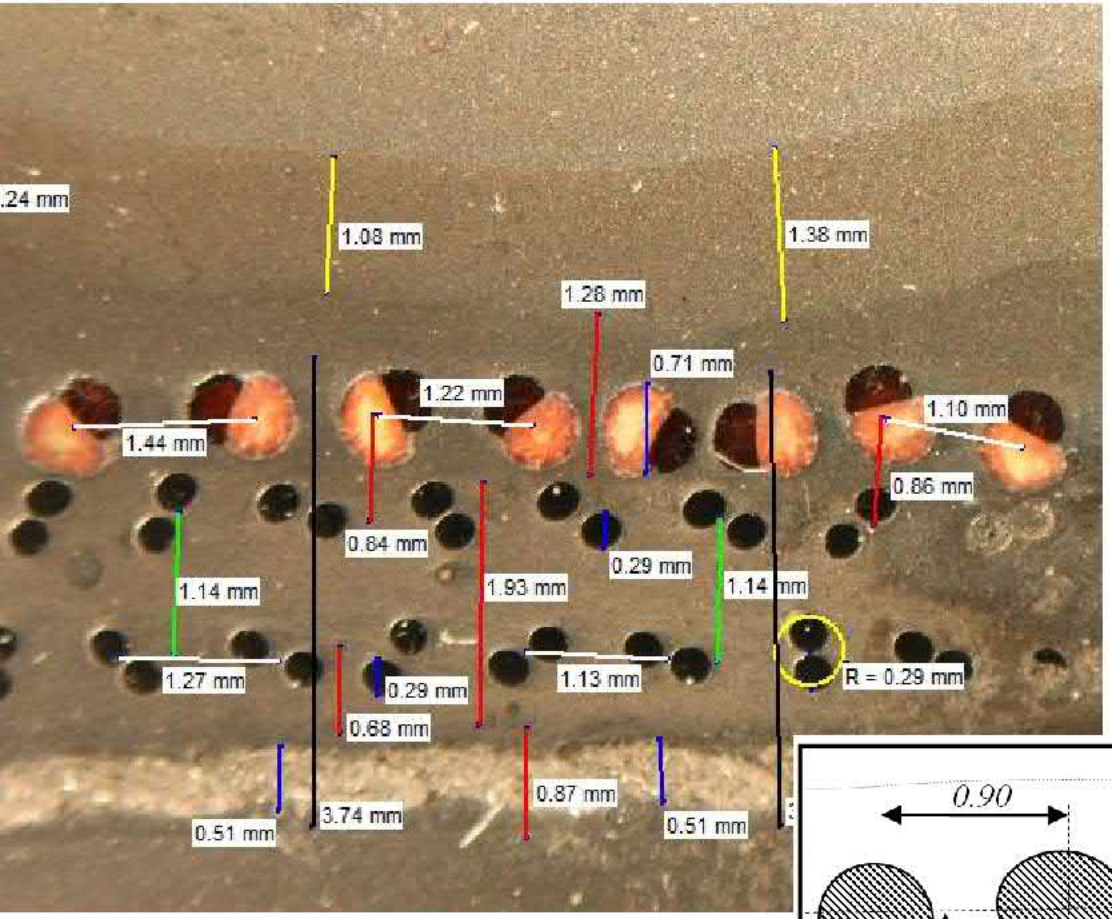

PHOTOGRAPHS ANALYSES

Thickness of layers *t* [mm]
Diameter of cords *D* [mm]
Construction of steel-cords
Number of steel-cords per decimeter width of one steel-cord belt layer (plumb on cords) [10cm^{-1}] (EPDM) ……

Structure of GEOMETRY in the tire-crown

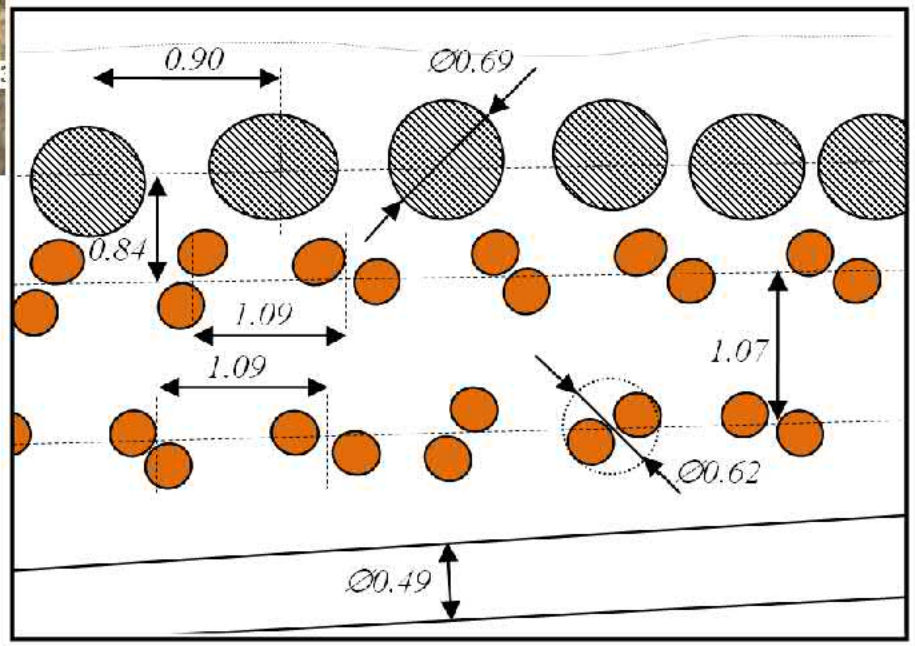

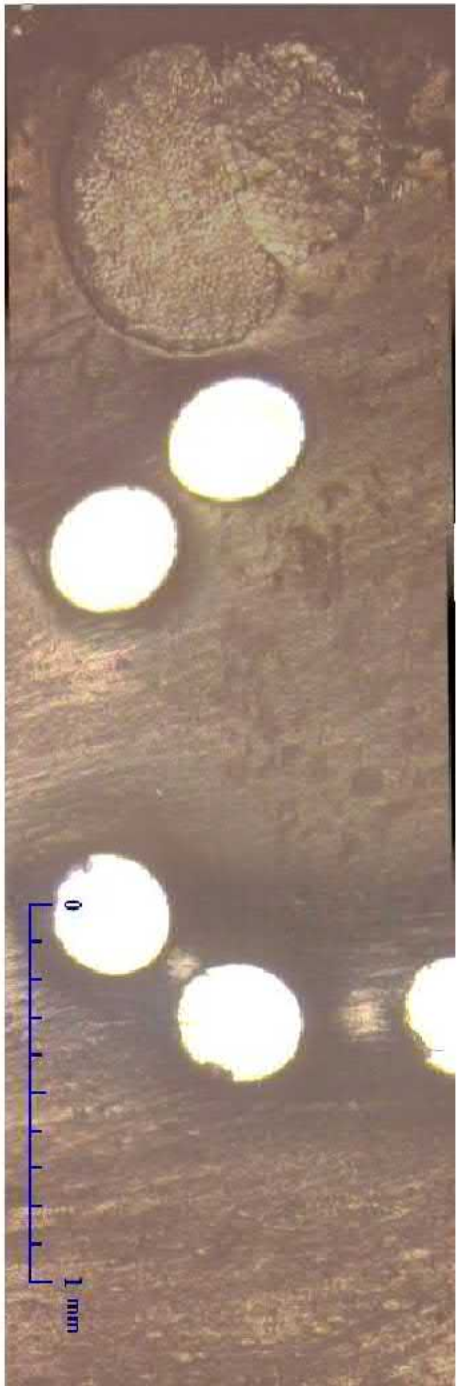

textile cord

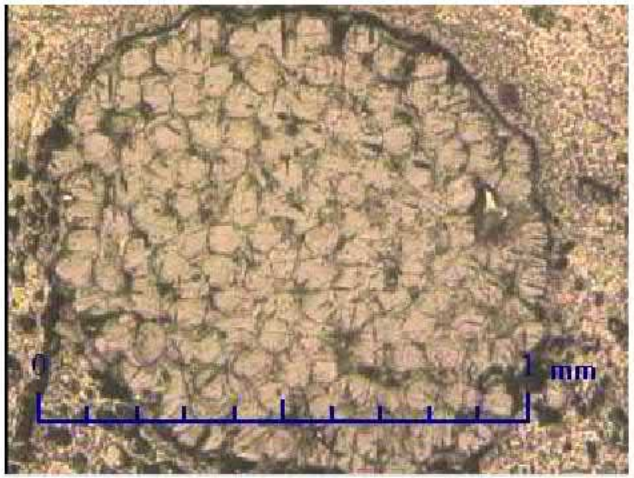

MICROSCOPY OBSERVATION

steel cord

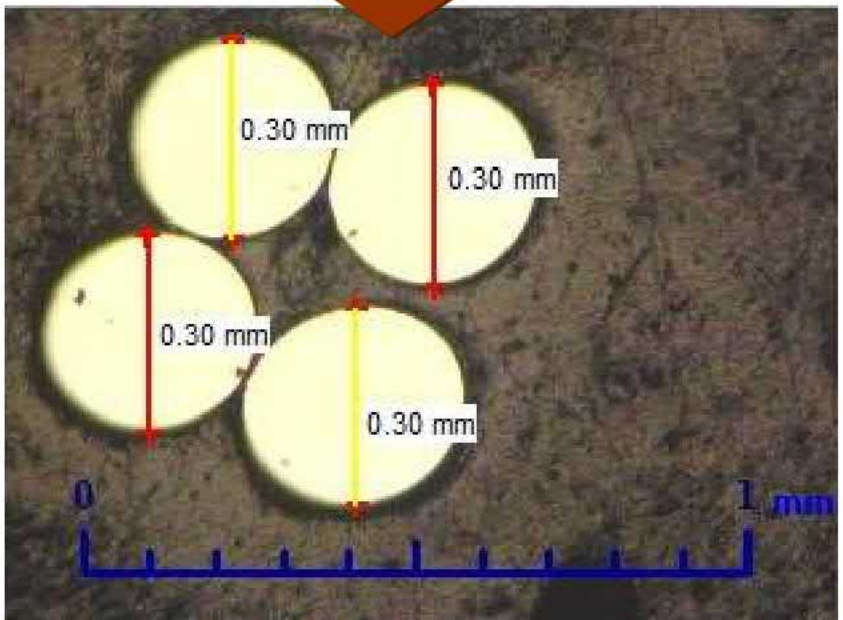

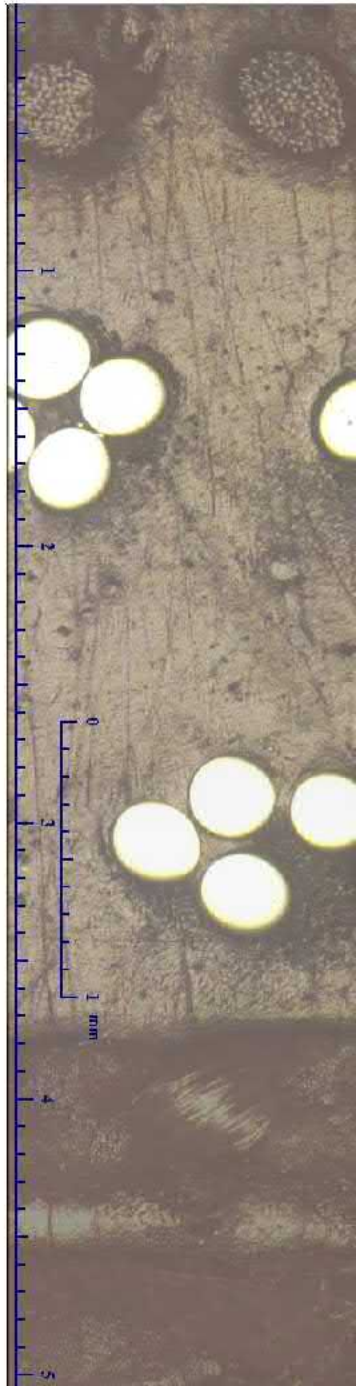

Composite structure parts of tire	Steel cord belt	Textile belt	Textile carcass
Number of layers [-]	2	1	1
Thickness of layers [mm]	2x0.98	1.28	0.92
Diameter of cords [mm]	0.62	0.69	0.49
Construction of steel cord belts	2x0.30		
Distance between middles of steel-cords in top and bottom layers [mm]	1.00÷1.14 1.07		
Spacing between middles of cords in layer [mm]	1.09 for top layer 1.09÷1.15 for bottom layer	0.90÷1.50 1.09	
Number of steel-cords per decimeter width of one steel-cord belt layer (plumb on cords) [$10cm^{-1}$]	920 for top layer 920÷960 for bottom layer		
Distance between middles of steel-cords in top layer of steel-cord belt and middles of textile cords in textile belt [mm]	0.69÷0.97 0.84		

Dynamic test DMA

Experimental tests were performed in order to obtain material characteristics and parameters of the selected parts of the tire casing as important material inputs into the calculations for verification and analysis of computer models with experimental data.

Samples were prepared from treads, alluvial mixtures and sidewalls of tree variously aged tire casings.

Dynamic DMA tests were performed on PYRIS Diamond test device from Perkin Elmer in the temperature range from -70 to 110 °C at frequency 1 Hz.

Dependencies of dynamic modules of elasticity from temperature obtained from DMA tests

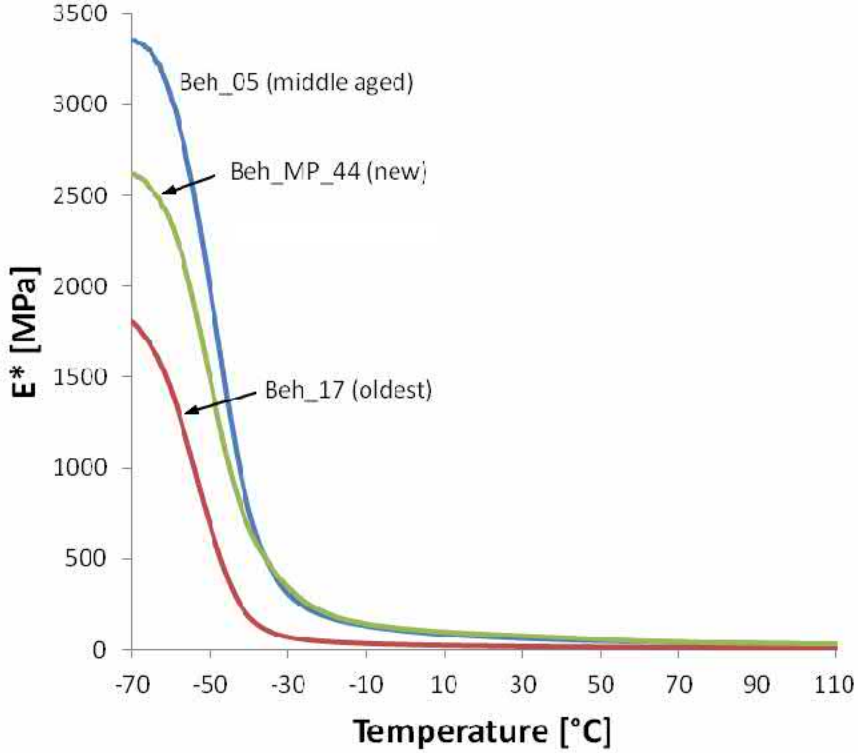

Dependency of elastic modulus E of treads from temperature*

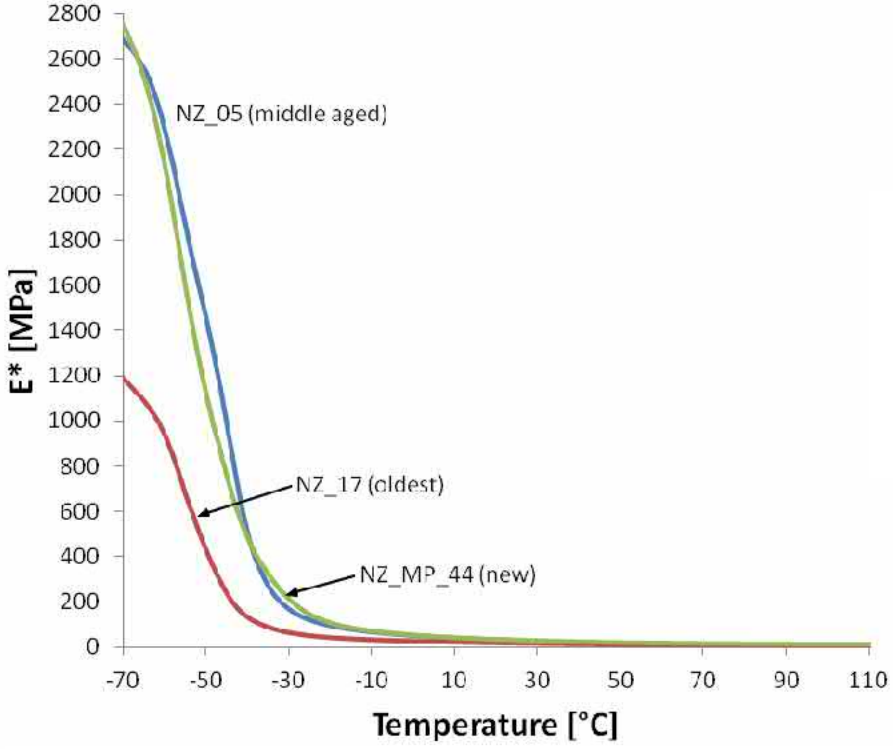

Dependency of modulus E of alluvial mixtures from temperature*

From the dependencies of load force from elongation static modules of elasticity were calculated.

Values of E of the samples at temperature 20 °C

Sample	*E* 05 (mid. aged) [MPa]	*E* 17 (oldest) [MPa]	*E* MP44 (new) [MPa]
Tread	5.34	11.22	20.07
Sidewall	1.02	1.52	0.65
Alluvial mixture	2.73	2.01	1.34

Values of dynamic modulus E at 20 °C*

Sample	E^* 05 (mid. aged) [MPa]	E^* 17 (oldest) [MPa]	E^* MP44 (new) [MPa]
Tread	72.70	18.21	86.74
Sidewall	21.06	13.98	33.01
Alluvial mixture	34.79	19.70	33.01

IRHD hardness tester the hardness of the selected variously aged tire casing parts was determined.

Values of IRHD hardness

Sample	*IRHD* MP44 (new) [-]	*IRHD* 05 (mid. aged) [-]	*IRHD* 17 (oldest) [-]
tread	72.83	73.50	79.33
sidewall	43.17	56.67	65.00
alluvial mixture	44.00	51.50	62.17

From the dynamic and static experiments modules of elasticity of tread, sidewall and alluvial mixture samples were determined and compared. The results show that the dynamic modules have much higher values than the static ones.

From the results of the IRHD hardness test can be clearly seen that hardness increases with age. This is most significant in the results for tread samples. From all of the results can be concluded that the oldest tire casing is significantly degraded.

Part 5 – DEGRADATION PROCESSES:

Degradation, Limit state, Corrosive test, Outputs from tensile tests, Microscopic evaluation of interaction of the cord – rubber (elastomer)

The part deals with experimental study of the adhesive bond between a steel-cord and non-linear matrix upon failure after corrosion test. The corrosion causes birth of dangerous delaminations on steel-rubber interface. Therefore, is necessary to deal with adhesive bond upon failure into microlocality. For experiments was used metallography observation and statically test for analyses of uniaxial stiffness. The obtained results from experiments will be used namely to computational modeling of steel belt of tire.

The knowledge about experimental modeling of tire from macrostructure and microstructure are necessary for computational modeling. The essential factor expressive influence on coherence of whole tire, are good adhesive bonds between reinforcement materials and rubber parts of tire.

The tire steel-cords are exposed to various chemical and thermal influences during cyclic loading states by tensile-compression in tire loading processes.

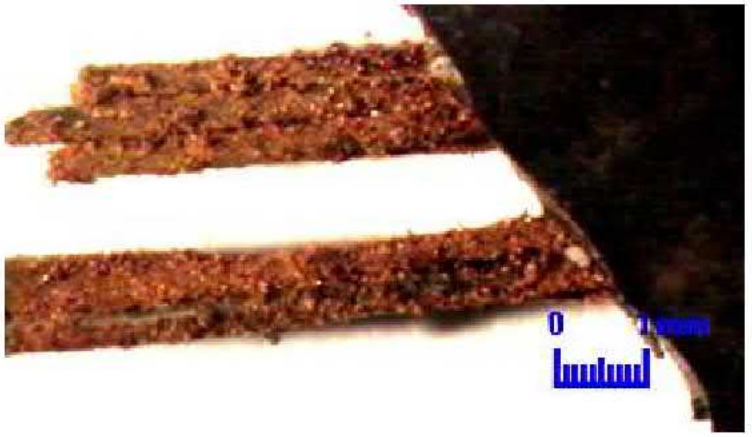

Mechanical

Temperature

Chemical

Corrosive

Vibratory

Combine

Applied load to cord

REQUIREMENTS ON TIRE CORD

- Failure resistance
- Crack propagation resistance
- Influenced temperature gradient
- Corrosive resistance
- Hardening mechanism
- Stiffness characteristic

Influence on behaviour and mechanical-physics properties of STEEL CORD BELT PLIES OF TIRE

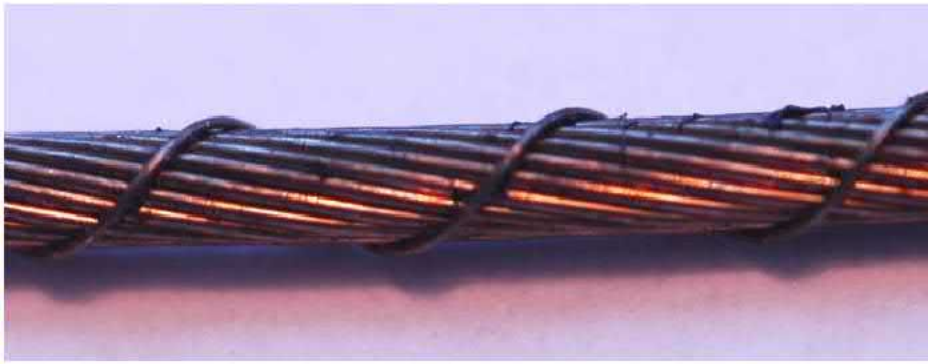

The adhesive bonds are affected by internal impacts (inserted during production, mounting) and external impacts (operating conditions, surrounding conditions etc.) or their interaction. It can be caused degradation on reinforcement-matrix adhesive bond. The degradation leads to failure into whole macro volume of tire. What isn't admissible from safety aspect of vehicle

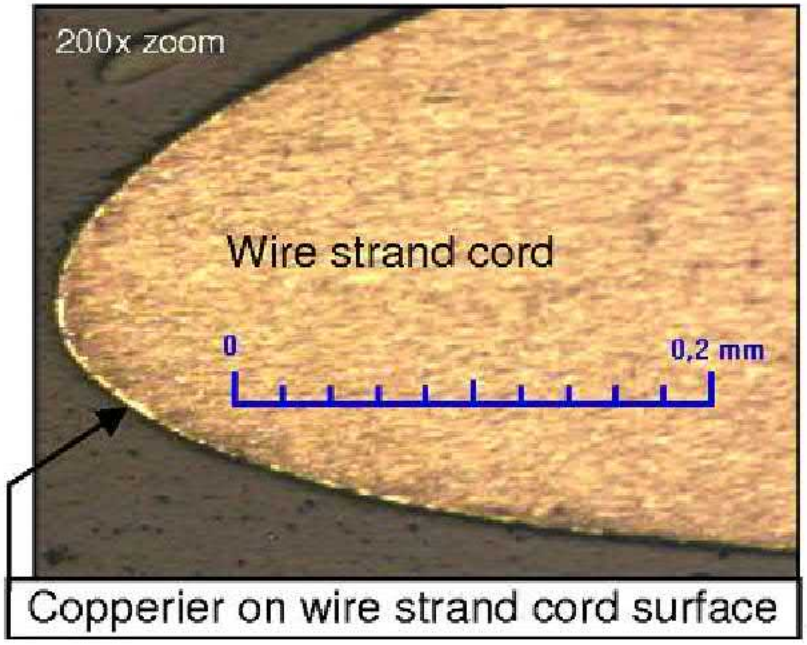

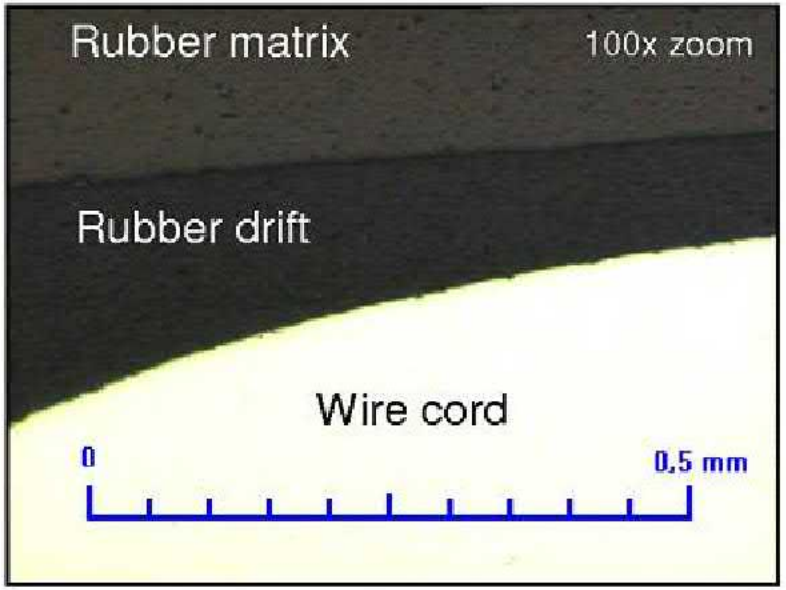

Bond between steel-cord and rubber

⇒ take in computational model

Microscopy with 100x-200x zoom

The light microscope was used for metallography observation of the adhesive bond between steel-cord and rubber upon failure after corrosion test in corrosion chamber under extreme conditions and statically tensile test. Together with metallography are performed experimentally analyses of uniaxial stiffness for using the obtained results for computational modeling . The selected samples of one-layer steel-belt of tire are effected to experiments. The reinforcement is wire form with radius 0.94 mm with surface treatment of cords.

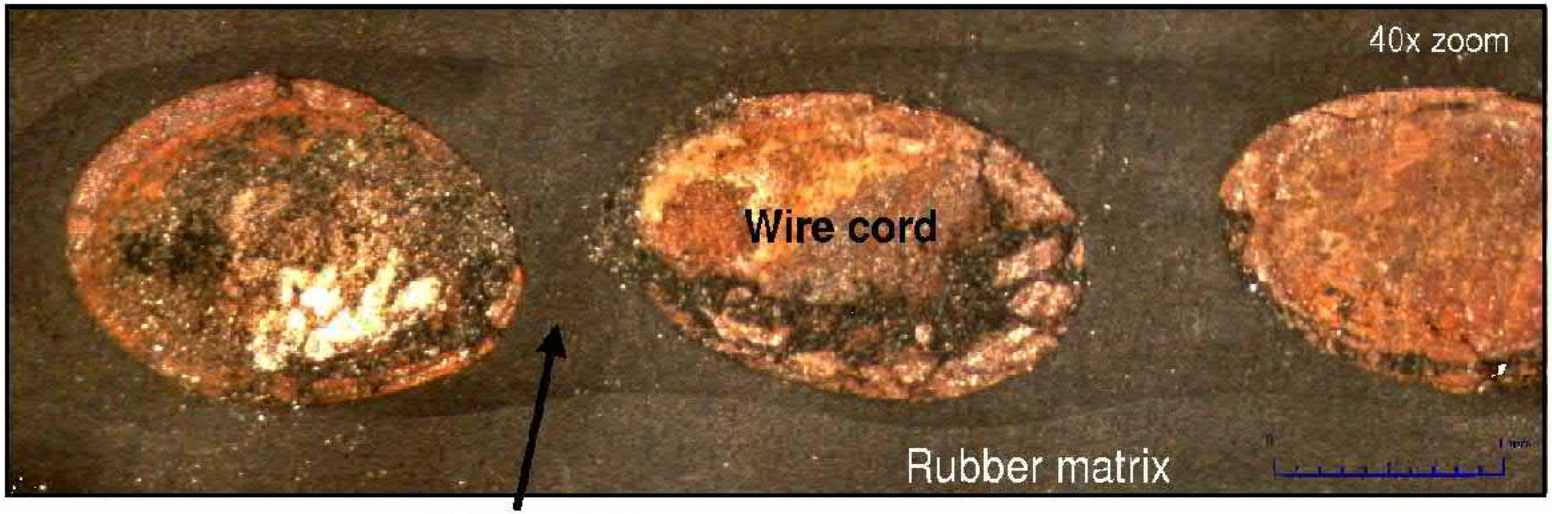

In addition if the tire is in use is defected in tire crown (e.g. defect caused by sharp object as a nail and after the repair is placed back into operation) the initiation of corrosion with faster process is being assumed. Consequently this can lead to gradual or sudden failure of the steel-cords and bonds of steel-cord and rubber with a serious car accident as a final consequence.

Any damage in the area of tire crown, namely into steel-cord belt, is perilous.

Tires are subject to internal and external effects which can more or less cause limit states leading to degradation processes.

The corrosion causes formation of oxides on steel-cord and rubber interface. The oxides accelerated of birth of dangerous delaminations after uniaxial test and so providing that fitting surface treatment of tire cords

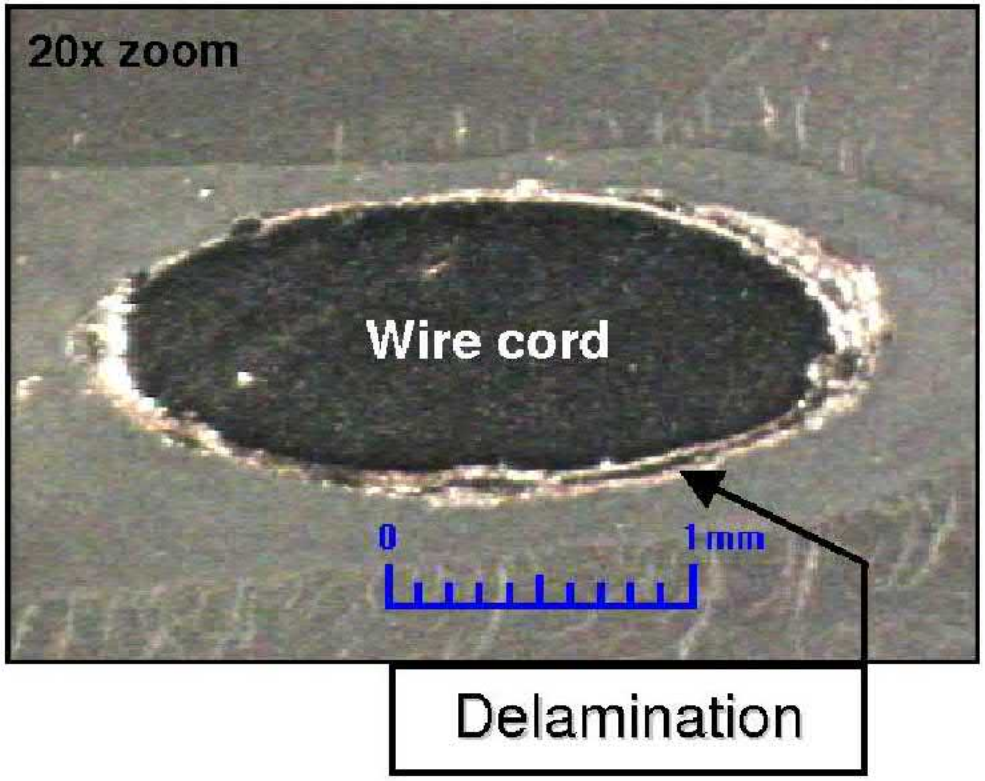

The oxide film is strongly affected on failure of adhesive bond which show comparison between test sample without corrosion only tensile loading and test sample after corrosion test together tensile test by tensile force in dependence on elongation. The tensile stiffness descended more than half in consequent on failure

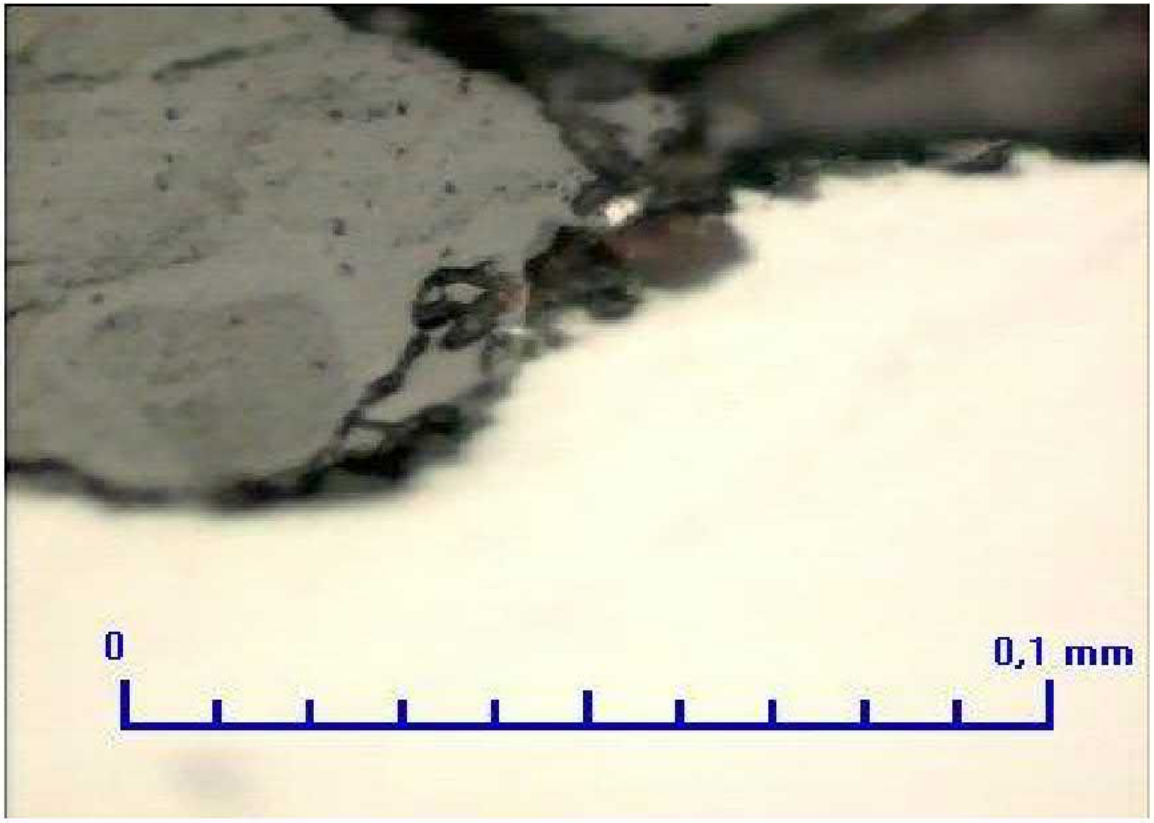

TYPES OF DEGRADATION PROCESSES OF TIRES according to

- **MORPHOLOGY** of exposure
  - WEAR
  - BULGING
  - CRACK
  - HOLE
  - "CORDS WORKING UP"
  - DESTRUCTION
- **LOCALES** (AREAS) of presence
  - inside of TIRE CROWN, TREAD
  - inside of SHOULDER
  - inside of SIDE-WALL
  - inside of BEAD
- **RANGE** of failure
  - in MATRIX of composite element
  - in REINFORCEMENT of composite element
  - in ONE element of tire
  - in TWO OR MORE elements of tire
  - in ALL elements of tire
- **SPEED** of degradation
  - DETERIORATION failure
  - IMMEDIATE failure
  - CUMULATIVE failure
  - COMBINED failure
- **INITIATION** of failure
  - in MANUFACTURING PROCESS
  - at STORAGE
  - in ASSEMBLY
  - at OPERATING
- **CAUSES** of failure
  - INCORRECT VULCANIZATION at manufacturing, BAD ADHESION BOND between cord and the matrix
  - SHARP OBJECT (stone, nail, ...)
  - COLLIDE with shoulder of road, ...
  - NON-PERFORMANCE OPERATIONAL REQUIREMENTS
  - OZONE IMPACT, TEMPERATURE IMPACT
- **CONSEQUENCE** of degradation in operation
  - **DELAMINATIONS and SEPARATIONS !**
  - **"CORDS WORKING UP" !**
  - TIRE-CASING DISRUPTION
  - AGING
  - PUNCTURE
  - CUT-OFF

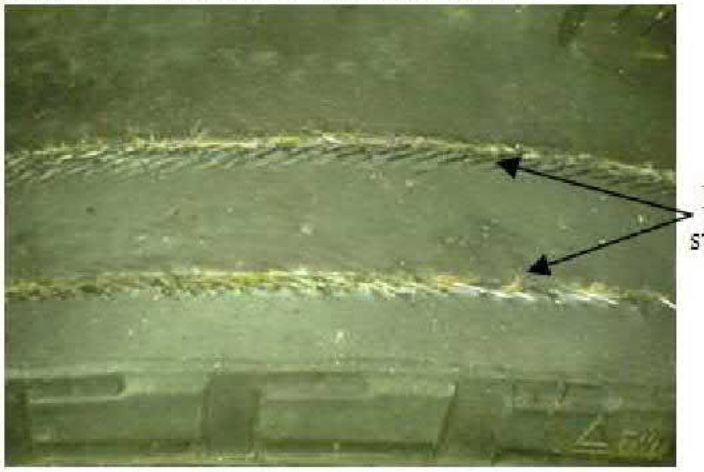

Extreme wear of tire on tread surface

„Cords working-up“

Tire life is affected by many factors (e.g. manufacturing way of a tire, its operation and handling, storage conditions of base materials for tire production etc.) while it's assumed an ideal adhesive bond among the rubber elements in matrix (e.g. an interface between tire tread and textile overlap belt) and the cord reinforcing and rubber drift inside tire carcass, and belts is assumed in this cases. For long life tires must resist during operating to surrounding effects, to negative effects of operation and to other effects, which could lead to wear and degradation processes as are e.g. delaminations.

Tires must resist during operating to surrounding effects, to negative effects of operation and to other effects, which could lead to wear and degradation processes as are e.g. delamination.

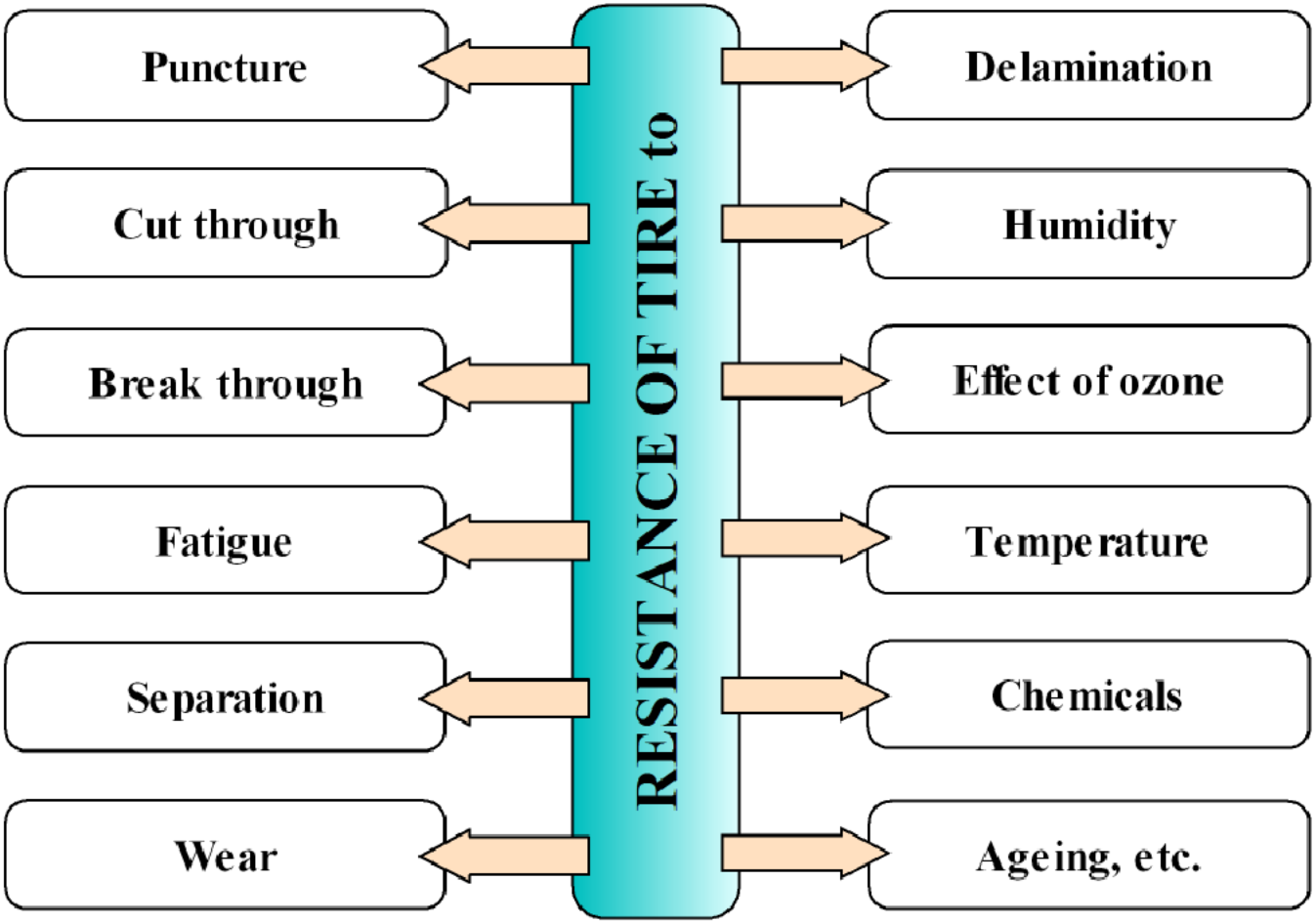

Resistance to the following effects is considered:

- Puncture – capability of tires to resist puncture by sharp objects;
- Cut-through – capability of tires (especially of the tread and sidewall) to resist contact with sharp objects;
- Breakdown – capability of tires to resist damage during short-term loading by concentrated forces;
- Fatigue – capability of tires to resist material fatigue and defects in consequence of repeated loading cycles;
- Separation and delamination – capability of structural tire components to maintain integrity of the system during operation;
- Humidity – tire elements must be able to resist degradation by contact with water;
- Ozone influence – capability of tires and of theirs components to resist degradation caused by ozone present in atmosphere;
- Temperature – tire components must be able to resist high and low ambient temperatures and also consequences of contact with the road;
- Chemicals – capability of tires and theirs components to resist degradation caused by chemicals (in winter – influence of salt solutions);
- Corrosion processes – capability of tire reinforcing cords to resist corrosion, etc.

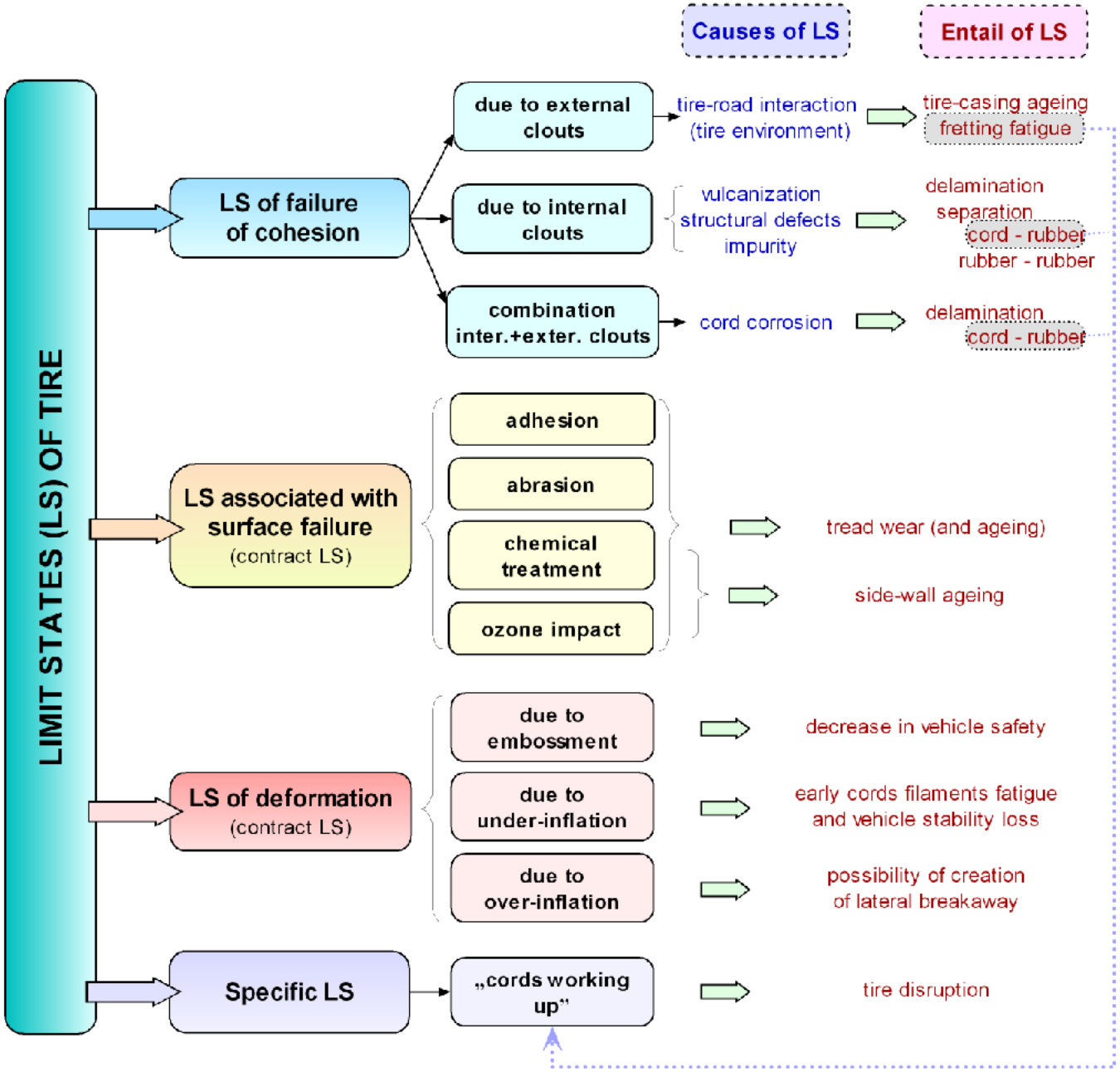
Causes of LS
Entail of LS
LIMIT STATES (LS) OF TIRE
LS of failure of cohesion
due to external clouts
tire-road interaction (tire environment)
tire-casing ageing
fretting fatigue
due to internal clouts
vulcanization
structural defects
impurity
delamination
separation
cord - rubber
rubber - rubber
combination inter.+exter. clouts
cord corrosion
delamination
cord - rubber
LS associated with surface failure (contract LS)
adhesion
abrasion
chemical treatment
ozone impact
tread wear (and ageing)
side-wall ageing
LS of deformation (contract LS)
due to embossment
decrease in vehicle safety
due to under-inflation
early cords filaments fatigue and vehicle stability loss
due to over-inflation
possibility of creation of lateral breakaway
Specific LS
„cords working up"
tire disruption

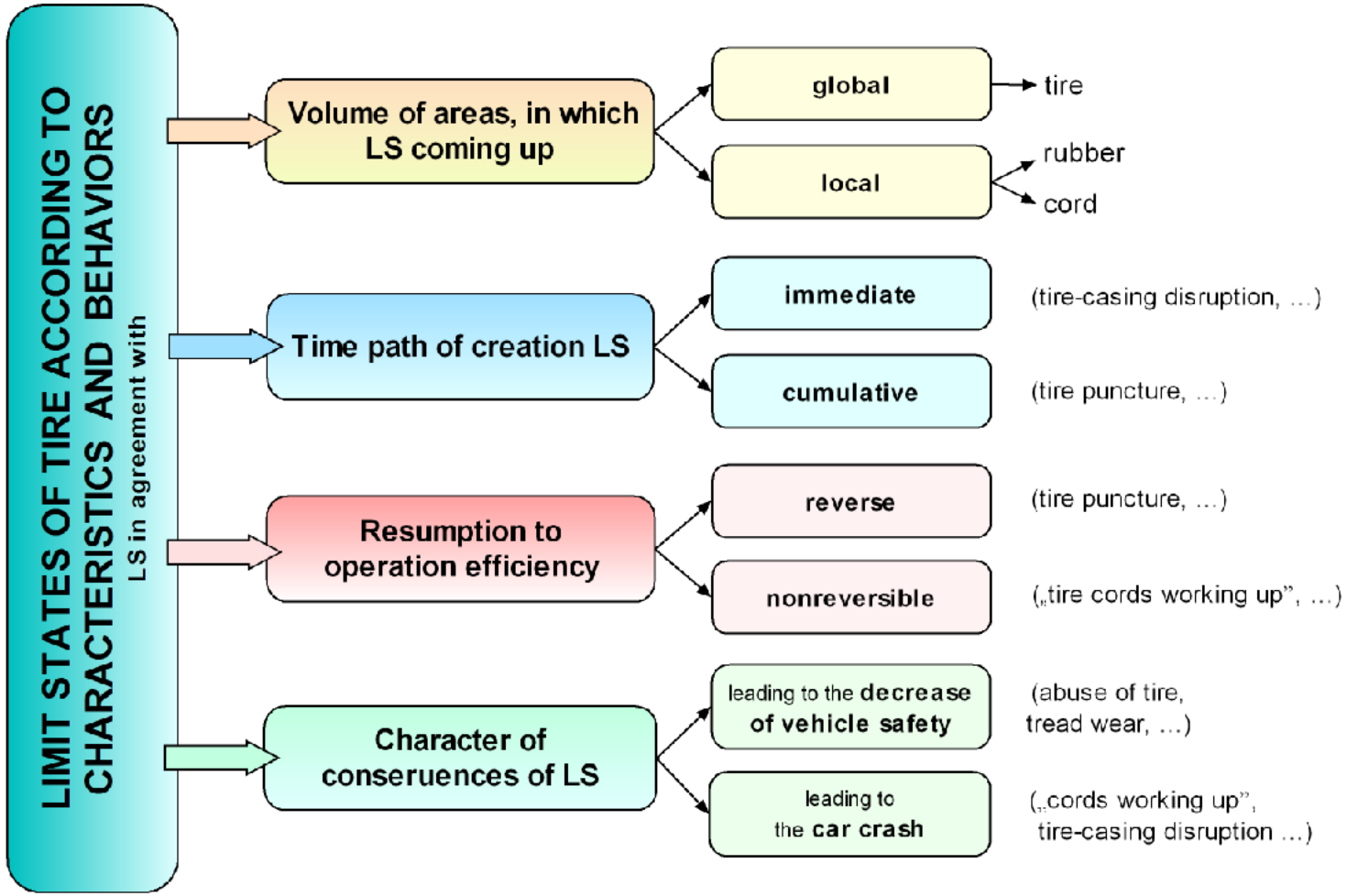
LIMIT STATES OF TIRE ACCORDING TO CHARACTERISTICS AND BEHAVIORS
LS in agreement with
Volume of areas, in which LS coming up
global
tire
local
rubber
cord
Time path of creation LS
immediate
(tire-casing disruption, ...)
cumulative
(tire puncture, ...)
Resumption to operation efficiency
reverse
(tire puncture, ...)
nonreversible
(„tire cords working up", ...)
Character of conseruences of LS
leading to the decrease of vehicle safety
(abuse of tire, tread wear, ...)
leading to the car crash
(„cords working up", tire-casing disruption ...)

CORROSION TEST

The corrosion chamber

500 hour by temperature 70°Celsius in saline application 5%

authors note: such extreme conditions should not ever appear in tire operations if proper conditions are kept

Steel-cords are exposed to various chemical and thermal influences ⇒ corroding process ⇒ adhesive bonds between cord-elastomer are damaged ⇒

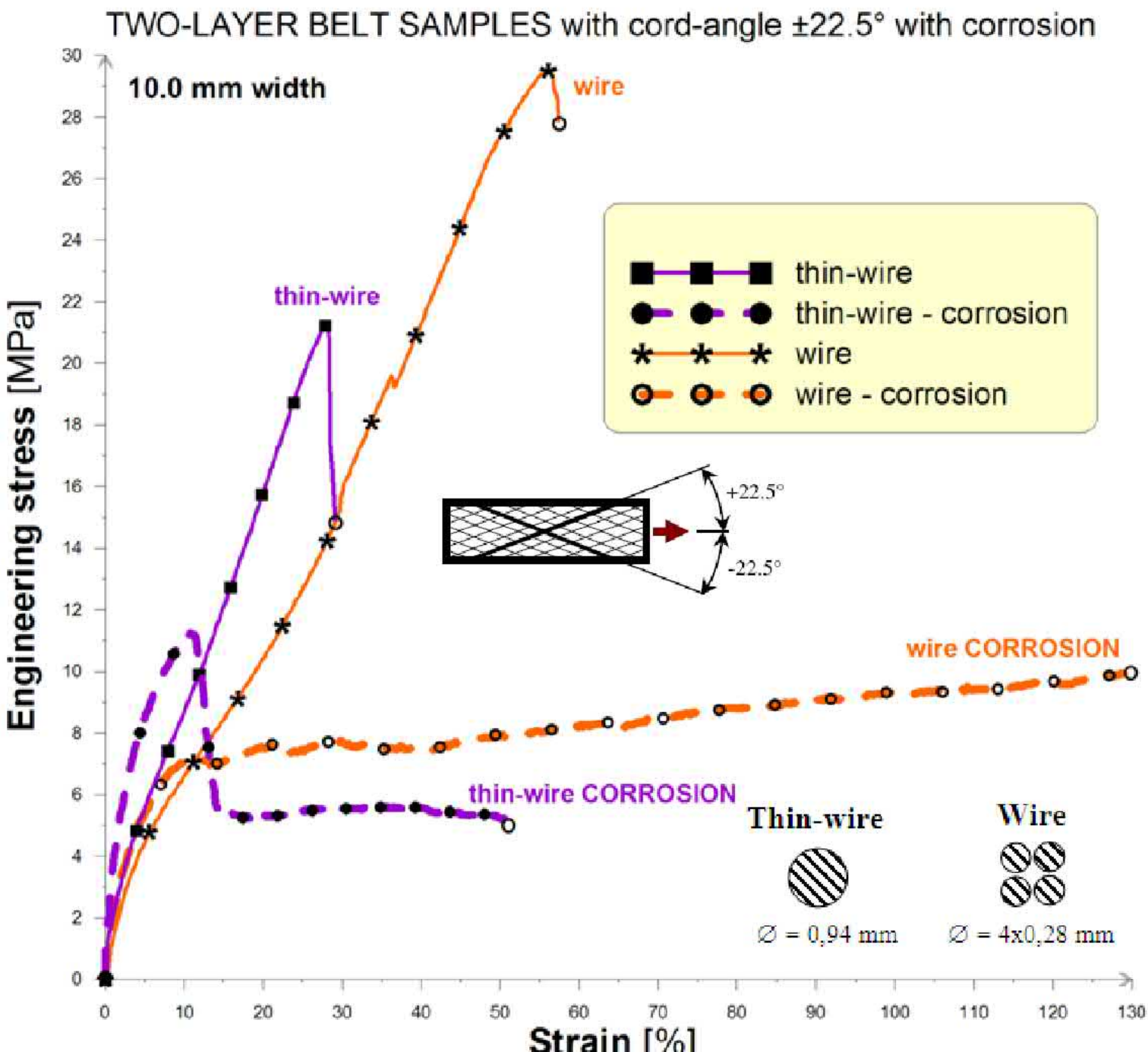
TWO-LAYER BELT SAMPLES with cord-angle ±22.5° with corrosion
10.0 mm width
wire
thin-wire
thin-wire
thin-wire - corrosion
wire
wire - corrosion
+22.5°
-22.5°
wire CORROSION
thin-wire CORROSION
Thin-wire
Wire
∅ = 0,94 mm
∅ = 4x0,28 mm
Engineering stress [MPa]
Strain [%]
0
2
4
6
8
10
12
14
16
18
20
22
24
26
28
30
0
10
20
30
40
50
60
70
80
90
100
110
120
130

CORROSION TEST
+ tensile test

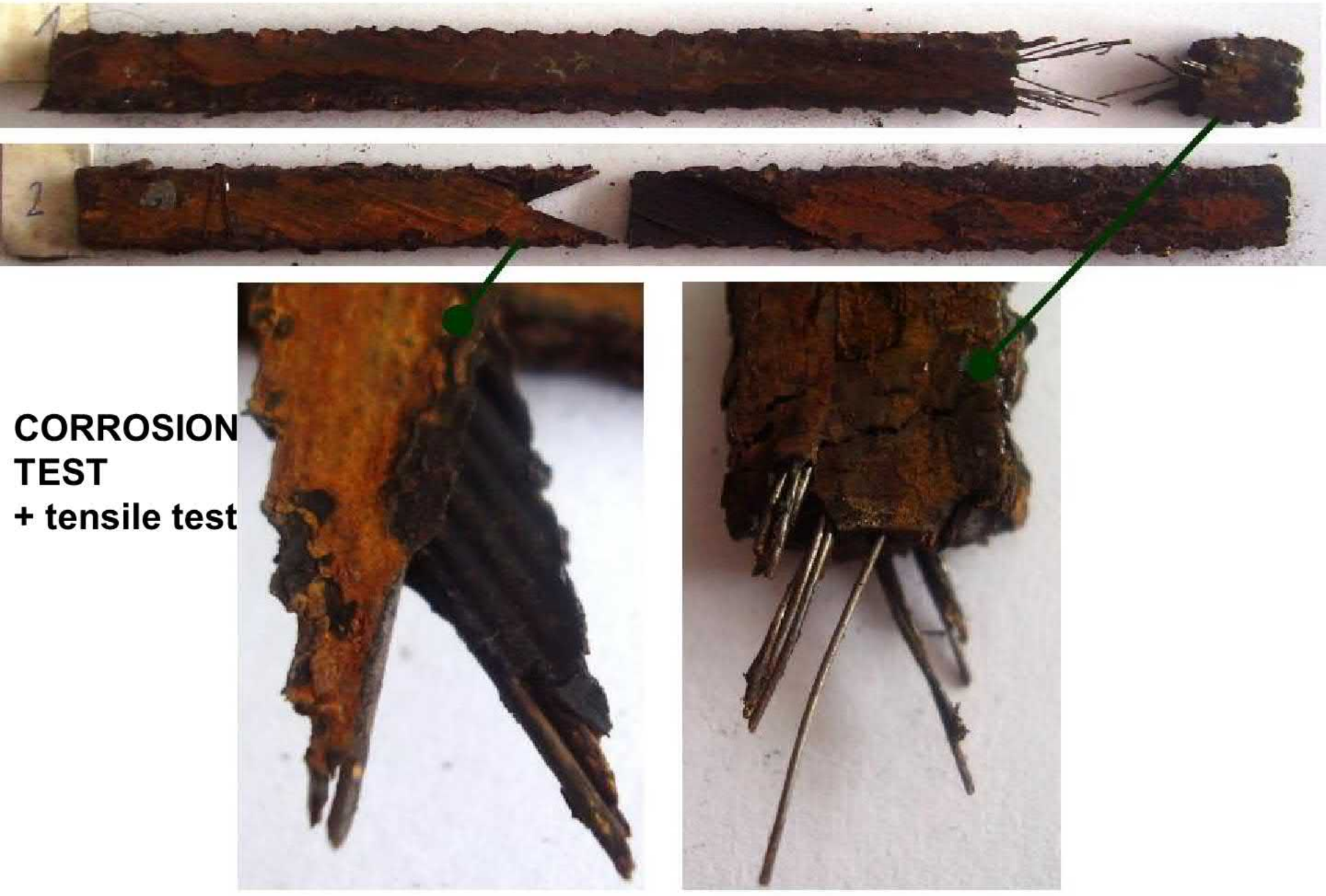

Fig.1. Specimens of steel-cord belt after failure with details of fracture area.

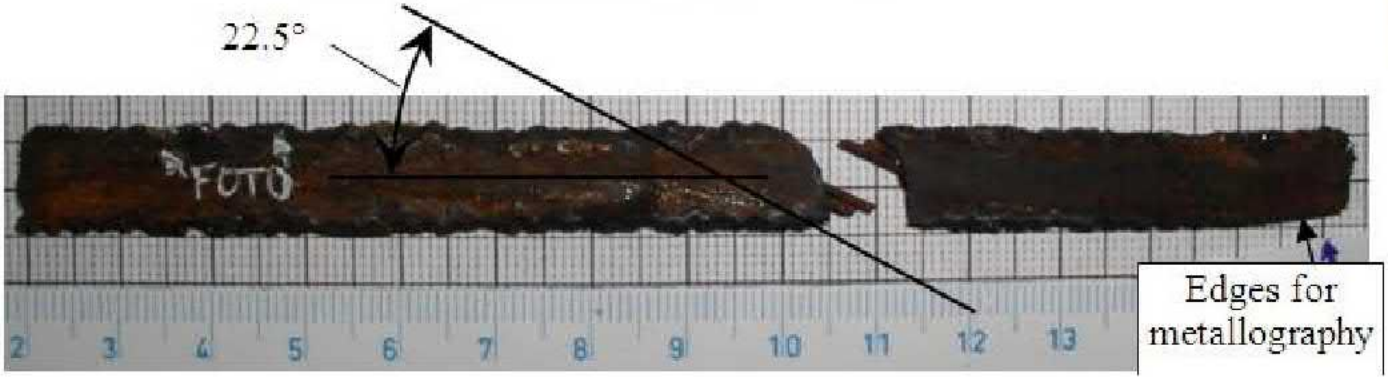

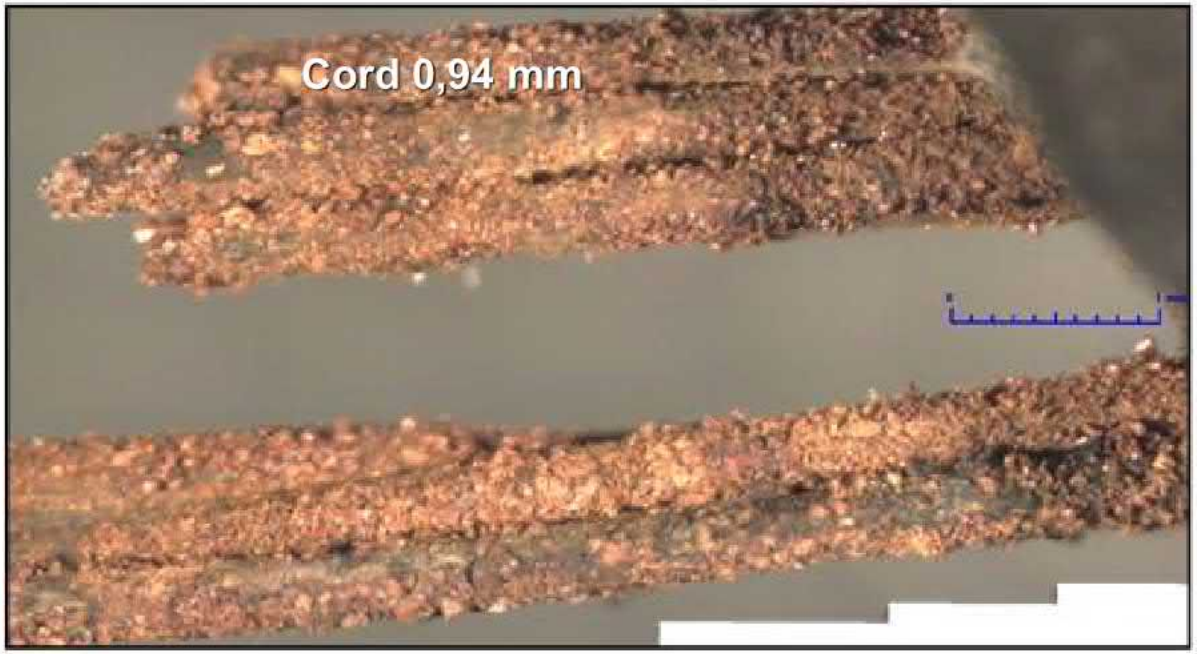

Microscopy with *100x-200x* zoom

Corrosion processes on cord surfaces is very dangerous!

drát
25°
lanko
4
5
6
7
8
9
10
11
12
13
14
15
16
17
18

Kord 0,94 mm
drátek
nánosový elastomer
elastomerová matrice

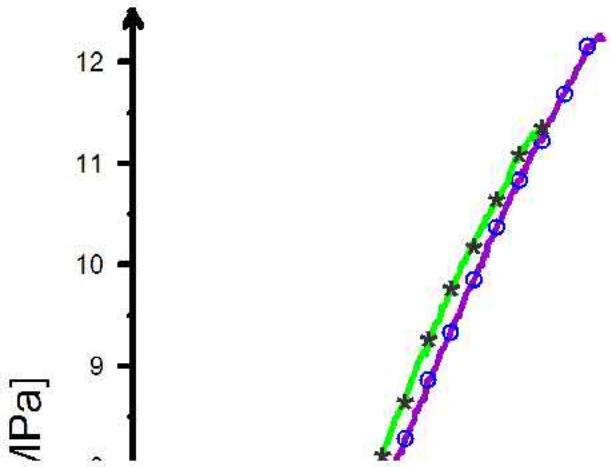

STRESS-STRAIN dependance of selected specimens with width 10 mm

- **FF3** thin-wire NESYM +67.5°/+22.5°
- **I** thin-wire one layer 22.5°, width 13.5 mm
- **EE3** wire NESYM +67.5°/+22.5°
- **BB3** thin-wire SYM ±45°

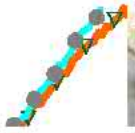

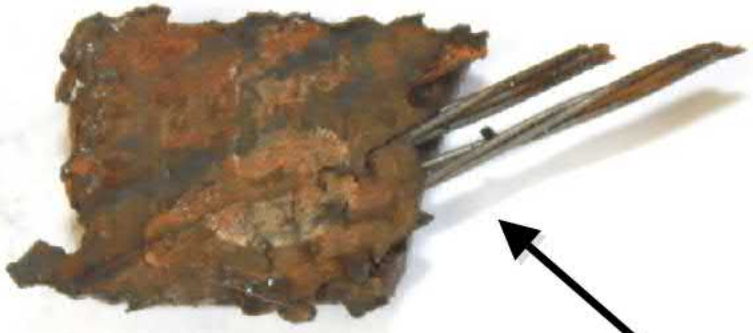

Specimens angle orientations

23°	NESYM +67.5°/+22.5°	SYM ±45°
I	EE3 and FF3	BB3

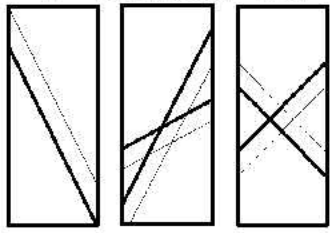

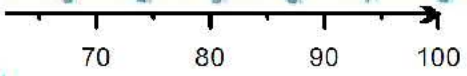

It is necessary to prepare of samples for microscopy observation of structures so that the samples included different:

- **Form of cord**;
- **Geometrical configurations and number of layers**;
- **Level of corrosion** impact of steel-cords – adhesive bonds (without corrosion, easy corrosion, after corrosion test behind extremely conditions).

For selected cords were accounted:

- **Uniformity of layer** of rubber drift on cord surfaces;
- **Surface treatment** of cords;
- **Interface between cord-rubber matrix** after tire production;

Structural change into microlocality of cord-rubber after corrosion.

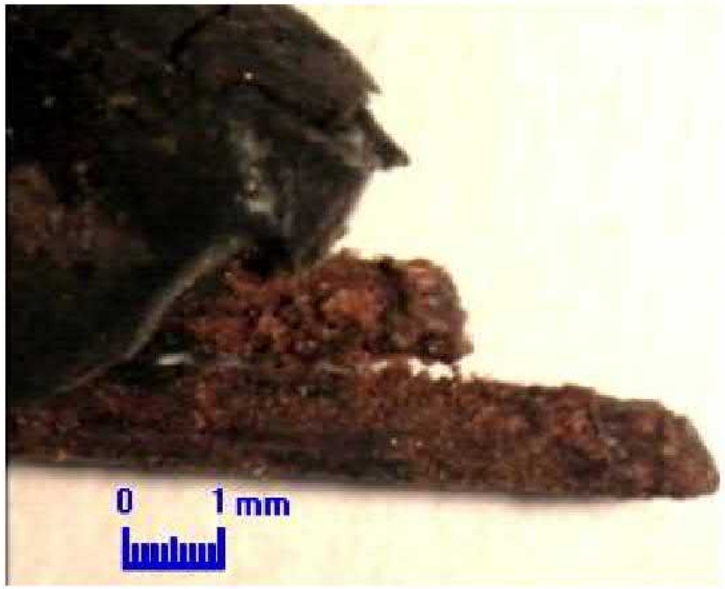
0 1 mm

0 1 mm

WIRE after production

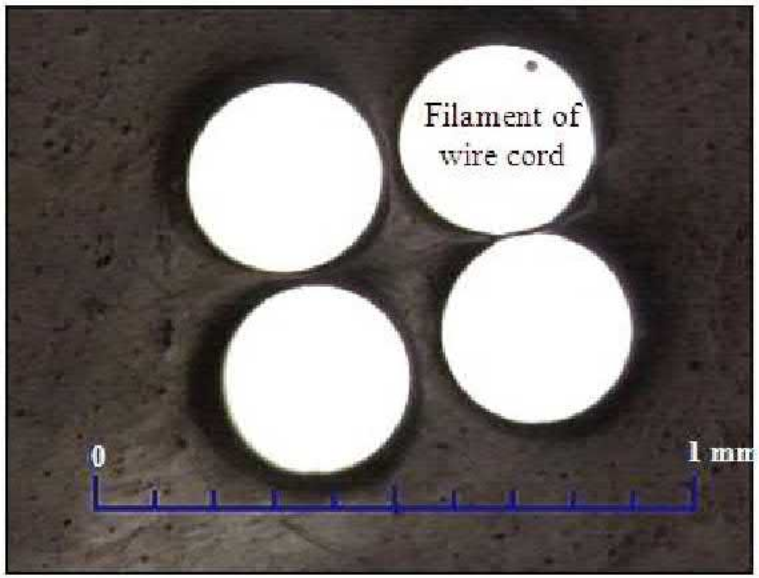

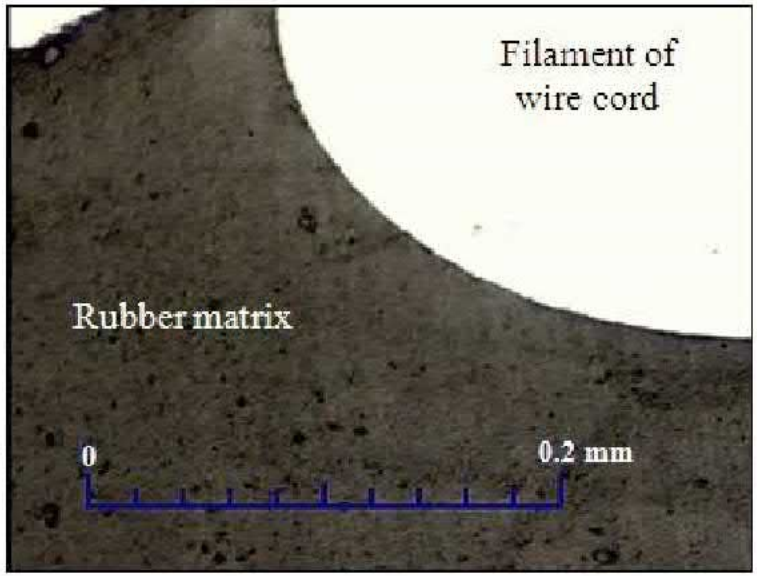

Good adhesive bond between wire steel cord 2+2×0.28 mm (cord consists of 4 filaments) and rubber after tire production (without corrosion)

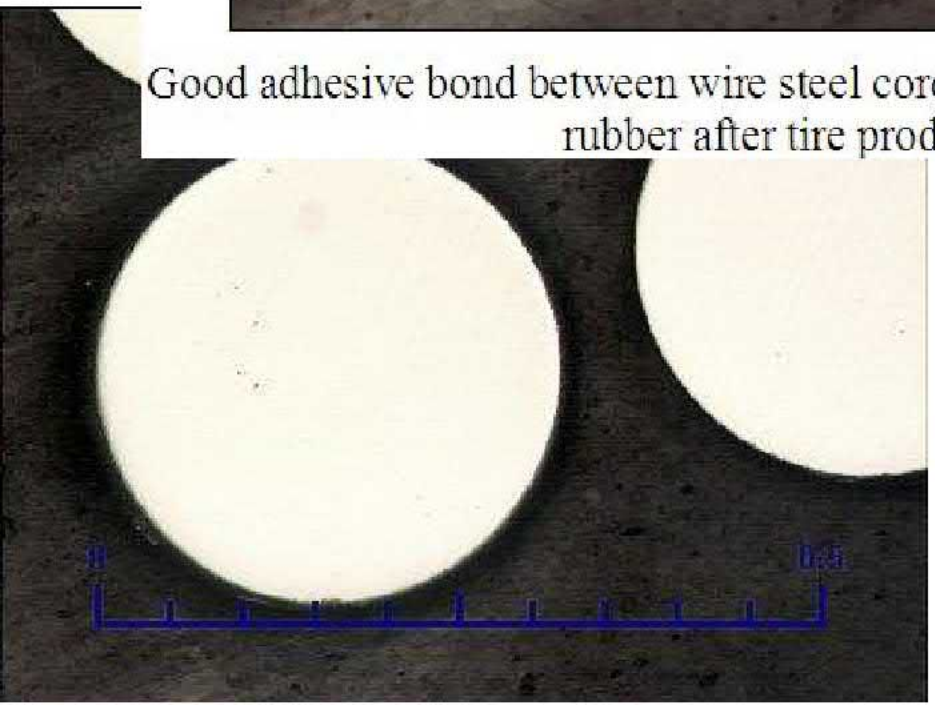

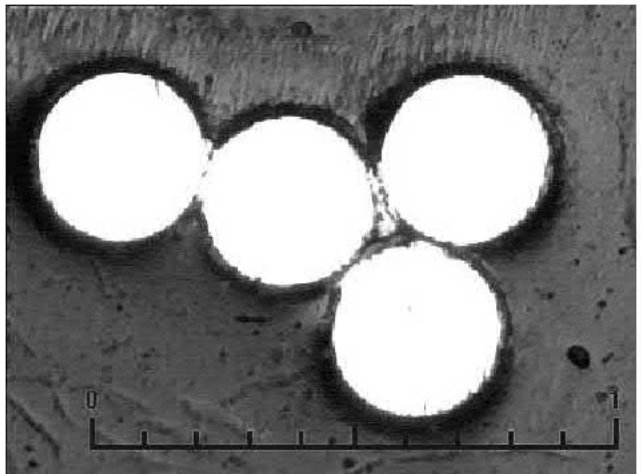

WIRE – after extreme corrosion

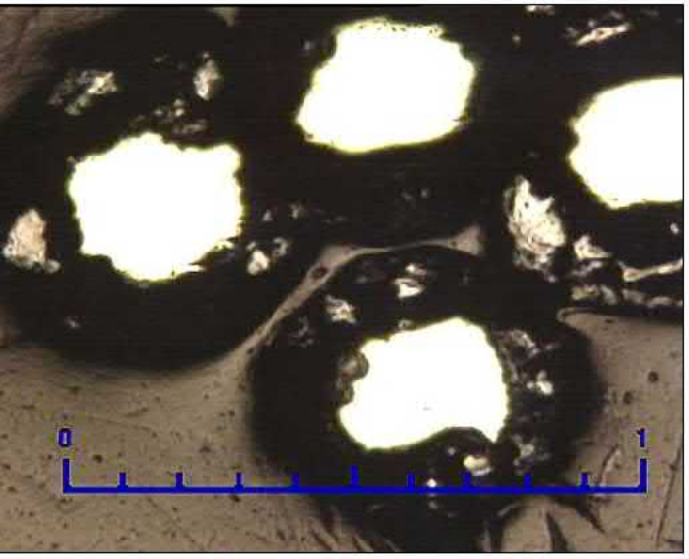

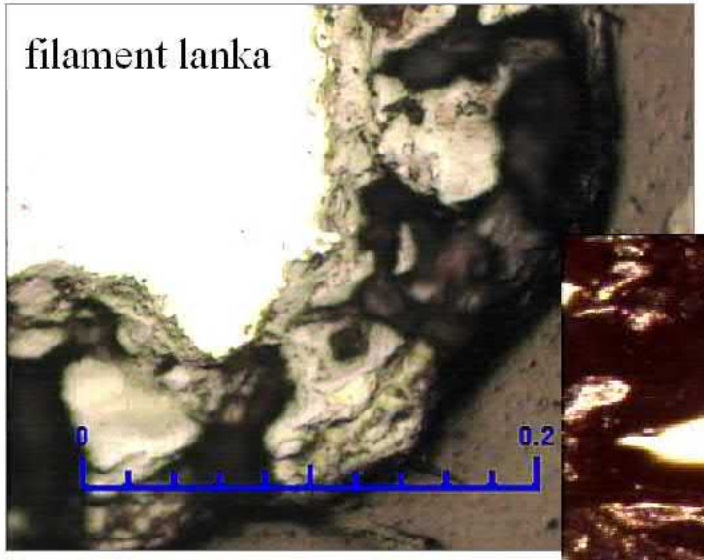

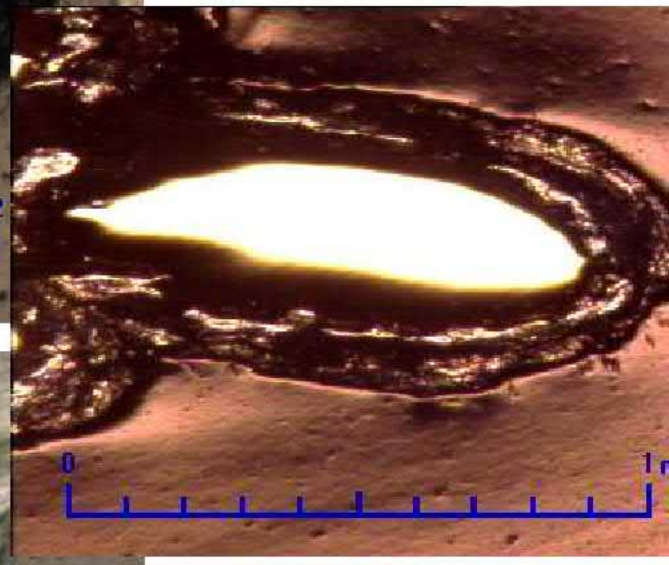

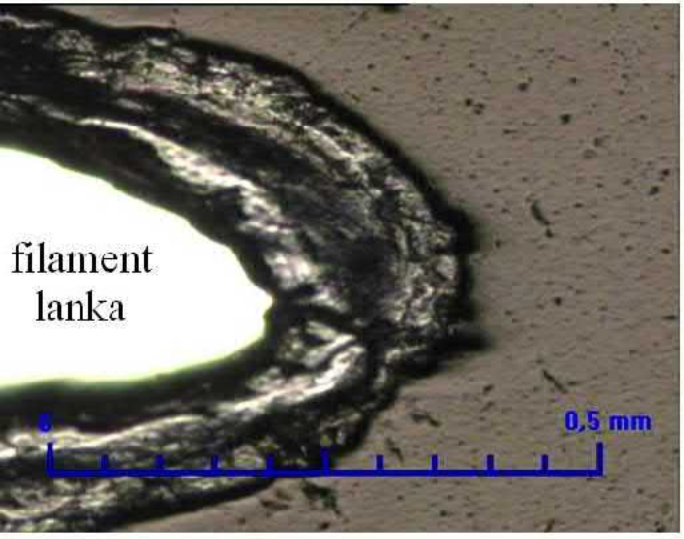

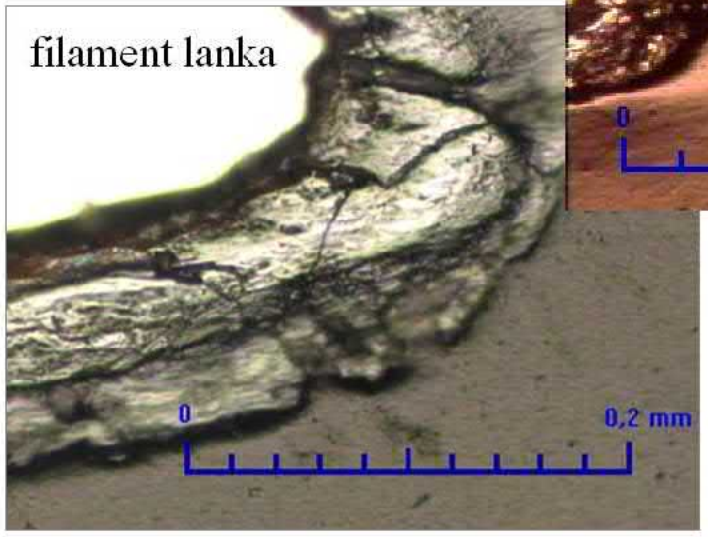

MICROSCOPY OBSERVATION

Detail of cord after extreme corrosion

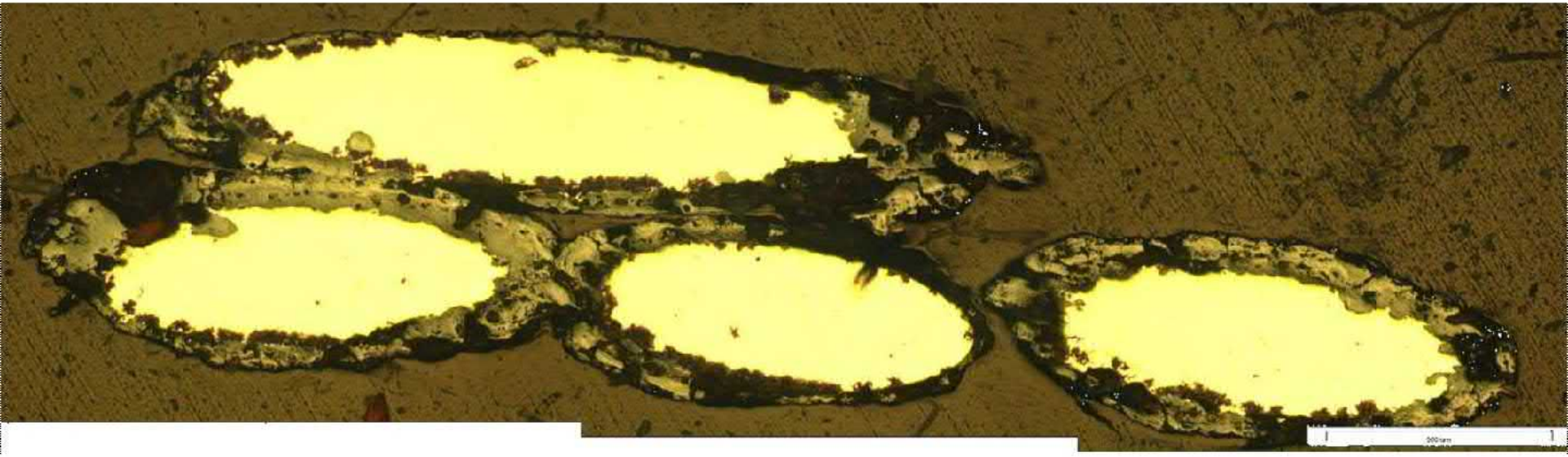

THIN-WIRE – after production

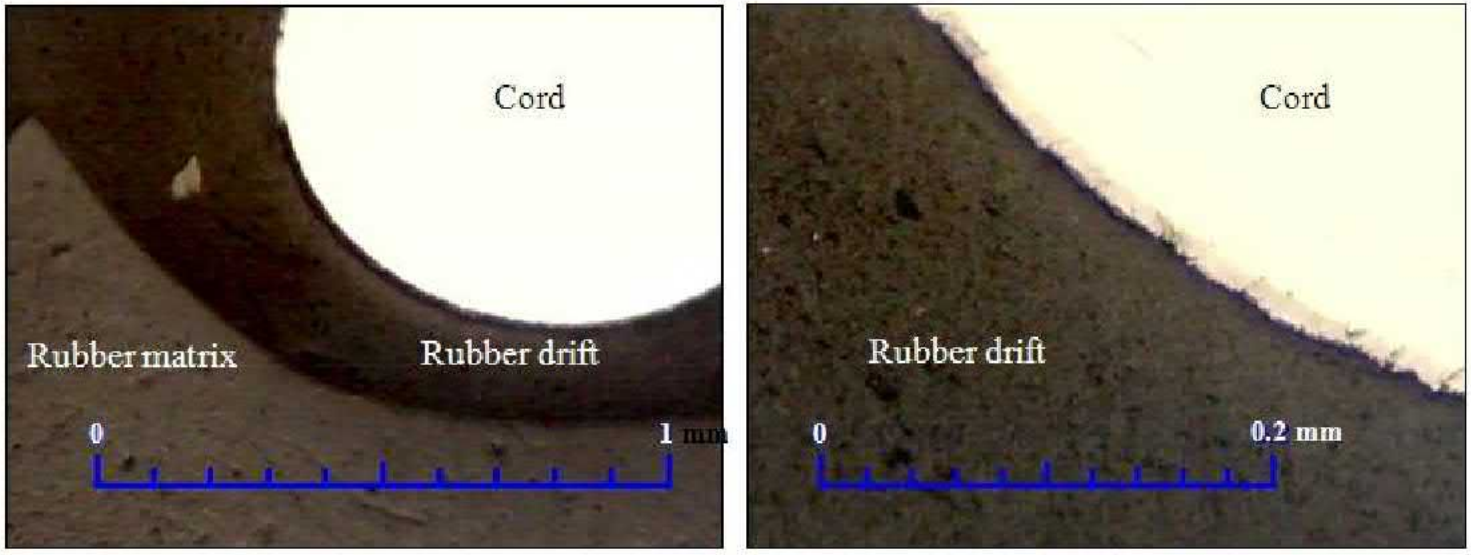

Good adhesive bond between thin-wire steel cord 0.94 mm and rubber drift after tire production (without corrosion)

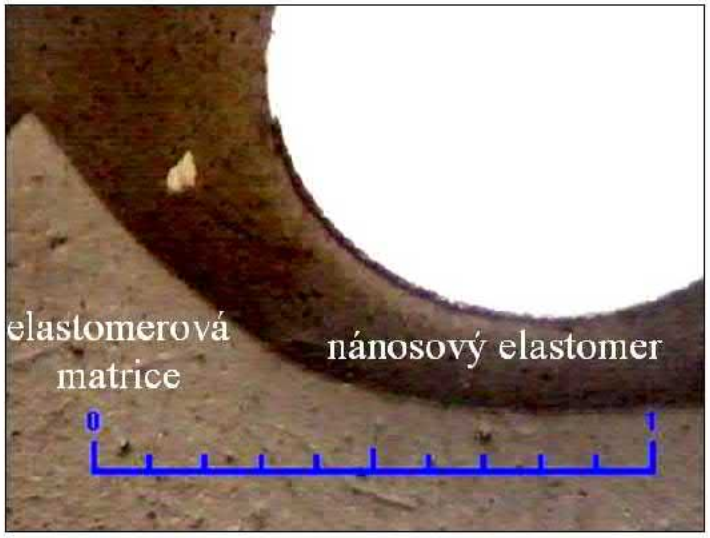
elastomerová
matrice
nánosový elastomer
0
1

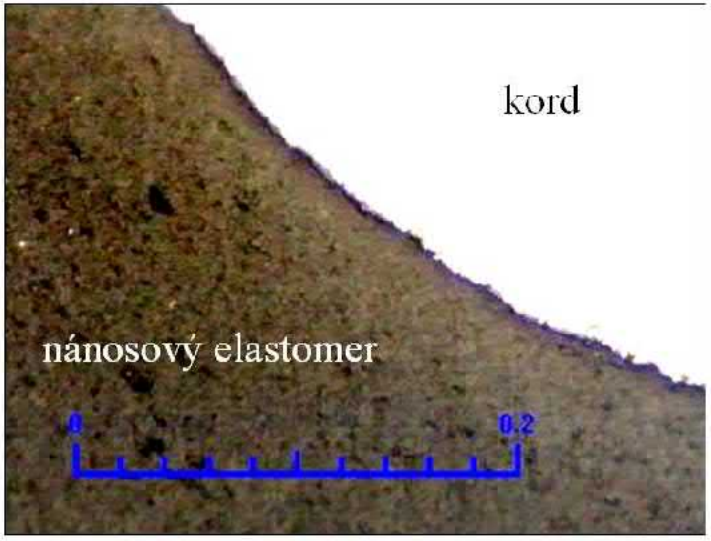
kord
nánosový elastomer
0
0.2

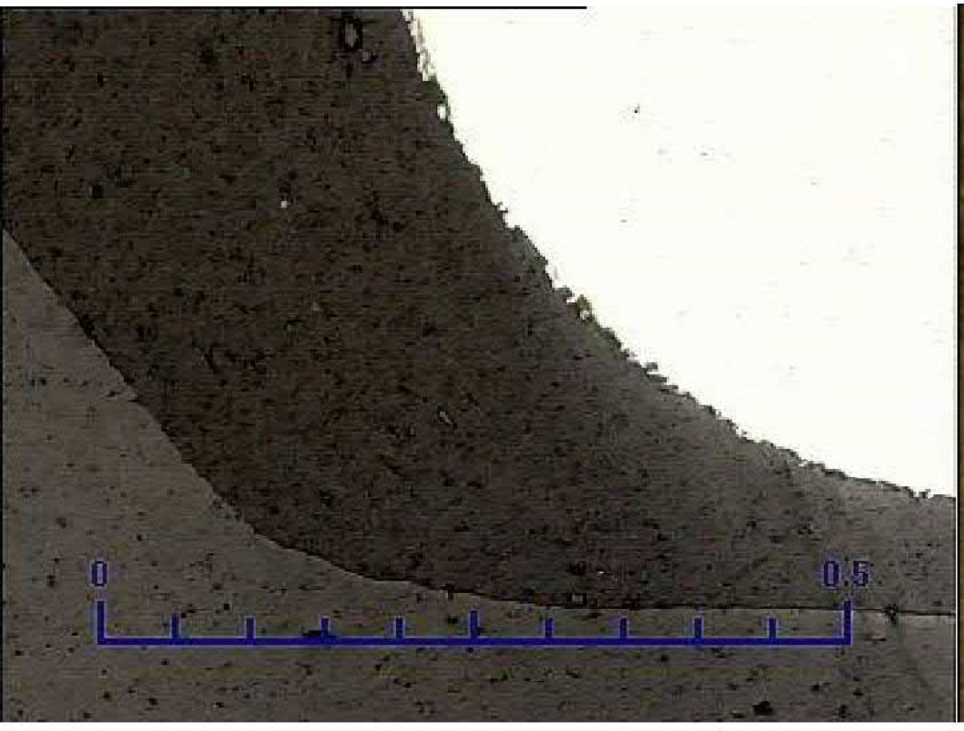
0
0.5

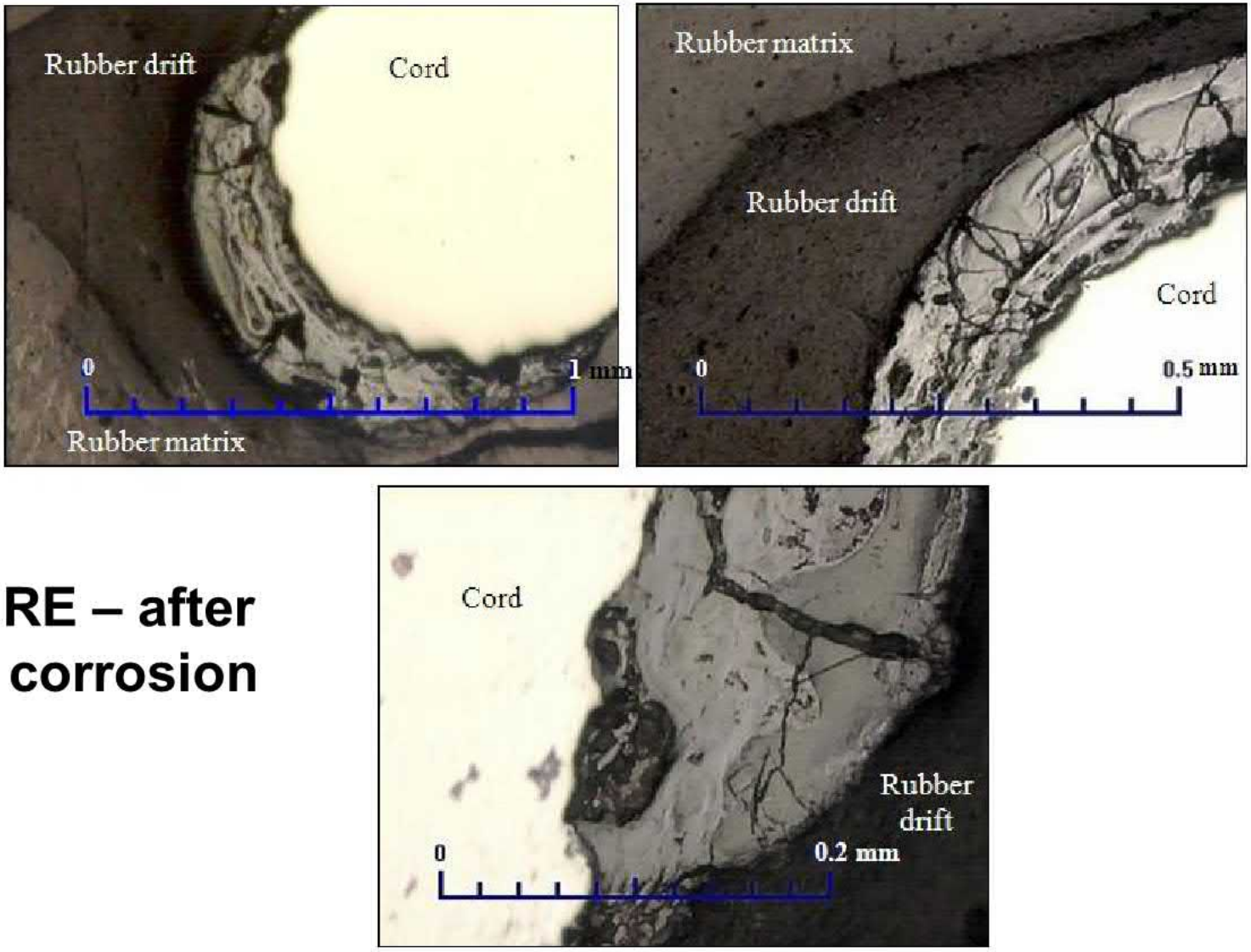

THIN-WIRE – after extreme corrosion

Damaged adhesive bond between thin-wire steel cord 0.94 mm and rubber drift after corrosive attack (with extreme corrosion and tensile loading) with detail of oxide on cord surfaces

extrémní korozní napadení

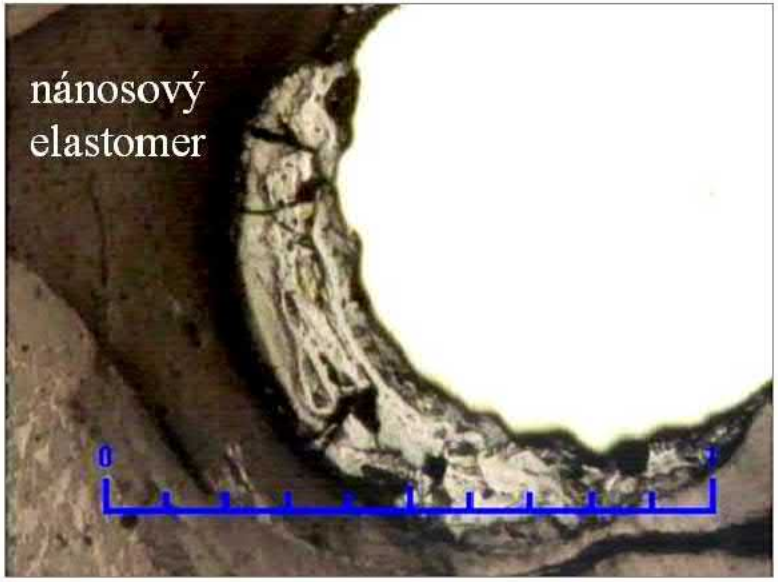

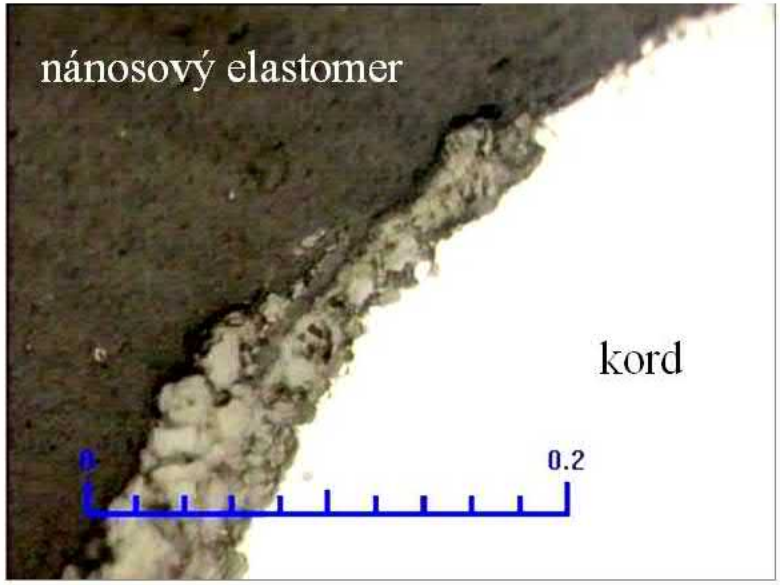

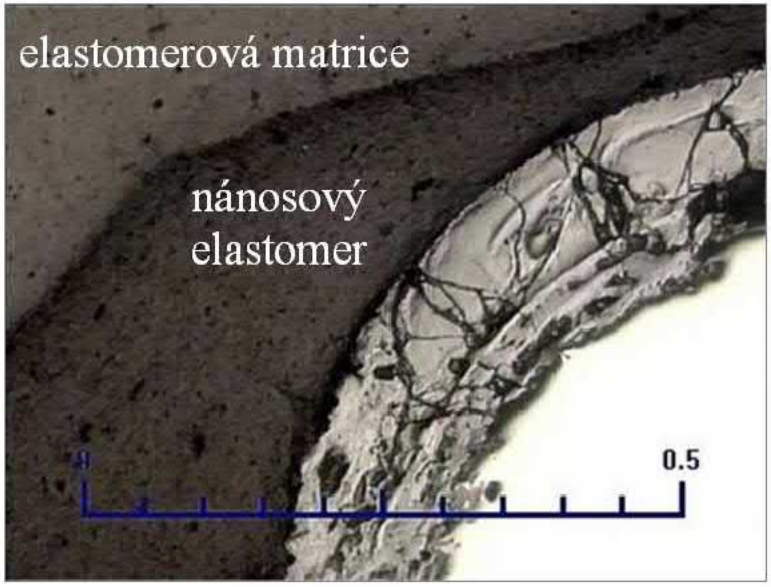

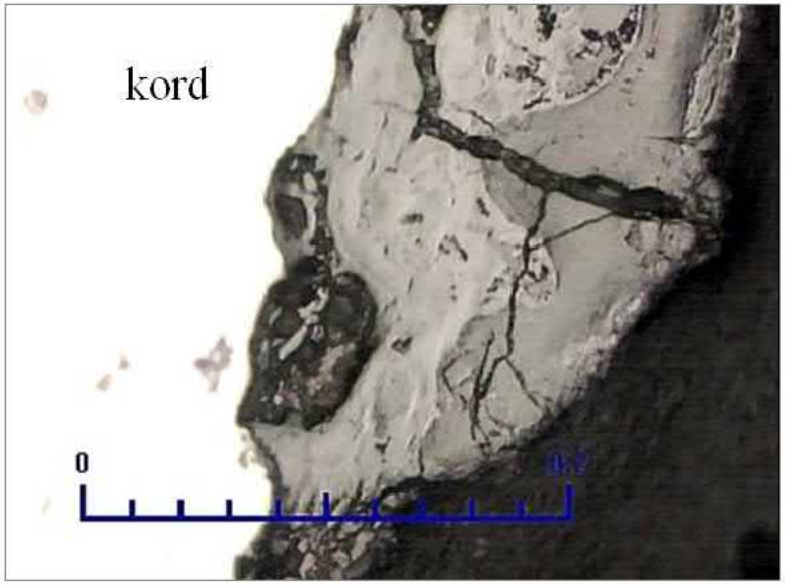

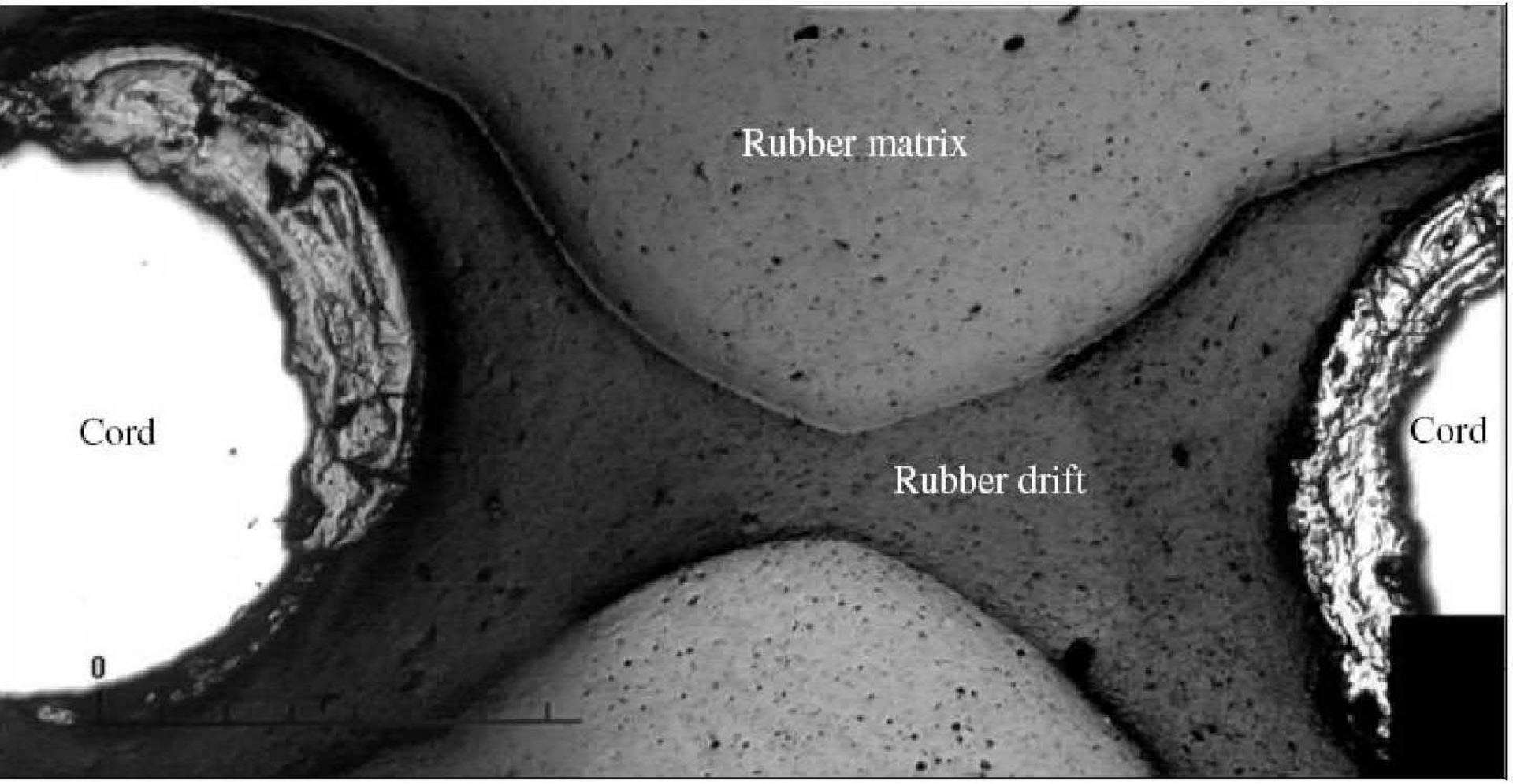
Rubber matrix
Cord
Rubber drift
Cord
0

On the base of corrosion tests is possible note:

- Arise of uniform surface corrosion;
- Fragility and hardness of corrosive layer;
- Quicker grow of oxides near cord surfaces;
- Fracture of oxide layer;
- Quality of cord-surfaces and surface treatment of cords with respect to corrosion attack;
- Decreased of material characteristics of steel-cord belt on the basic of tensile tests.

- Any damage in the area of tire crown is perilous.
- If extreme corrosion on cords then cord surface treatment lost function of corrosive protection.
- If cords are with corrosion then adhesive bonds between cord-rubber matrix are damaged and safety of steel-cord belt plies and also tire is decreased.
- For predication of damaged belt ply is possible used combination of computational with experimental modeling.

On the basis of experiments of tested samples from tire are lost their mechanical and physical properties in exposition to critical corrosion loading. Whereby these property losses are lead to decrease suitability of tires in operation namely where tires are exposed to heavy duty and also where small initiation can be caused one wire cord burst or steel cords burst into concrete part of tire or whole tire disruption.

Sample specification: wire cord; one layer steel-cord belt with cord-angle 65° with respect to loading direction; width 8.5 mm

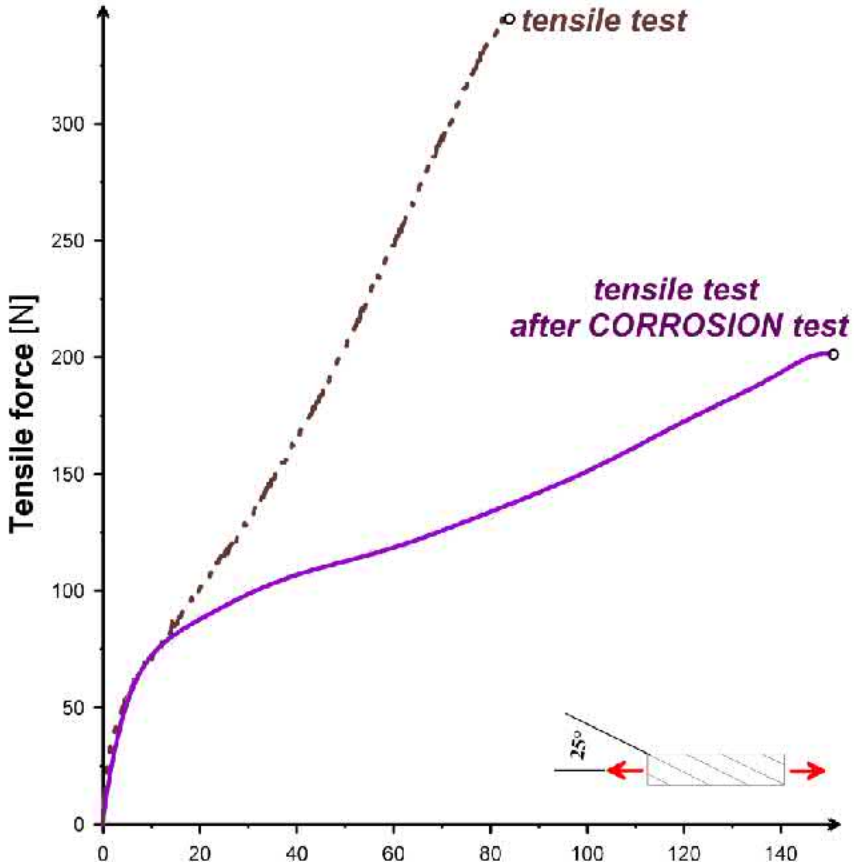

Computational models of belt:

- **Without** adhesive bonds including (it is model reinforcement-matrix);
- **With** adhesive bonds including (it is model reinforcement-adhesive bond-matrix) – adhesive bonds will be included influence of corrosion attack, drift rubber and surface treatment of cords. Then this model based on higher level knowledge with inclusion of all necessary input data.

It is necessary take into consideration:

- **Adhesive bond** cord-rubber;
- **Matrix relations** with reinforcing cords;
- **Non-uniformity in cord location** on cross-section of steel-cord belt.

Part 6 – COMPUTATIONAL MODELLING OF TIRE: FEA by program ANSYS, Parts of tire, Elastomer, Determination of Mooney-Rivlin parameters, Comparison of experiment results with simulation results of tire parts

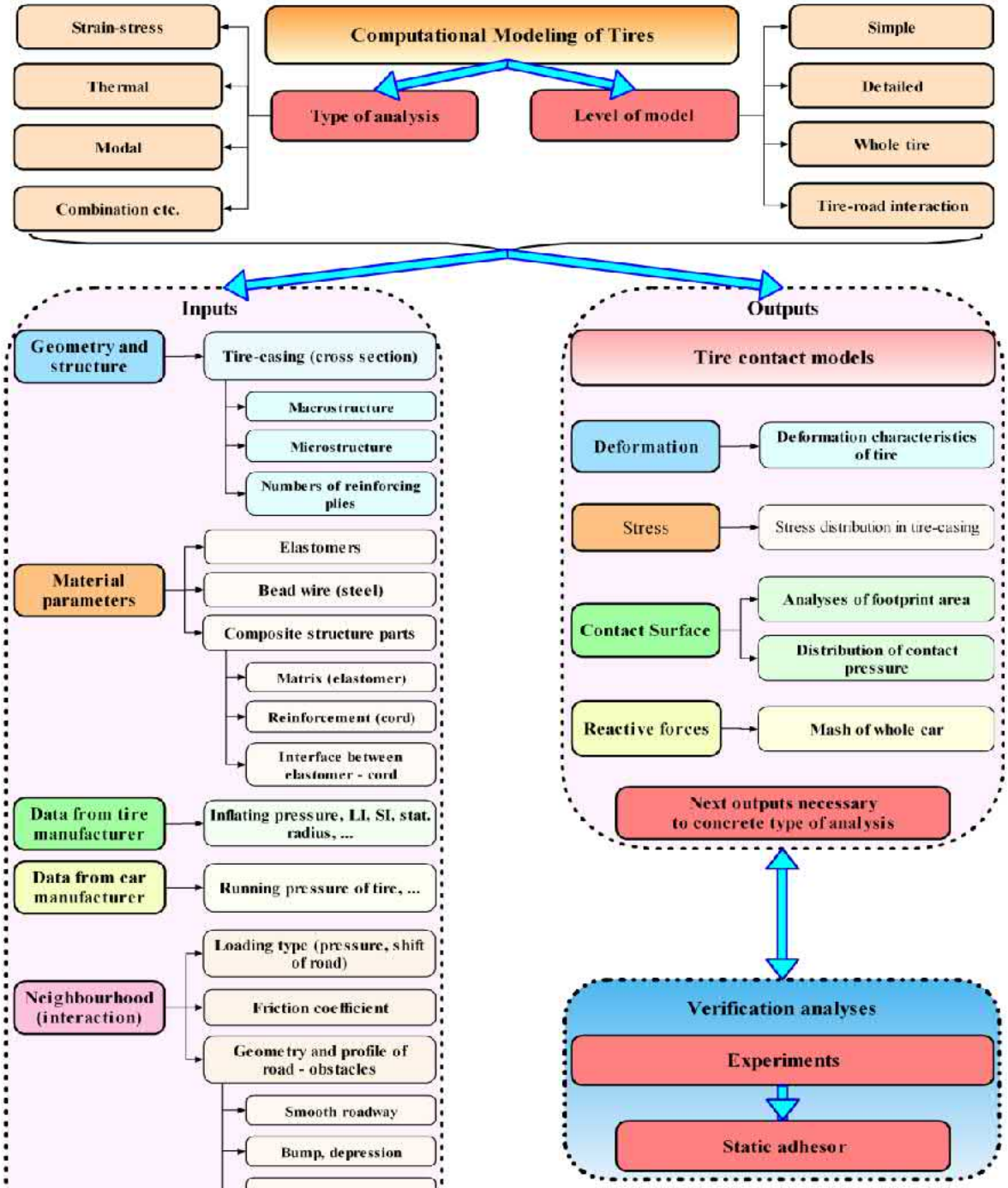
Computational Modeling of Tires
Type of analysis
Level of model
Strain-stress
Thermal
Modal
Combination etc.
Simple
Detailed
Whole tire
Tire-road interaction
Inputs
Geometry and structure
Tire-casing (cross section)
Macrostructure
Microstructure
Numbers of reinforcing plies
Material parameters
Elastomers
Bead wire (steel)
Composite structure parts
Matrix (elastomer)
Reinforcement (cord)
Interface between elastomer - cord
Data from tire manufacturer
Inflating pressure, LI, SI, stat. radius, ...
Data from car manufacturer
Running pressure of tire, ...
Neighbourhood (interaction)
Loading type (pressure, shift of road)
Friction coefficient
Geometry and profile of road - obstacles
Smooth roadway
Bump, depression
Outputs
Tire contact models
Deformation
Deformation characteristics of tire
Stress
Stress distribution in tire-casing
Contact Surface
Analyses of footprint area
Distribution of contact pressure
Reactive forces
Mash of whole car
Next outputs necessary to concrete type of analysis
Verification analyses
Experiments
Static adhesor

For creations of computational models of tires it is necessary to have good knowledge about:

- **Complete tire geometry parameters,**
- **Structure of tire-casing from macrostructure point of view,**
- **Number of composite layers and their geometrical configurations (namely thickness),**
- **Construction of steel-cord belt which are used into tire (as angle and number of cords per meter width of belt layer),**
- **Construction and material of cords into tire (with specification of construction),**
- **Material parameters of elastomer matrixes and cords as reinforcements,**
- **Complete loading conditions (as inflation pressure into tire, loading force, shape of unevenness) etc.**

For creation computational models of parts of tires (as model of belt layers of tires) it is necessary to have next knowledge about:

- **Microstructure of interface between cords – elastomer after tire production (by microscopy),**
- **Surface treatment of cords (as thickness of surface),**
- **Uniformity of layer of elastomer drift on cord surfaces (as adhesive bond),**
- **Next e.g. structural change into microlocality of steel-cords – elastomer after degradation process as corrosion attack.**

Tire by laminate theory

One-layer, cord angle = 0

One-layer, cord angle ≠ 0

(transform)

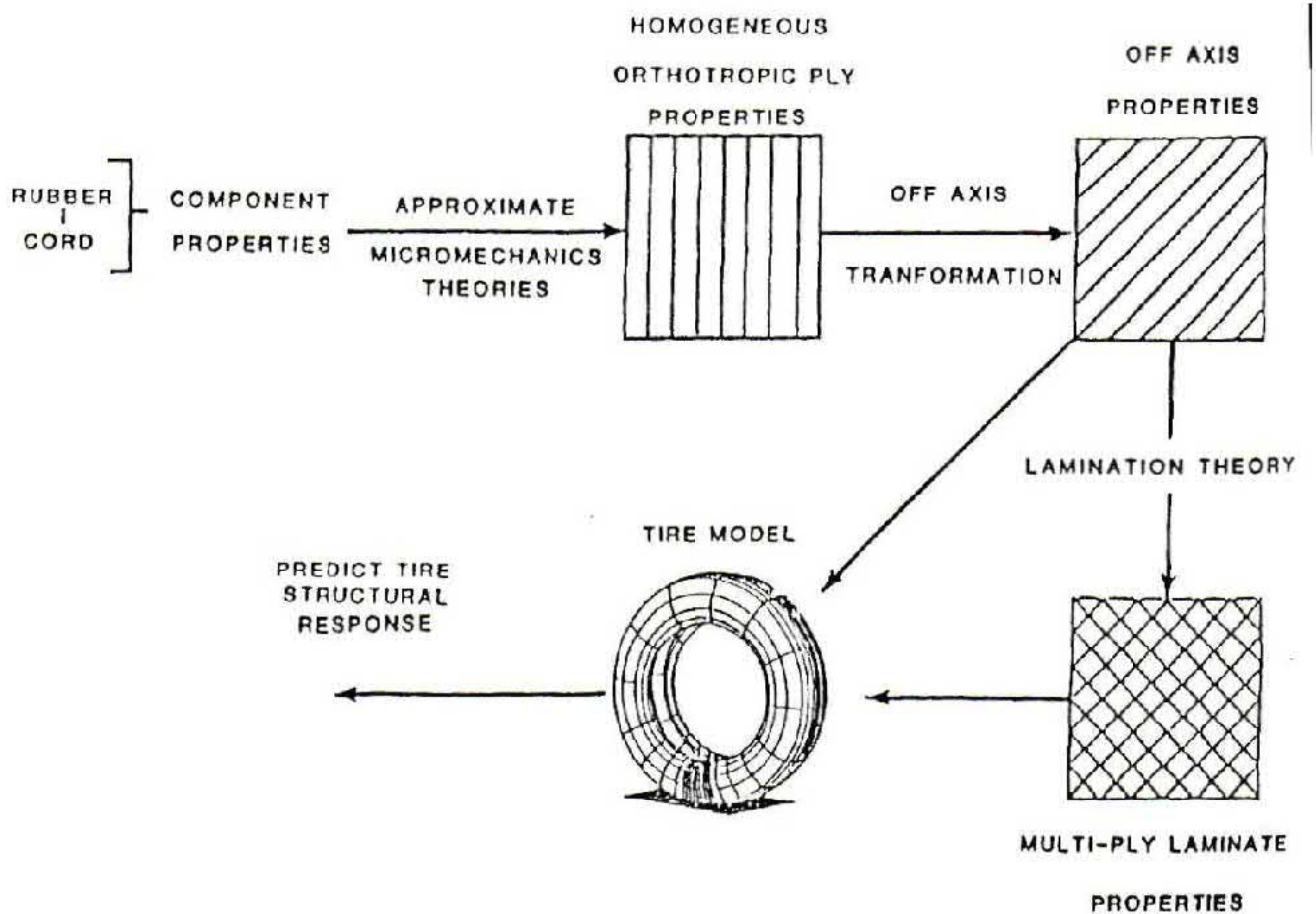

Multi-layers

(two-layers)

APPROACHES

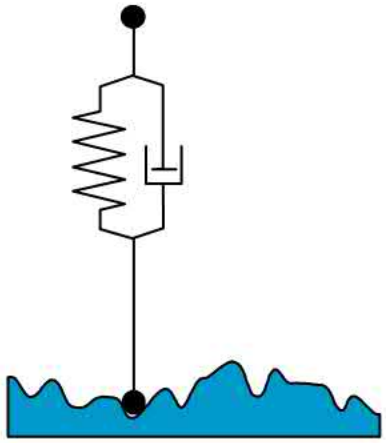

point contact

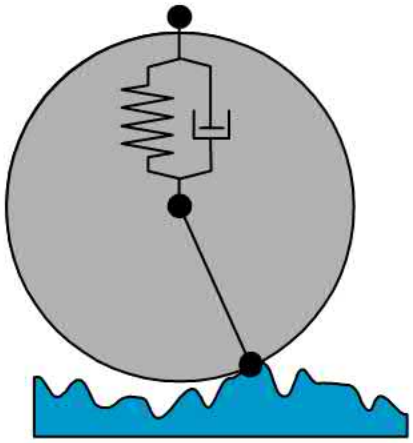

roller contact

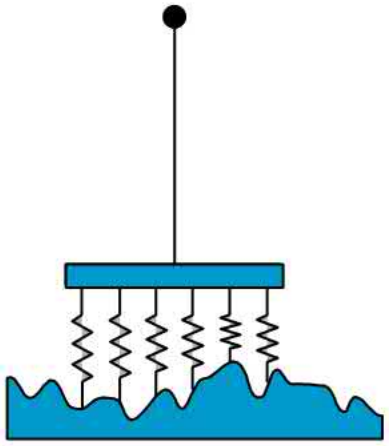

fixed footprint

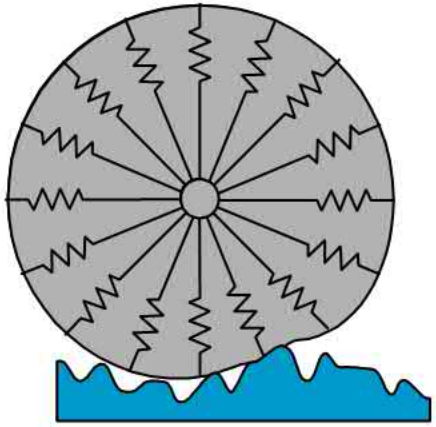

radial spring

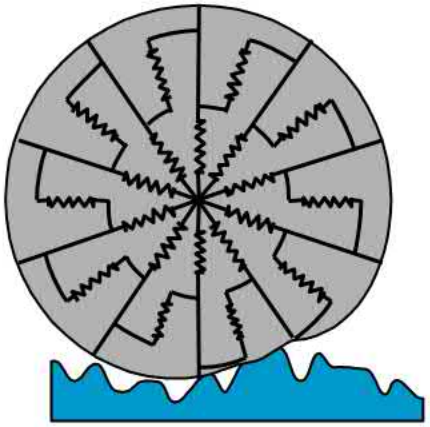

radial-interradial spring

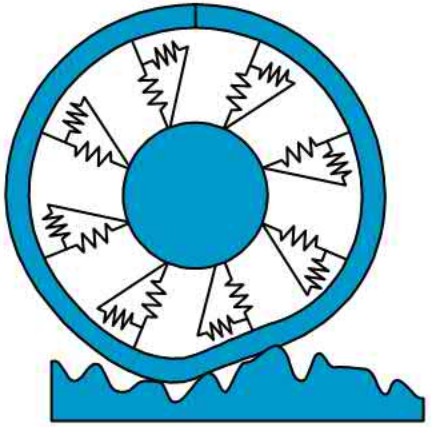

flexible ring

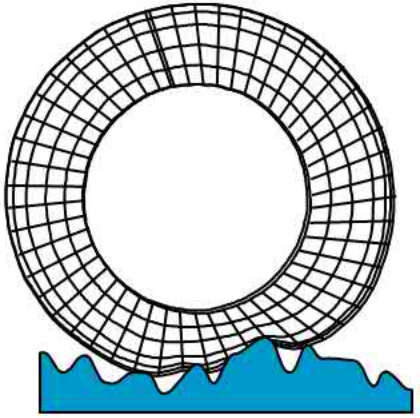

finite element

Before I start two explain these enveloping models I will give overview of other, different enveloping models.

As already explained the point contact model is not able to describe the tire behaviour correctly. No lengthening of the response and no swallowing of obstacles.

The rigid roller model is able to lengthen the response, but is not able to swallow obstacles.

The major problem of the fixed footprint model and the radial spring model is that there is no connection between adjoining springs, i.e. there is always a continues contact patch.

All other models, the radial-interradial spring model, the flexible ring model and the finite element model are able to describe the tire response rather well. The computational effort is however very large.

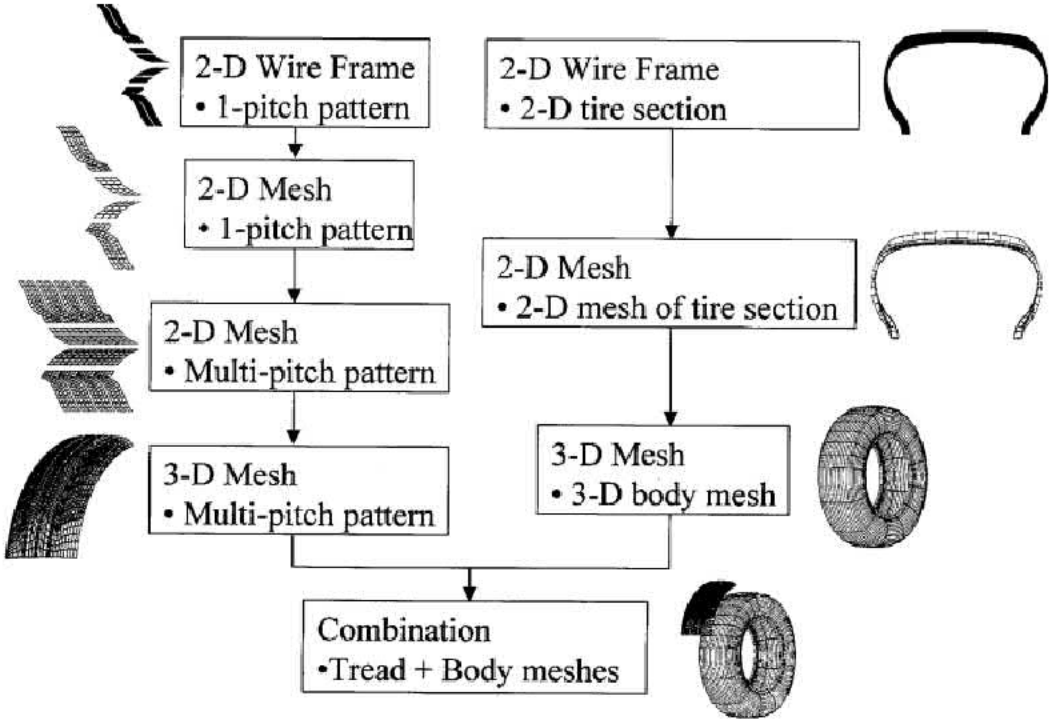

Fig. 4. 3D tire meshing process considering the detailed tread blocks.

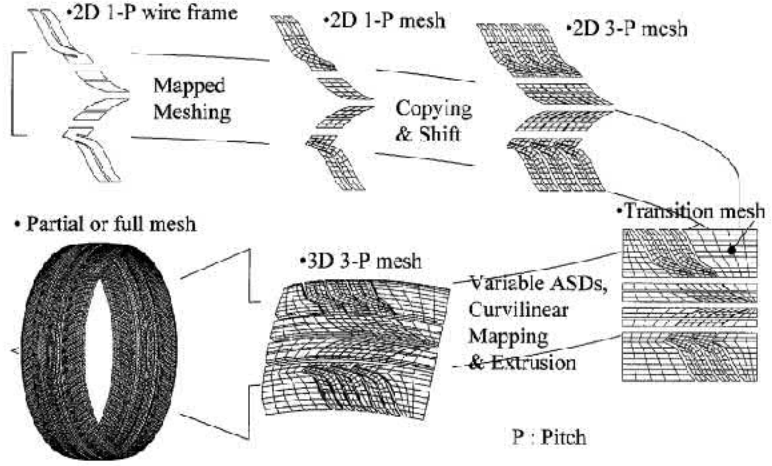

Fig. 5. Procedure for generating tread meshes (no need of the transition mesh for the full tread mesh).

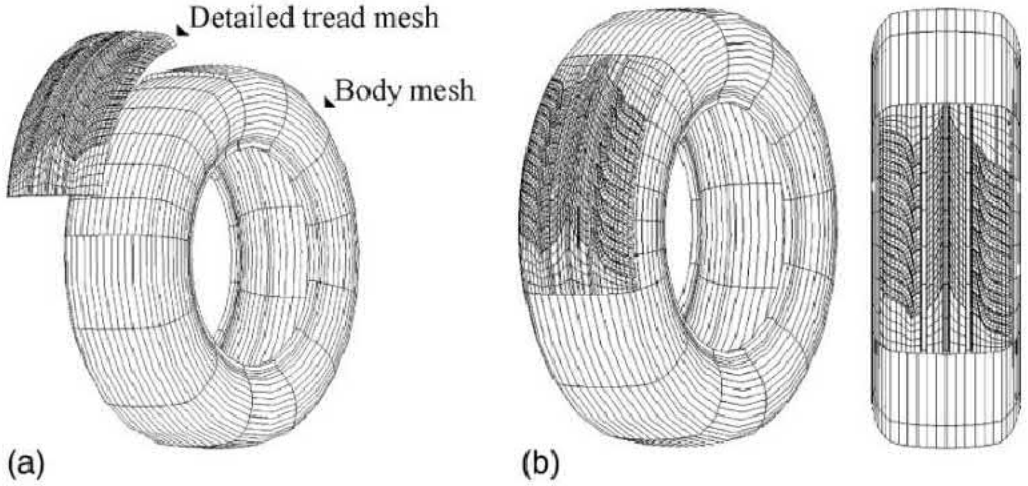

Fig. 10. 3D tire model with partial tread mesh: (a) before assembling; (b) after assembling.

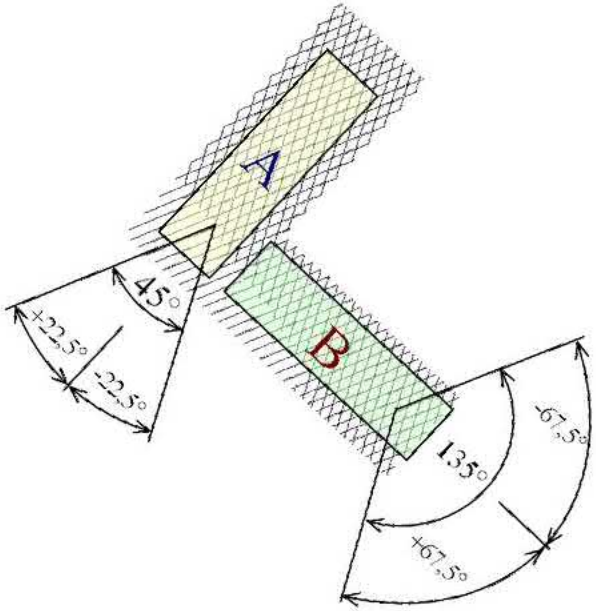

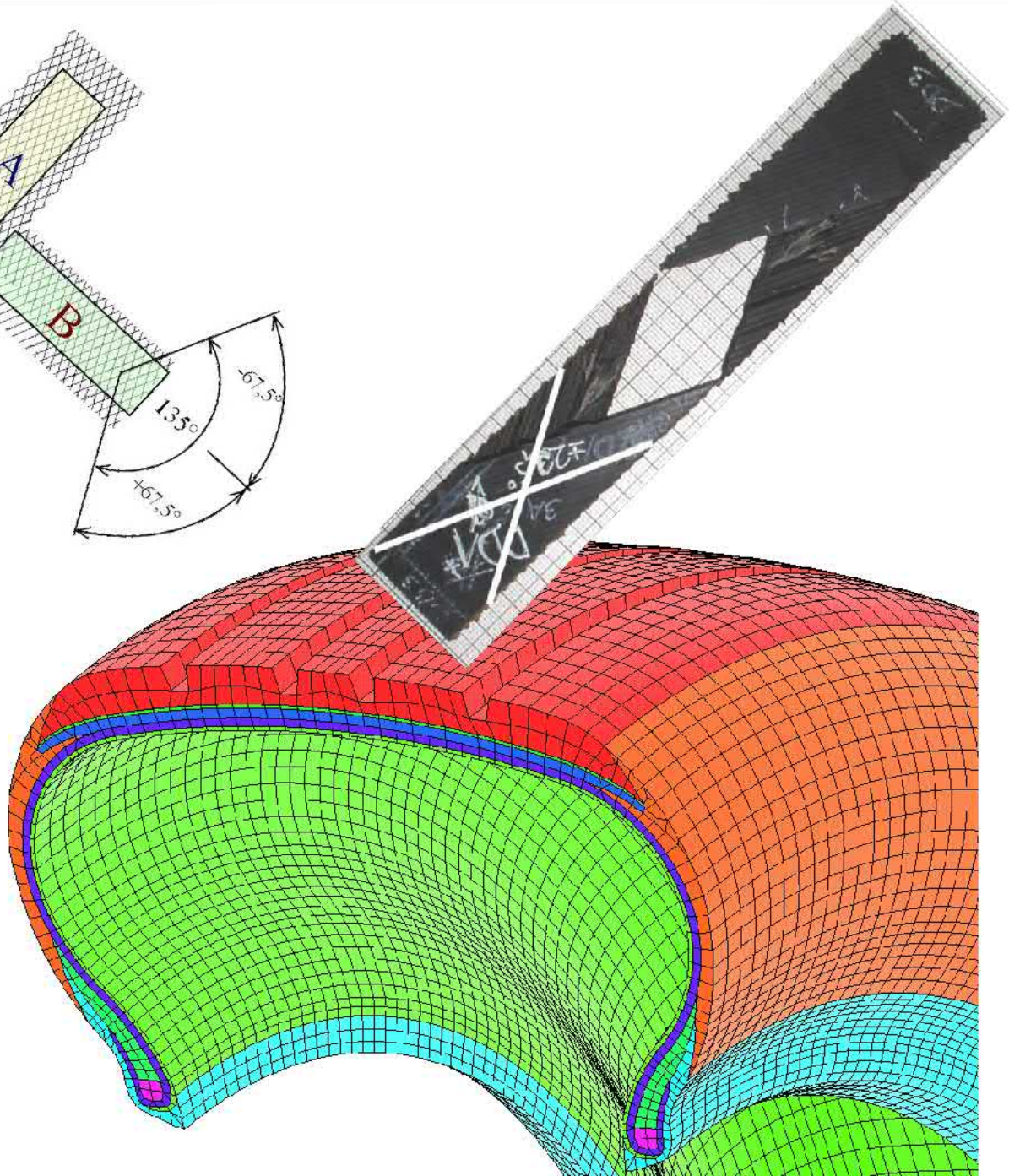

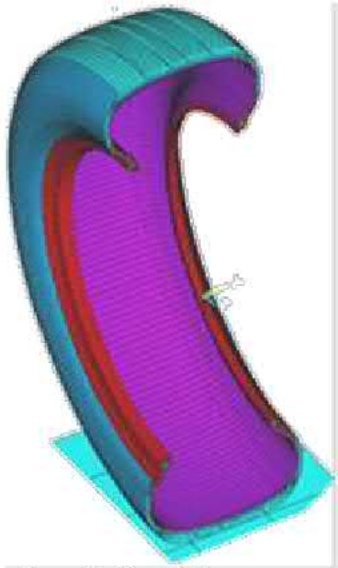

Fourth part of model:
36 000 elements
155 000 nodes

GEOMETRICAL AND MATERIAL PARAMETERS of matrixes and reinforcements into tire 165/65 R 13 (on the basic on measurement into cross-section by author)

Composite structure parts of tire			Steel-cord belt	Textile overlap belt	Textile tire carcass
Geometrical parameters	Number of layer [-]		2	1	1
	Thickness of layer [mm]		0.95	0.80	0.95*
	Cord	Diameter [mm]	0.60	0.40*	0.48*
		Cord-angle [°]	±23	0	90
		Texture [m^{-1}]	961	420*	1160
		Spacing between cords ** [mm]	1.04	2.38*	0.86*
		Volume of cord in whole layer [%]	28.6	6.6*	21.6
Material parameters	Stress modulus for matrix E [MPa]		12	21*	12
	Poisson ratio for matrix ν [-]		0.4995	0.4995	0.4995
	Stress modulus for reinforcing E [MPa]		180 000	11 000	3 400
	Poisson ratio for reinforcing ν [-]		0.3	0.66	0.4

* – only orientation value; ** – spacing determined by texture.

Mooney-Rivlin parameters for elastomer parts of tire.

Mooney-Rivlin parameters		C10 [MPa]	C01 [MPa]
Tread		0.417	0.519
Inner liner		0.109	0.259
Bead elastomer		0.692	0.371
Sidewall with Tread side edge		0.532	0.065
Bead bundle		-0.111	1.945
Elastomer drift	for steel-cord belt	0.638	0.284
	for textile overlap belt	0.548	0.112
	for textile tire carcass	0.328	0.119

M-R parameters

$$\sigma = 2\cdot\left(\lambda-\frac{1}{\lambda^2}\right)\cdot\left(C_1-\frac{C_2}{\lambda}\right)\Rightarrow\frac{\sigma}{2\cdot\left(1-\frac{1}{\lambda^3}\right)}=C_1\cdot\lambda+C_2$$

$$Y = A\cdot X + B \Leftrightarrow \frac{\sigma}{2\cdot\left(1-\frac{1}{\lambda^3}\right)}=C_1\cdot\lambda+C_2$$

$$Y = C_{10}\cdot\lambda + C_{01}$$

$$\sigma = \left(C_{10}\cdot\lambda+C_{01}\right)\cdot 2\cdot\left(1-\frac{1}{\lambda^3}\right)$$

Lambda λ = Epsi + 1

$$\sigma = \left(C_{10}\cdot\left(Epsi+1\right)+C_{01}\right)\cdot 2\cdot\left(1-\frac{1}{\left(Epsi+1\right)^3}\right)$$

Excel sigma = [C10*(Epsi+1)+C01]*2*[1-1/(Epsi+1)_3]

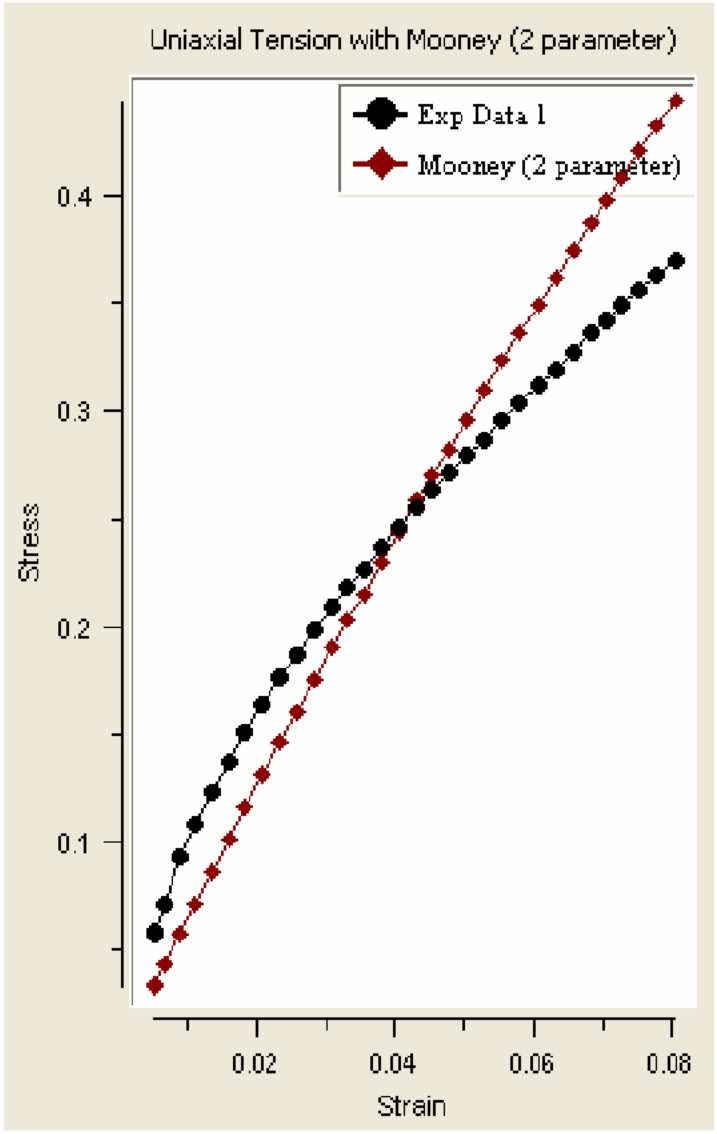
Uniaxial Tension with Mooney (2 parameter)
Exp Data 1
Mooney (2 parameter)
Stress
0.1
0.2
0.3
0.4
0.02
0.04
0.06
0.08
Strain

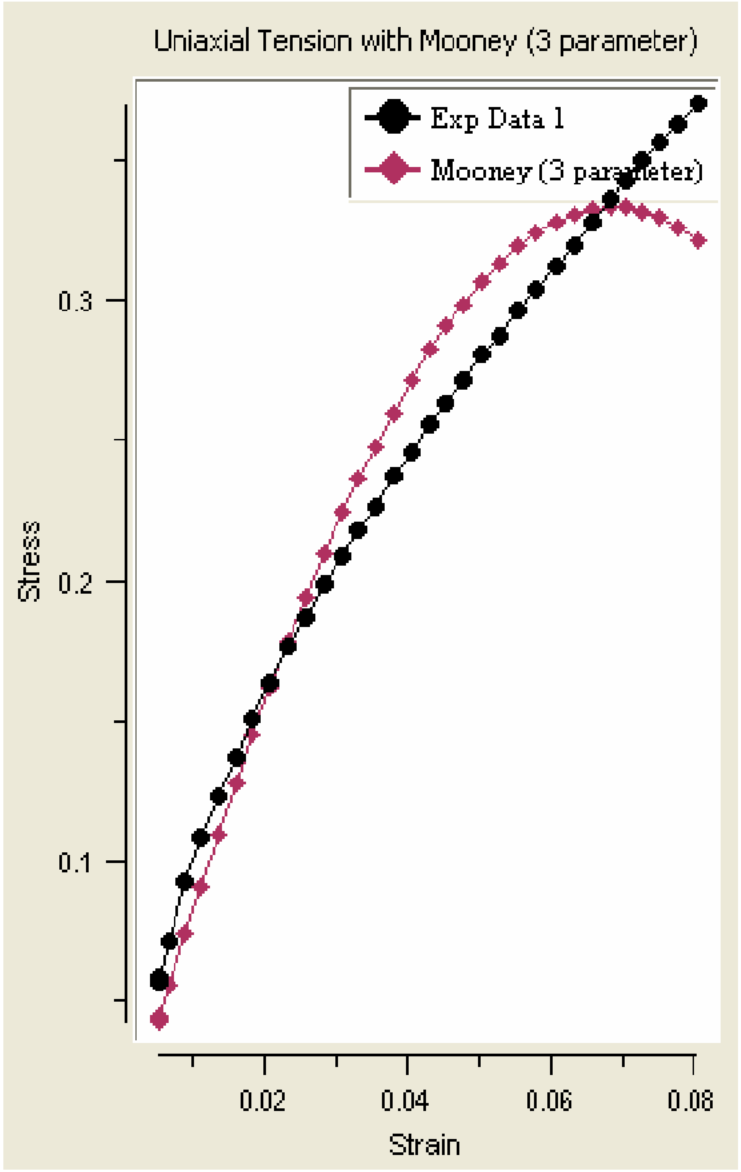
Uniaxial Tension with Mooney (3 parameter)
Exp Data 1
Mooney (3 parameter)
Stress
0.1
0.2
0.3
0.02
0.04
0.06
0.08
Strain

Material parameters of elastomer matrixes

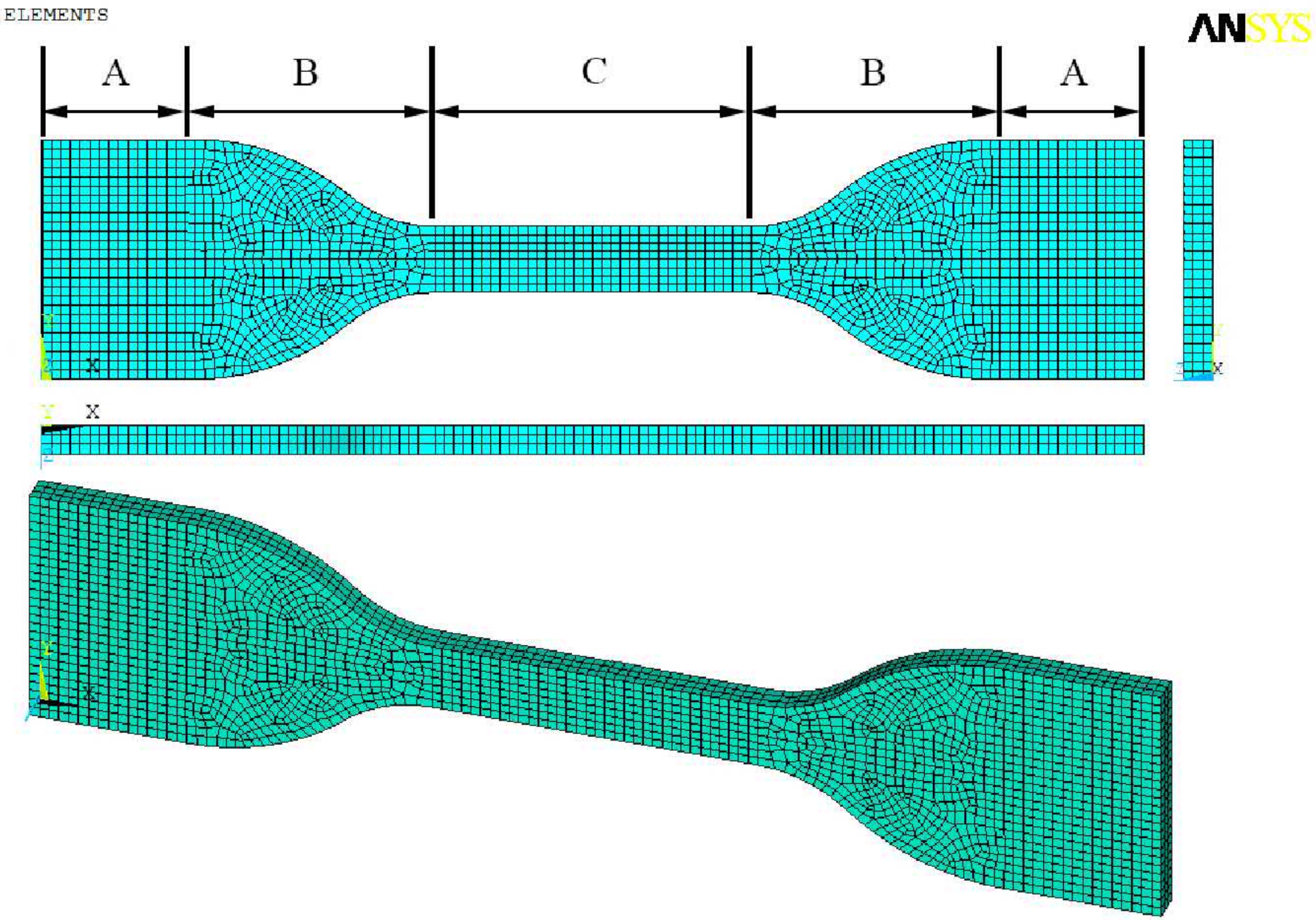

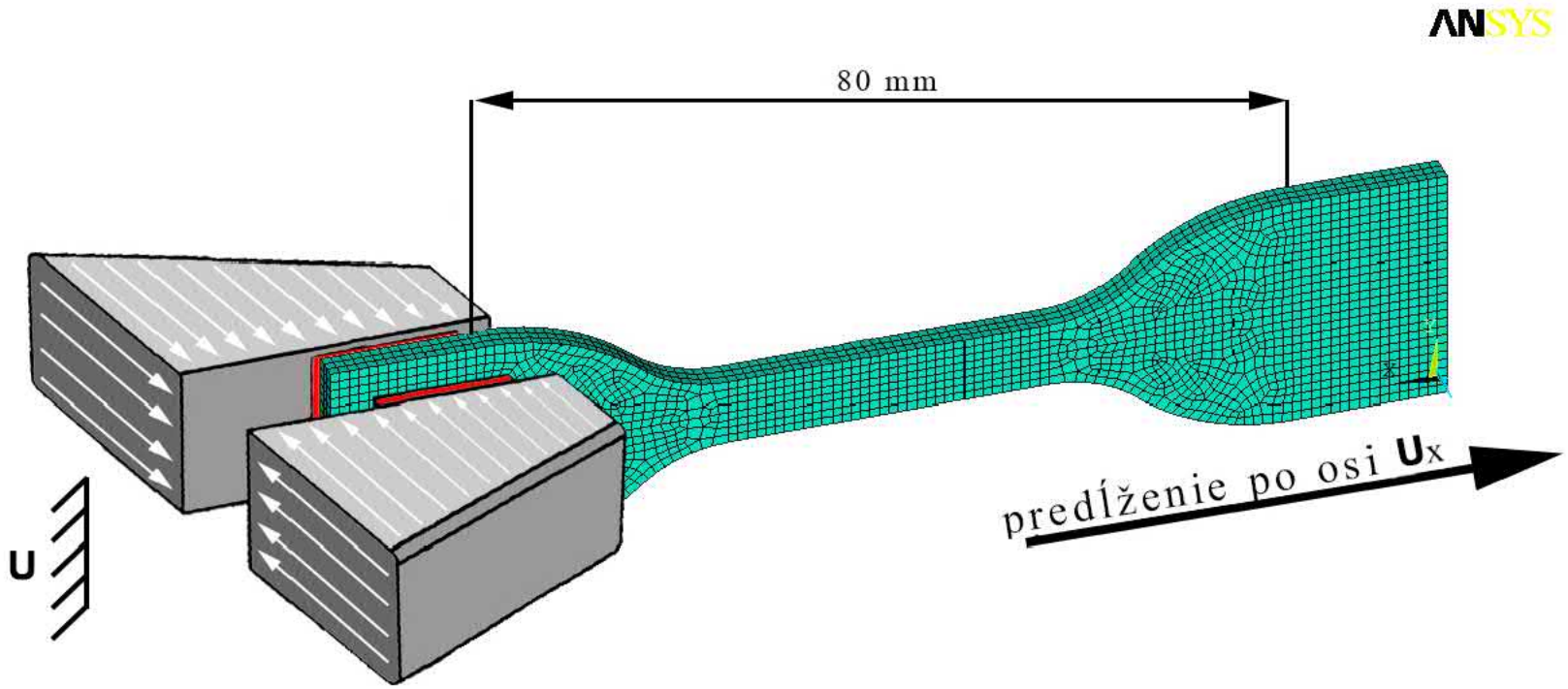
ANSYS
80 mm
predĺženie po osi Ux
U

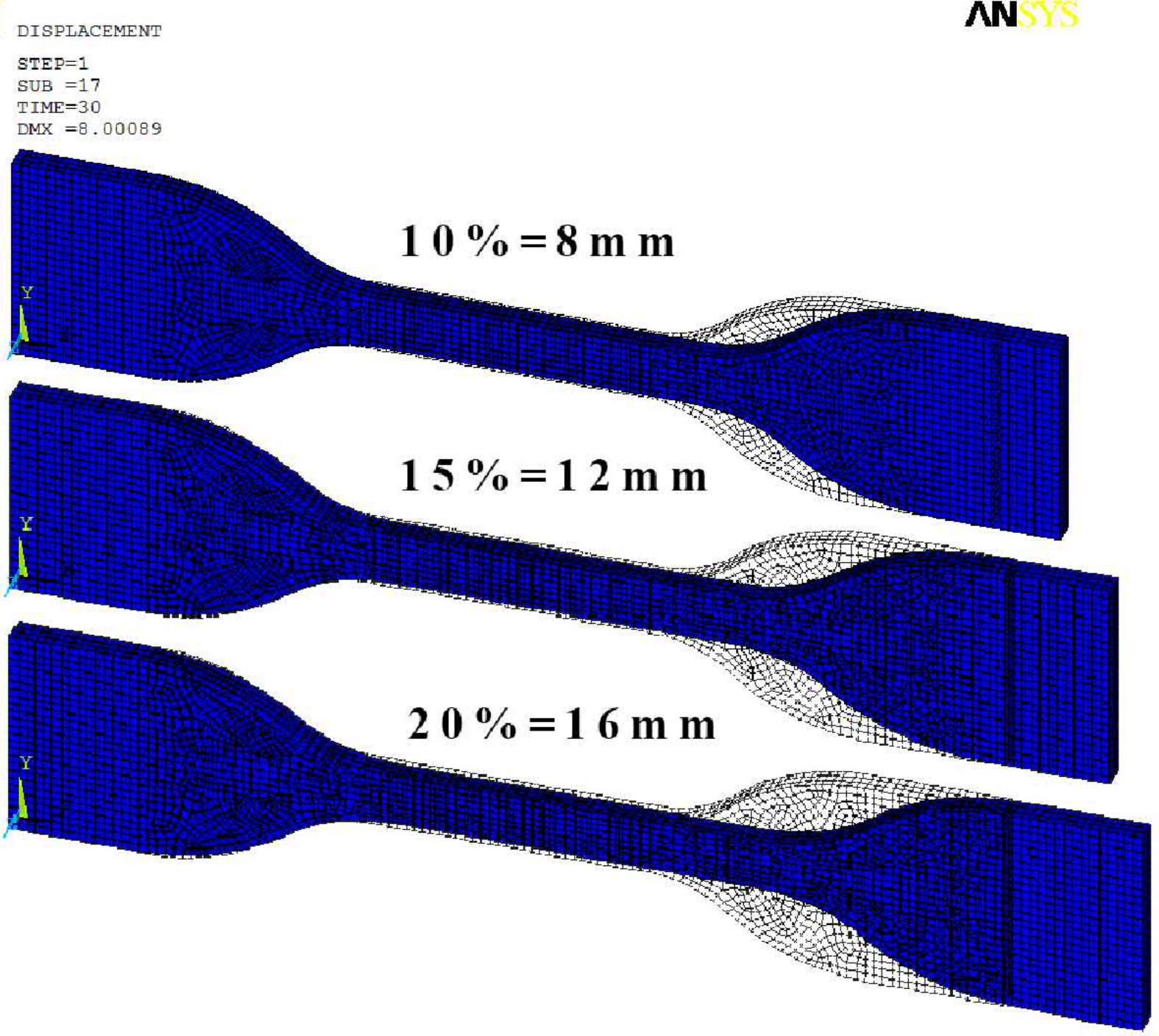
DISPLACEMENT
STEP=1
SUB =17
TIME=30
DMX =8.00089
10 % = 8 mm
15 % = 12 mm
20 % = 16 mm
Y
Y
Y

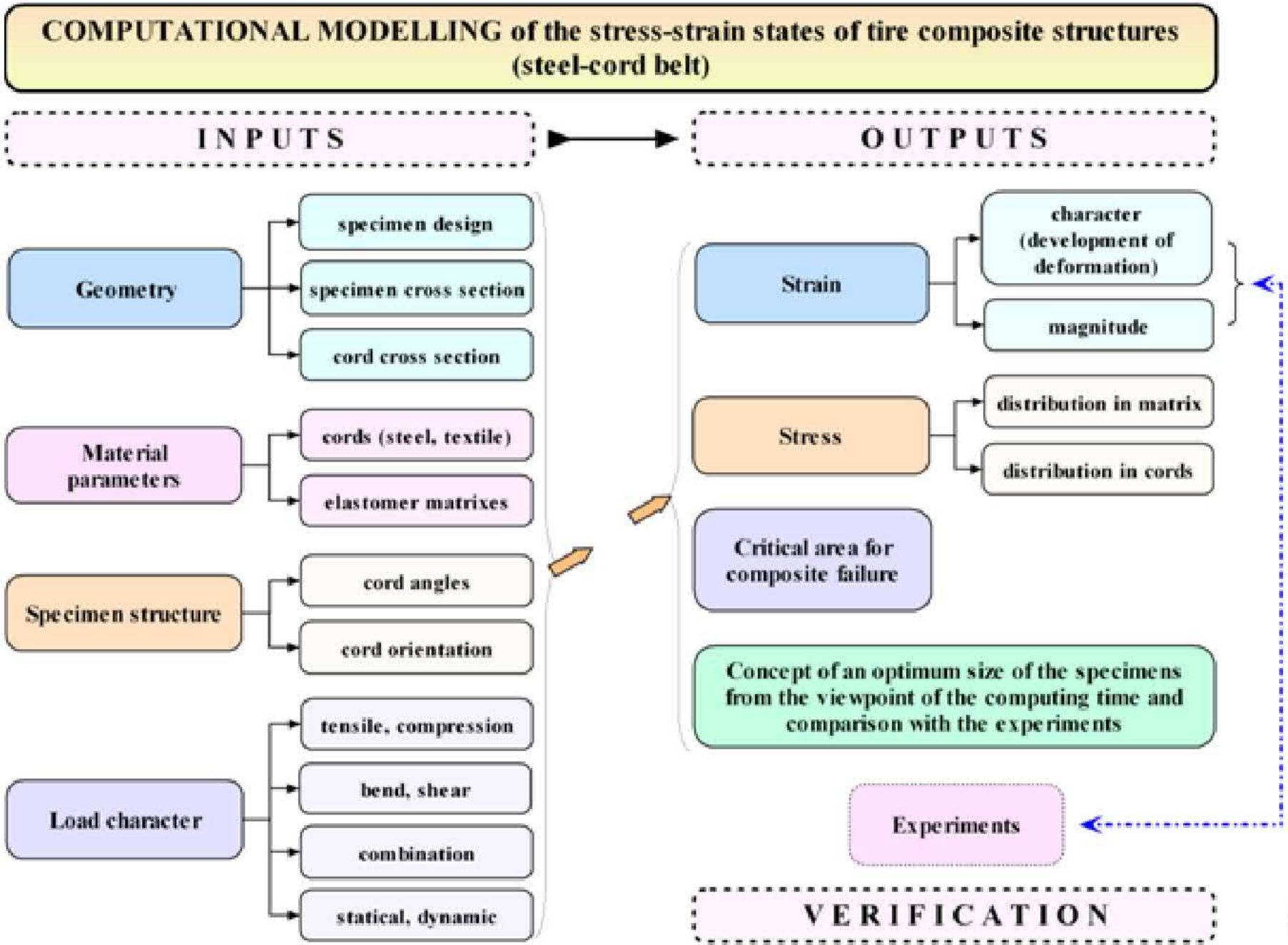
COMPUTATIONAL MODELLING of the stress-strain states of tire composite structures (steel-cord belt)
INPUTS
OUTPUTS
Geometry
specimen design
specimen cross section
cord cross section
Material parameters
cords (steel, textile)
elastomer matrixes
Specimen structure
cord angles
cord orientation
Load character
tensile, compression
bend, shear
combination
statical, dynamic
Strain
character (development of deformation)
magnitude
Stress
distribution in matrix
distribution in cords
Critical area for composite failure
Concept of an optimum size of the specimens from the viewpoint of the computing time and comparison with the experiments
Experiments
VERIFICATION

model without adhesive bond

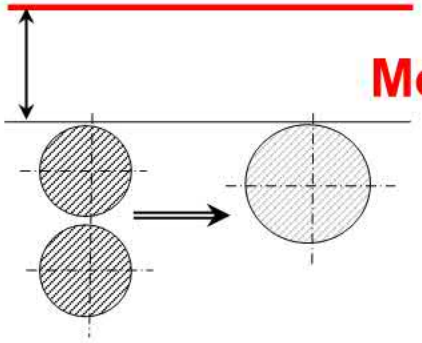

Modul of inertial

Material parameters for non-linear matrix = Mooney-Rivlin hyperelastic model

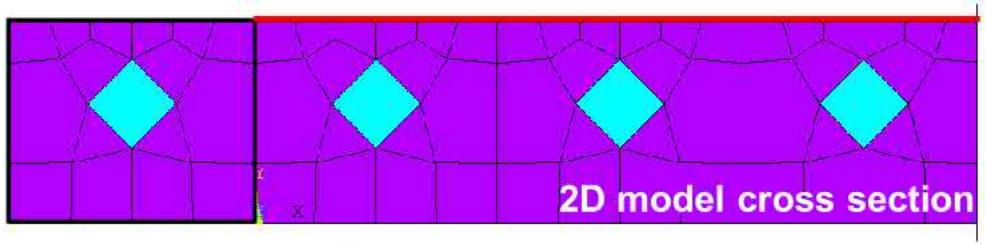

„basic“

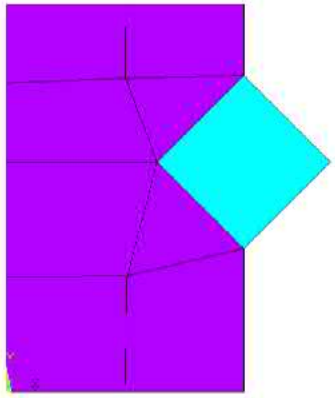

3D model

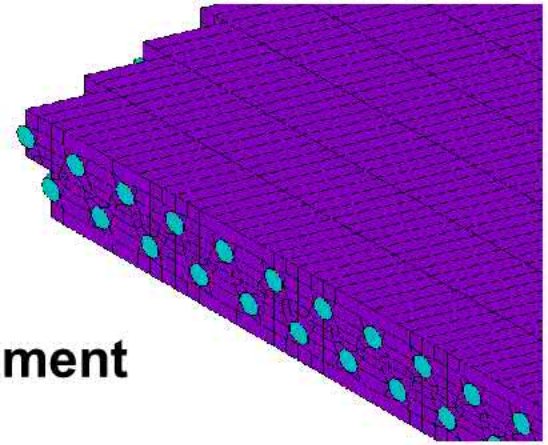

Cord by solid or beam element

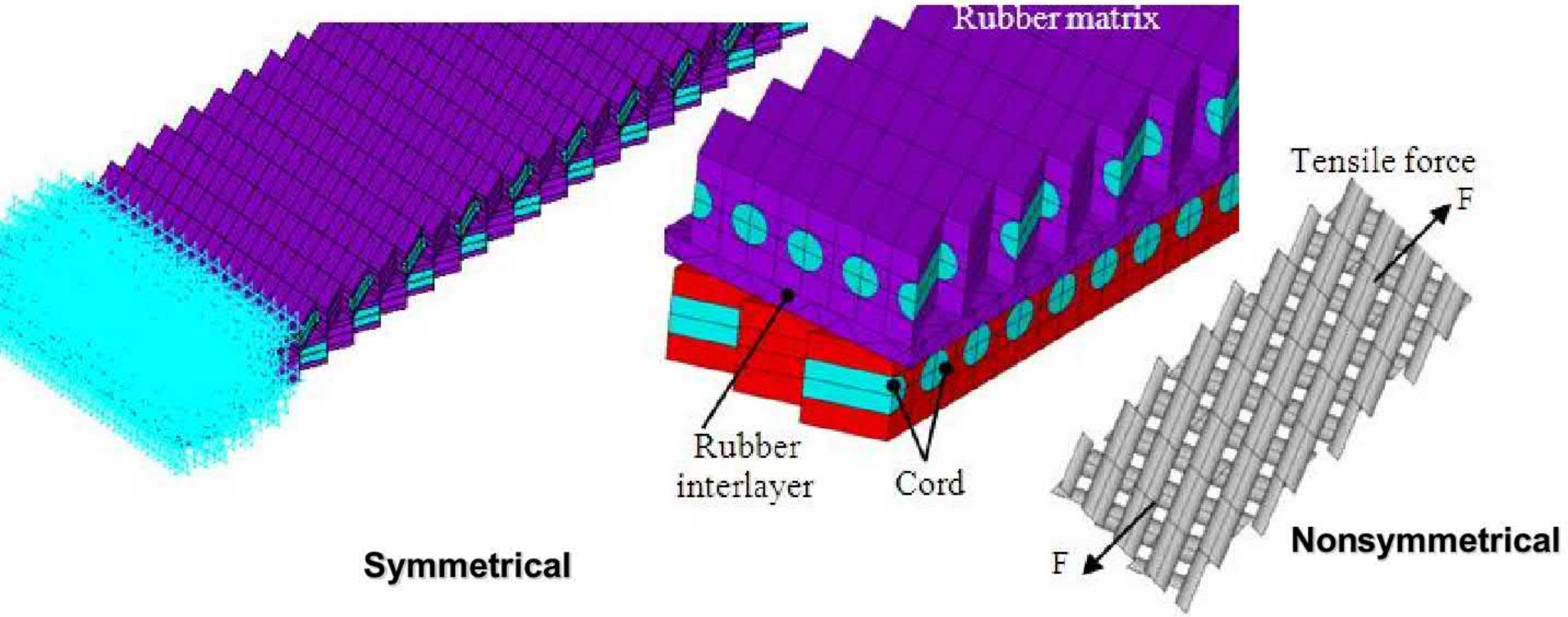

Tensile Bend

One-layer / Two-layer

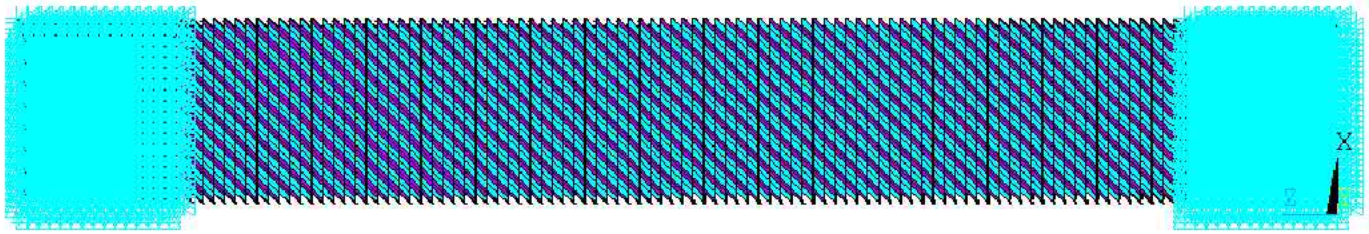

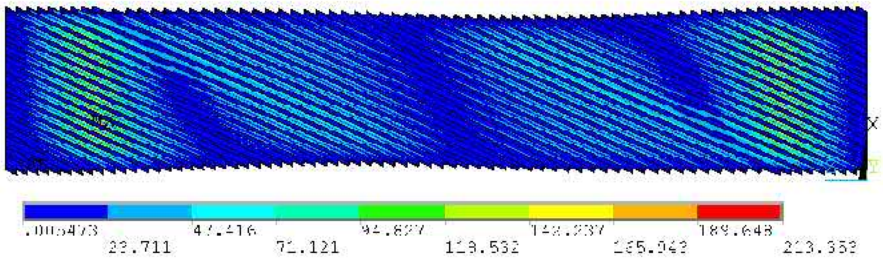

One-layer 23°
stress [MPa]
- **cord stress**
- **matrix stress**

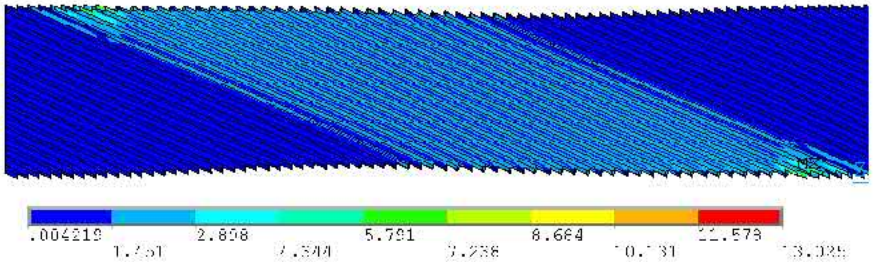

TENSILE

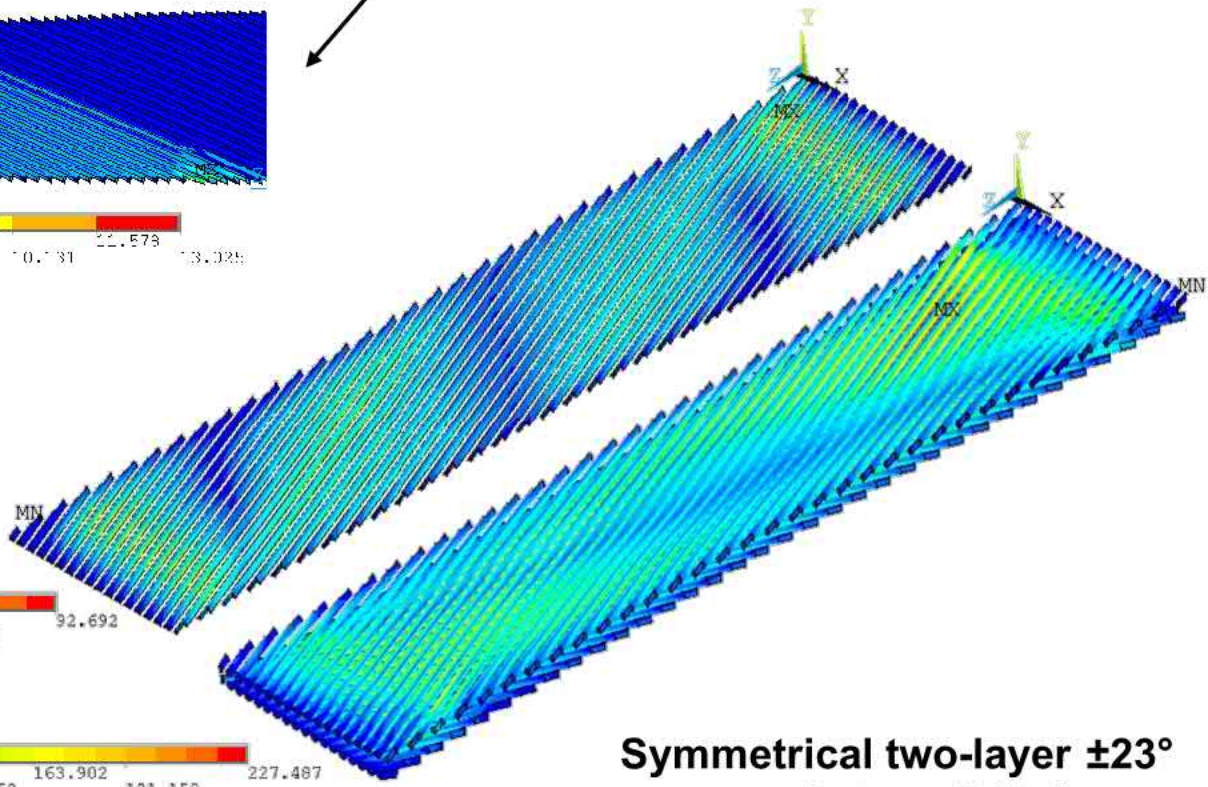

Symmetrical two-layer ±23°
cord stress [MPa]

23° two-layer tensile test

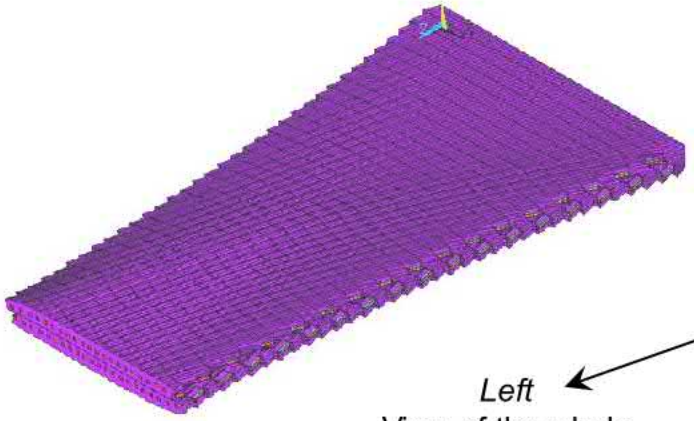

Left
View of the whole specimen

Centre
Top view of the upper surface of the bottom layer of a two-layer specimen (i.e. the "place of contact" of the upper and bottom layer of the specimen).

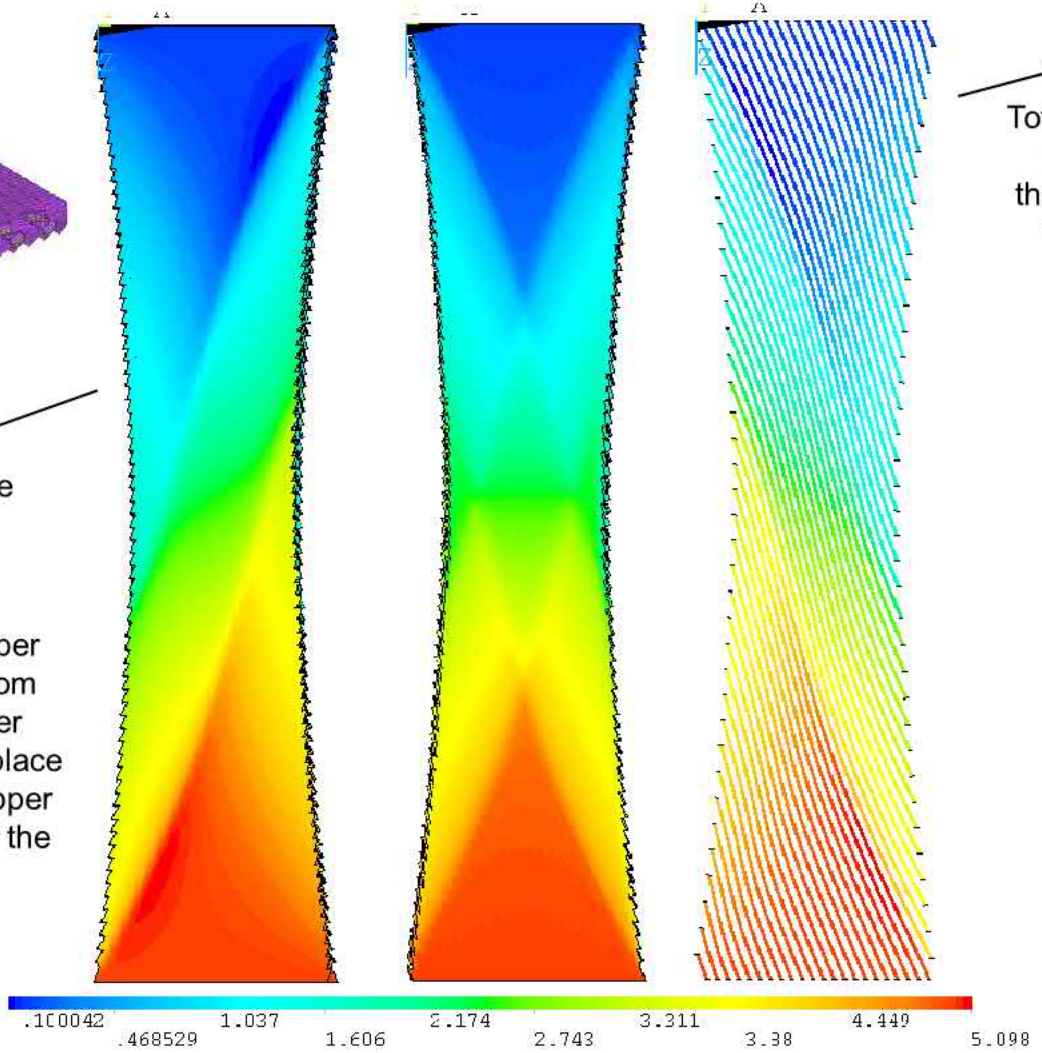

Right
Total displacements in the cords in the bottom layer of the specimen.

Displacements along specimen **length**

23° specimen – tensile test

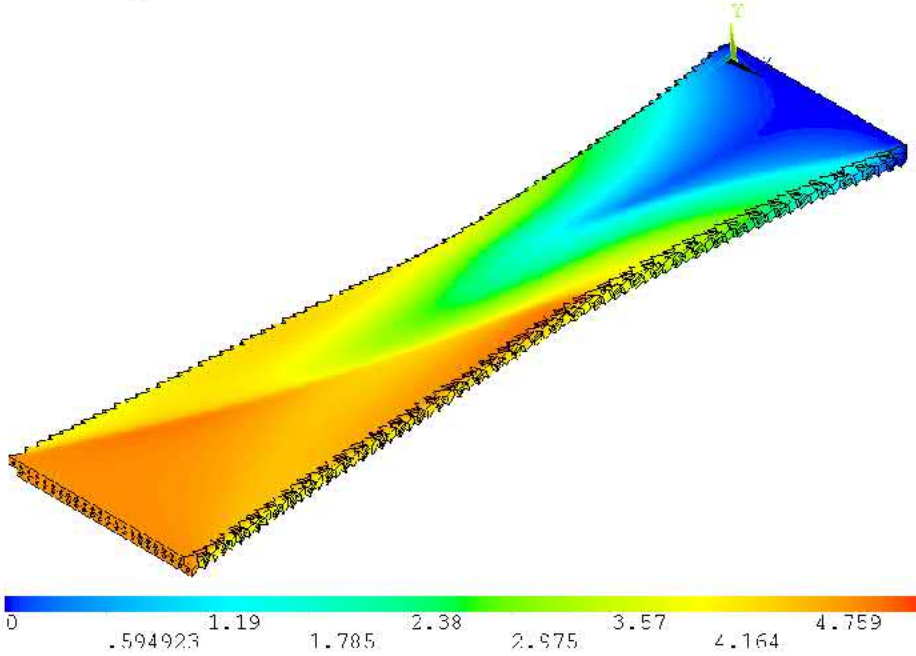

⇐ Two-layer specimen

Single-layer specimen ⇓

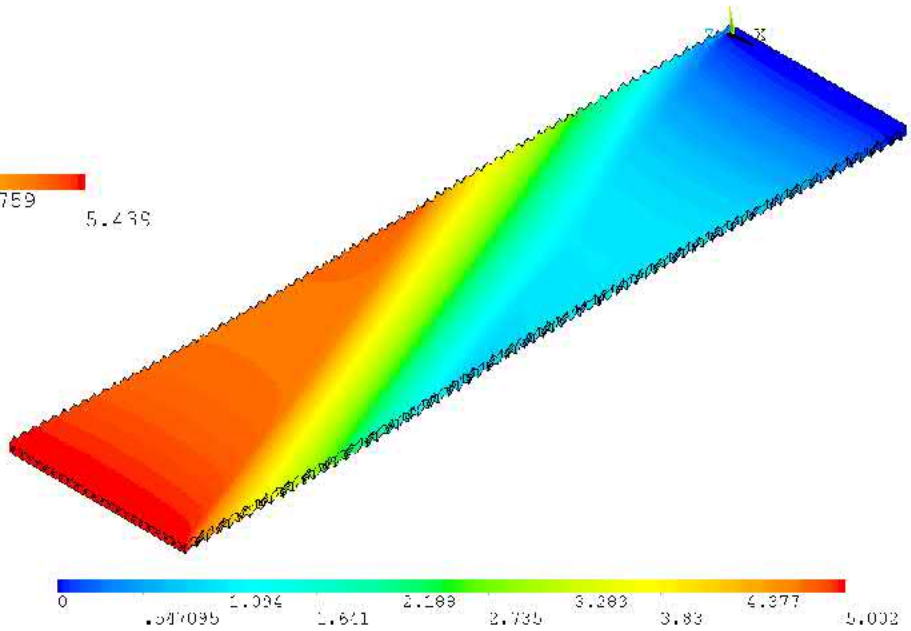

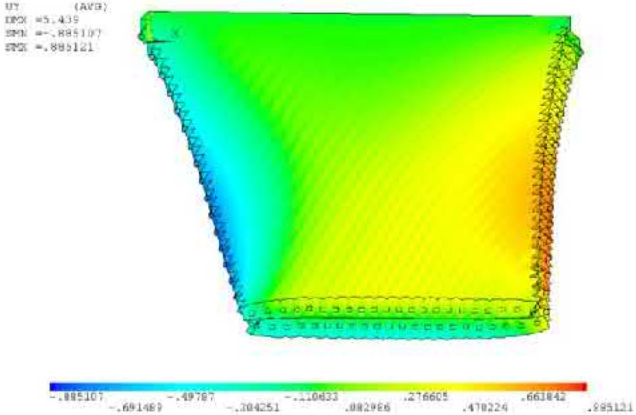

Total displacements and comparison with a single-layer specimen

30° – tensile, 10 mm width

Force [N] ↑

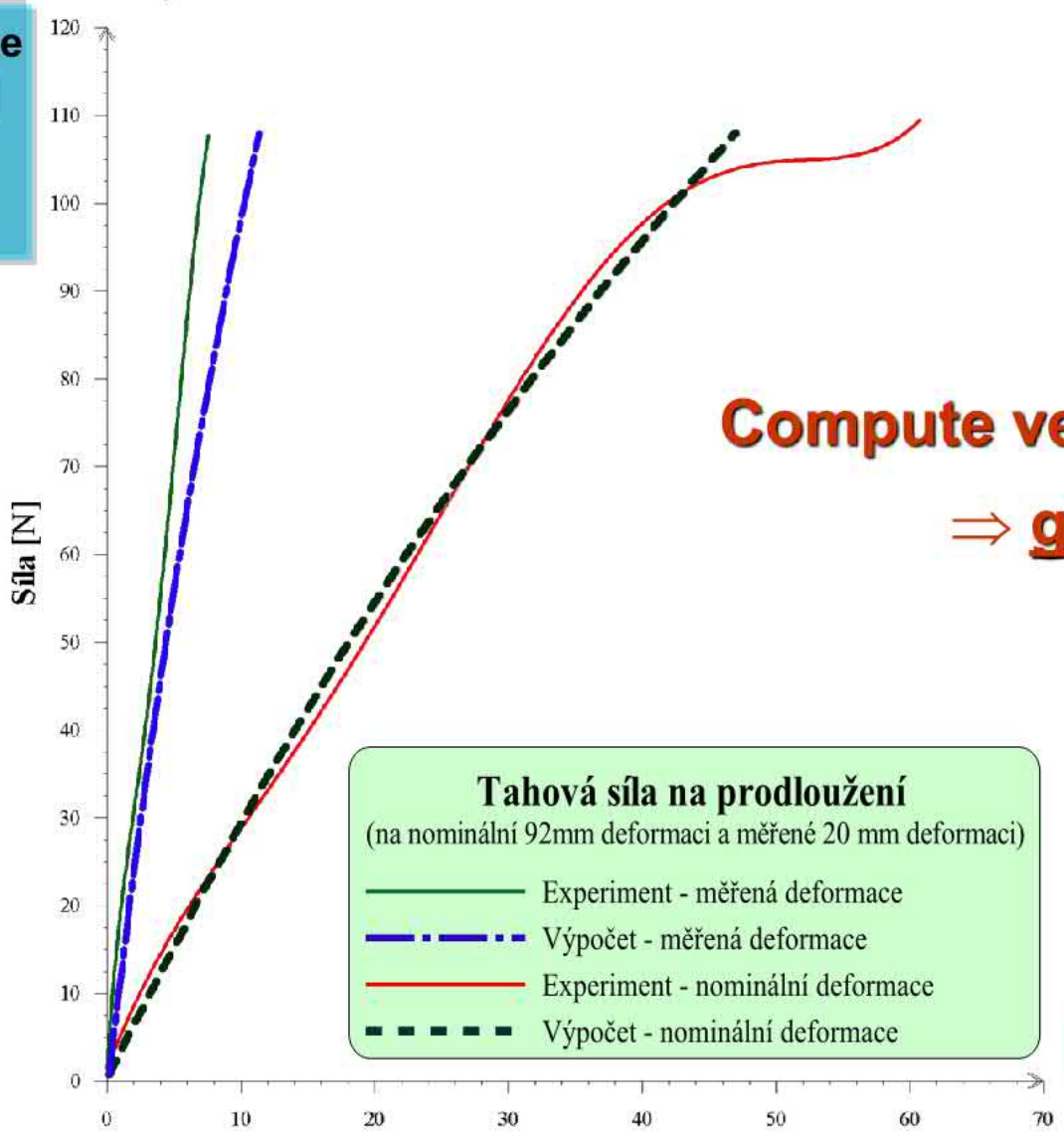

Compute vers. experiment:

⇒ **good**

→ Elongation [mm]

60° – bend, 5.6 mm width

Force [N]

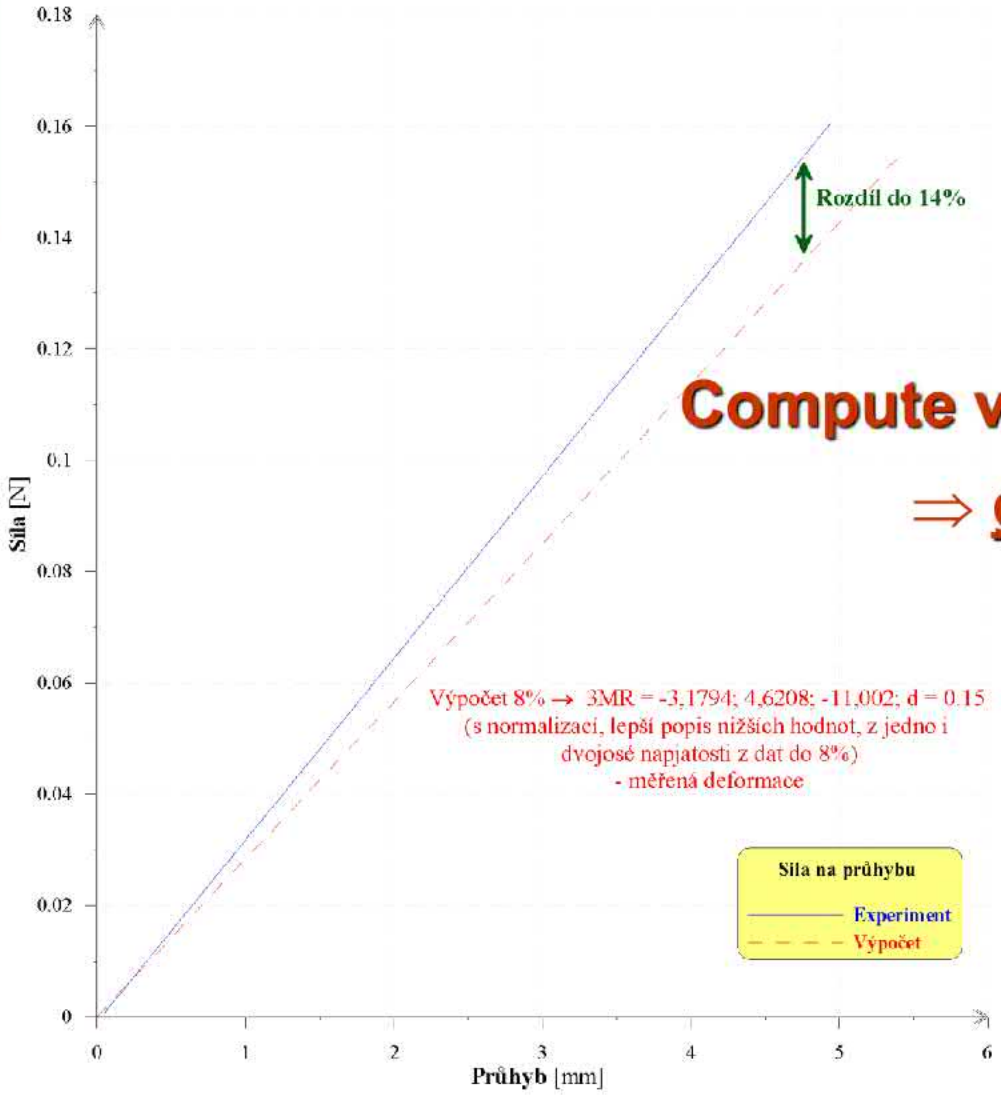

Compute vers. experiment:

⇒ good

→ Deformation [mm]

23° – BEND / 4 mm

⇐ Two layers / one layer

⇓

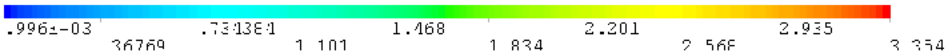

67° – BEND / 4 mm

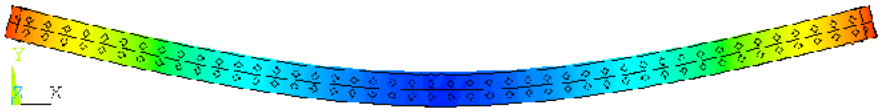

⇐ Two layers / one layer

⇓

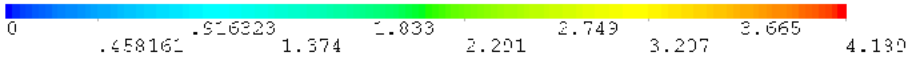

model with bond cord-rubber

This specific area between the cord and the rubber in the computational models of the steel-belt leads to the decreasing of the cord diameters.

Thickness of this area is also determining parameter for correct consideration of adhesion and degradation processes in the border of steel cord/drift rubber/rubber matrix.

model with bond cord-rubber

The way of adhesive bond incorporation in way of considering the replacement by third material will be show on the next figure. The model of half of one steel-belt layer with the reinforcement formed by compact wire is being concerned. Original border of cord-matrix (i.e. steel-cord diameter) is illustrated with dash line.

model with bond cord-rubber

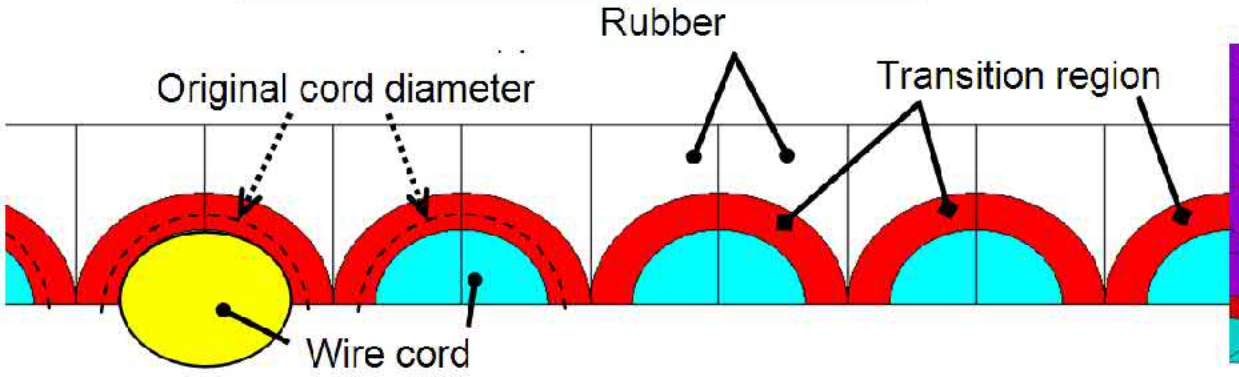

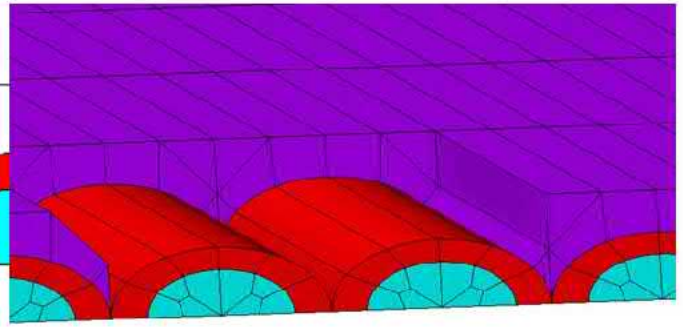

Meshing of FEM model

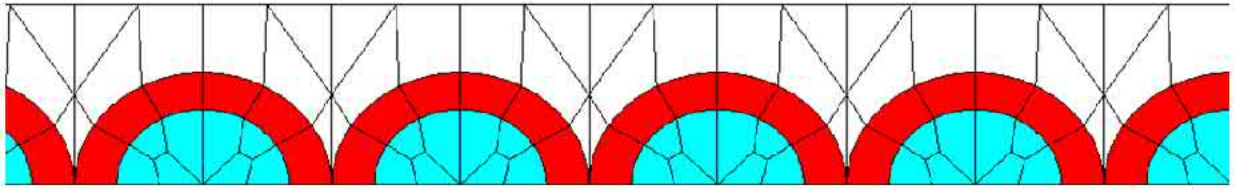

Design of computational model of wire steel-cord belt (half of one-layer with orientation angle 30°) with adhesive bond

Sample output - Stress von Mises into cord [MPa]

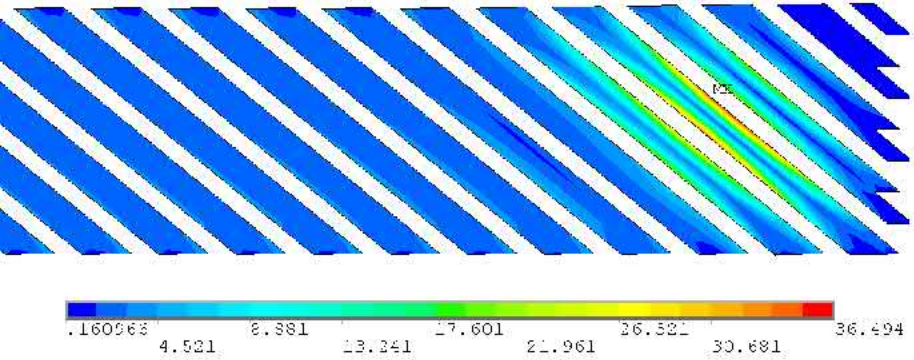

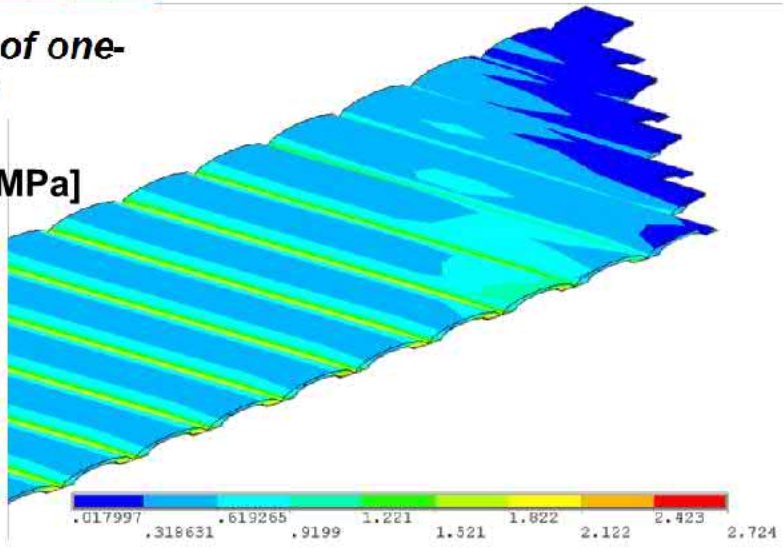

COMPUTATIONAL MODEL OF STEEL-CORD BELT for STRESS-STRAIN ANALYSES

- material parameters of **matrix** (Mooney-Rivlin) and cord,
- **optimalization** (computational time, type of analyses),
- „**open**“⇒ **other analyses** (after supplementation of necessary input data to the models, analyses of thermal field, dynamical form of loading, eventually combination these loading states will be possible),
- outputs are **inputs to FEA model of tire**,
- model of steel-cord belt with degradation (**CORROSION**).

Macro and microstructure of steel-cord belt (interface cord-rubber by microscopy).

Corrosion test of sample of steel-cord belt.

Part 7 – CREATION OF COMPUTATIONAL MODELS:

Geometrical parameters, Material parameters (characteristics) as input for computational model, Replacement of belt structure for FEA of tire

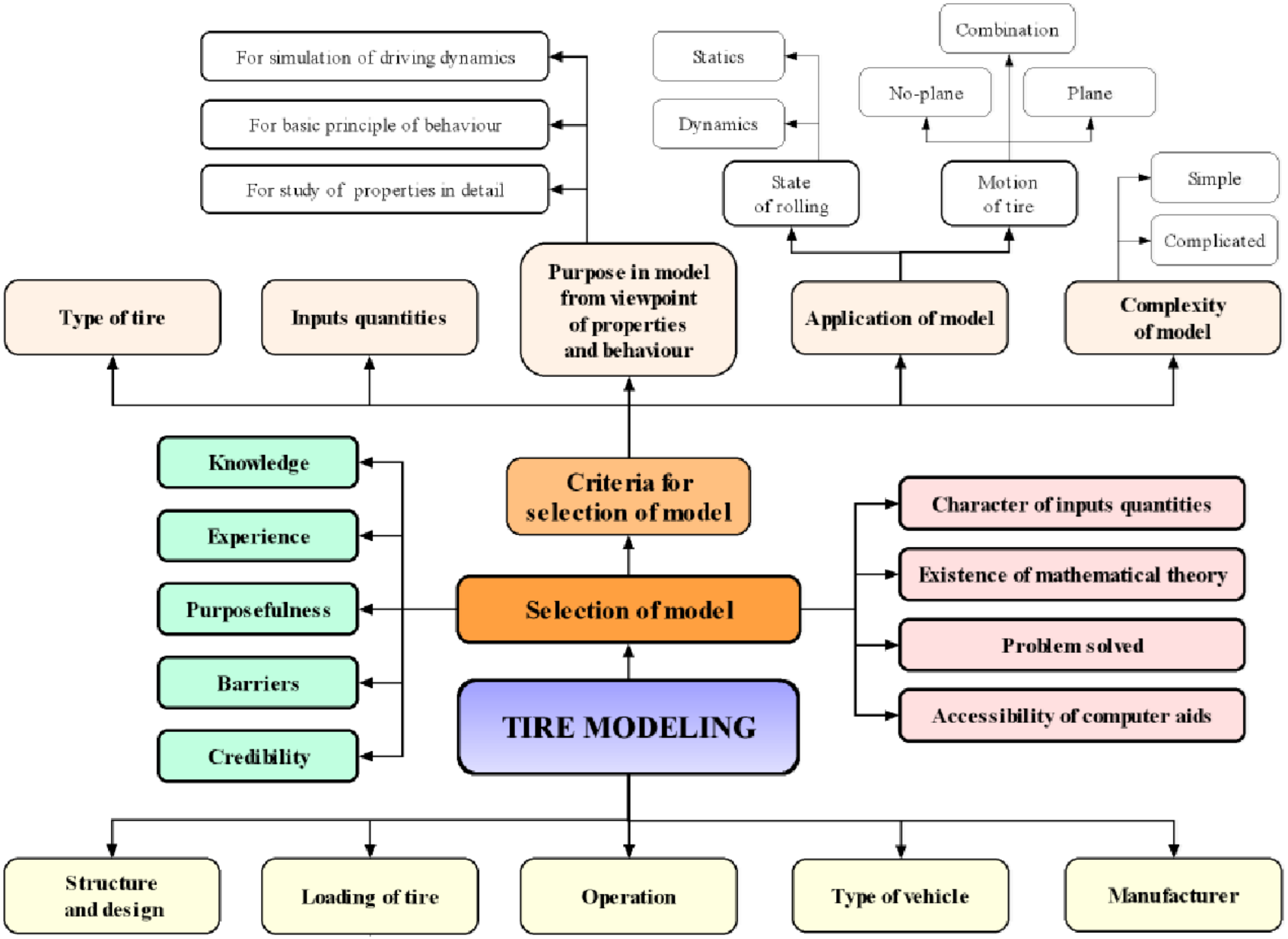

Criteria for choosing of tire computational models and requirements

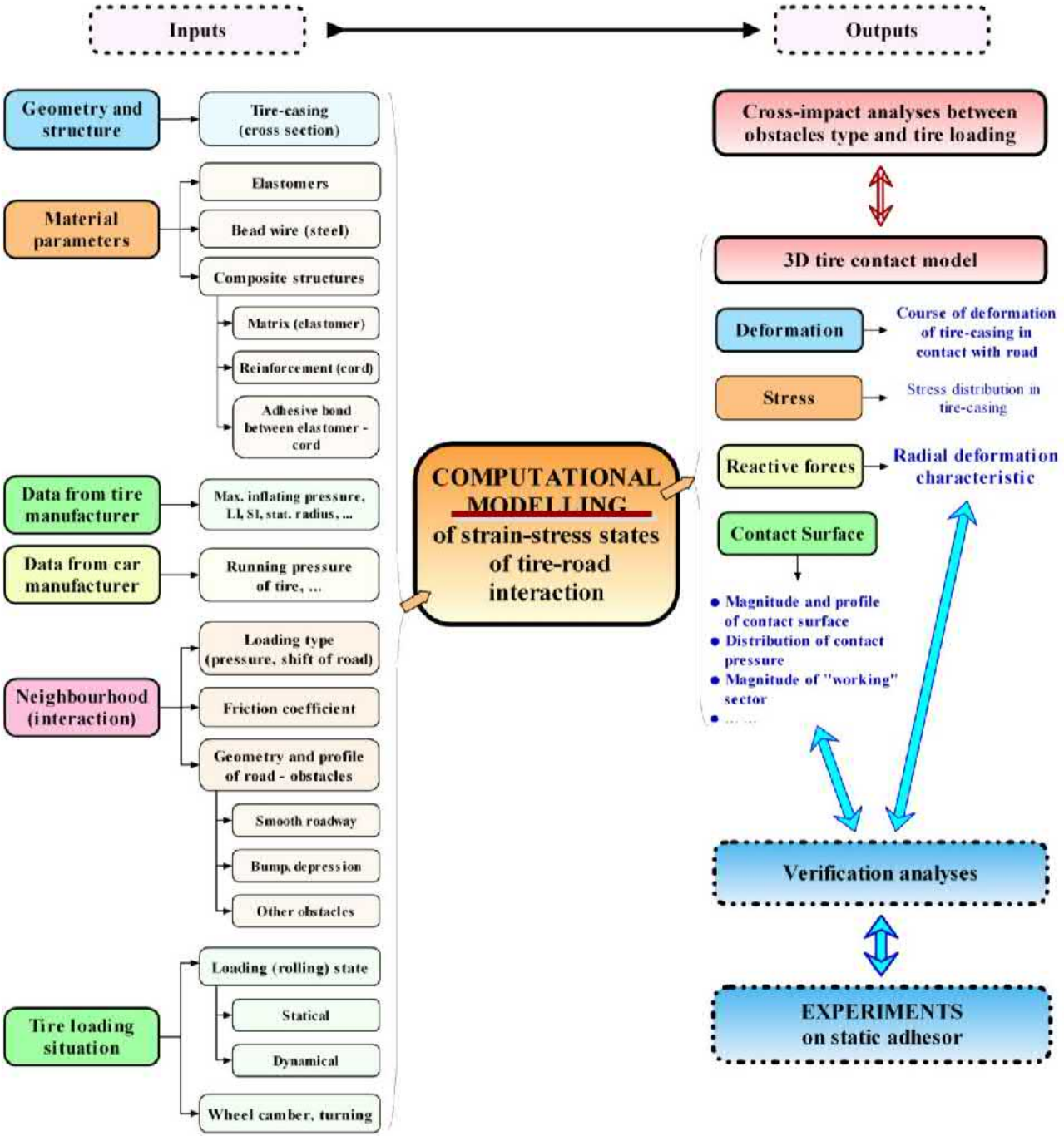

Necessary inputs to computational models of tire

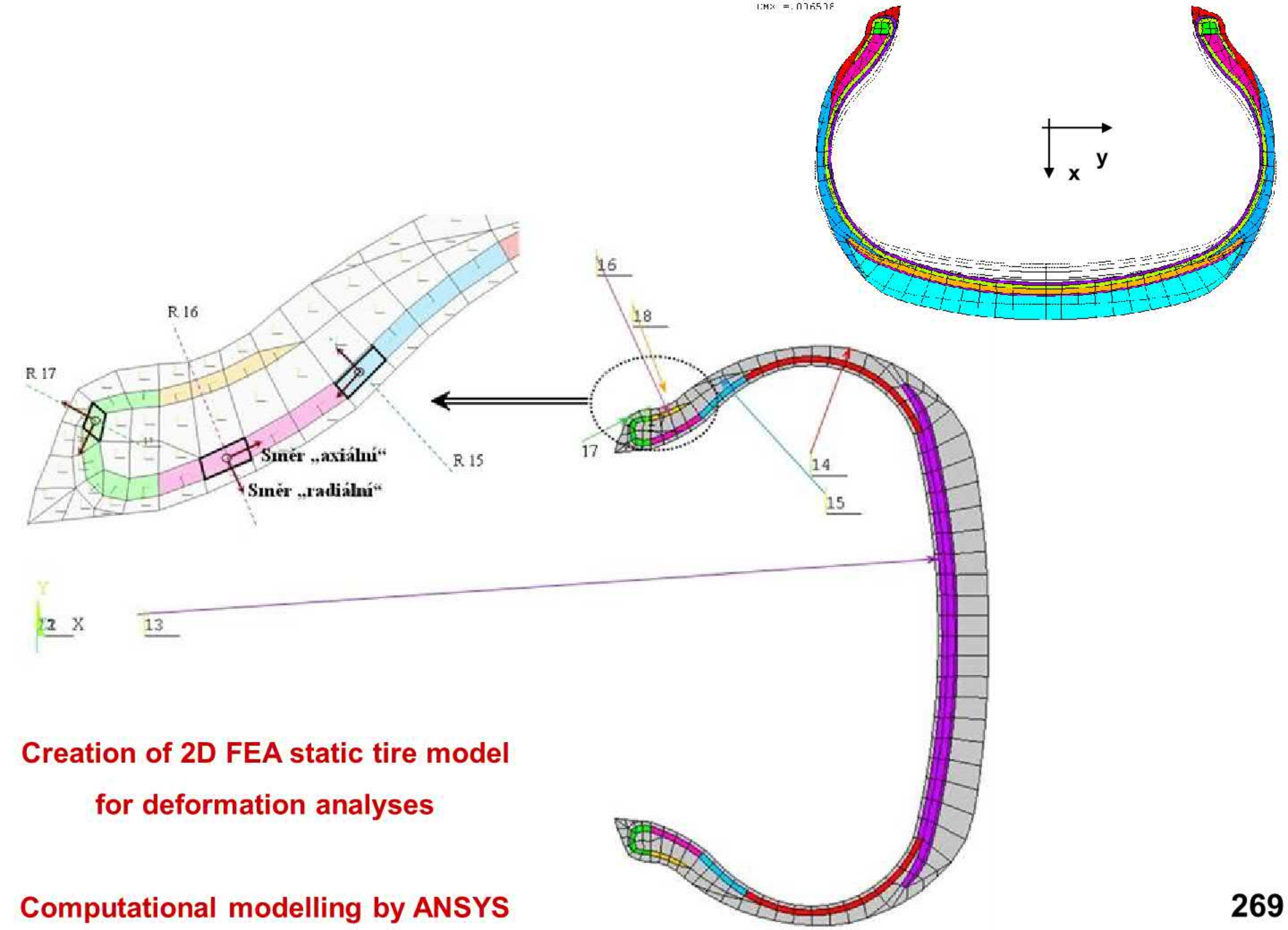

Creation of 2D FEA static tire model

for deformation analyses

Computational modelling by ANSYS

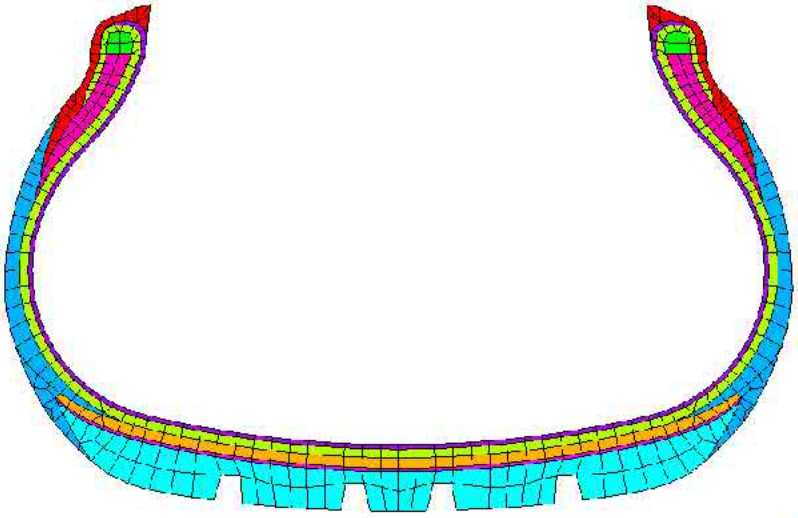

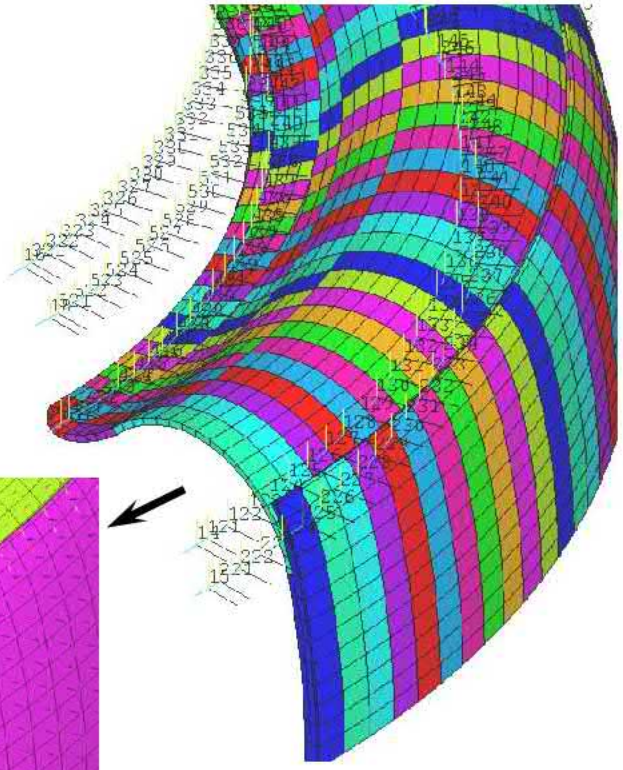

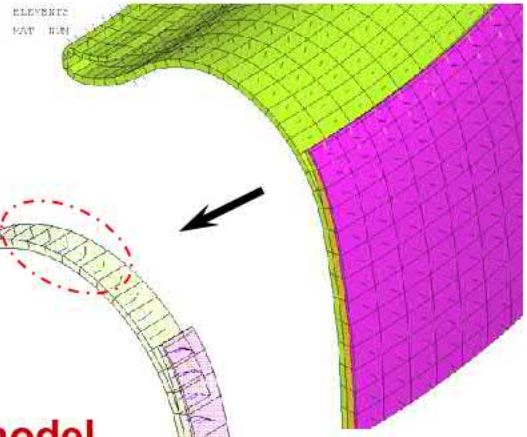

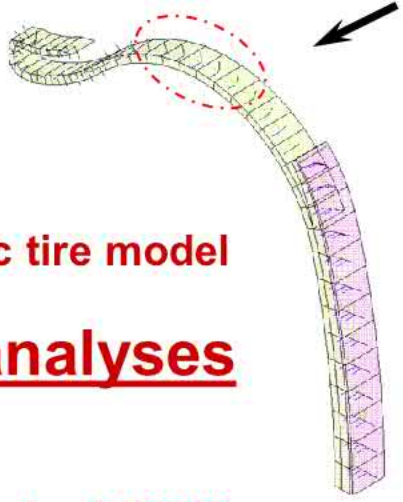

Creation of 3D FEA static tire model

for stress-strain analyses

Computational modelling by ANSYS

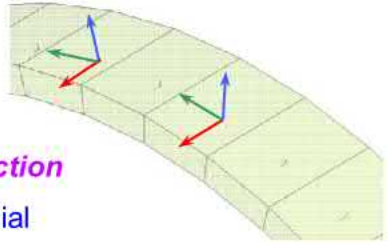

Direction

- radial
- peripheral
- axial (meridian)

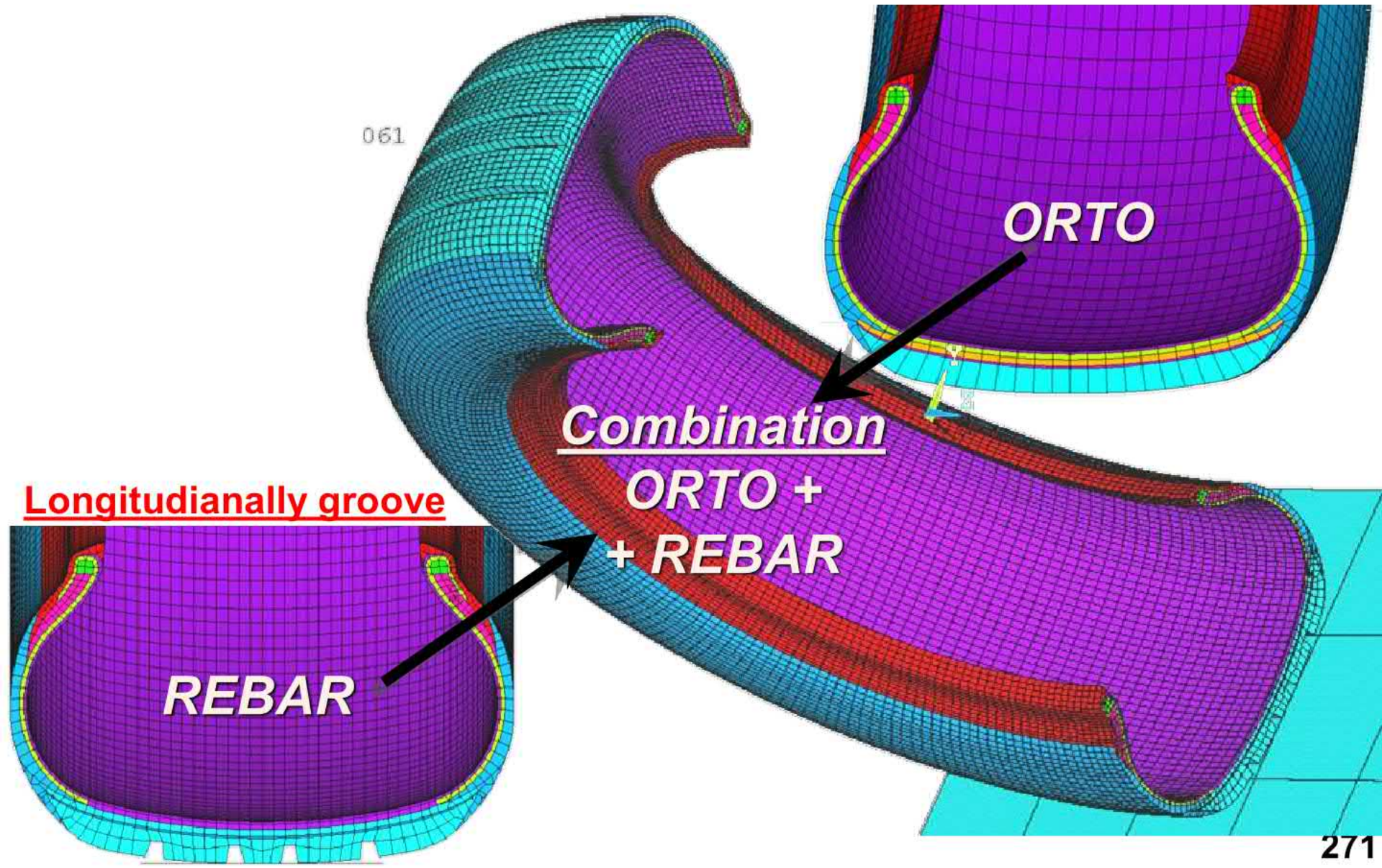
061
ORTO
Combination
ORTO +
+ REBAR
Longitudianally groove
REBAR

165/65 R13

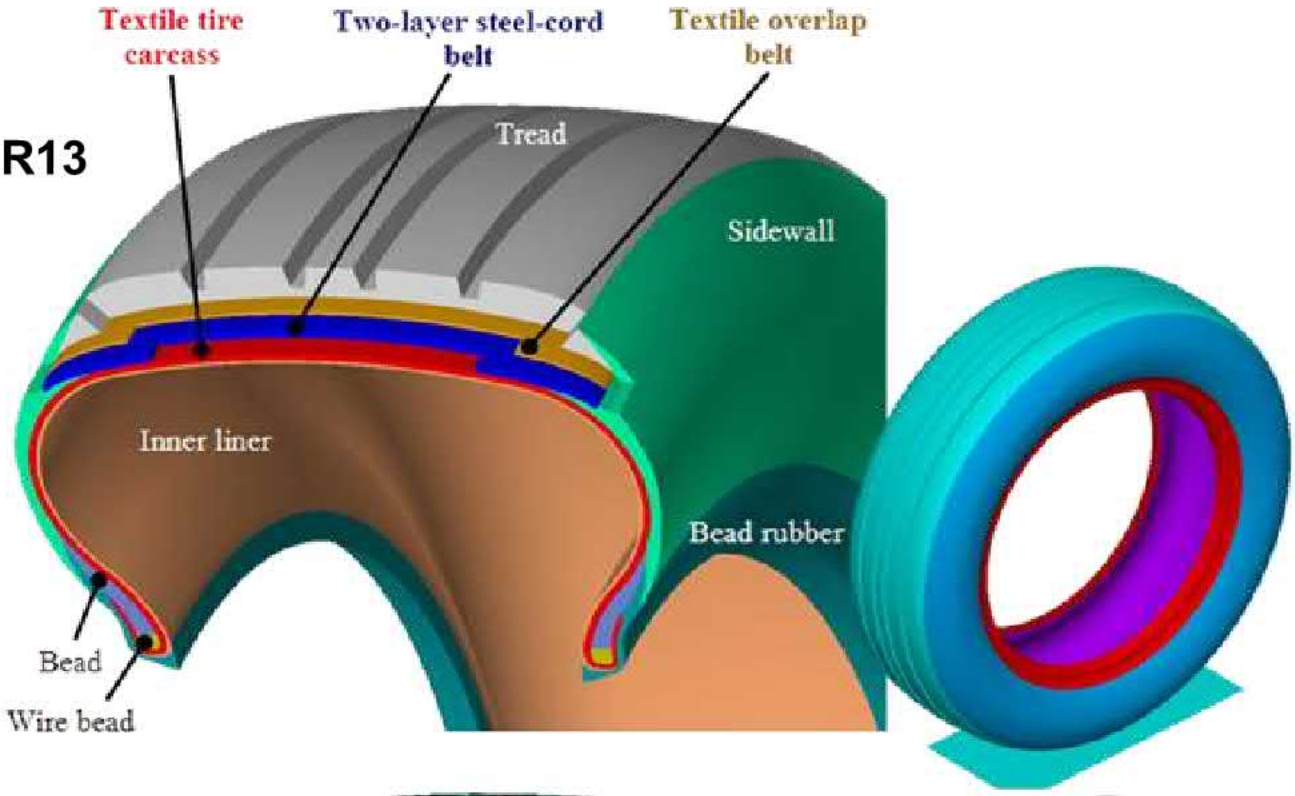

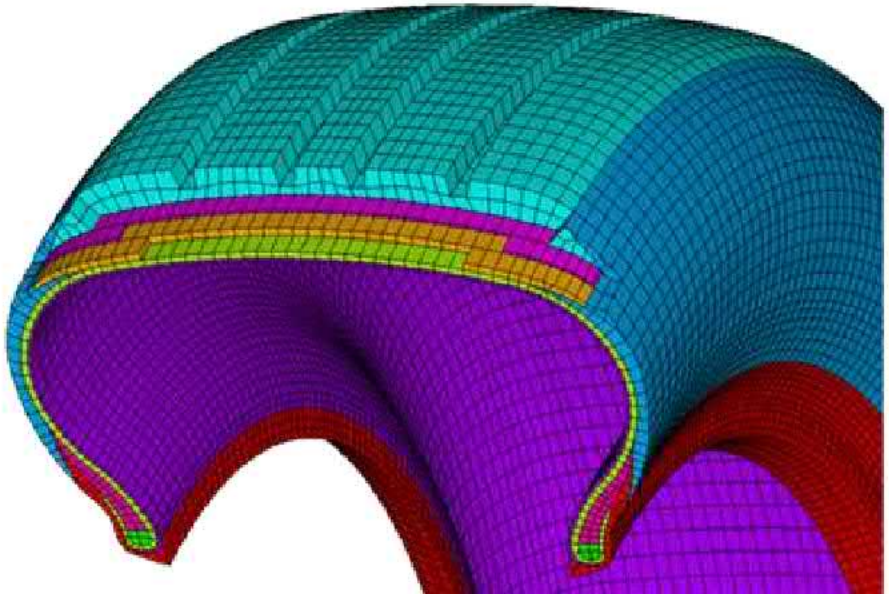

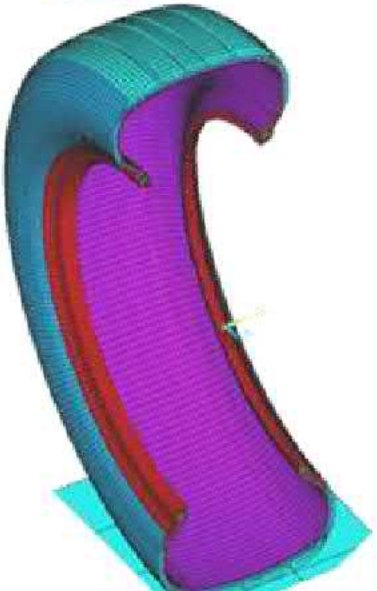

Fourth part of model:

36 000 elements

155 000 nodes

Material parameters of composite structures for ANSYS

Composite structures \ Orthotropic material parameters			Young module Ex / Ey / Ez[1] [MPa]	Main Poiss. ratio[2] PRxy / PRyz / PRxz [-]
Steel-cord belt	Homogenization one-layer variant ORTHO1		12.0 / 22.2 / 55.0	0.5384 / 0.2801 / 0.1025
	Homogenization two-layer	variant **ORTHO2A**	12.0 / 23.1 / 717.0	0.2706 / 0.1724 / -0.0480
		variant **ORTHO2B**		0.3122 / 0.0740 / -0.0234
		variant **ORTHO2C**	12.0 / 23.1 / 550.0	0.4362 / 0.0924 / -0.0399
Textile overlap belt			21.0 / 25.4 / 745.3	0.8227 / 0.0174 / 0.0132
Textile tire carcass			12.0 / 745.1 / 21.8	0.0076 / 0.4776 / 0.5481

Modulus of shear

Complete MATERIAL PARAMETERS OF COMPOSITE STRU

Material parameters	Stress modules Ex / Ey / Ez[1] [MPa]	Main Poisson ratios PRxy / PRyz / PRxz [-]	Shear modules Gxy / Gyz / Gxz [MPa]
Steel-cord belt	12.0 / 23.1 / 717.0	0.3122 / 0.0740 / -0.0234	5.6 / 16.7 / 12.4
Textile overlap belt	21.0 / 25.4 / 745.3	0.8227 / 0.0174 / 0.0132	6.0 / 23.4 / 19.9
Textile tire carcass	12.0 / 745.1 / 21.8	0.0076 / 0.4776 / 0.5481	11.6 / 20.6 / 4.5

Detail of steel-cord belt into FEA model of tire = **impossible**.

In relation to the computational models, the composite component parts are not able to be implemented up to the level of reinforcing cords for reason of the time difficulty as well as the large number of the finite elements. The composite component parts are partially taken into account in the form of specified stiffness or in other words, the composite component parts are partially replaced with definite stiffness.

$\Rightarrow$ necessary steel-cord belt **replace by**

Different descriptions of composite structure parts into tire computational models

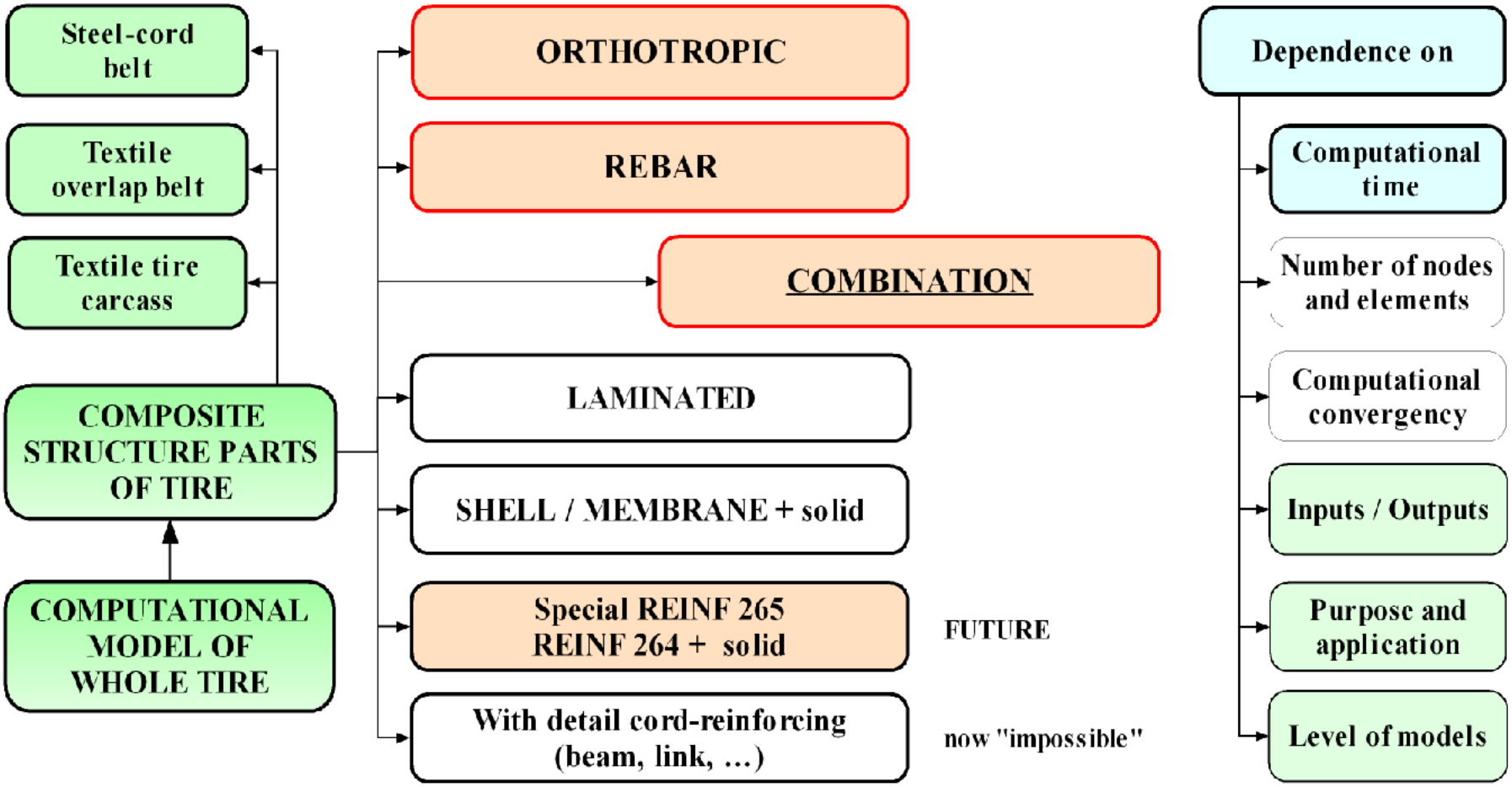

The suitable selection of the mentioned replacement is influenced by the specific factors including computational time, knowledge of the required materials parameters and expected results of accuracy.

- Replacement of steel cord belt with orthotropic material (marked as ORTHOTROPIC)

Two layers of steel cord belt with symmetrically crossed reinforcements are homogenized together and they exhibit the properties of the orthotropic material which represents the elastomeric layer with cords (homogenization of two layers in order to make only one layer). Materials parameters are specified by experimental process on the basis of which the values of constants of elasticity for steel cord belt in individual directions of tire casing are obtained. The mentioned replacement is often used in practice. The difficulty of this method is connected with the correct determination of Poisson's ratios which have to be calculated in order to obtain the appropriate coordinate system of computational model representing the tire casing. Based on the sensitive analysis, high sensitivity was determined for some Poisson's ratios and it means that only slight change can cause the significant change in stiffness parametres of the belt as well as the whole tire casing.

- Replacement of the areas with so called “rebar” reinforcing finite element (marked as REBAR).

The area of the steel cord belt is expressed by one homogeneous material with parameters which is equal to materials parametres of matrix referring to linear isotropic material. The reinforcement can be defined by real constants including angles of cord, volume measure of reinforcement with its specified by cord material. The reinforcement can be simply expressed by help of volume ration but in relation to this volume ration, there is not real configuration of cords in belt. In comparison with orthotropic material, the utilization of the rebar element in computational model leads to the increase of the computational time because of more sensitive discretization.

- Replacement based on combination of orthotropic material with rebar element (marked as COMBINATION)

This method represents the combination of the advantages relating to the both methods mentioned above.

- Replacement of the areas with layers (“laminated”) finite element (marked as LAMINATED) or shell finite element (marked as SHELL / MEMBRANE + solid)

This replacement of the steel cord belt is based on assignation of real constants to the given type of element and the given constants include angles of cord and the number of layers standing for the specified reinforcing element of tire casing while the parametres of the orthotropic material are also assigned. It is necessary to point out that the given orthotropic material represents the homogenization of the individual steel cord belt layers. Steel cord belt with two layers consists two layers which are positioned in a parallel way. The mentioned layers are described by help of real constants representing cord angles and by parameters of orthotropic material which is identical for both layers. In relation to the mentioned two layers, the third layer can be placed between these two layers and this third layer represents elastomeric interlayer which is between layers of steel cord belt. The two-layered steel cord belt can be also made up of five parallel layers and the order of the given layers. This introduced replacement is the closest to real description of the two-layered steel cord belt.

The Poison's ratios of the orthotropic material describing each one layer of steel cord belt and could be determined more precisely in comparison with the case where the replacement of steel cord belt is obtained with orthotropic material or in other word, by homogenization of two layers of steel-cord belt leading to creation of one part only.

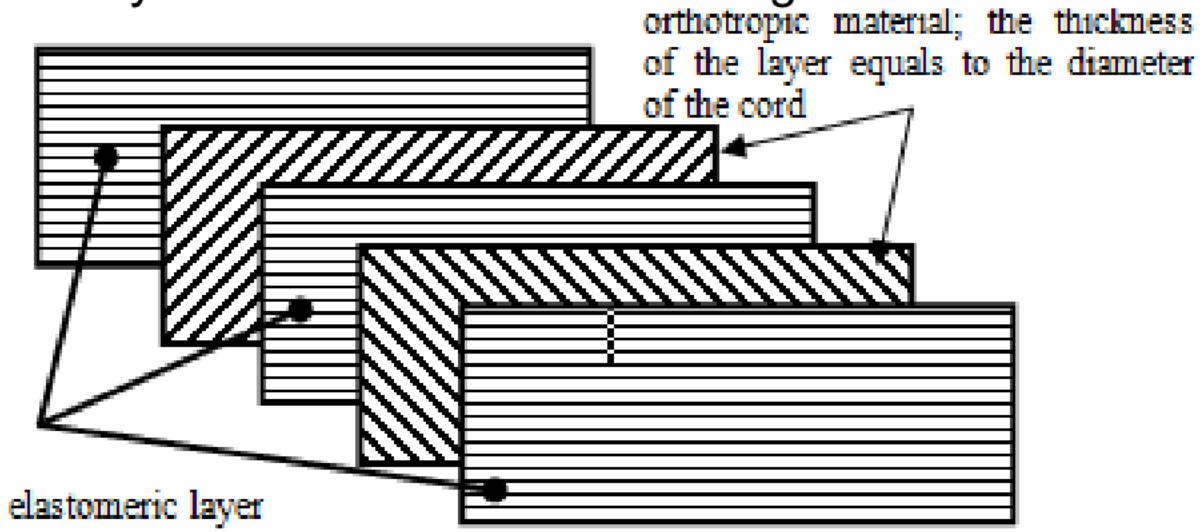

The definition of the two-layered steel-cord belt by help of "laminated" finite element.

- Replacement of steel cord belt by special reinforcing finite element

Relating to the description of the steel cord belt for tire casing, the special type of element is recommended during the operation in ANSYS software and this new special type of element is Reinf265, which is assigned to the areas of the steel cord belt with Solid186 type of element. Considering FEM, there is not a lot of available information in relation to the mentioned type of the element and therefore, the utilization of Reinf is going to be the subject of authors' investigation from the aspect of the replacement of the steel cord belt as well as other tire composite components.

The computation modeling and calculations of long-fiber composites are very difficult because the accurate materials characteristics of matrixes and reinforcement are needful but these accurate materials characteristics have to be obtained from the experiments.

The obtained information on geometric arrangement of reinforcements can be used also for optimization of arrangement of cords in the tire casing in order to gain better stiffness parameters standing for individual directions.

✓ **ORTHOTROPIC material model**

input: **9 material parameters** (E, ν, G).

✓ **REBAR element** (concret Solid65 = 8-nodes!)

Steel-cord belt = **material parameters matrix**.

Cord = real constant.

input: + material parameters of matrix and cord

+ real constants = angle and volume %.

e.g. well obstacles

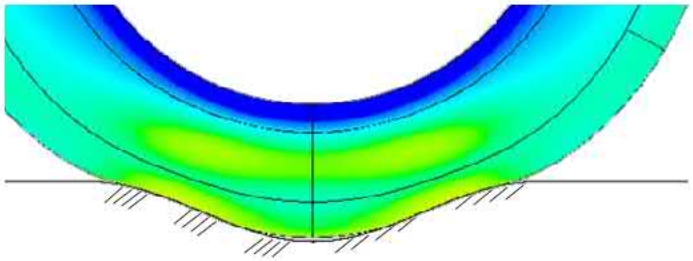

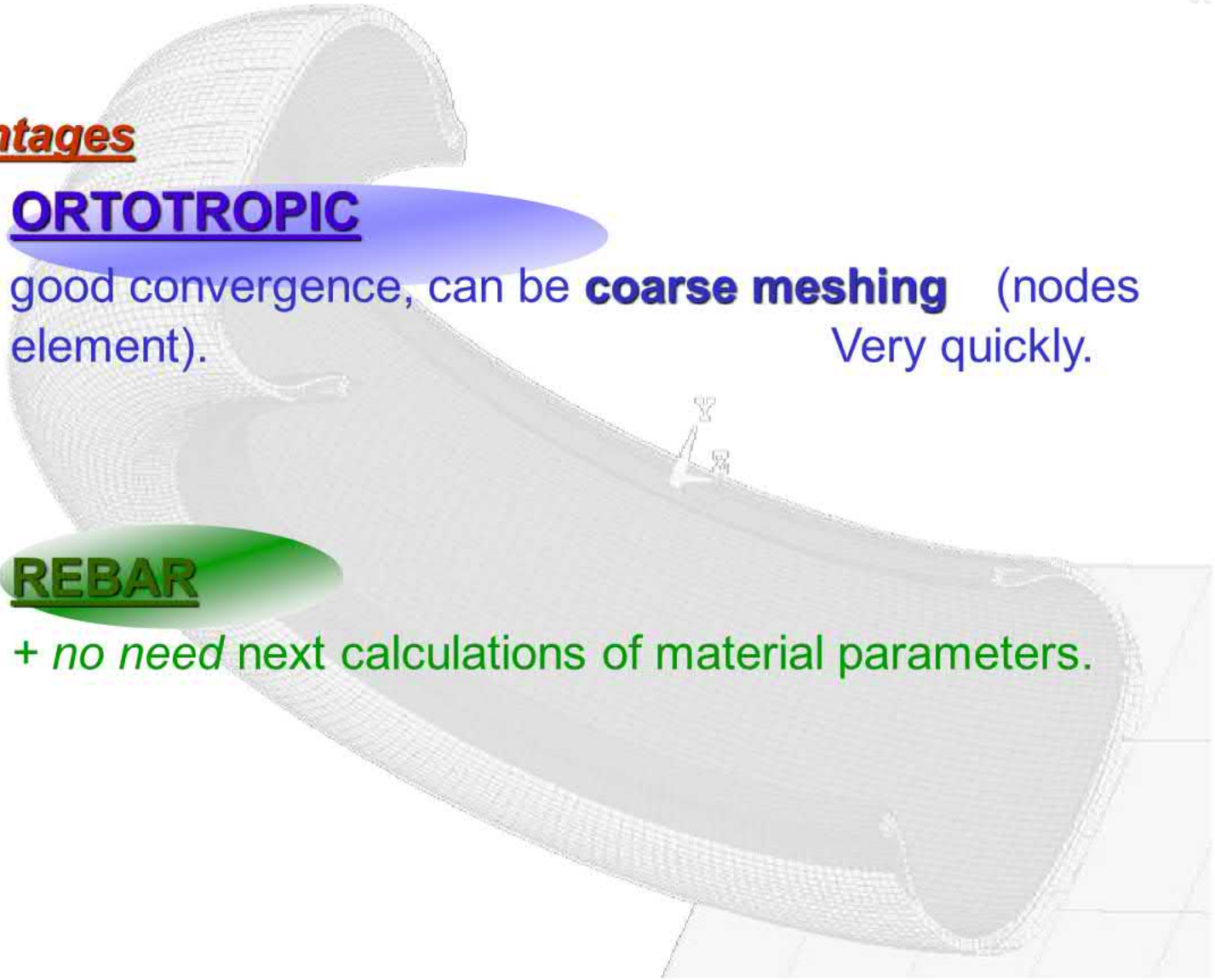

Advantages

✓ **ORTOTROPIC**

\+ good convergence, can be **coarse meshing** (nodes element). Very quickly.

✓ **REBAR**

\+ *no need* next calculations of material parameters.

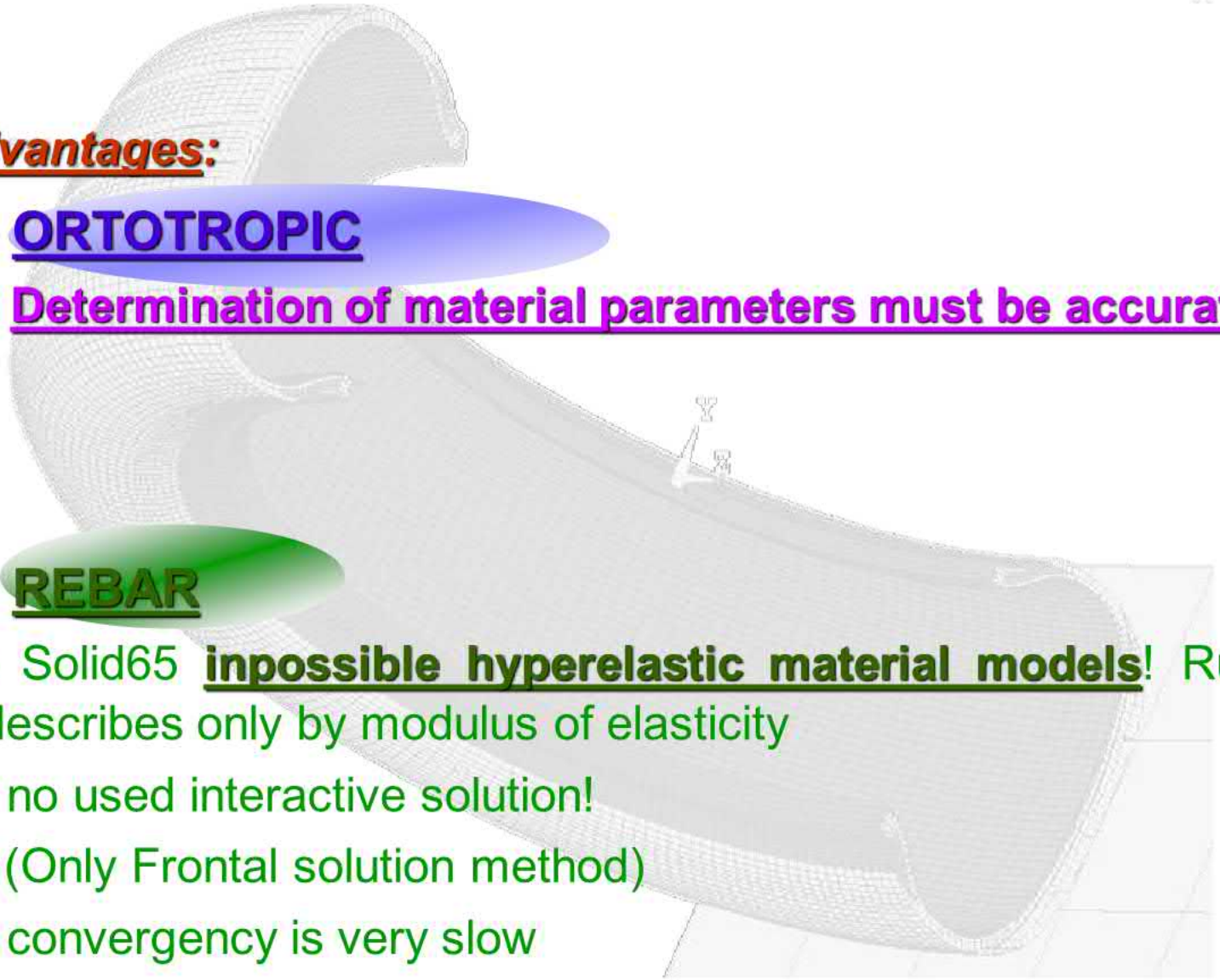

Disadvantages:

✓ **ORTOTROPIC**

- **Determination of material parameters must be accurate.**

✓ **REBAR**

- Solid65 **inpossible hyperelastic material models**! Rubber describes only by modulus of elasticity
- no used interactive solution!
  (Only Frontal solution method)
- convergency is very slow

Part 8 – OUTPUTS FROM SIMULATIONS: Simulation of tire-road interactions, Outputs from plane surfaces and obstacles, Dynamic loading, Modal analysis

Different descriptions of composite structure parts into tire computational models

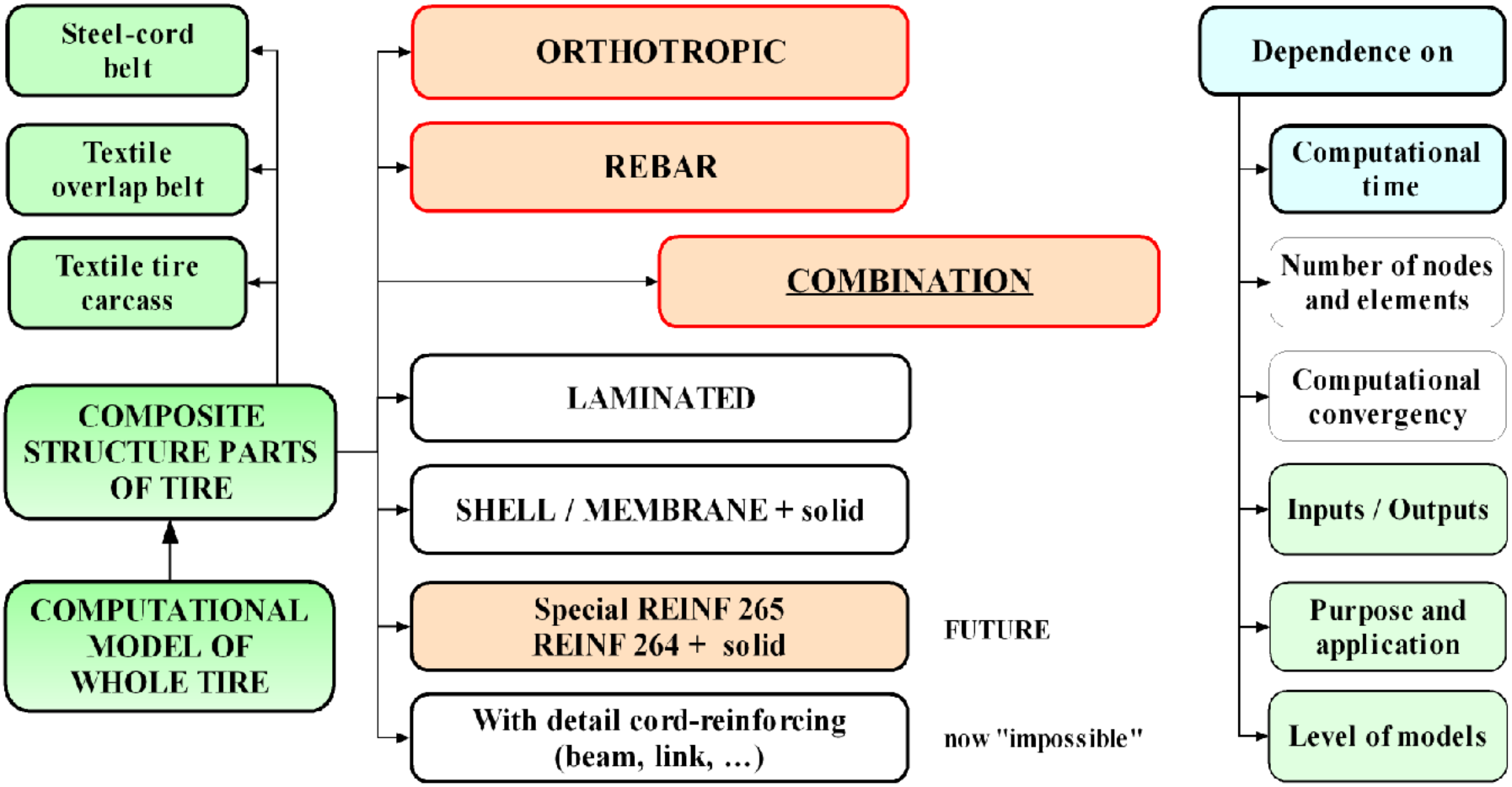

✓ **ORTHOTROPIC** material model

input: **9 material parameters** (E, ν, G).

✓ **REBAR** element (concret Solid65 = 8-nodes!)

Steel-cord belt = **material parameters matrix**.

Cord = real constant.

input: + material parameters of matrix and cord

+ real constants = angle and volume %.

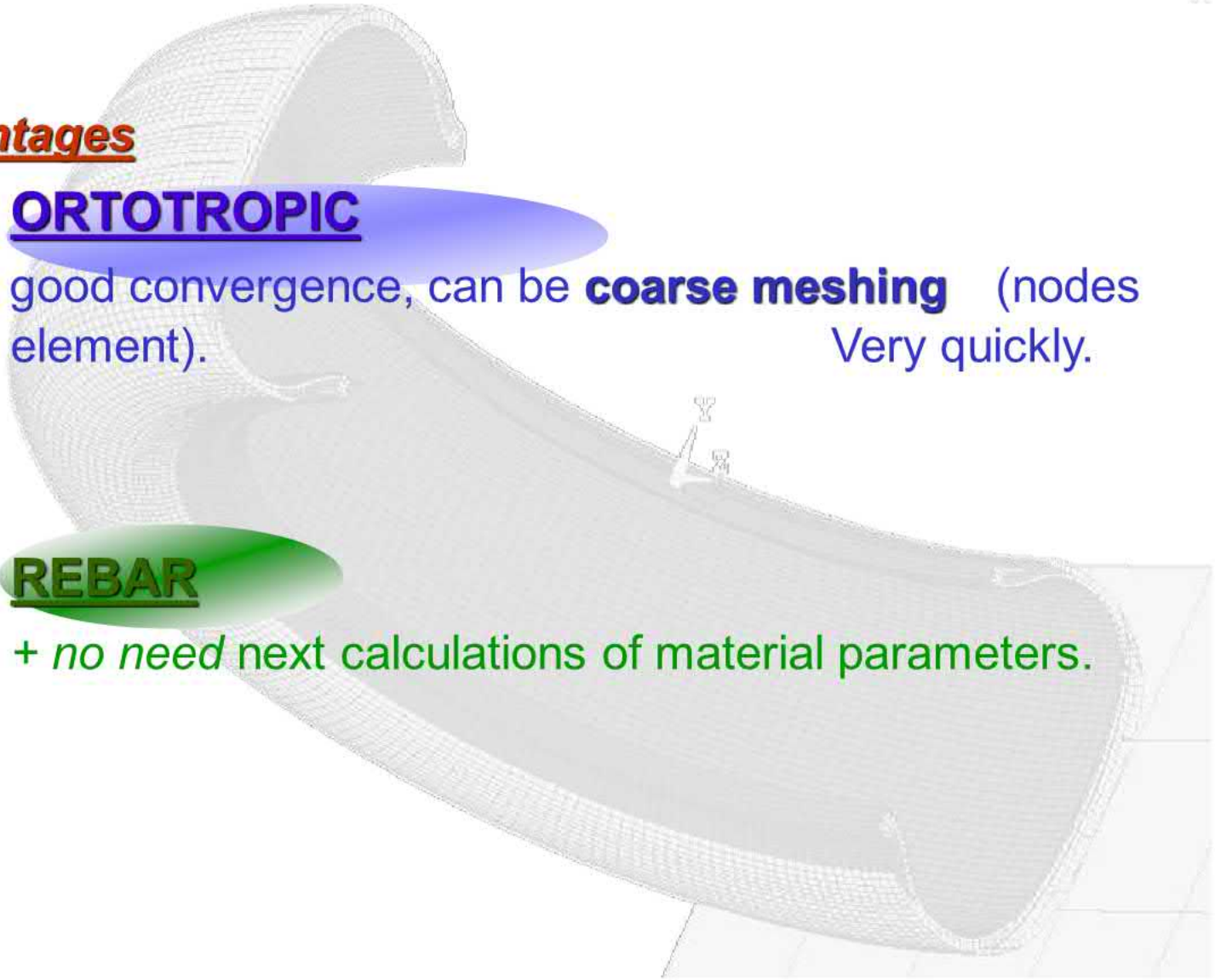

Advantages

✓ **ORTOTROPIC**

\+ good convergence, can be **coarse meshing** (nodes element). Very quickly.

✓ **REBAR**

\+ *no need* next calculations of material parameters.

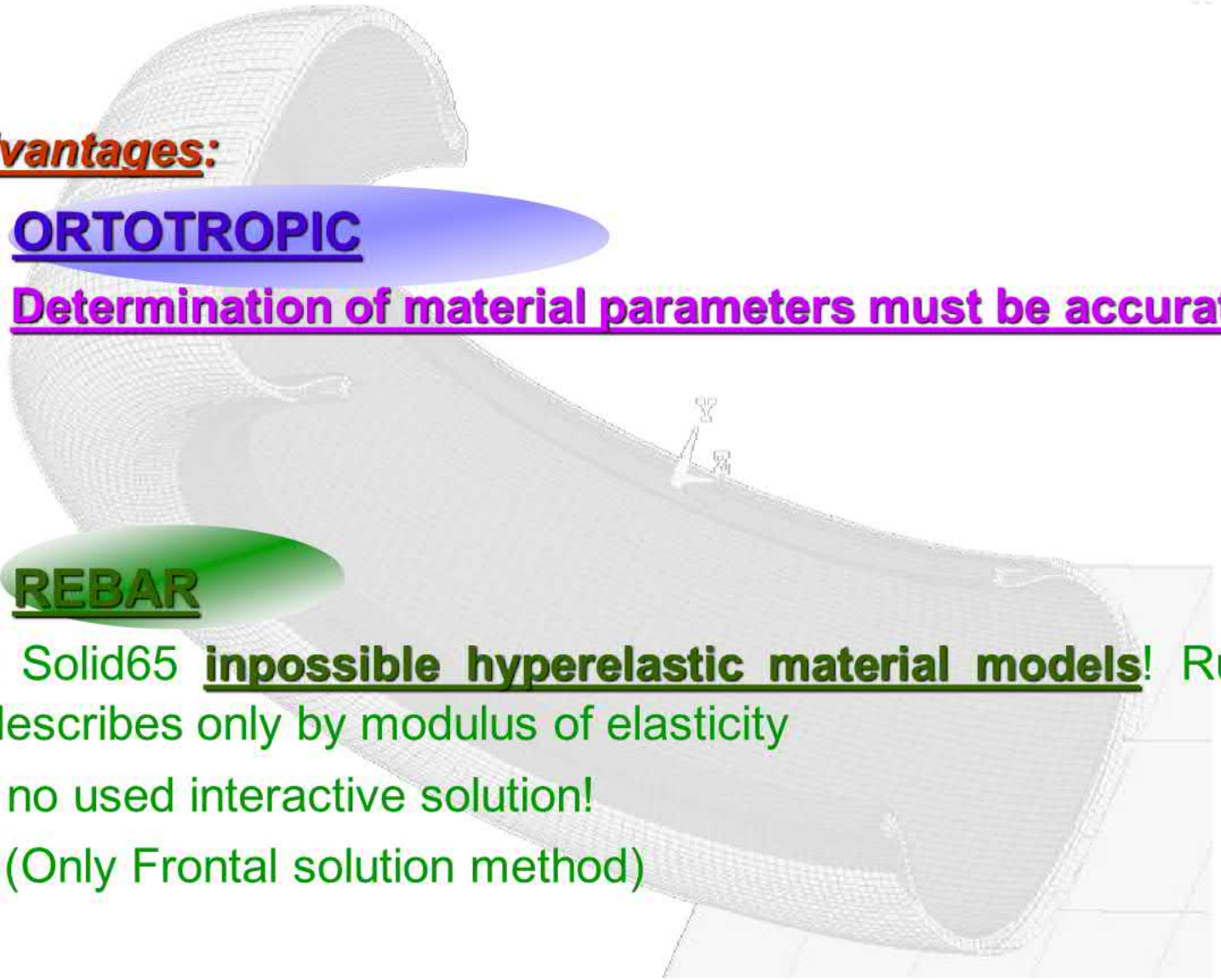

Disadvantages:

✓ **ORTOTROPIC**

- **Determination of material parameters must be accurate.**

✓ **REBAR**

- Solid65 **inpossible hyperelastic material models**! Rubber describes only by modulus of elasticity
- no used interactive solution!
  (Only Frontal solution method)

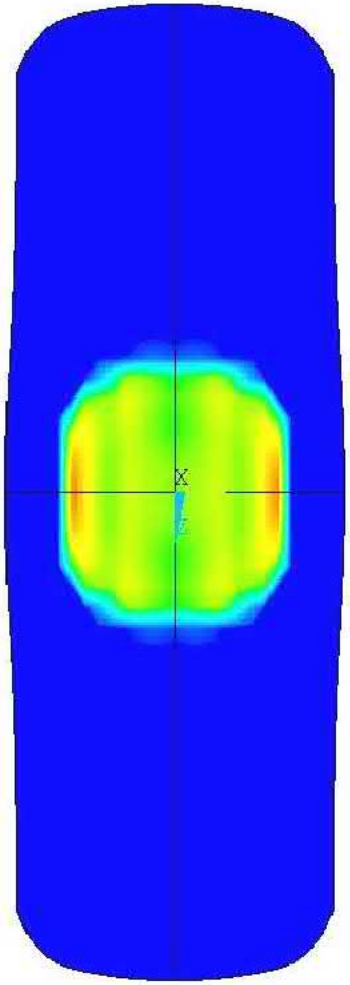

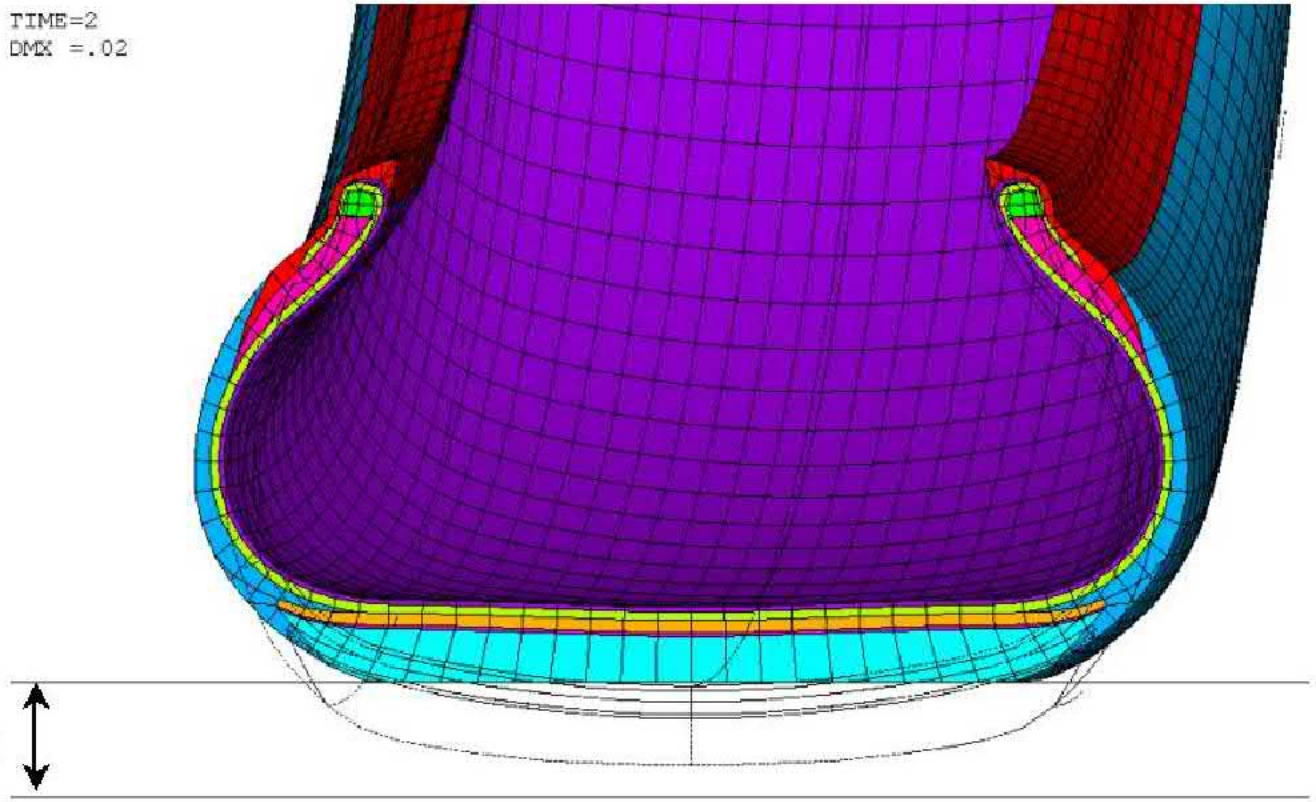

Slick tire

Plane surface

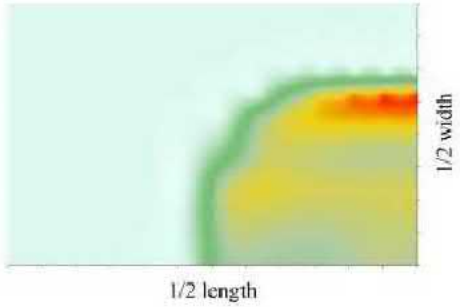

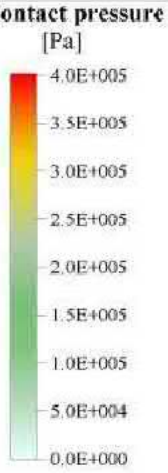

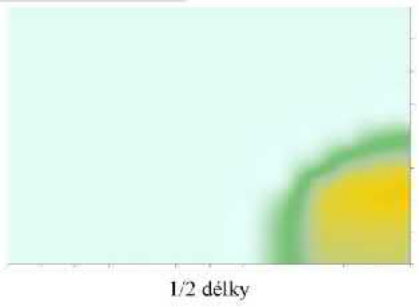

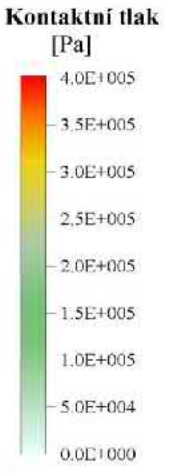

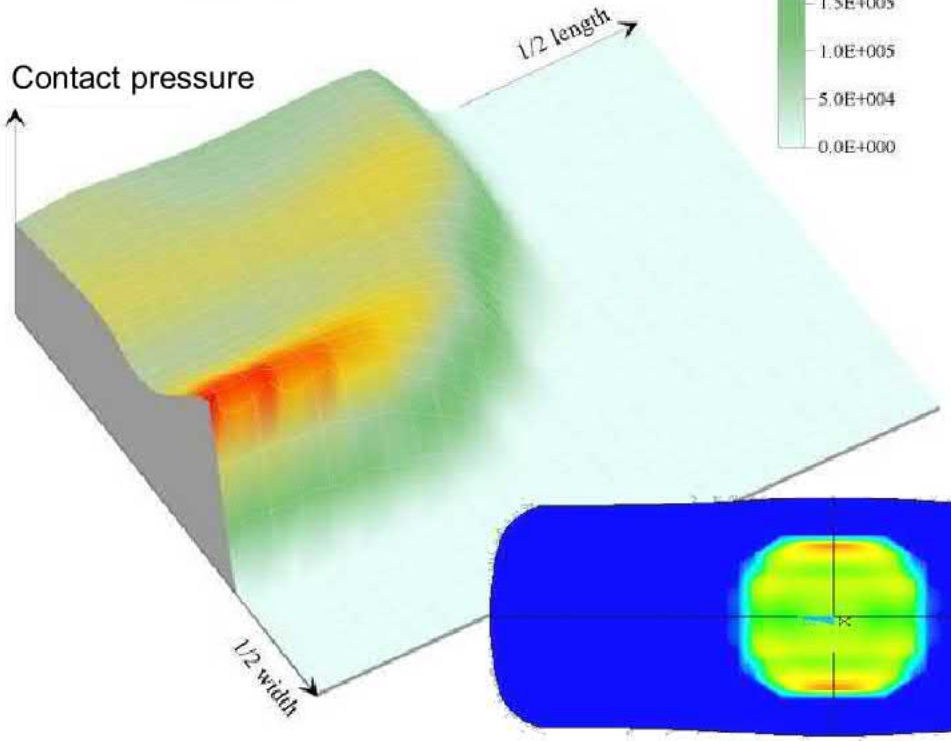

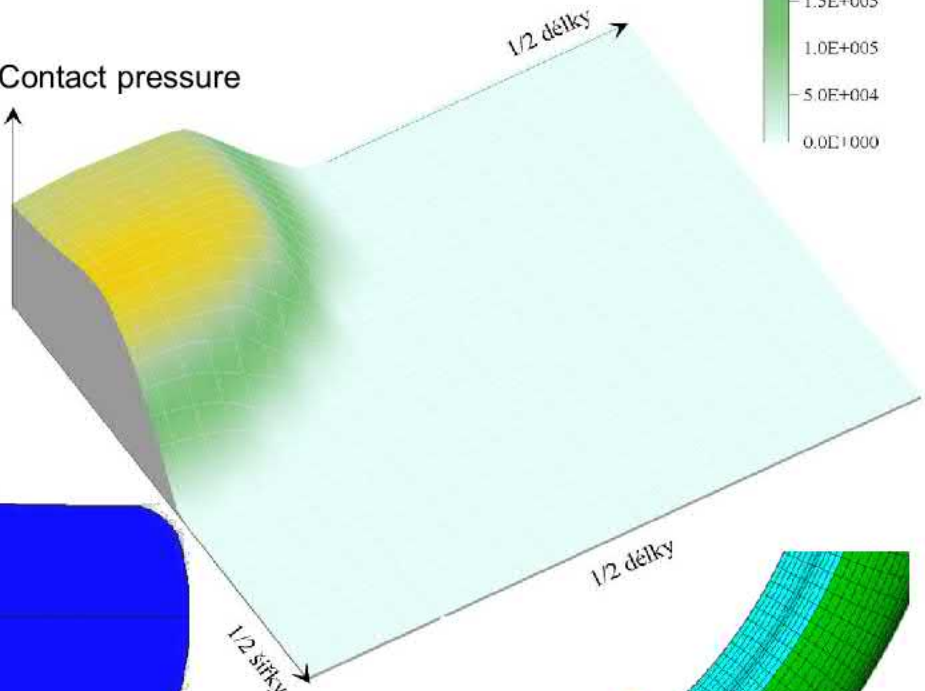

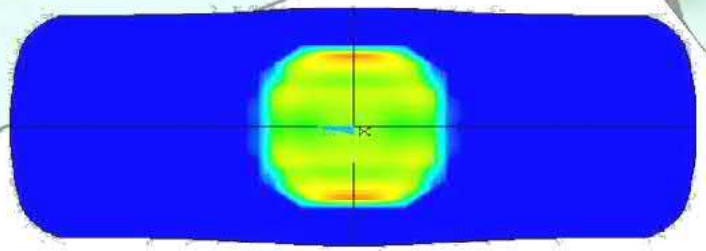

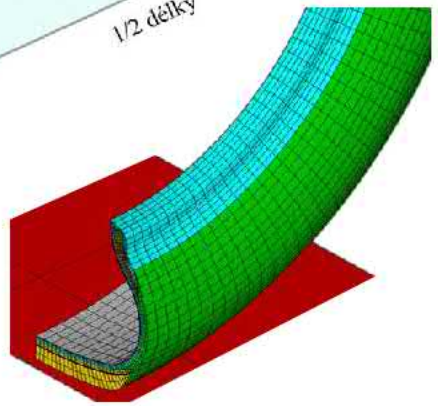

Radial deformation

„great“ deformation 20.0 mm ⇔ small“ deformation 10.4 mm

Plane surface

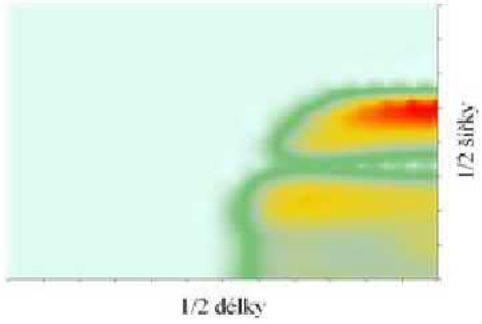

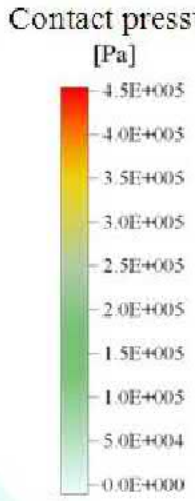

„great“ deformation

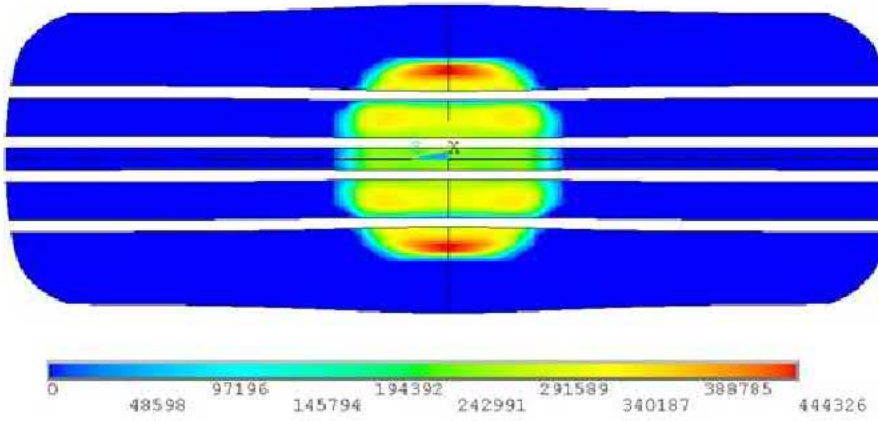

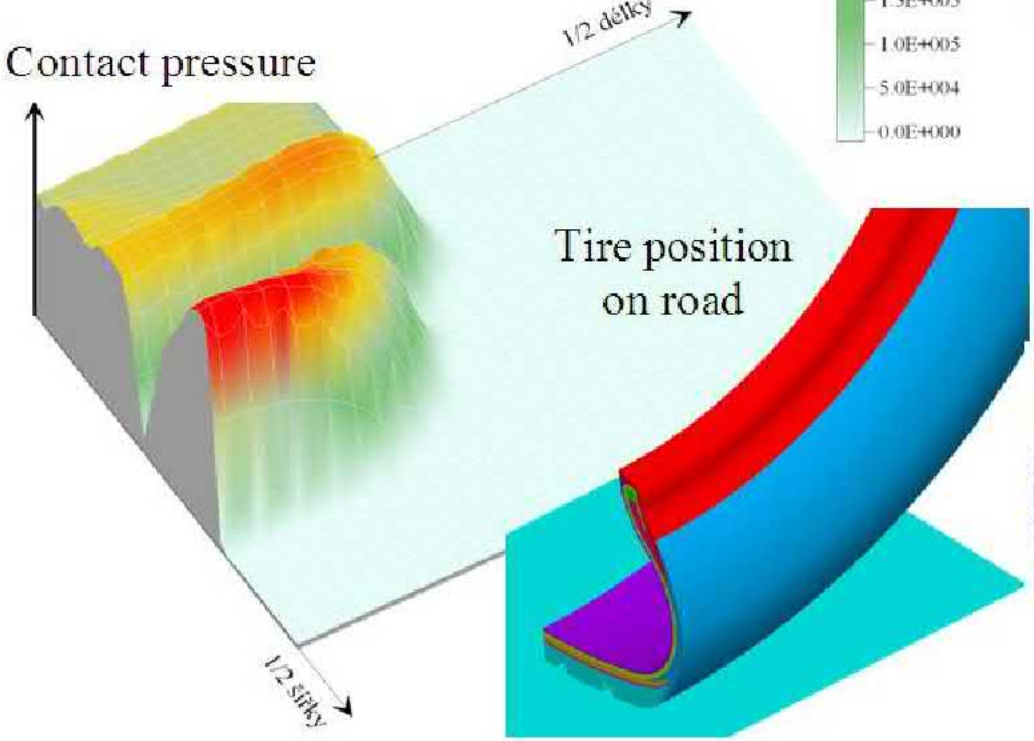

„small“ deformation

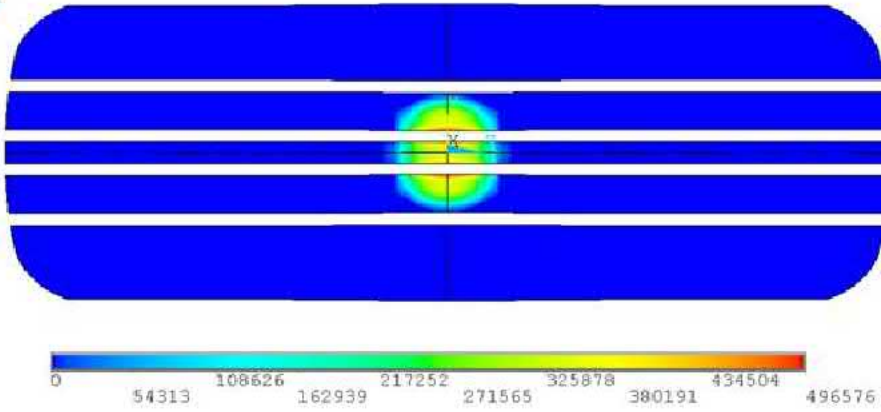

PROFILES OF OBSTACLES

Due to the fact that the profiles of road obstacles have neither been standardized nor published, in the present paper ***convex and concave sinusoidal obstacles were defined*** with a period of 150 mm. The height (amplitude) of the obstacle was set equal to the magnitude of the tyre-road "shift "– 20 mm.

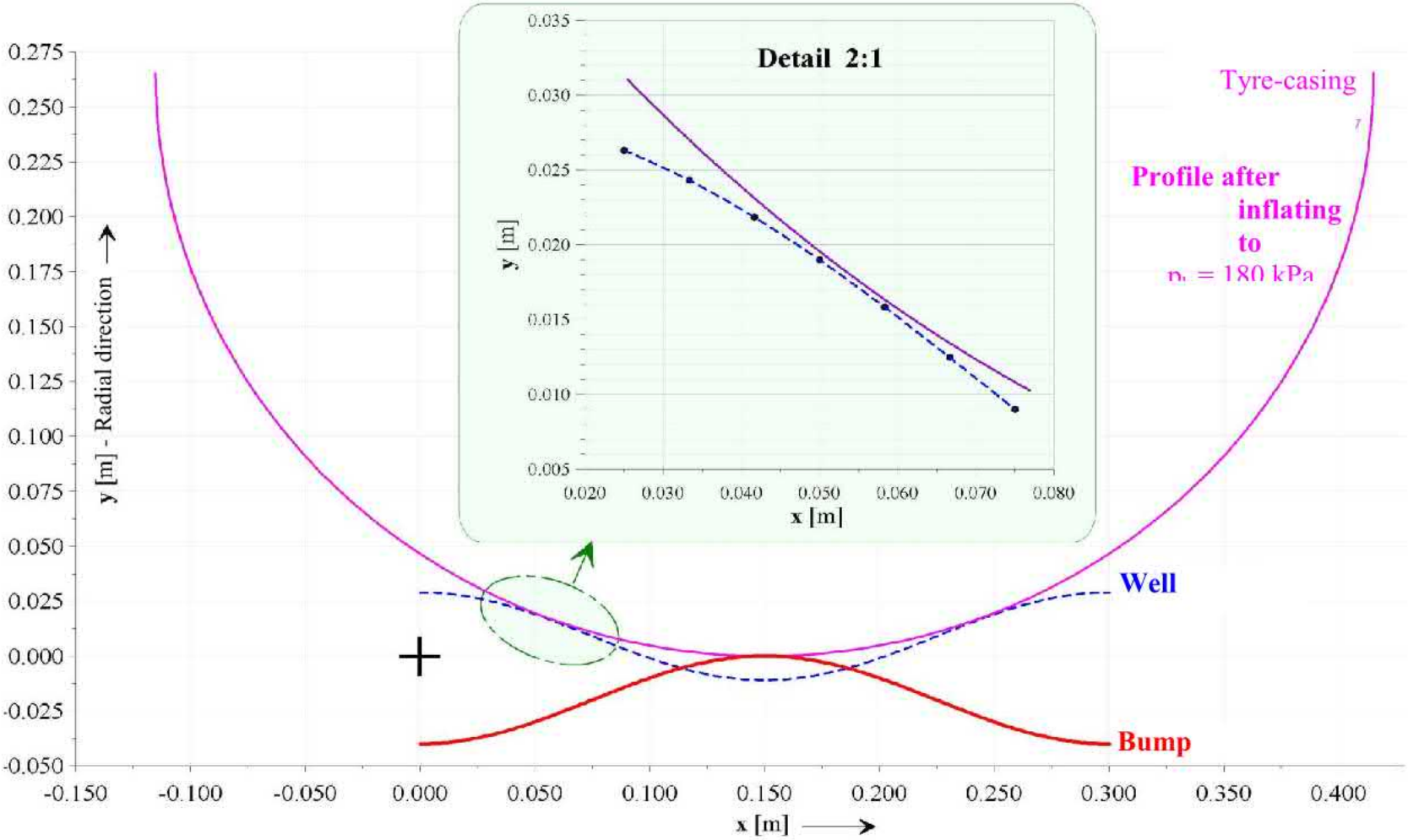

Definition of sinusoidal obstacles for contact calculation problems

Well obstacles

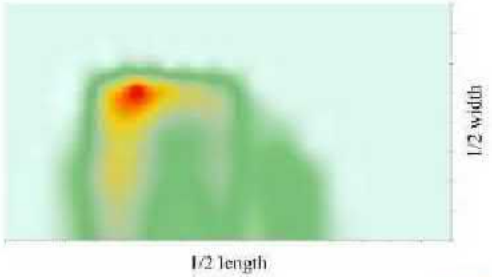

Contact pressure

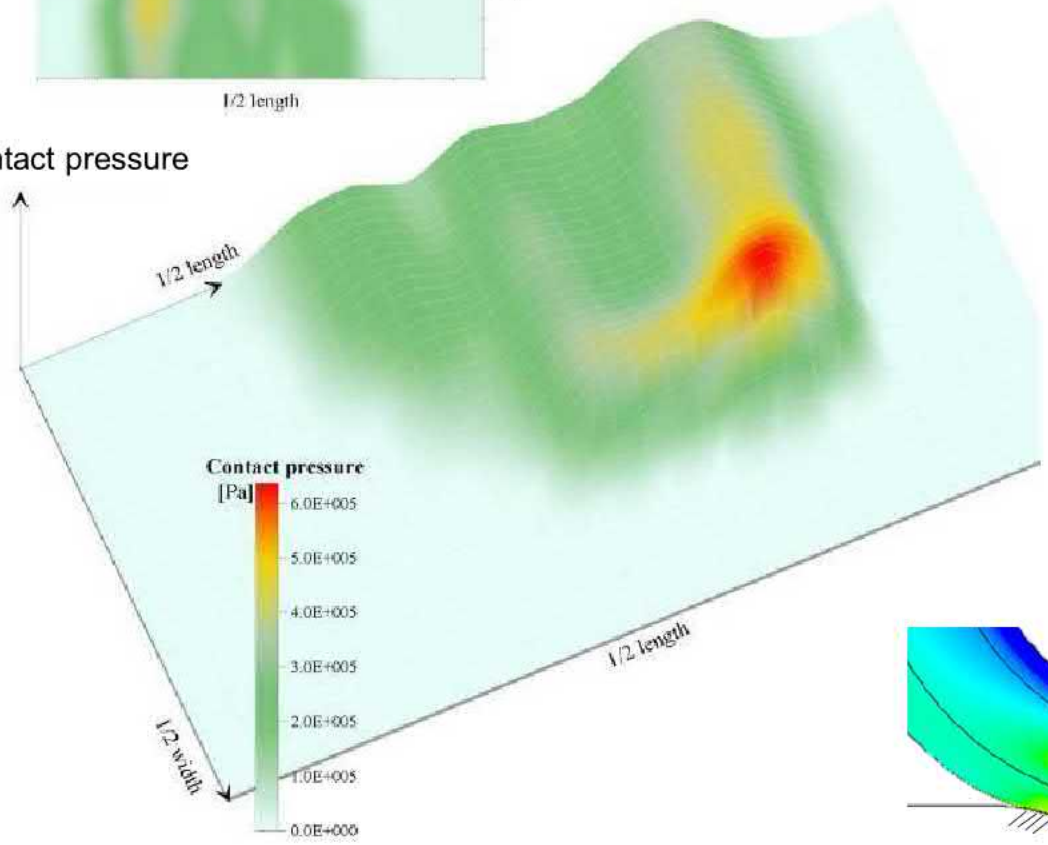

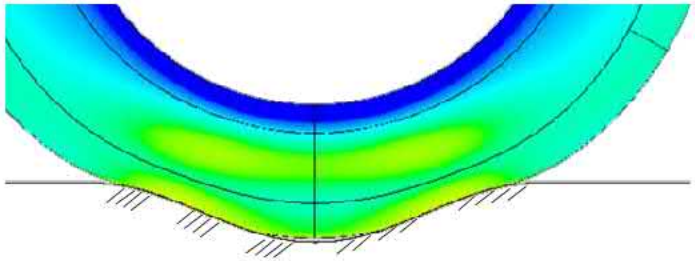

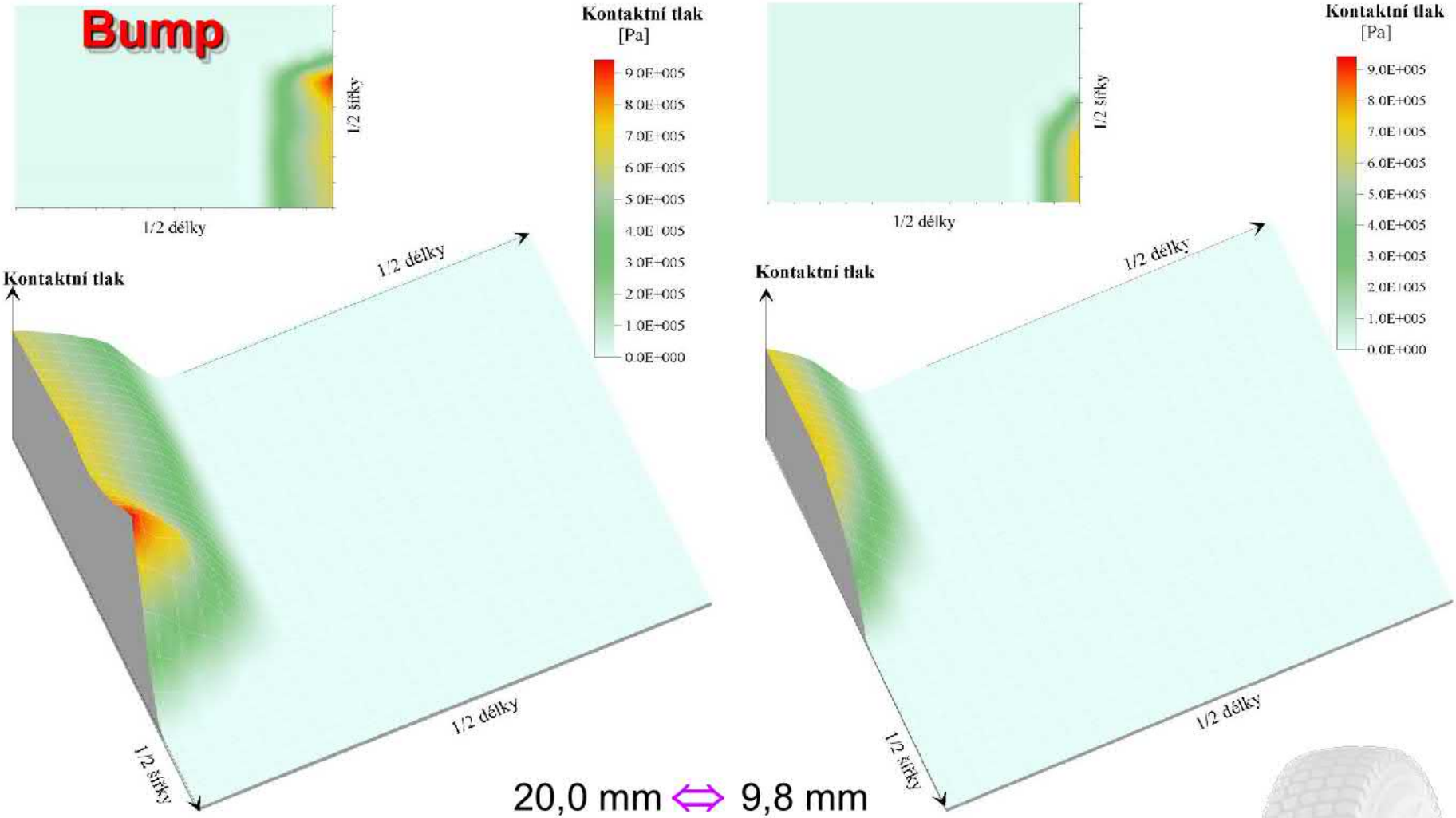
Bump
1/2 šířky
1/2 délky
Kontaktní tlak
[Pa]
9.0E+005
8.0E+005
7.0E+005
6.0E+005
5.0E+005
4.0E+005
3.0E+005
2.0E+005
1.0E+005
0.0E+000
Kontaktní tlak
1/2 délky
1/2 délky
1/2 šířky
20,0 mm ⇔ 9,8 mm
1/2 šířky
1/2 délky
Kontaktní tlak
1/2 délky
1/2 šířky
1/2 délky
Kontaktní tlak
[Pa]
9.0E+005
8.0E+005
7.0E+005
6.0E+005
5.0E+005
4.0E+005
3.0E+005
2.0E+005
1.0E+005
0.0E+000

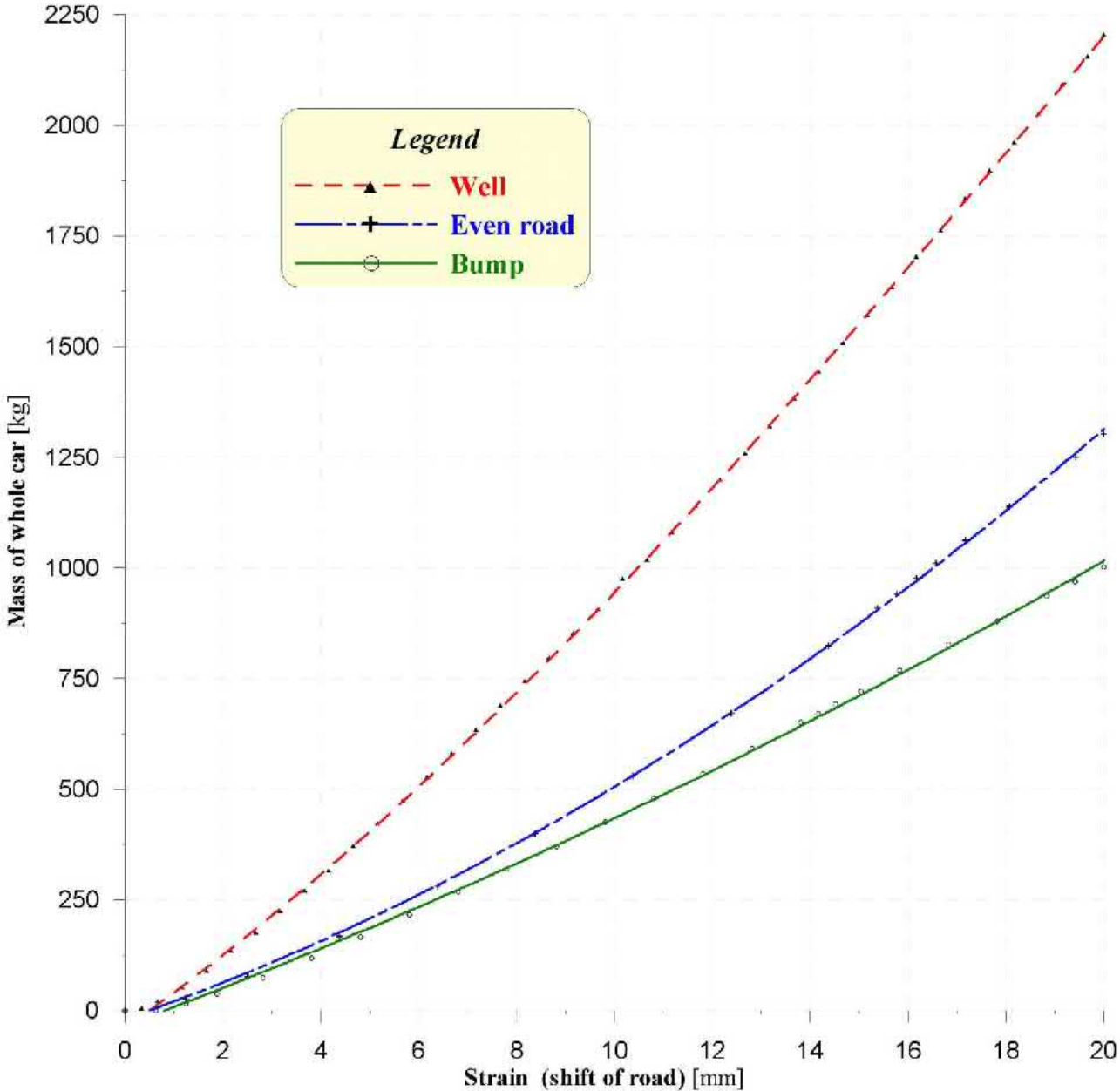
Legend
Well
Even road
Bump
Mass of whole car [kg]
Strain (shift of road) [mm]
2250
2000
1750
1500
1250
1000
750
500
250
0
0
2
4
6
8
10
12
14
16
18
20

Modal analyses

130.0 = 2*4,5

169.7 = 2*4

197.8 = 2*3.5 / 2*3.5

Interaction with plane surface

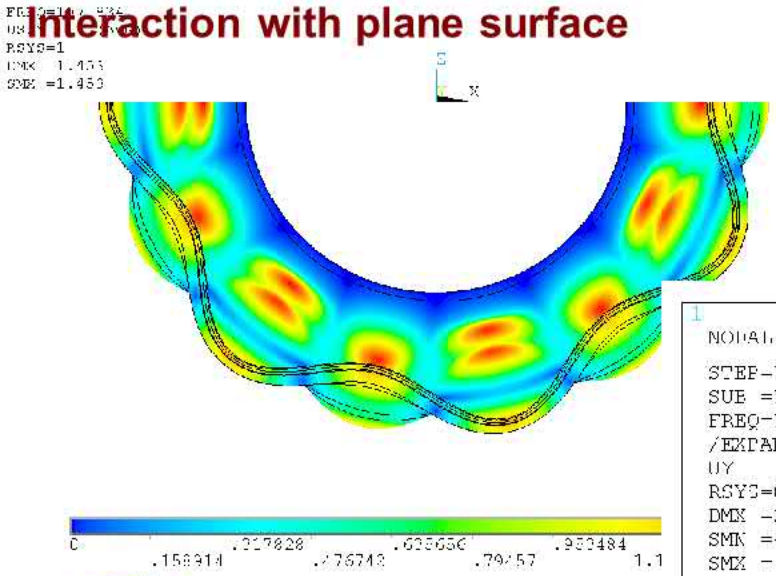

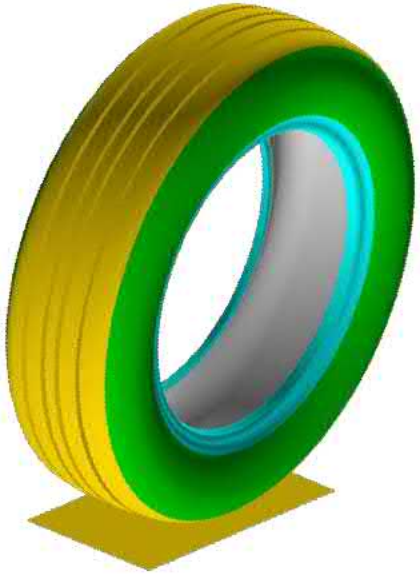

Unloaded tire – natural frequency

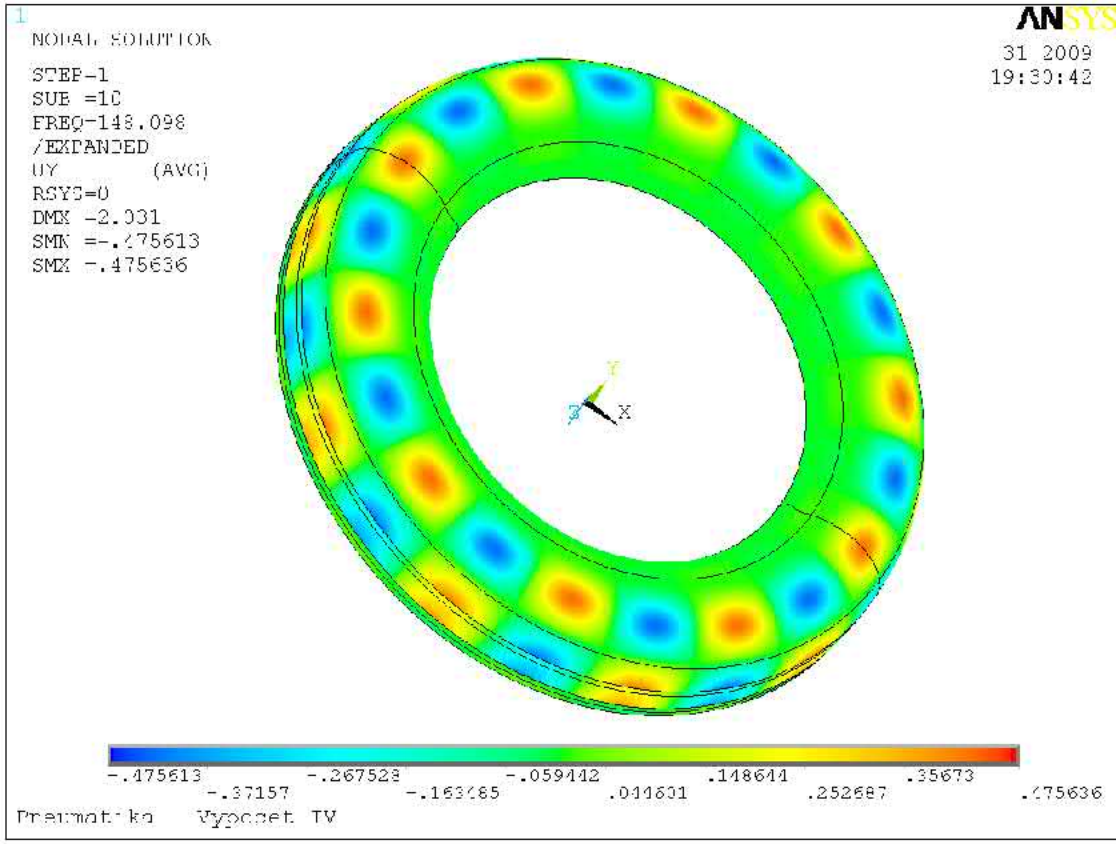

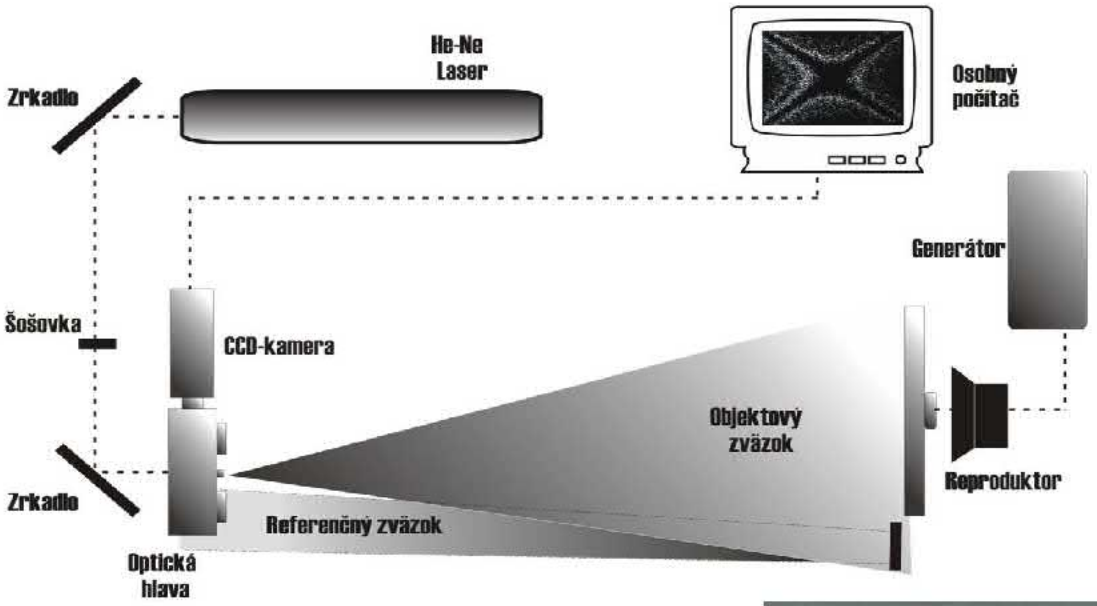

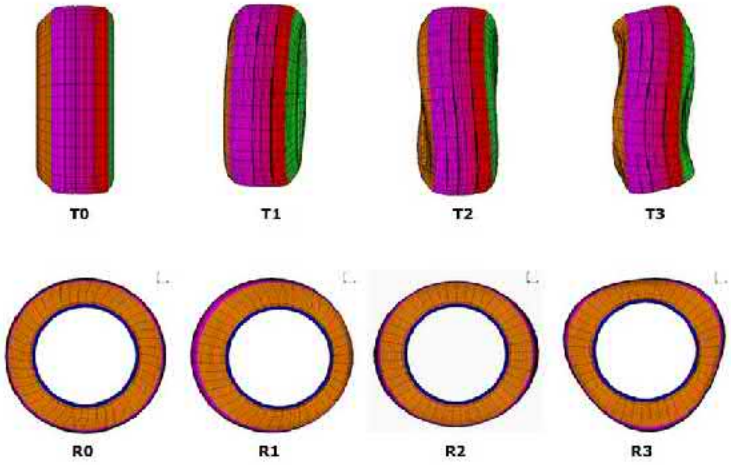

(T) axiálne módy, (R) radiálne módy

ESPI experiment

measurement of Matador tire MP12 82T 165/65 R13

Modes	Value of own frequencies Hz	Amplitude μm	Number of oscillating fields	Frequency by ESPI	Vizualization field of tire
T1	78	3,9	2	–	–
T2	121	3,8	4	120	Fig.4
T3	180	3,7	6	179	Fig.5
R1	100	4,0	2	–	–
R2	135	3,4	4	136	Fig.6
R3	165	3,2	6	166	Fig.7
R4	189	3,0	8	188	Fig.8
R5	208	2,8	10	208	Fig.9
R6	240	1,9	12	239	Fig.10

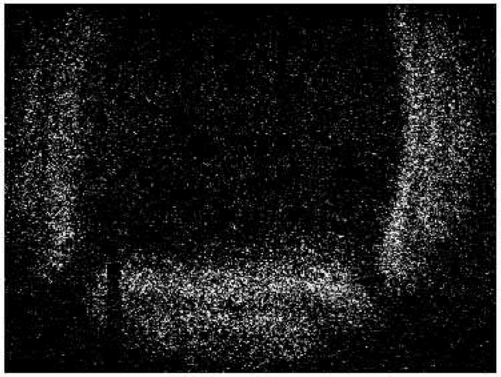

Tire vibration field at a frequency of 120 Hz.

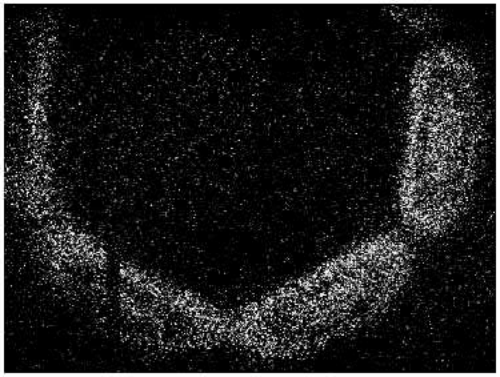

179 Hz

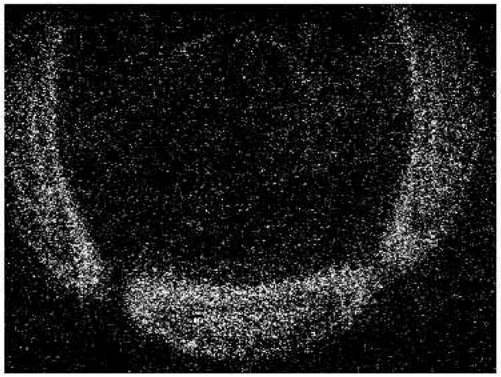

Tire vibration field at a frequency of 136 Hz

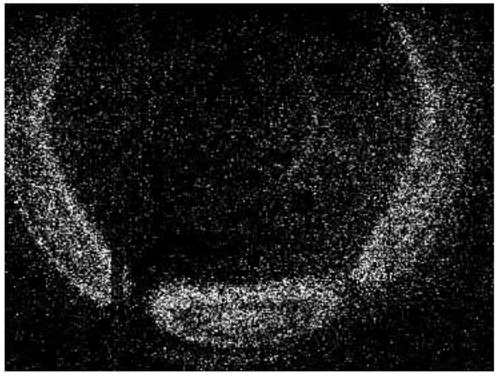

166Hz

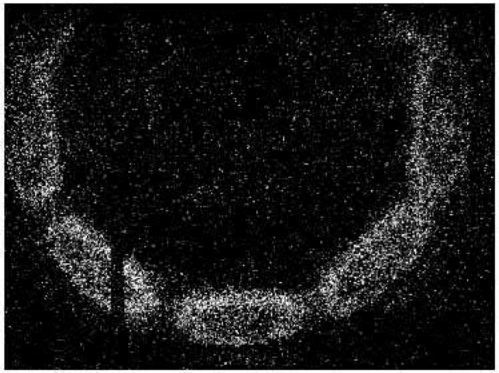

Tire vibration field at a frequency of 188 Hz

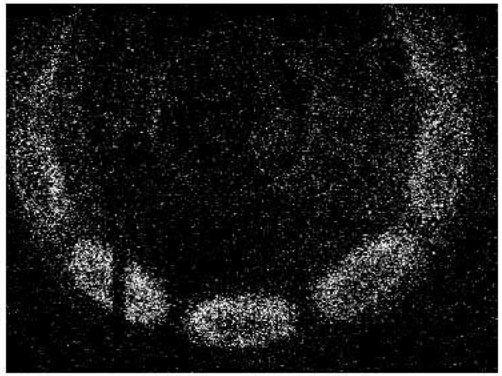

208 Hz

Axiálne módy plášťa 165/65 R13

Módy	Vlastné frekvencie (MARC) [Hz]	Vizualizácia
Axiál 1	100	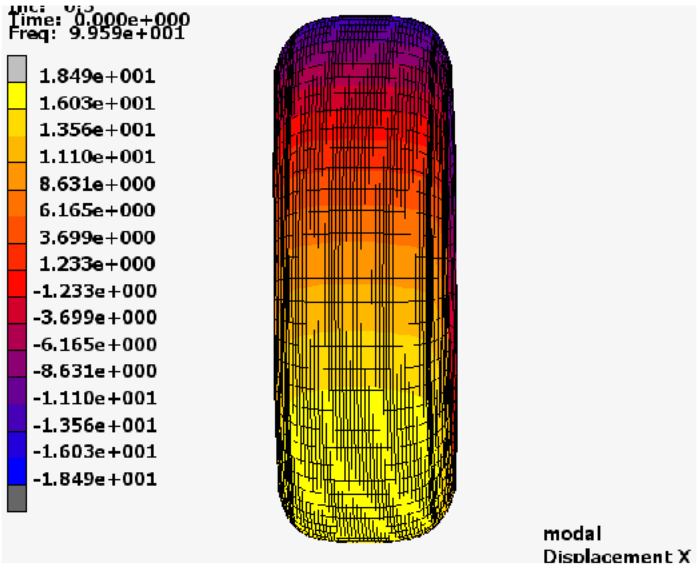
Axiál 2	135	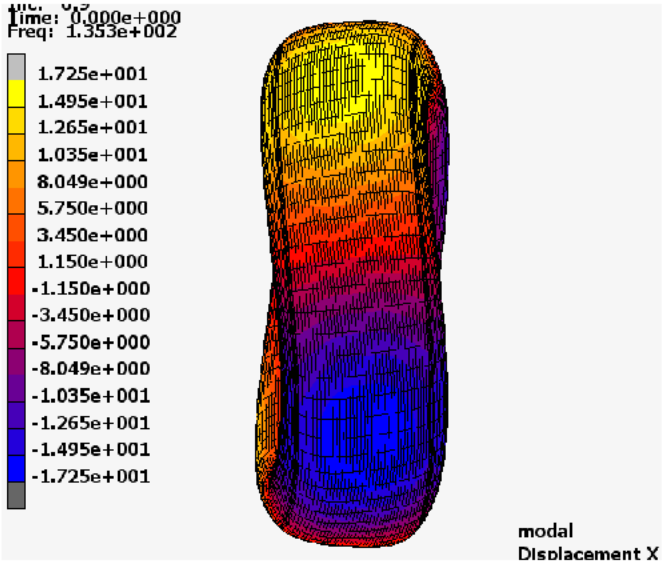

Axiálne módy plášťa 165/65 R15

Módy	Vlastné frekvencie (MARC) [Hz]	Vizualizácia
Axiál 3	183	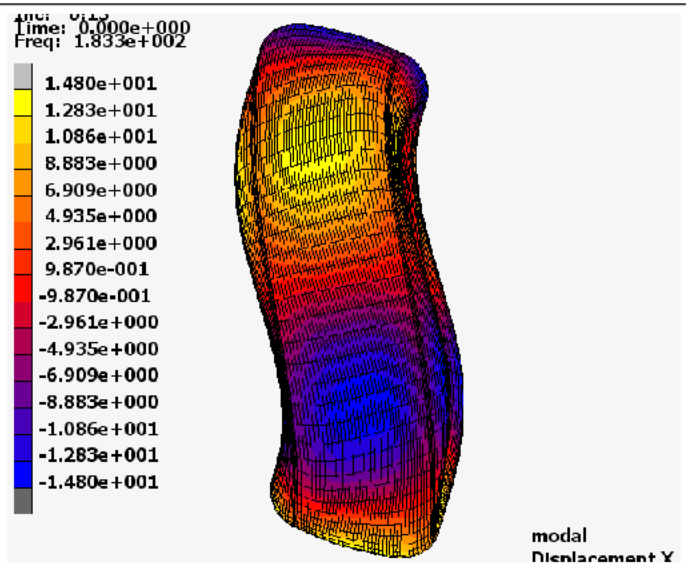
Axiál 4	219	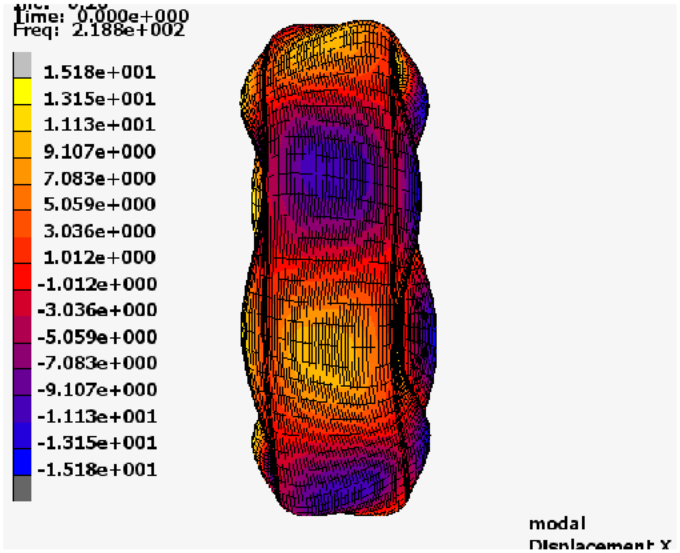

Axiál 5	245	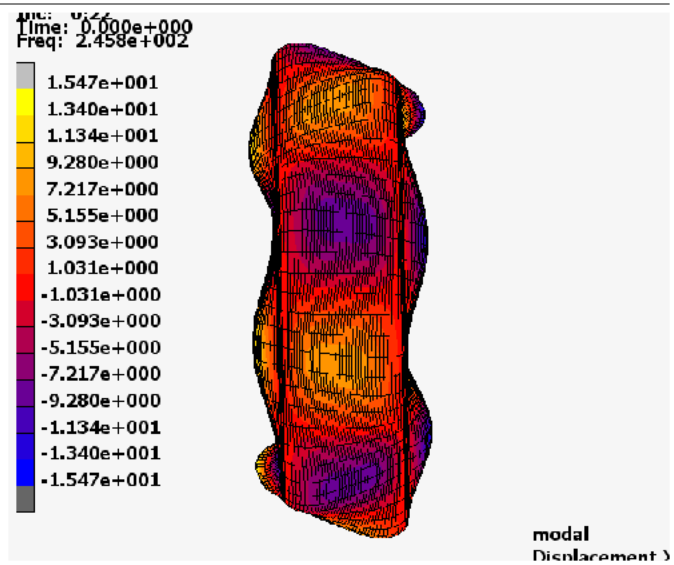

Time: 0.000e+000
Freq: 2.458e+002
1.547e+001
1.340e+001
1.134e+001
9.280e+000
7.217e+000
5.155e+000
3.093e+000
1.031e+000
-1.031e+000
-3.093e+000
-5.155e+000
-7.217e+000
-9.280e+000
-1.134e+001
-1.340e+001
-1.547e+001
modal

Radiálne módy plášťa 195/75 R14

Módy	Vlastné frekvencie (MARC) [Hz]	Vizualizácia
Radiál 1	107	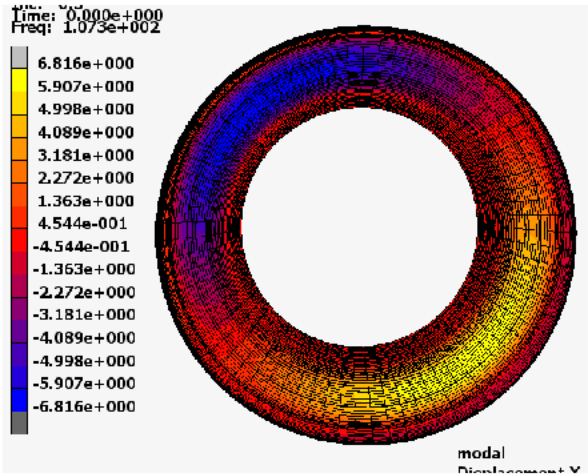
Radiál 2	131	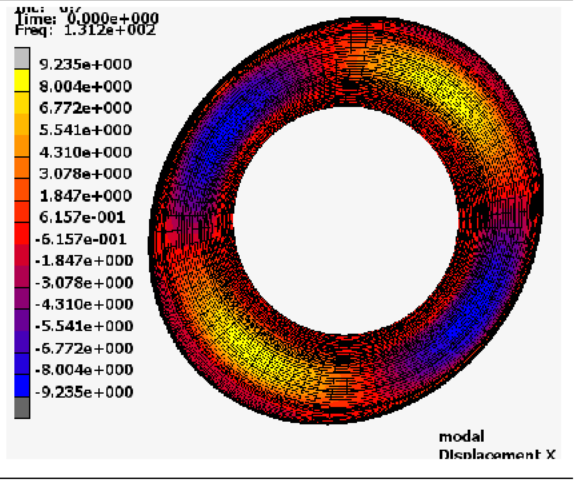

Radiál 3	156	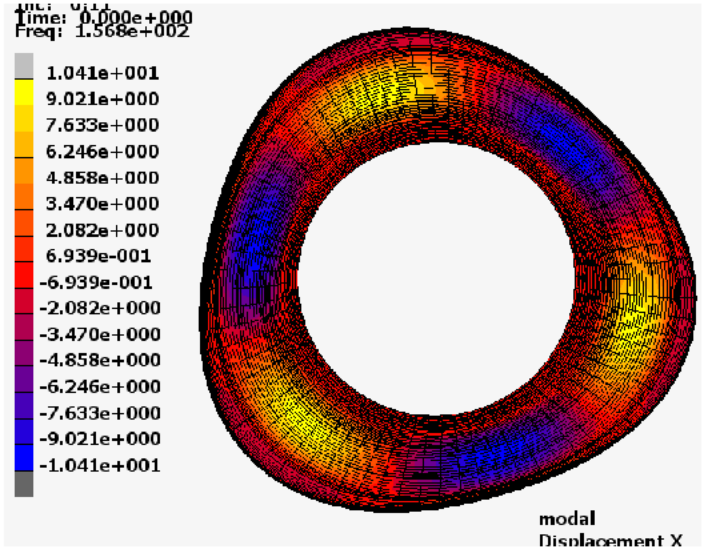
Radiál 4	185	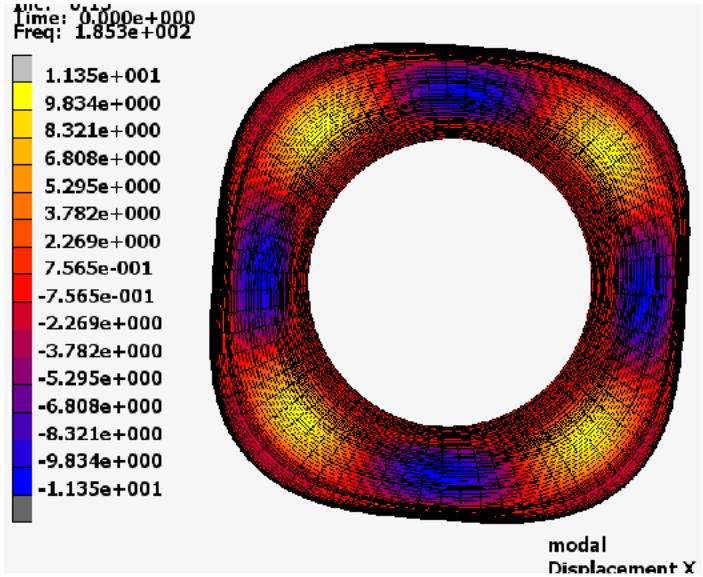

Radiál 5	215	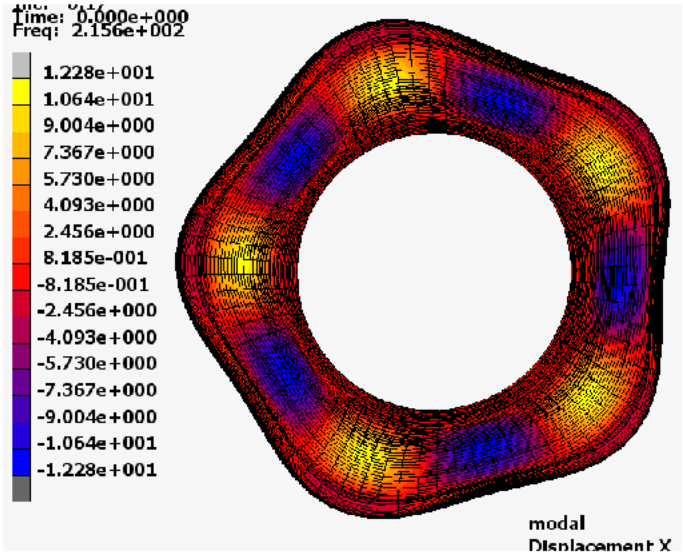
Radiál 6	246	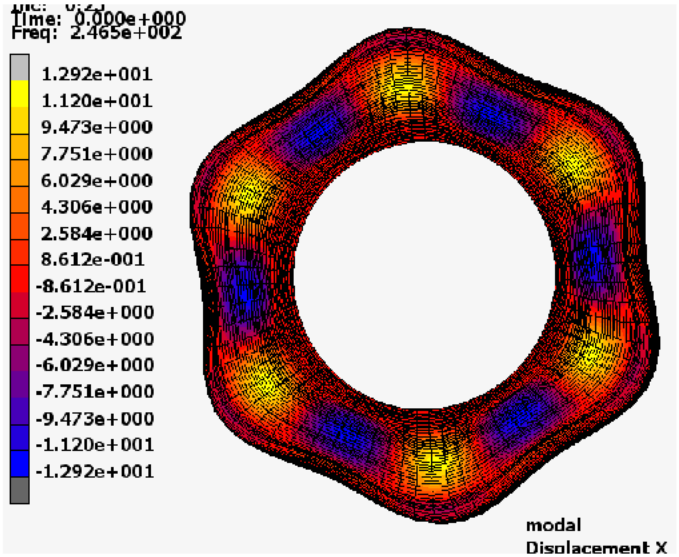

Axiálne módy plášťa 205/55 R16

Módy	Vlastné frekvencie (MARC) [Hz]	Vizualizácia
Axiál 1	71	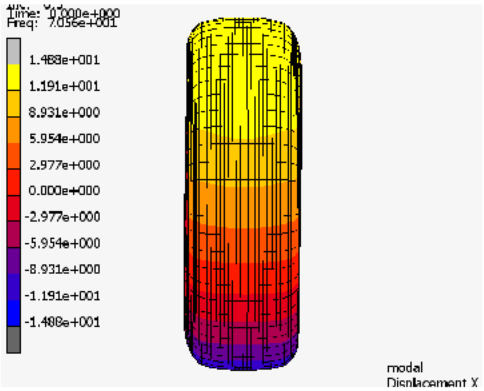
Axiál 2	117	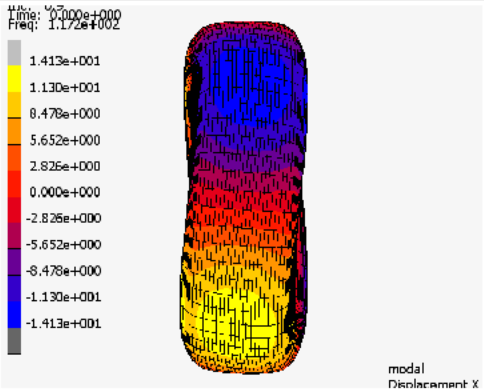
Axiál 3	167	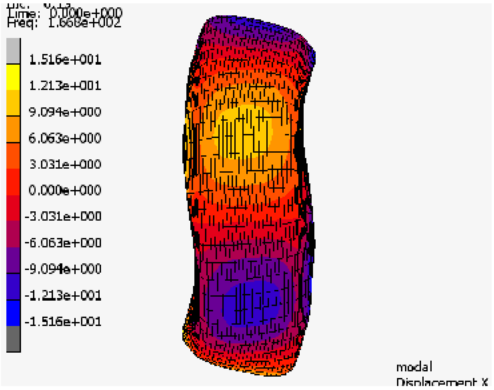

Axiálne módy plášťa 205/55 R16

Módy	Vlastné frekvencie (MARC) [Hz]	Vizualizácia
Axiál 4	201	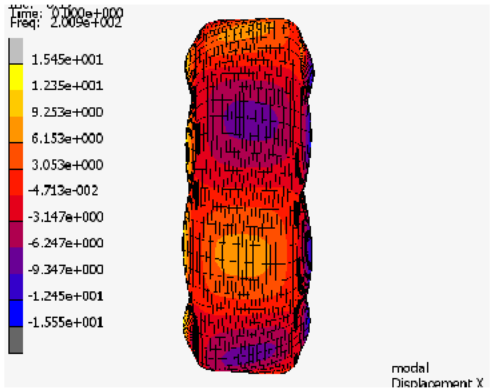
Axiál 5	229	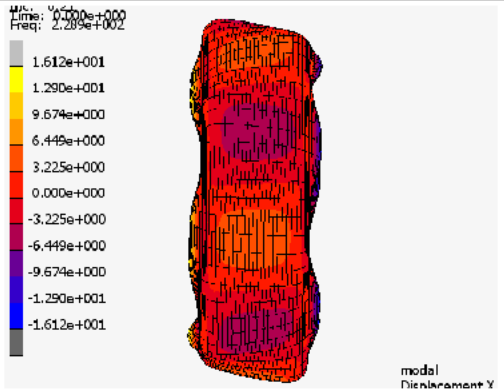
Axiál 6	256	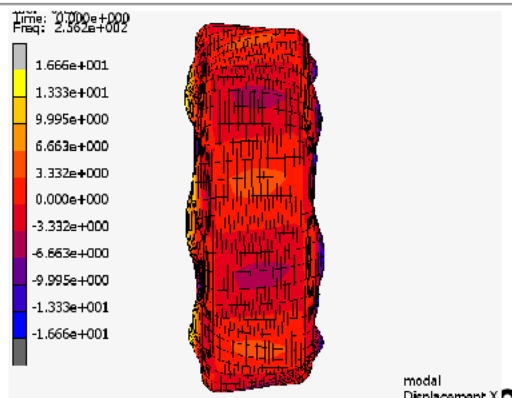

Radiálne módy plášťa 205/55 R16

Módy	Vlastné frekvencie (MARC) [Hz]	Vizualizácia
Radiál 1	85	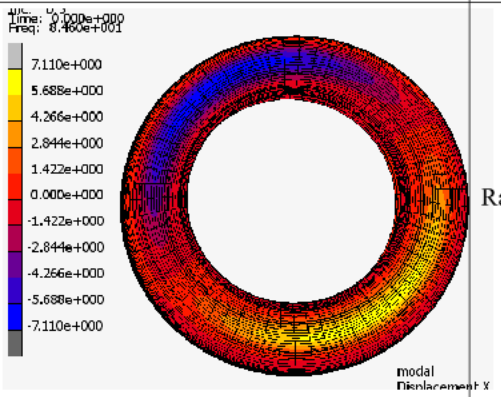
Radiál 2	111	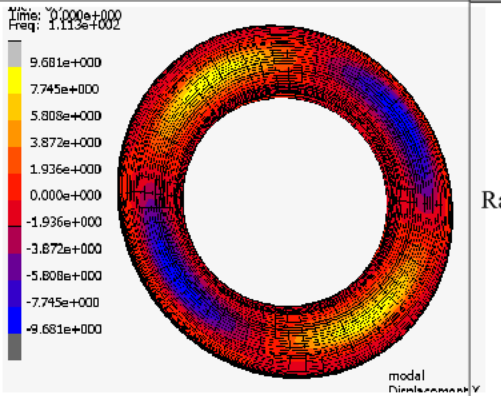
Radiál 3	139	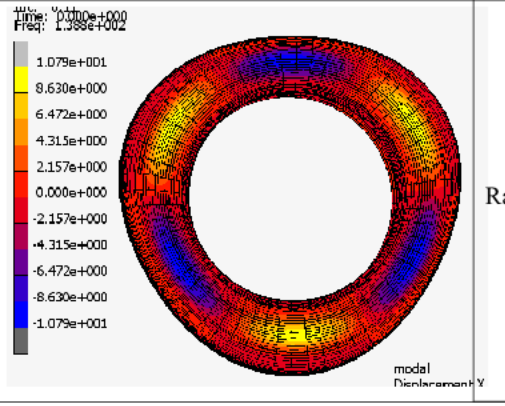

Radiálne módy plášťa 205/55 R16

Módy	Vlastné frekvencie (MARC) [Hz]	Vizualizácia
Radiál 4	170	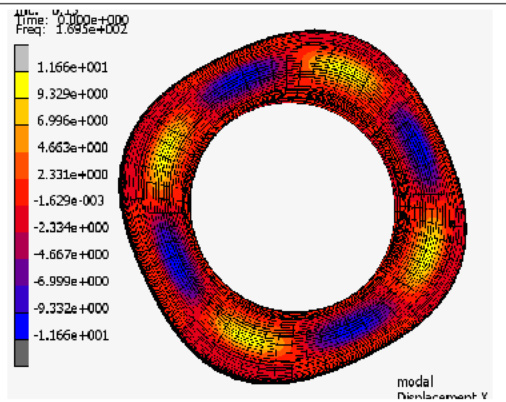
Radiál 5	202	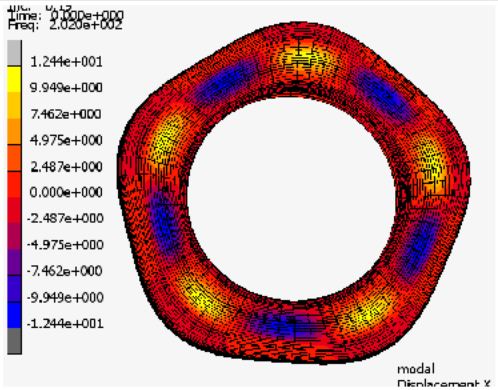
Radiál 6	234	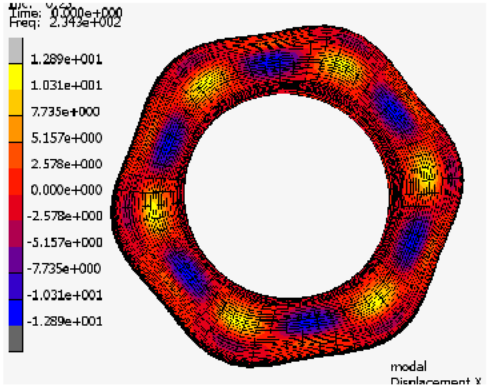

Radiálne módy plášťa pneumatiky 205/55 R16

Módy	Rezonančné frekvencie (ESPI) [Hz]	Vizualizácia
Radiál 1	-	-
Radiál 2	123	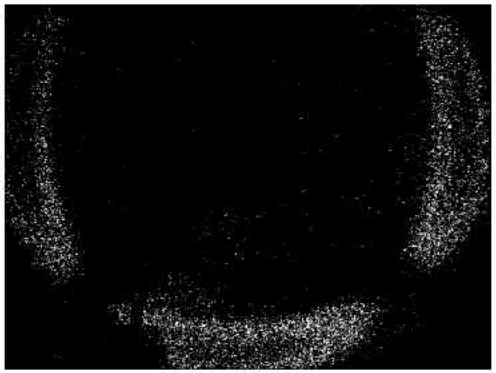
Radiál 3	133	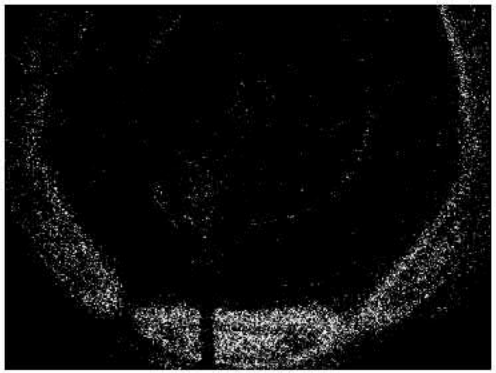
Radiál 4	154	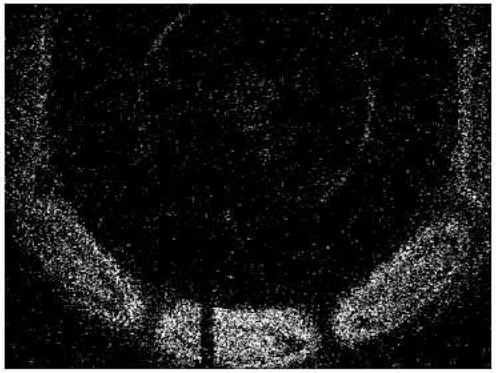

ESPI vs. MARC 165/65 R13

Mode	ESPI (Experiment) [Hz]	MARC [Hz]	Difference [%]
Axiál 1	-	99	-
Axiál 2	120	135	11,1%
Axiál 3	179	183	5,3%
Axiál 4	-	219	-
Axiál 5	-	245	-
Axiál 6	-	270	-
Radiál 1	-	107	-
Radiál 2	136	131	3,7%
Radiál 3	166	156	6%
Radiál 4	188	185	1,6%
Radiál 5	208	215	3,3
Radiál 6	239	246	2,8

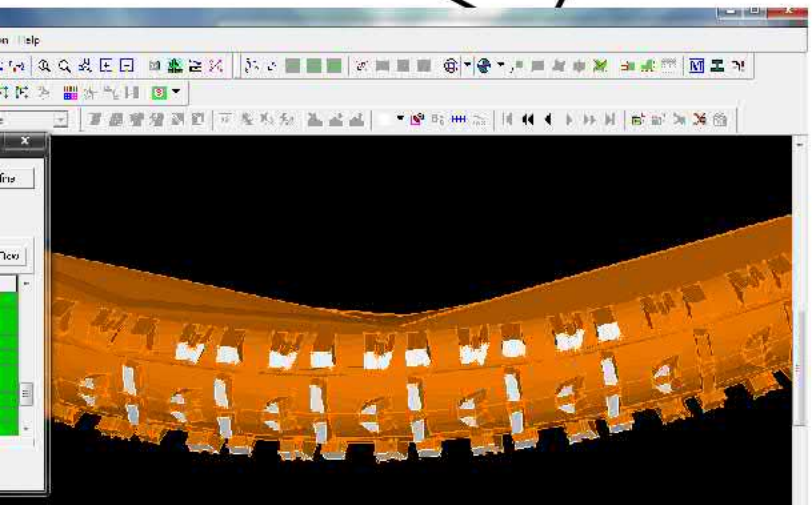

The reinforcements are not included in the computational model because this model serves as a debugging model. The material parameters were specified by one type of material only, with modulus of flexibility 90 GPa and Poisson number 0.45.

COMPUTATIONAL MODELLING

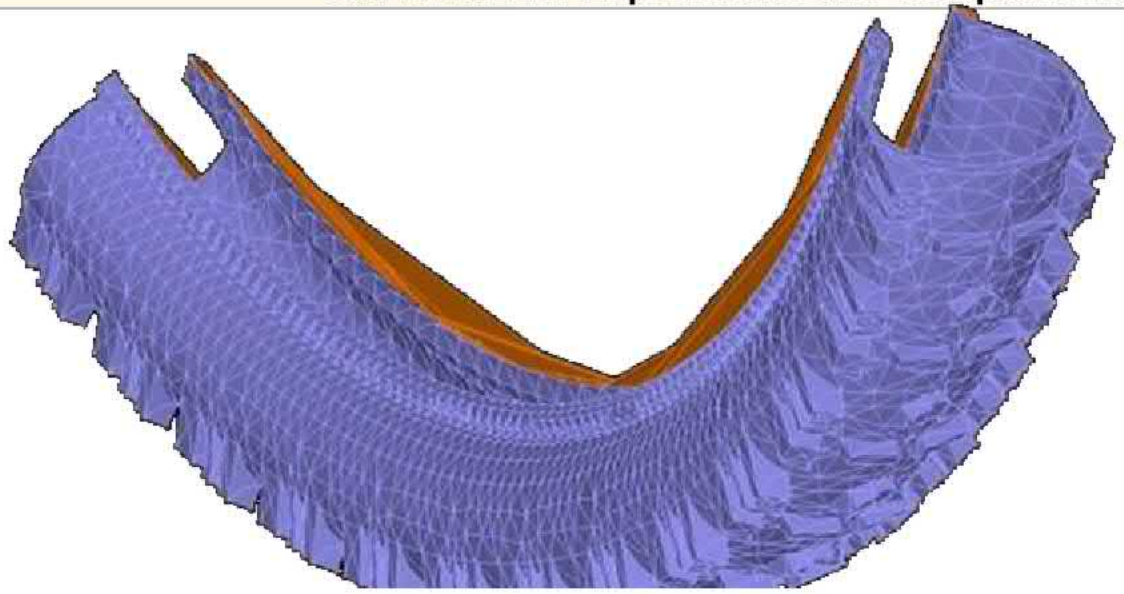

Meshing of quarter of computational model in FEM program

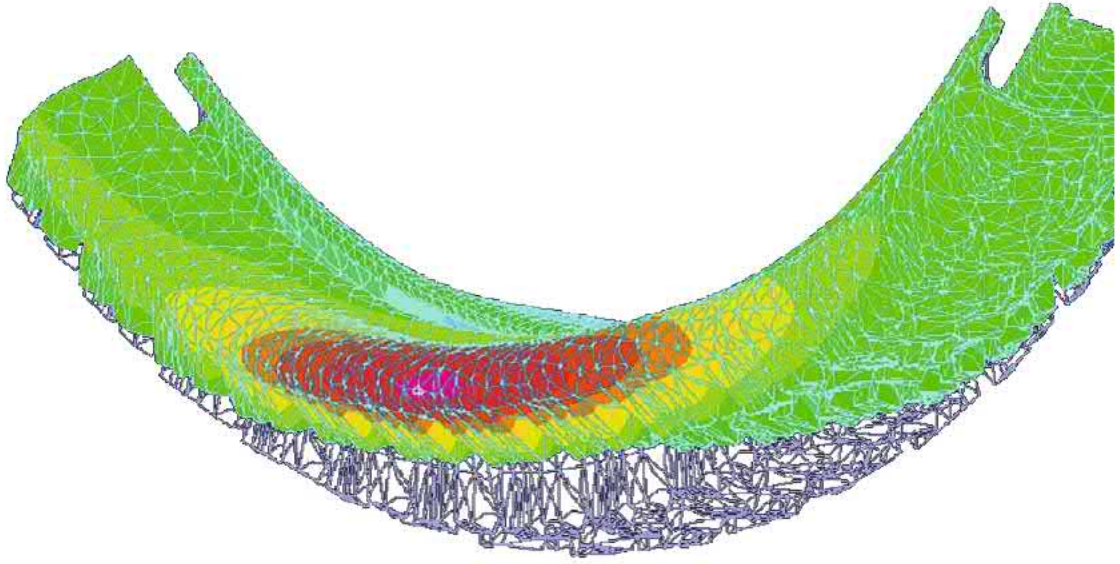

Deformation of tire

Part 9 – INTEREST INFORMATION: Optimalization of computational time, Material parameters and their sensitivity to the precision of results, Structure of truck tire, Freeware (CADEC) for compute of composite material parameters

205/55 R16

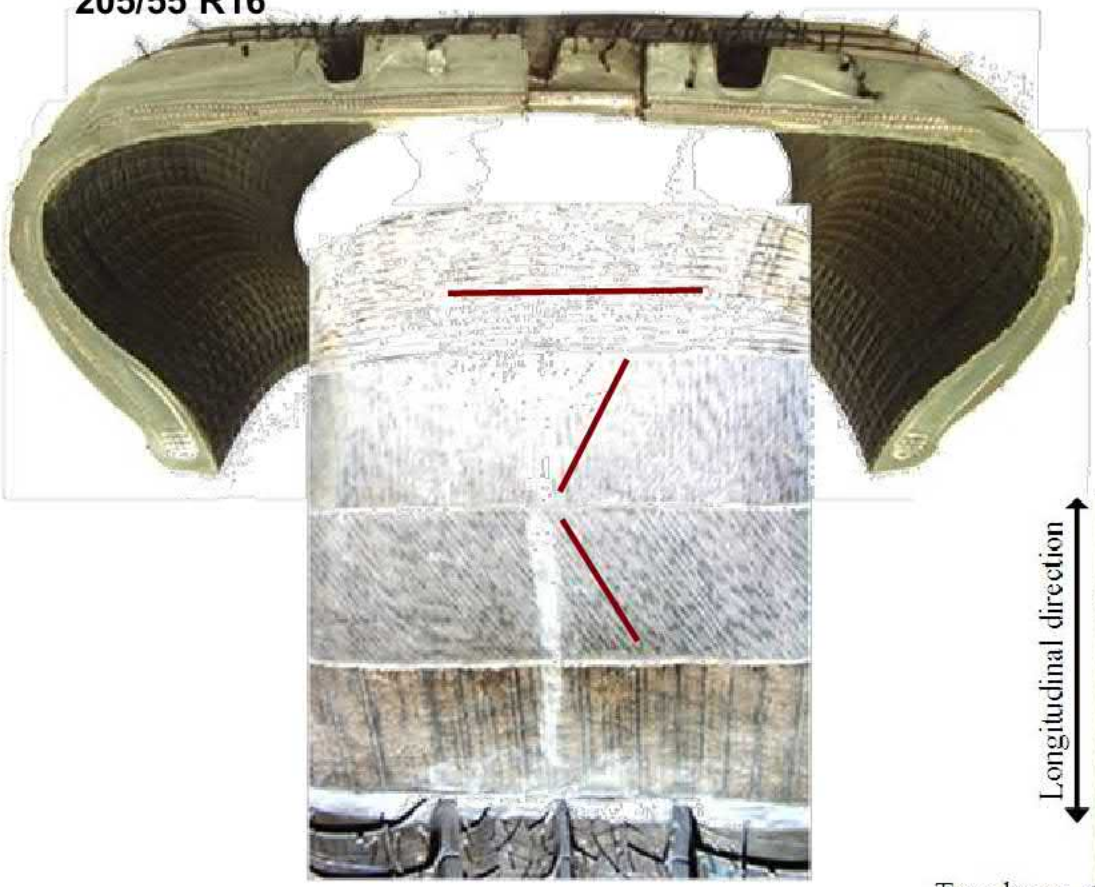

TRUCK radial tire – structure of belts of tire crown

Matador 22.5”

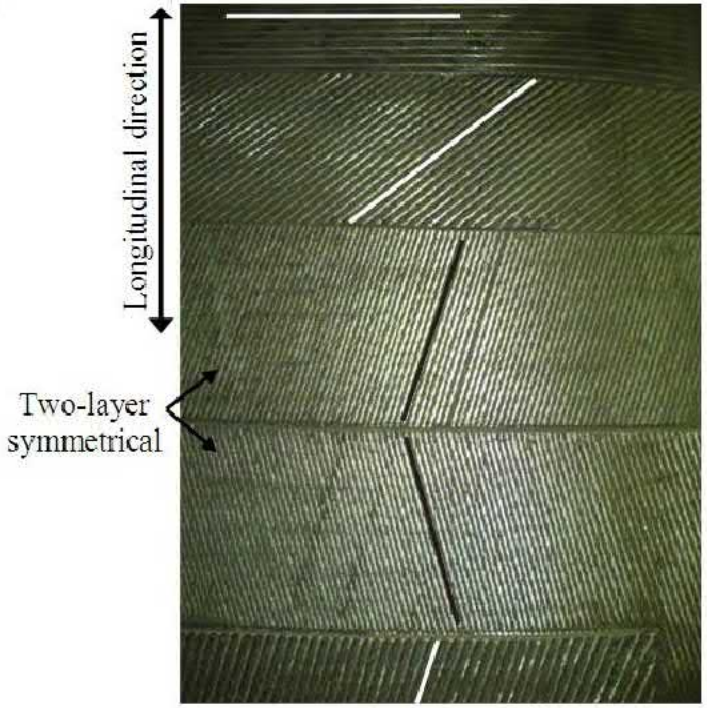

Structure of truck tire in the middle of tire crown

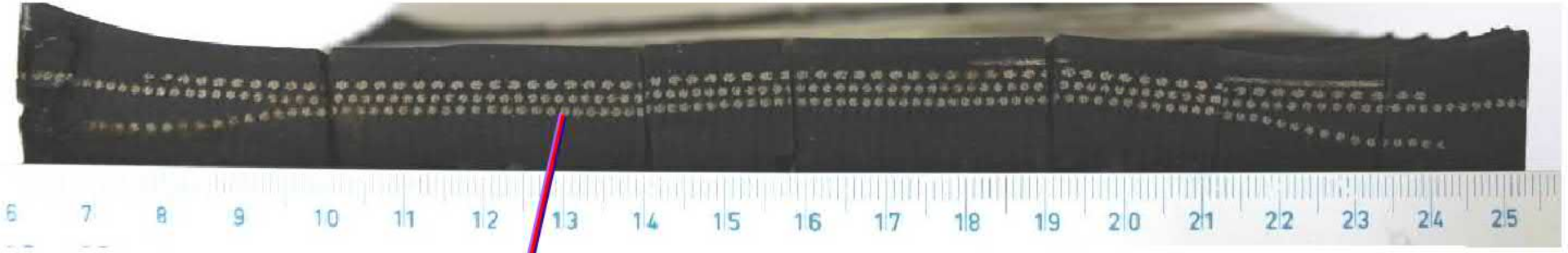
6
7
8
9
10
11
12
13
14
15
16
17
18
19
20
21
22
23
24
25

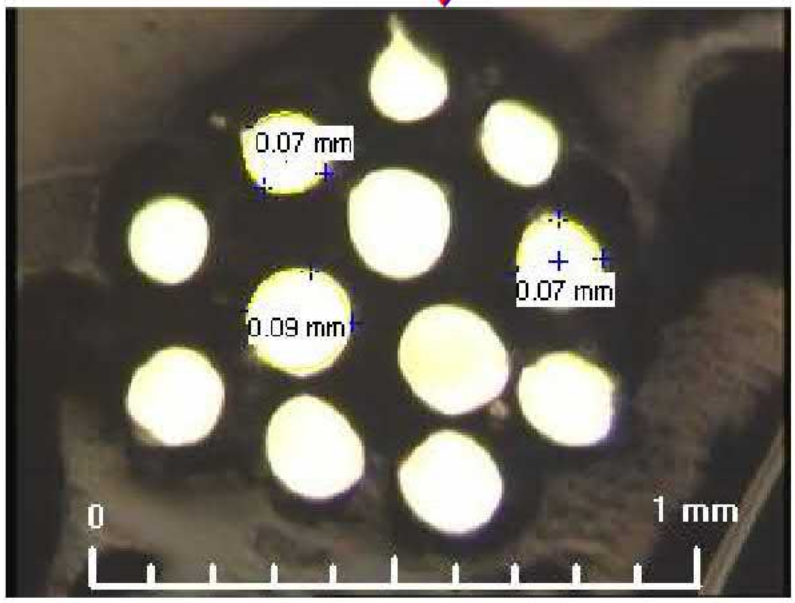
0.07 mm
0.07 mm
0.09 mm
0
1 mm

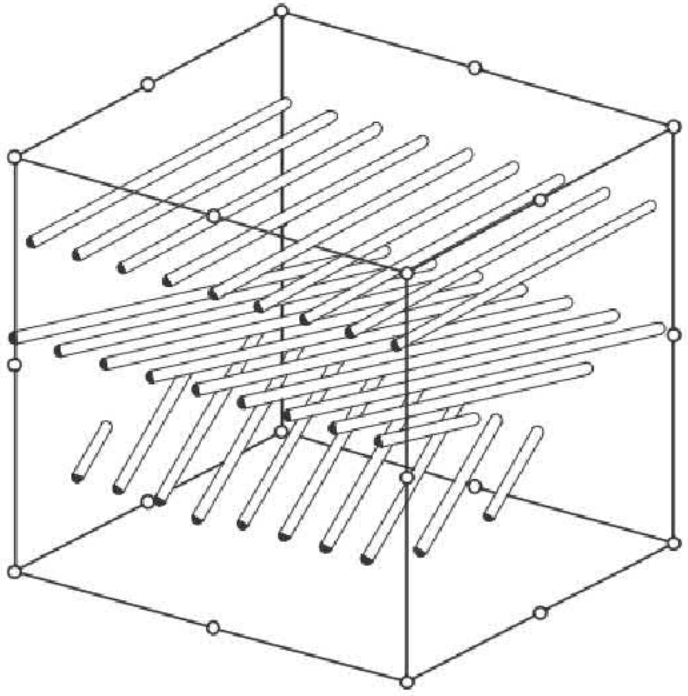

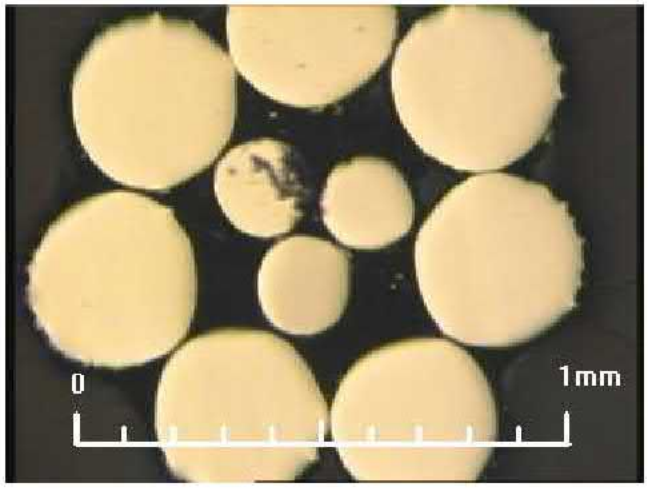
0
1mm

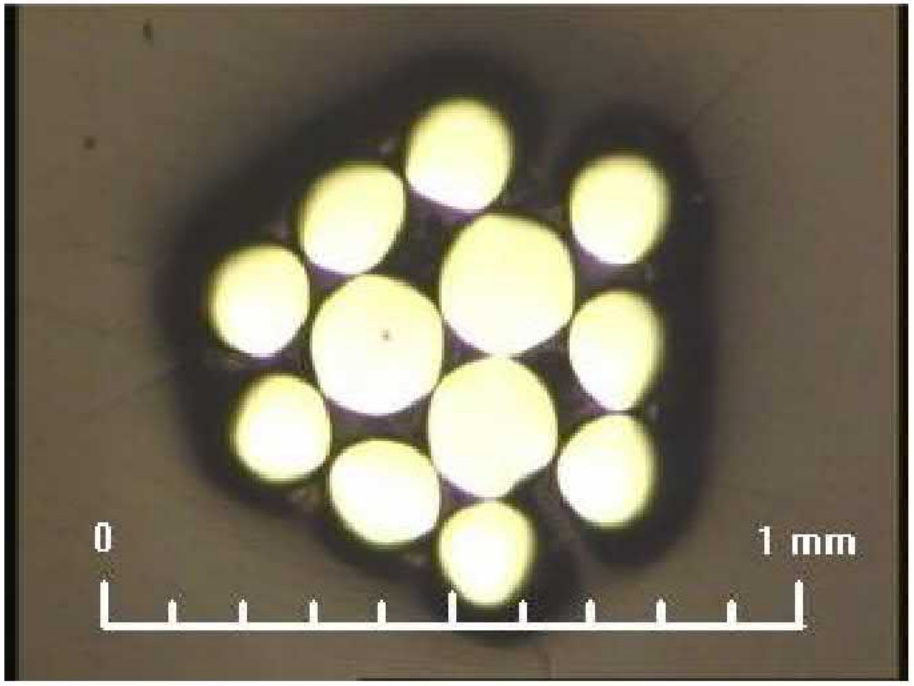
0
1 mm

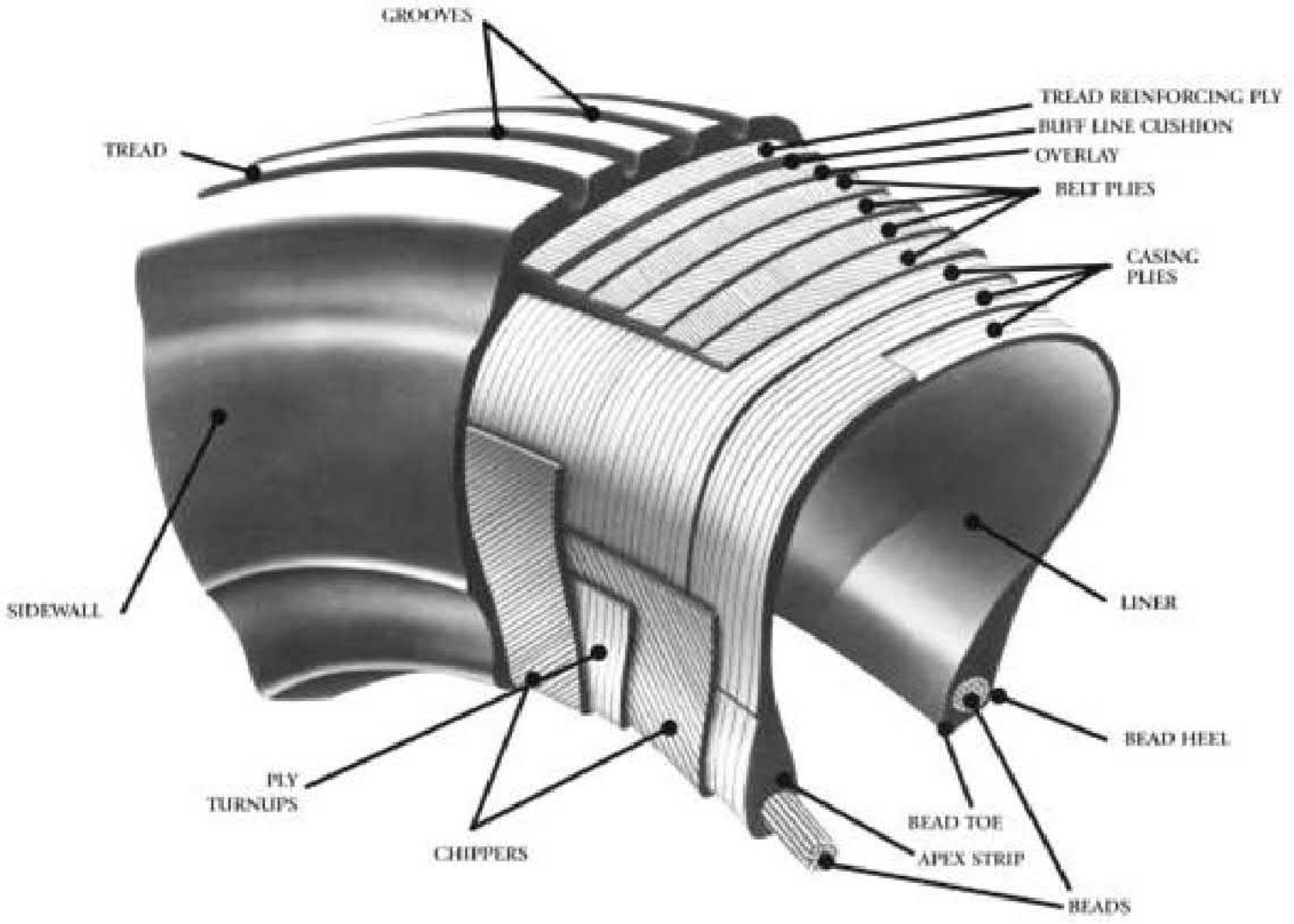
GROOVES
TREAD
TREAD REINFORCING PLY
BUFF LINE CUSHION
OVERLAY
BELT PLIES
CASING PLIES
SIDEWALL
LINER
BEAD HEEL
PLY TURNUPS
CHIPPERS
BEAD TOE
APEX STRIP
BEADS

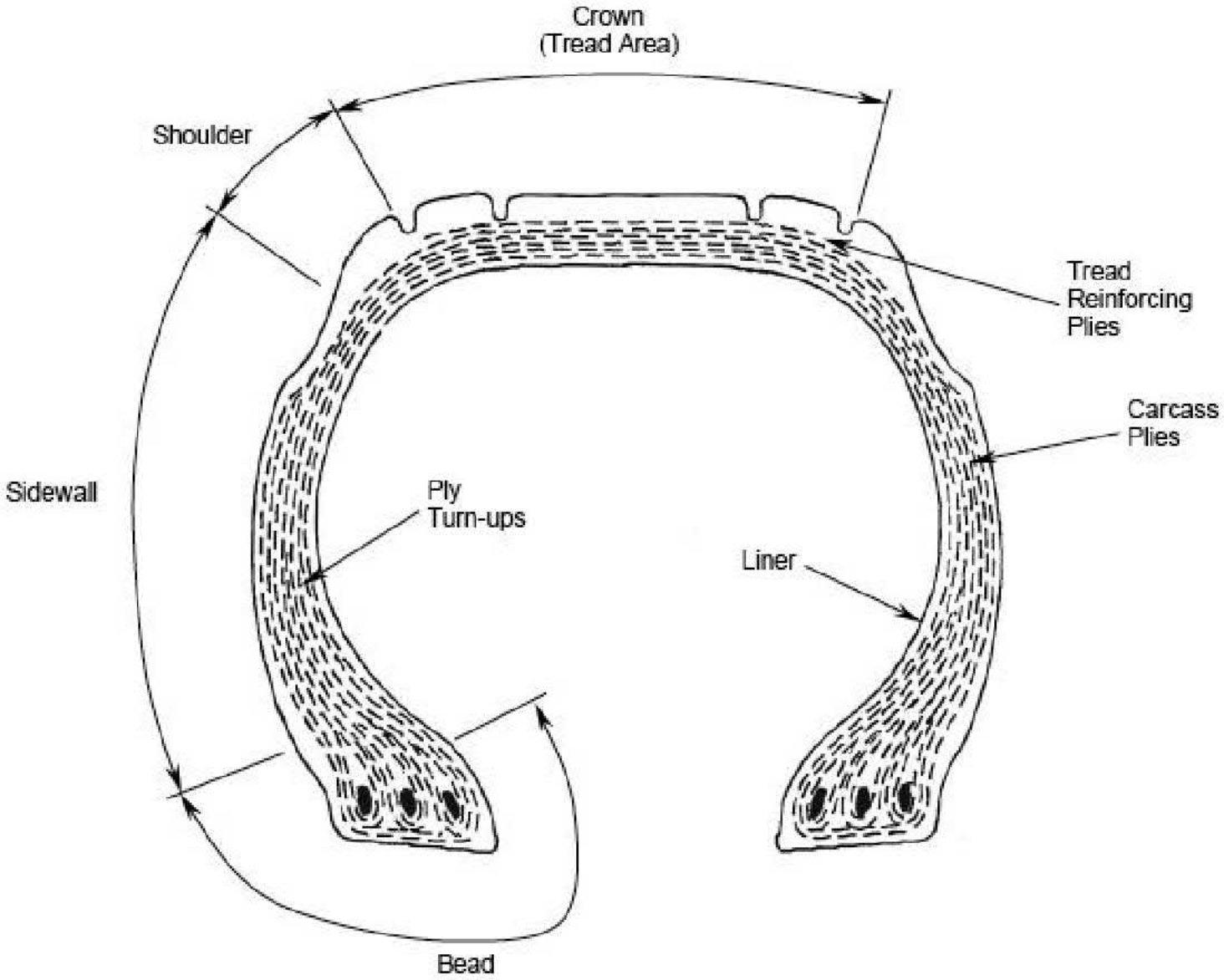
Crown
(Tread Area)
Shoulder
Tread
Reinforcing
Plies
Carcass
Plies
Sidewall
Ply
Turn-ups
Liner
Bead

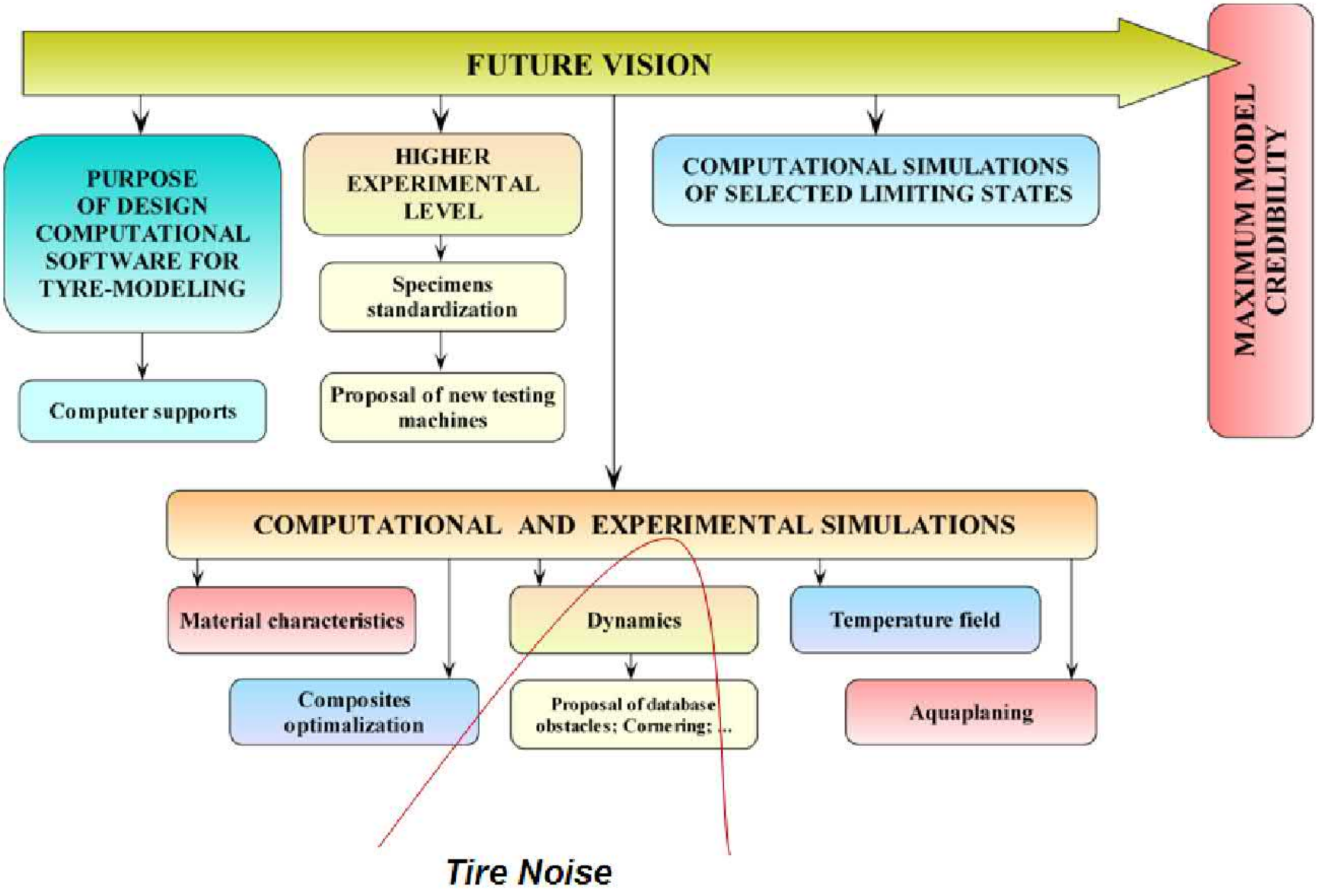
FUTURE VISION
MAXIMUM MODEL CREDIBILITY
PURPOSE OF DESIGN COMPUTATIONAL SOFTWARE FOR TYRE-MODELING
HIGHER EXPERIMENTAL LEVEL
COMPUTATIONAL SIMULATIONS OF SELECTED LIMITING STATES
Specimens standardization
Computer supports
Proposal of new testing machines
COMPUTATIONAL AND EXPERIMENTAL SIMULATIONS
Material characteristics
Dynamics
Temperature field
Composites optimalization
Proposal of database obstacles; Cornering; ...
Aquaplaning
Tire Noise

Cycle loading

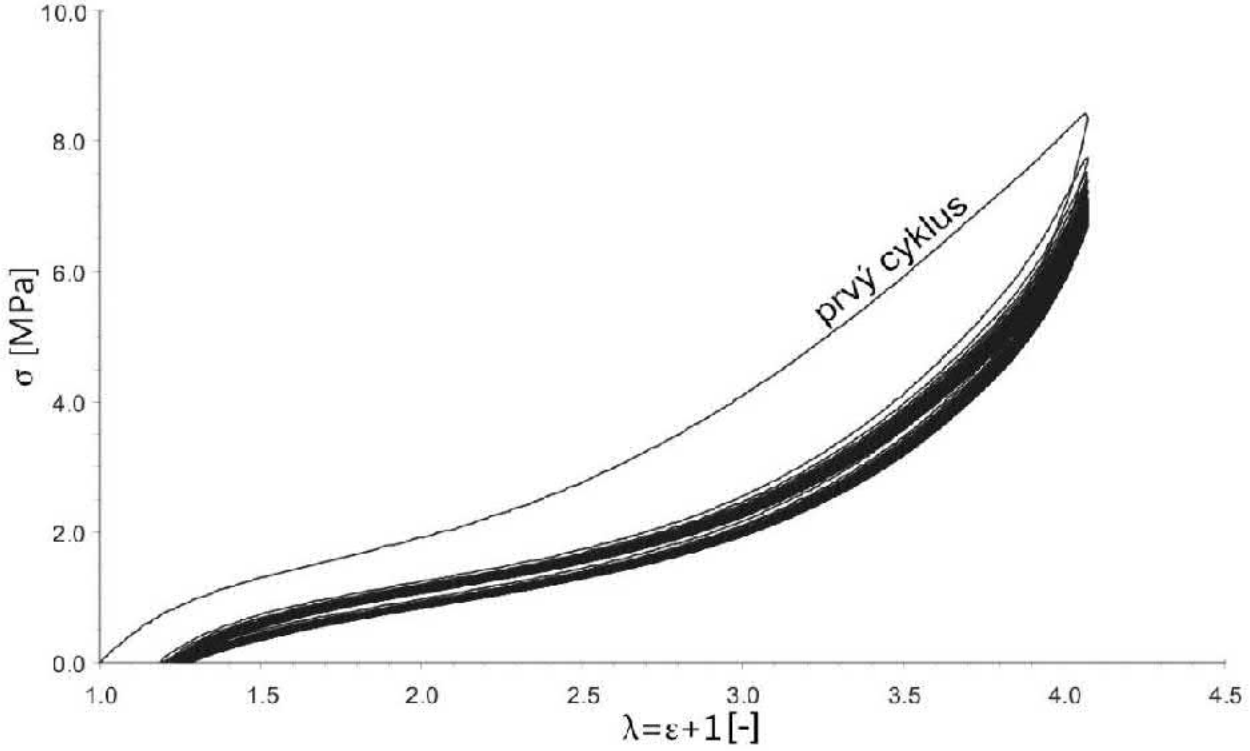

Cycle loading

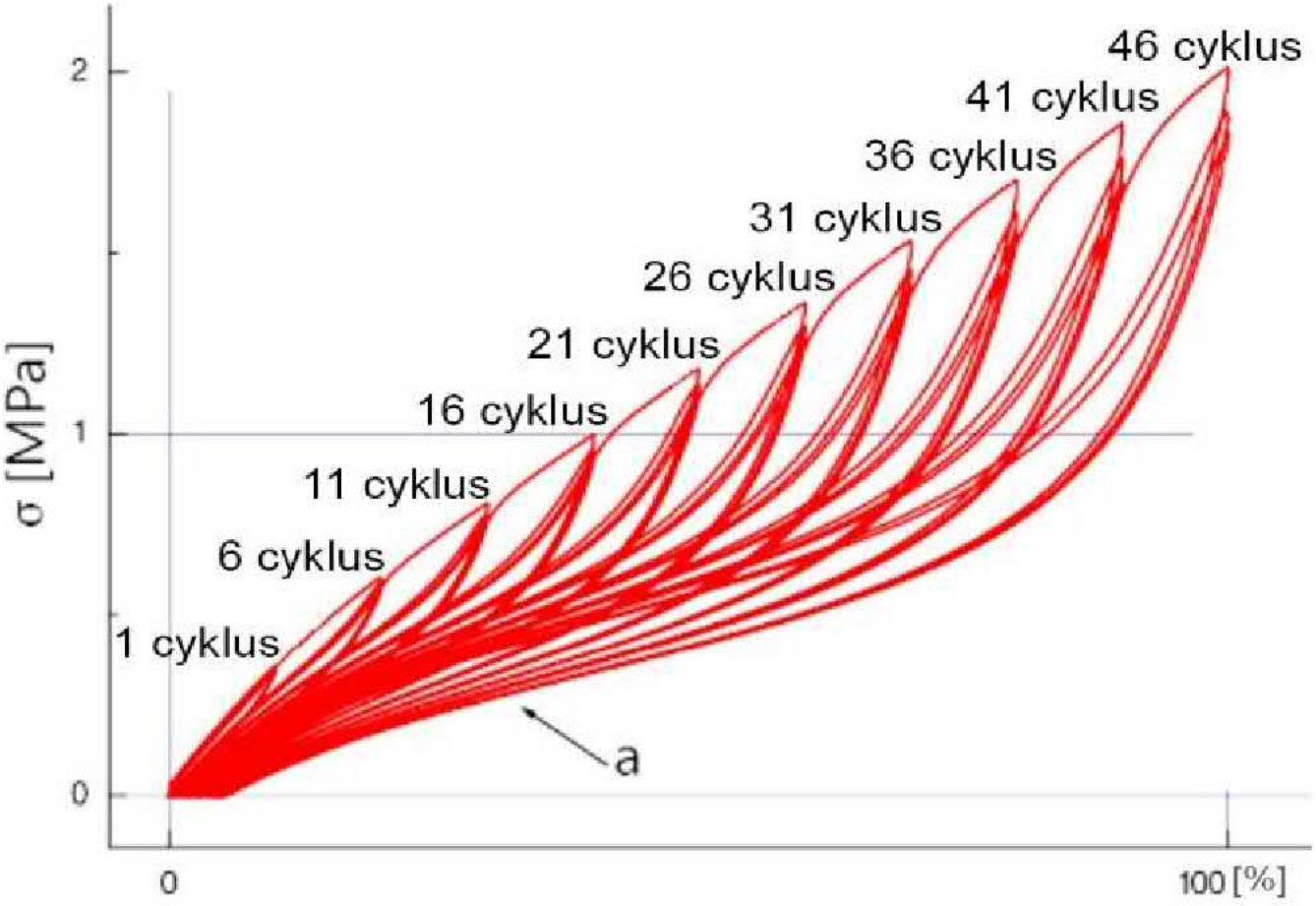

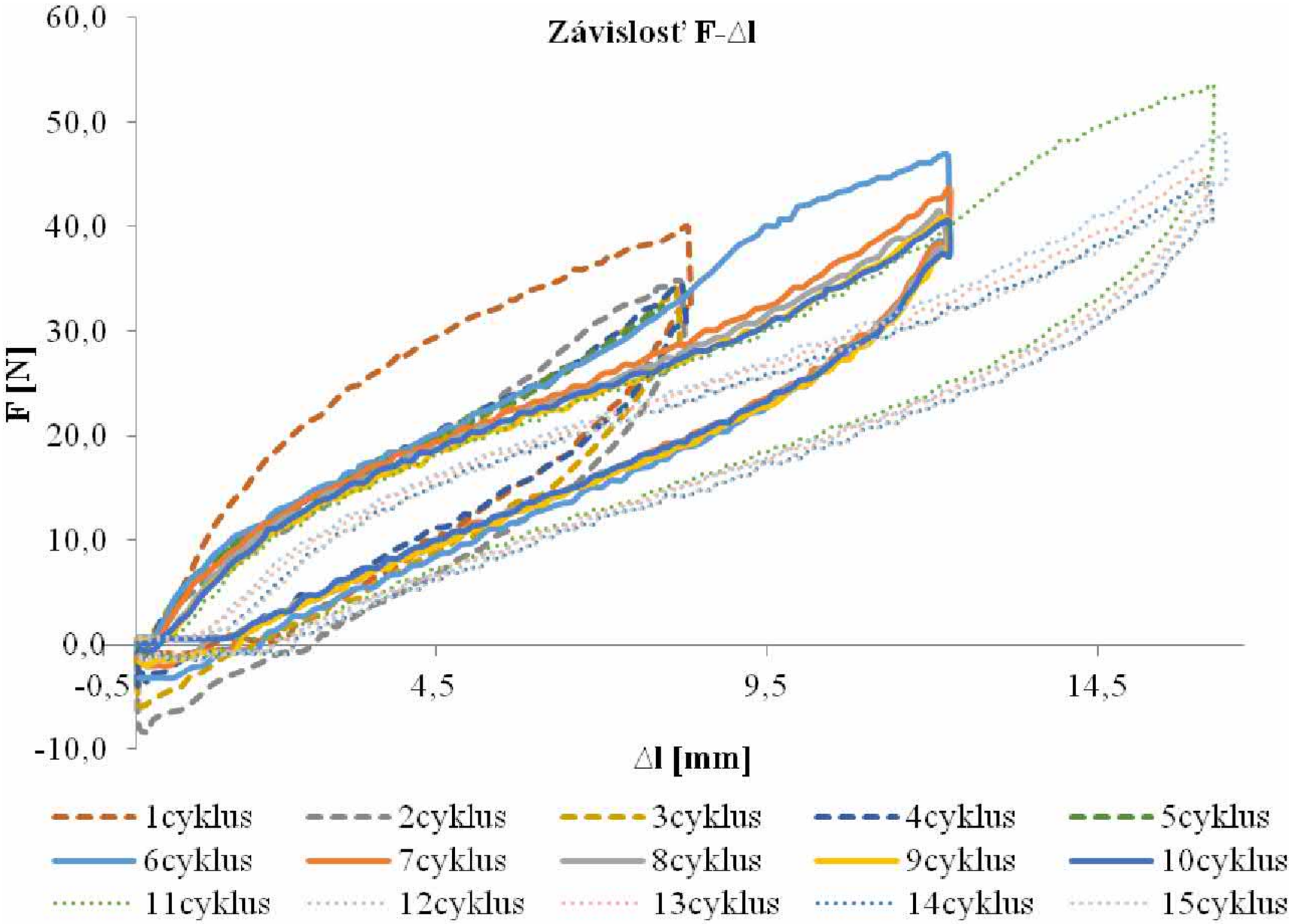
Závislosť F-Δl
60,0
50,0
40,0
30,0
20,0
10,0
0,0
-10,0
F [N]
-0,5
4,5
9,5
14,5
Δl [mm]
1cyklus
2cyklus
3cyklus
4cyklus
5cyklus
6cyklus
7cyklus
8cyklus
9cyklus
10cyklus
11cyklus
12cyklus
13cyklus
14cyklus
15cyklus

Cycle loading

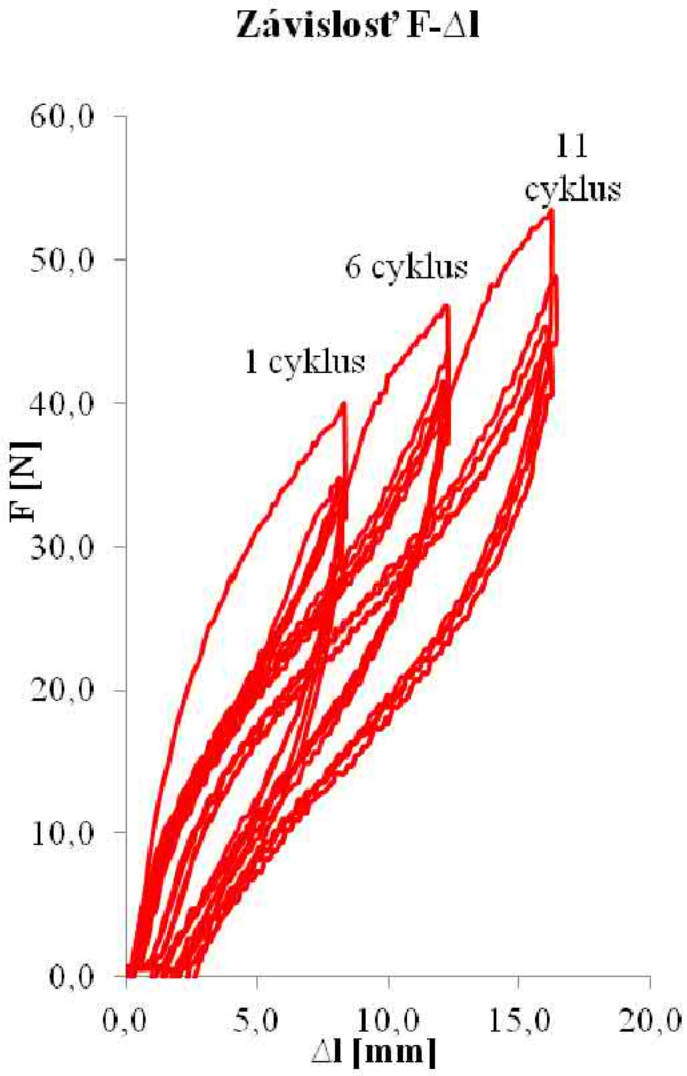

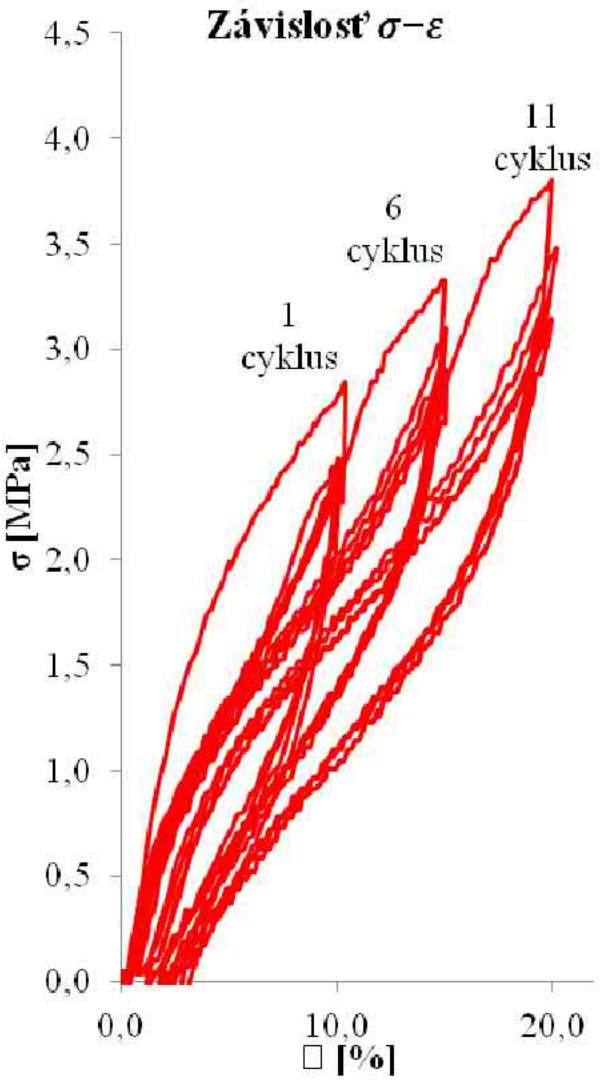

Cycle loading

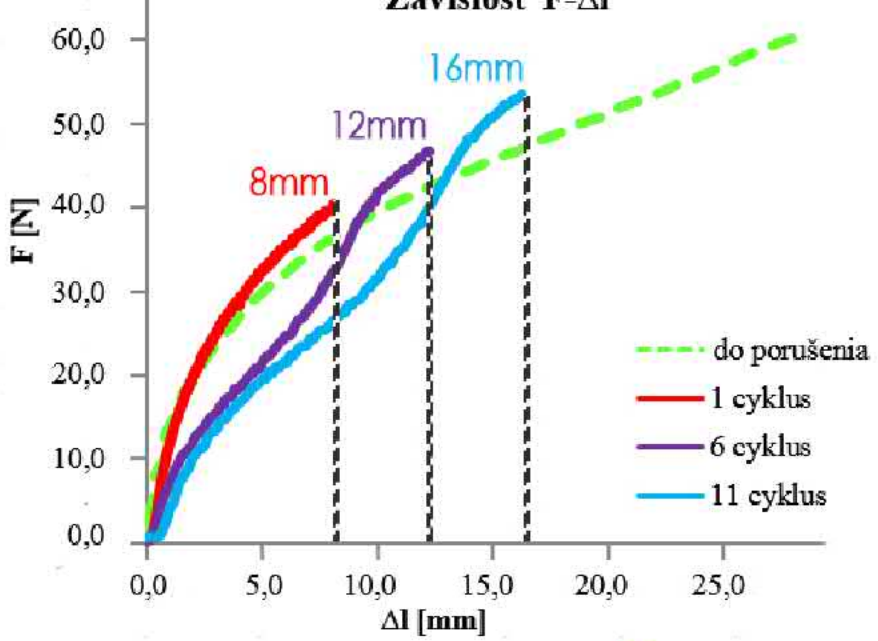

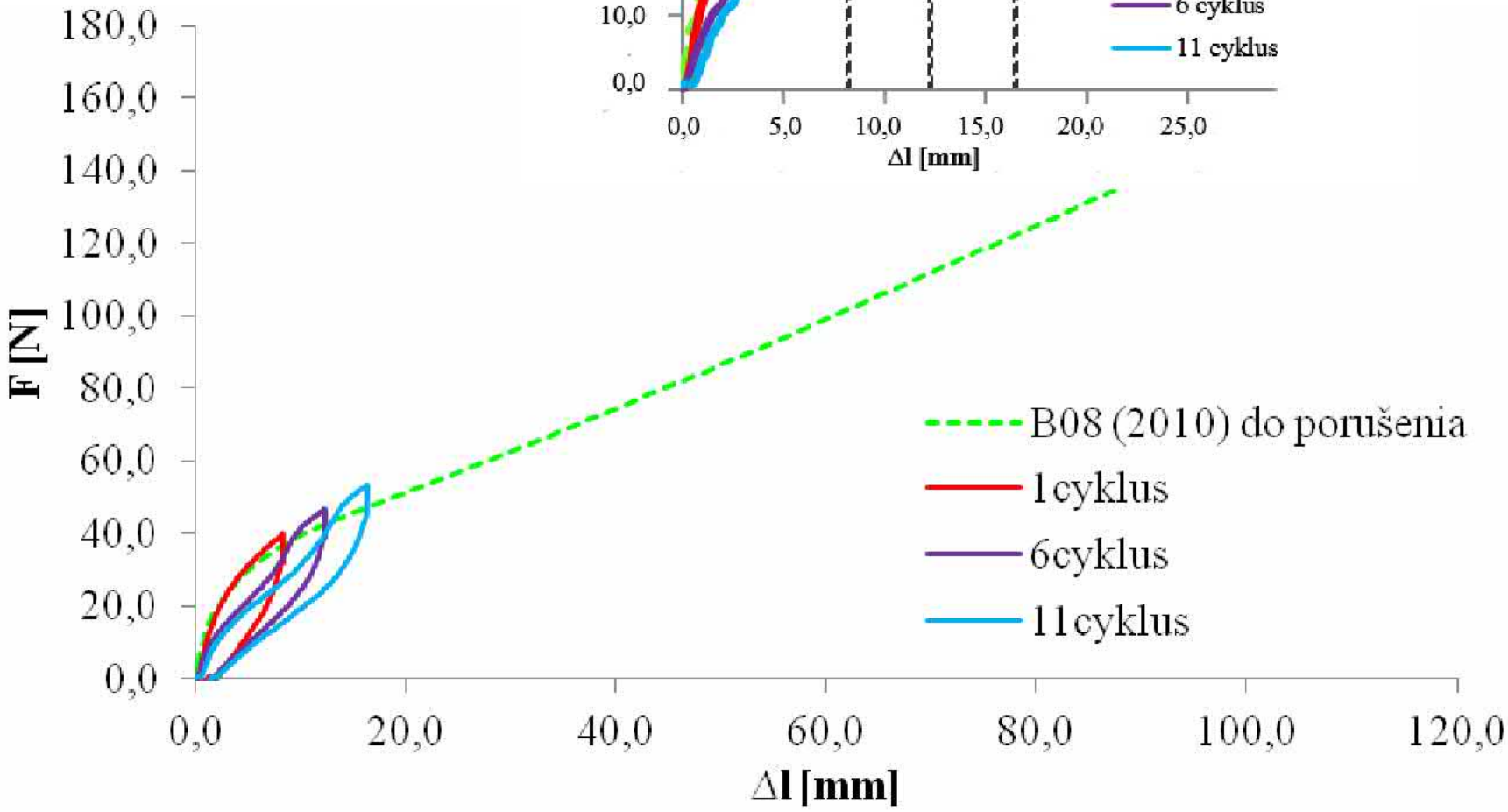

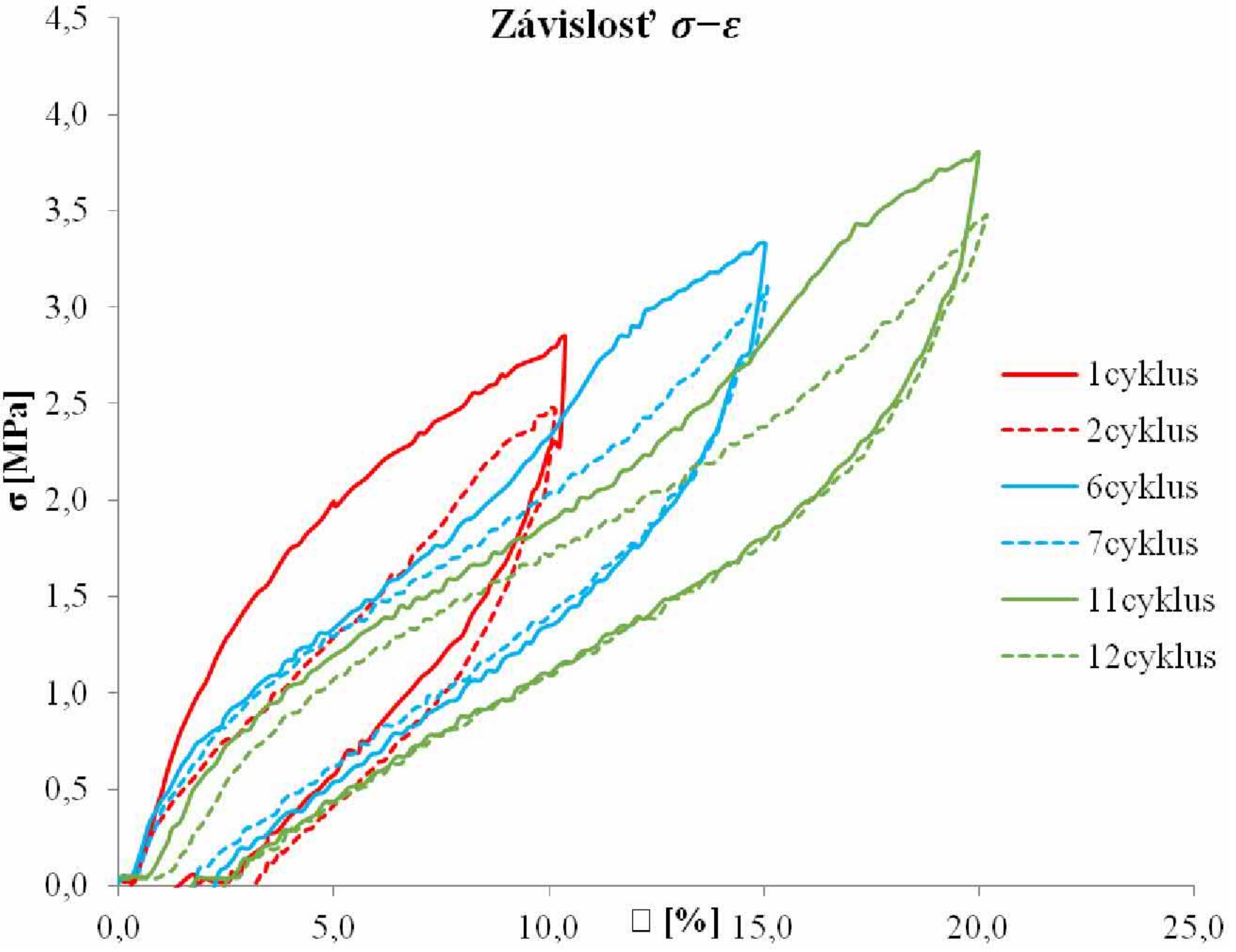
Závislosť σ−ε
σ [MPa]
4,5
4,0
3,5
3,0
2,5
2,0
1,5
1,0
0,5
0,0
0,0
5,0
10,0
□ [%]
15,0
20,0
25,0
1cyklus
2cyklus
6cyklus
7cyklus
11cyklus
12cyklus

Cycle loading

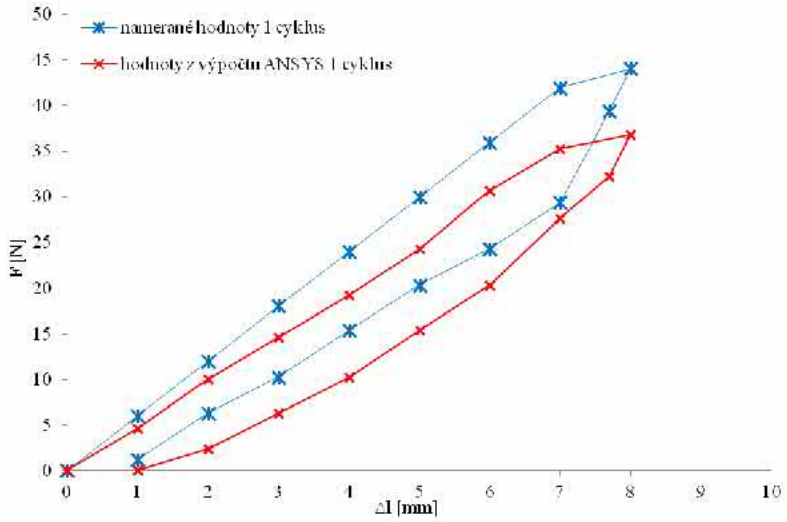

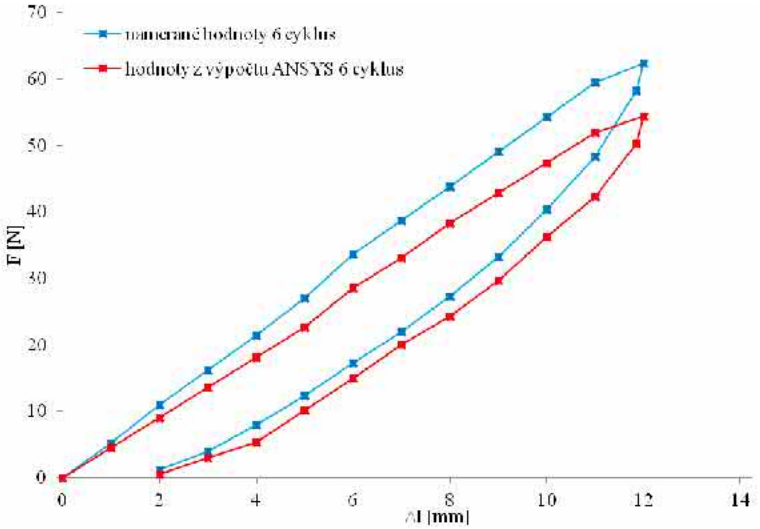

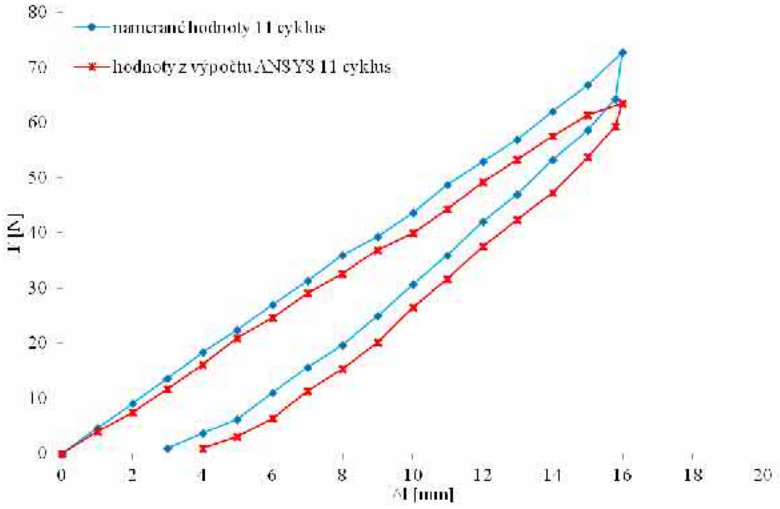

Design of Method for Cyclic Tensile Loading of Composites

The universal testing device: Autograph AG-X plus 5 kN – Schimadzu with video-extensometer is used for cyclic loading in temperature chamber. Software Trapenzium X Control is used.

Before carrying out the mechanical tests, the geometric parameters of test samples it were proposed and test conditions with respect to the current standards and test equipment opportunities were determined.

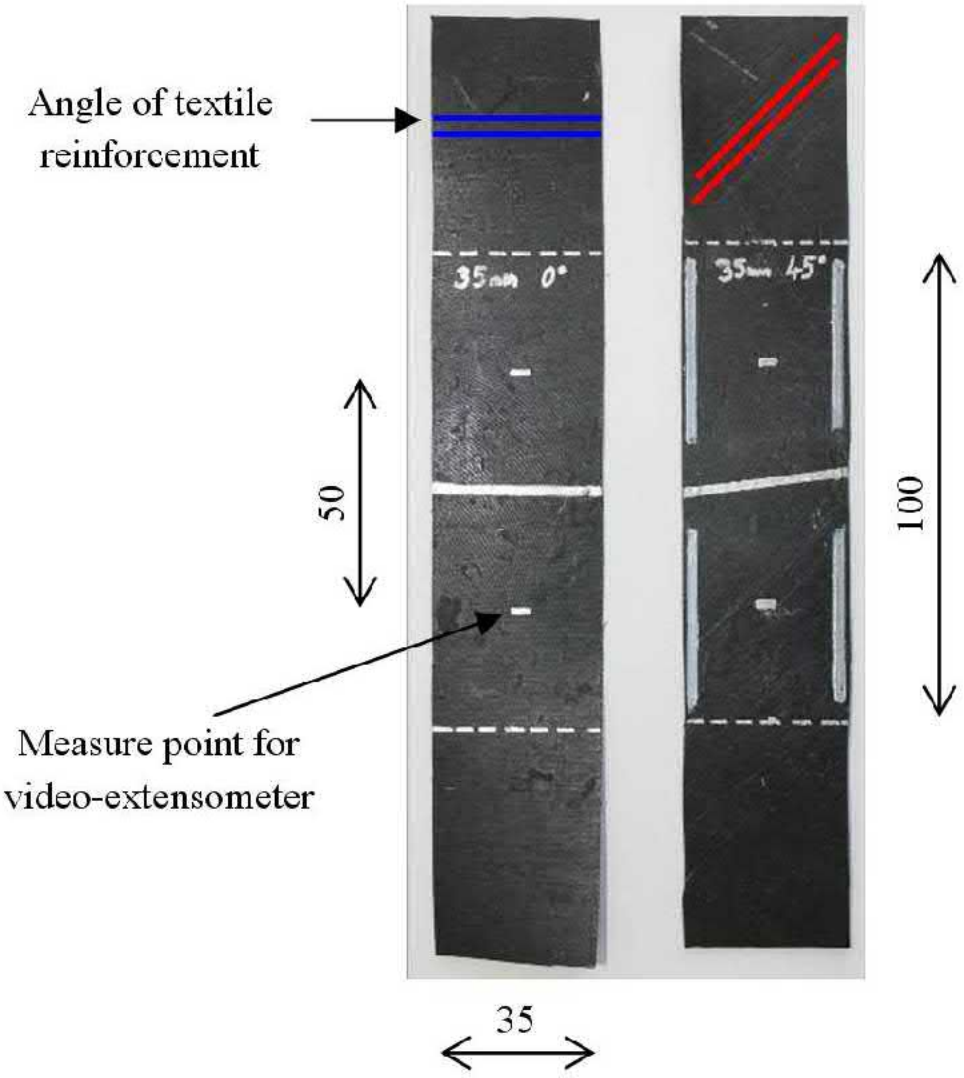

The PA 66 is used as textile reinforcement for tests of cyclic loading. The composite specimens with textile reinforcement's angles 0° (textile reinforcement is perpendicular to the direction of loading), 45° and 60° are used for cyclic tests.

The geometrical parameters of specimens are: specimen's length is 195 mm, width is 35 mm, initial length between the clamps of test machine is 100 mm and specimen's thickness is 1.05 mm. The EPM is 870 m-1. The initial length between the points for video-extensometer is 50 mm.

The loading speed is 250 mm/min for cycle tests and 50 mm/min for preload by force value 2 N.

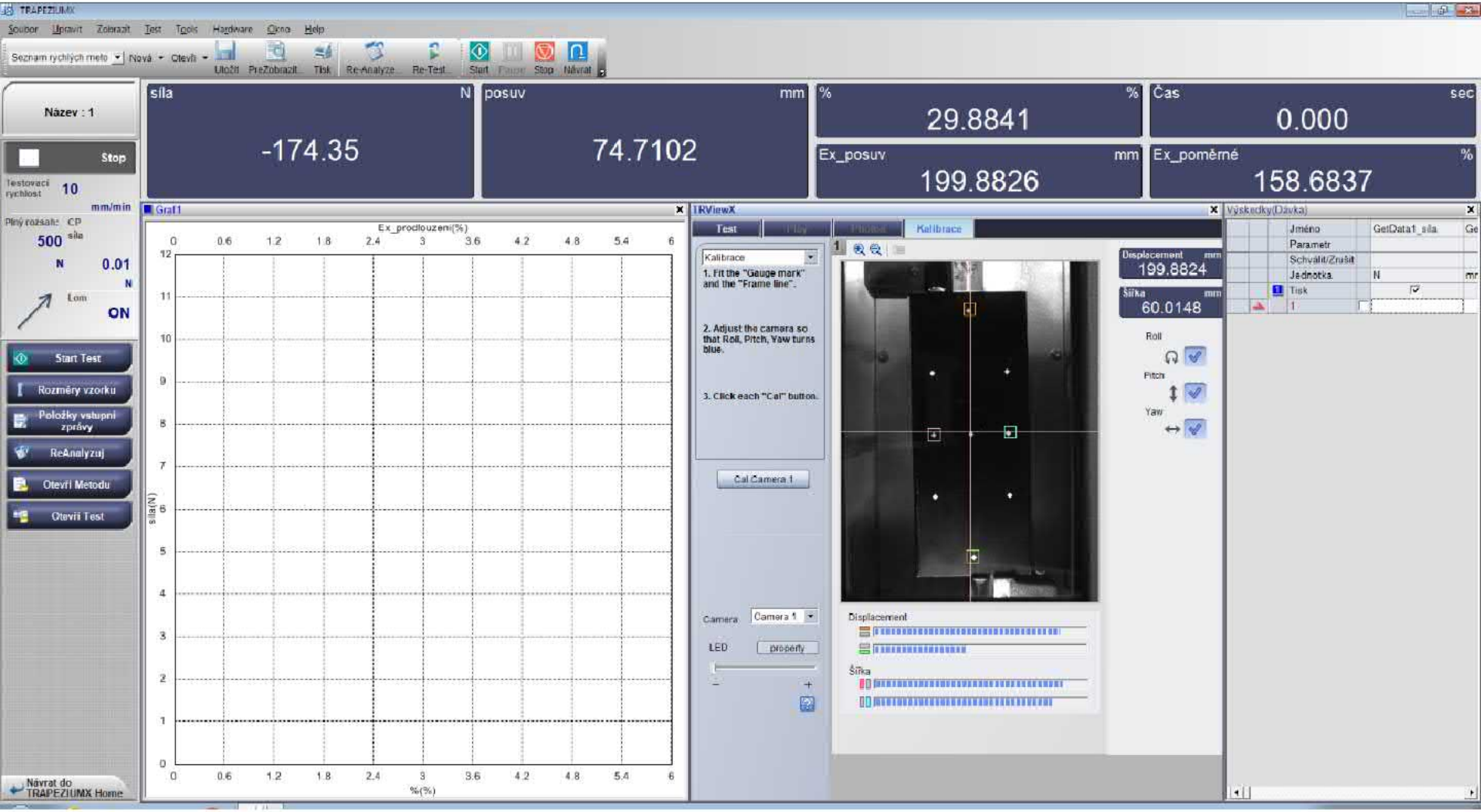

Calibration process

The five cycle loops are used. Every cycle loop consists of five cycles. Every cycle is defines as loading to certain percent of elongation between clamps of test machine and unloading to certain percent of elongation between clamps of test machine.

For angles 0 and 45° the first cycle loop consists of cycles with loading to 30% and unloading to 3% of elongation (not 0% because negative force is not possible during tensile testing for certain composite specimens with textile reinforcement). The second loop consists of cycles with elongation higher by 10%: loading to 40% and unloading to 10% of elongation. The third loop consists of five cycles which have loading to 50% and unloading to 20% of elongation, the fourth loop with cycles has loading to 60% and unloading to 30% of elongation. The fifth loop has cycles with different elongations, the loading to 60% is the same as fourth loop and unloading is 5% of elongation.

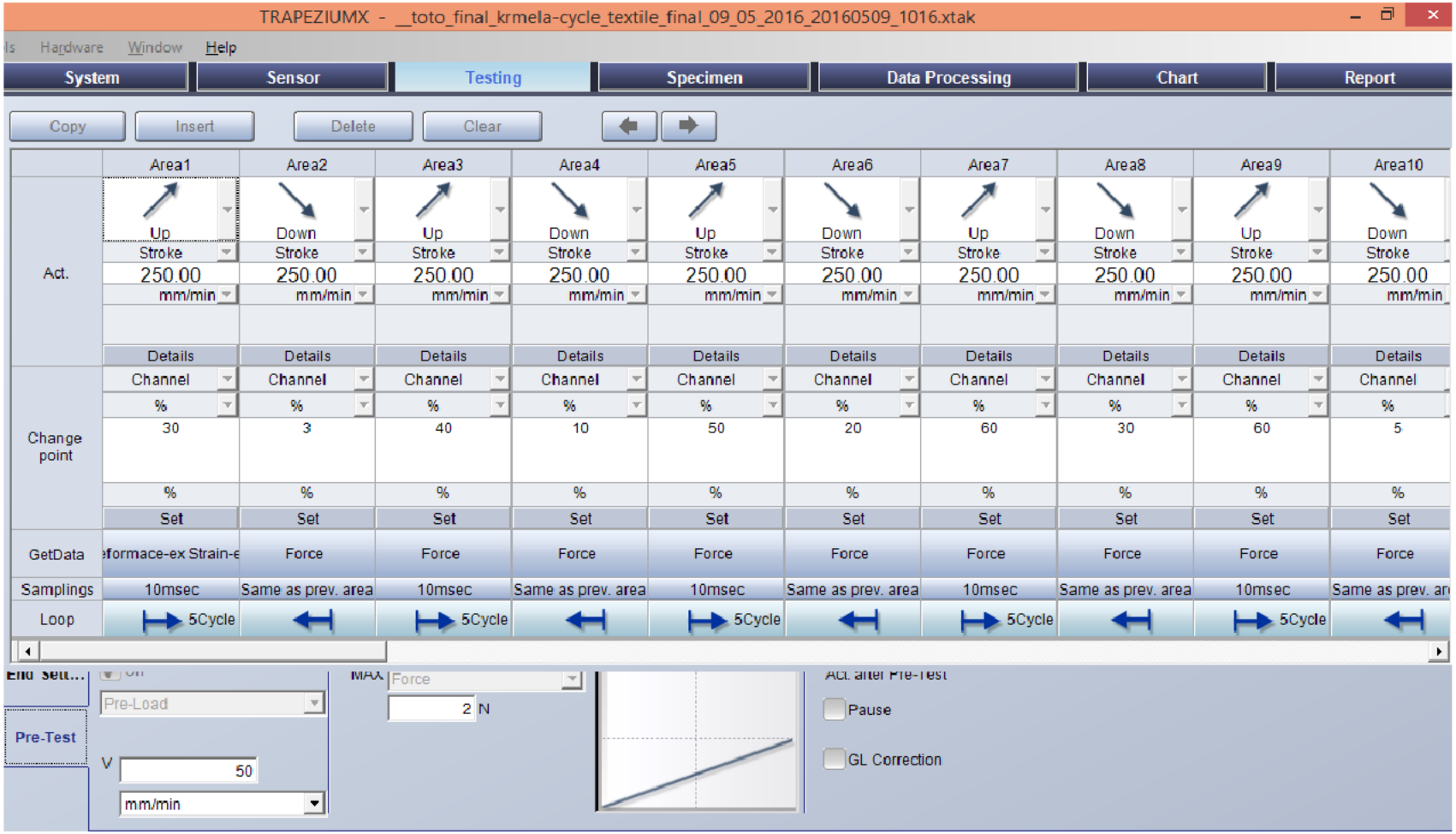

Method for cyclic tensile loading by Trapenzium X Control

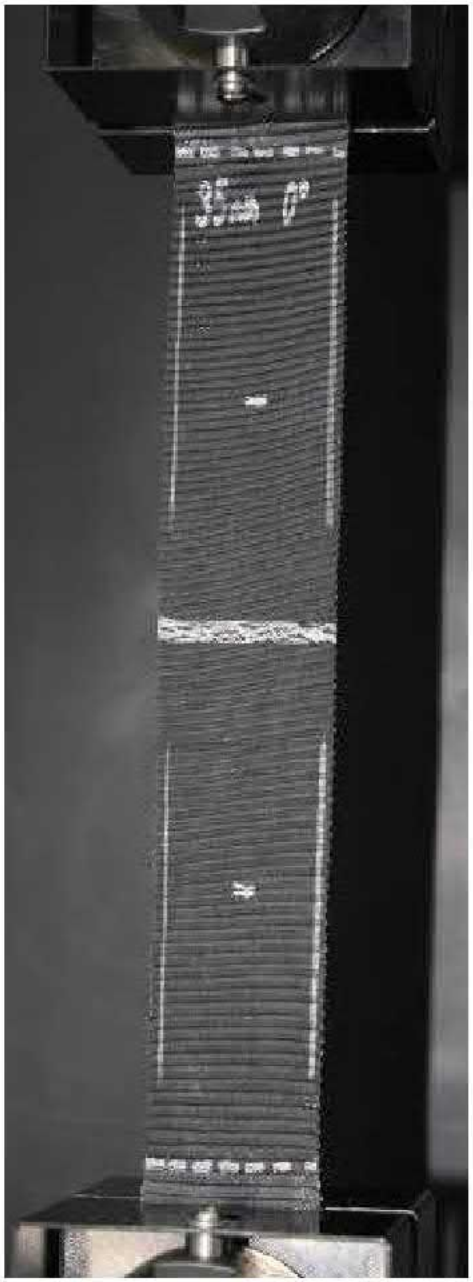

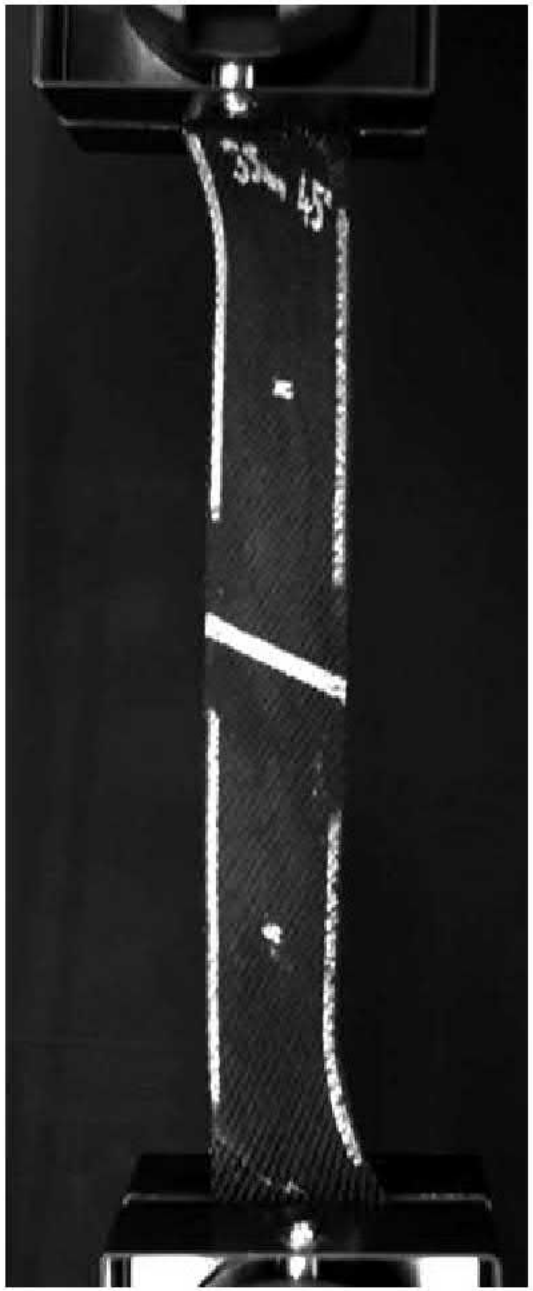

Photos of specimens for deformation 100 mm

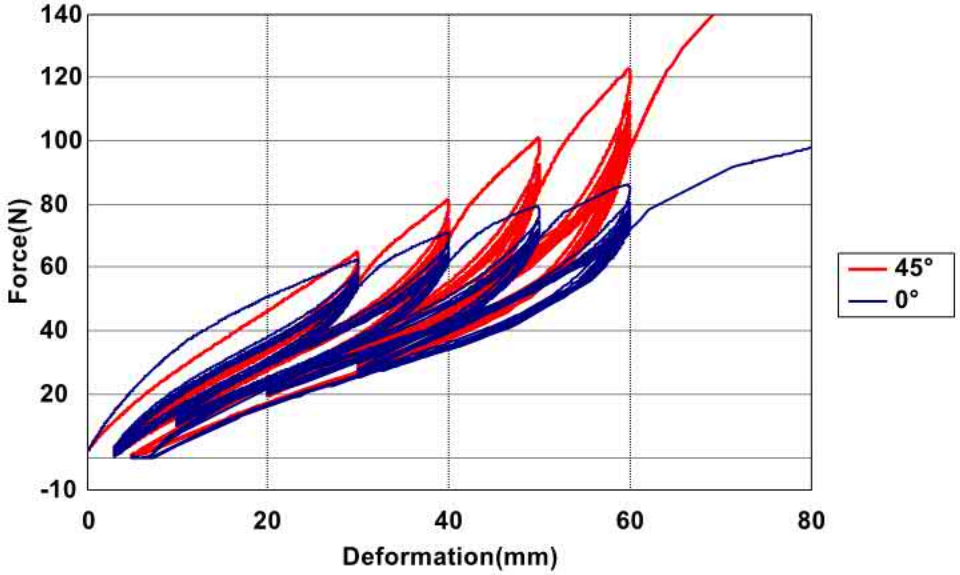

Dependence of force on deformation

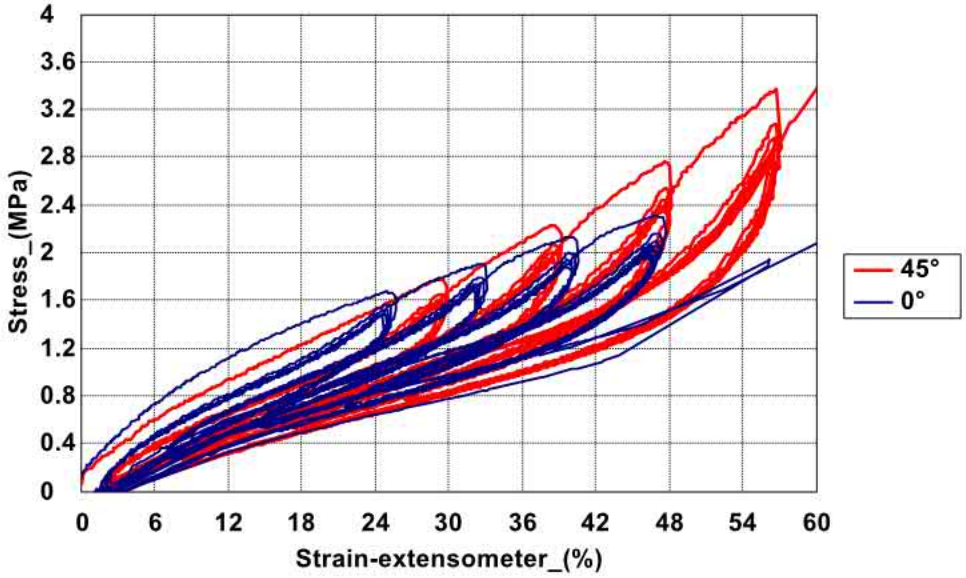

Dependence of stress on strain on extensometer

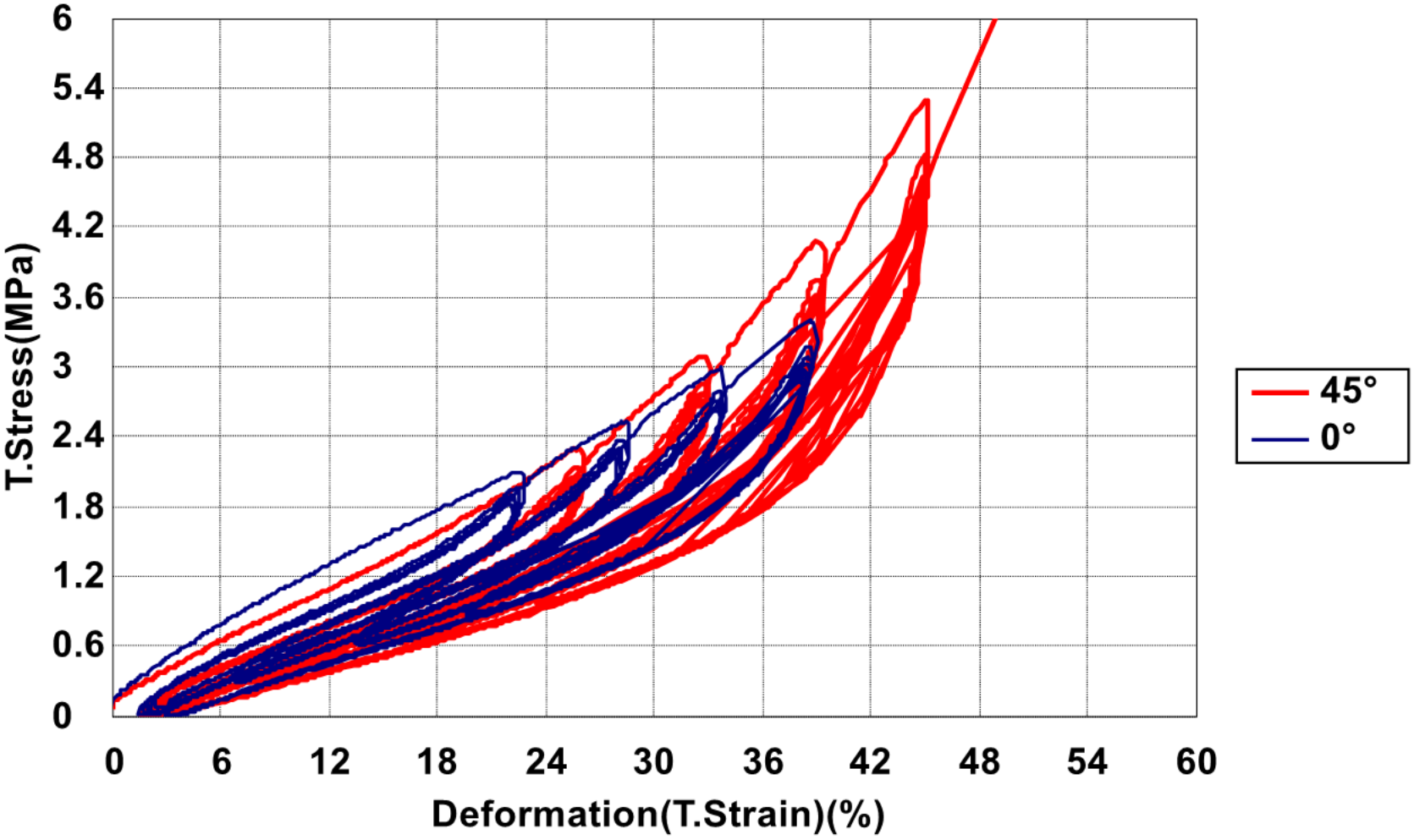

Dependence of true stress on true strain on extensometer

Composite after tests of cycle loading

Dependences of true stress on elongation between points for video-extensometer (marking as elongation ex.) are on:

for cord angle 45°;

for cord angle 0°;

and for cord angle 60° (different method).

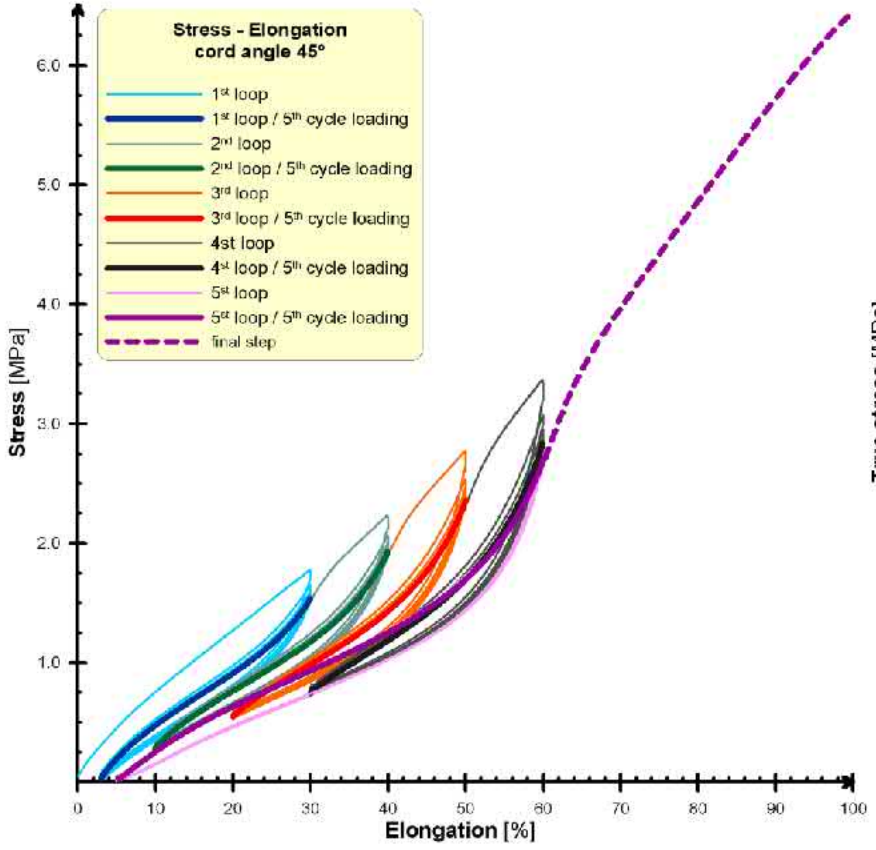

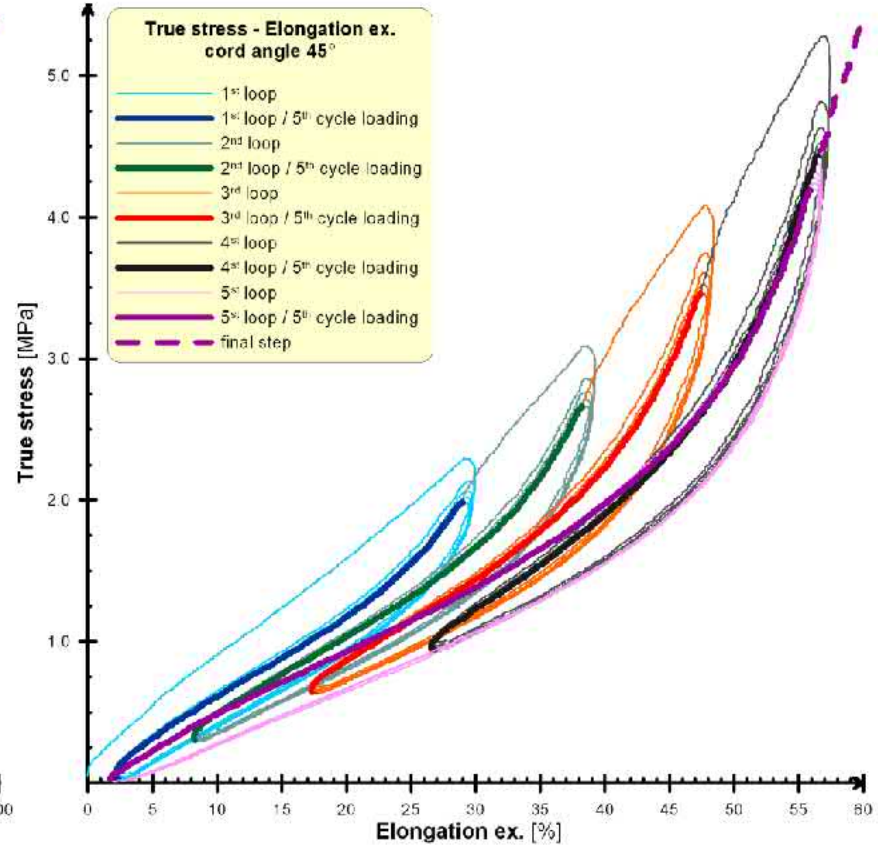

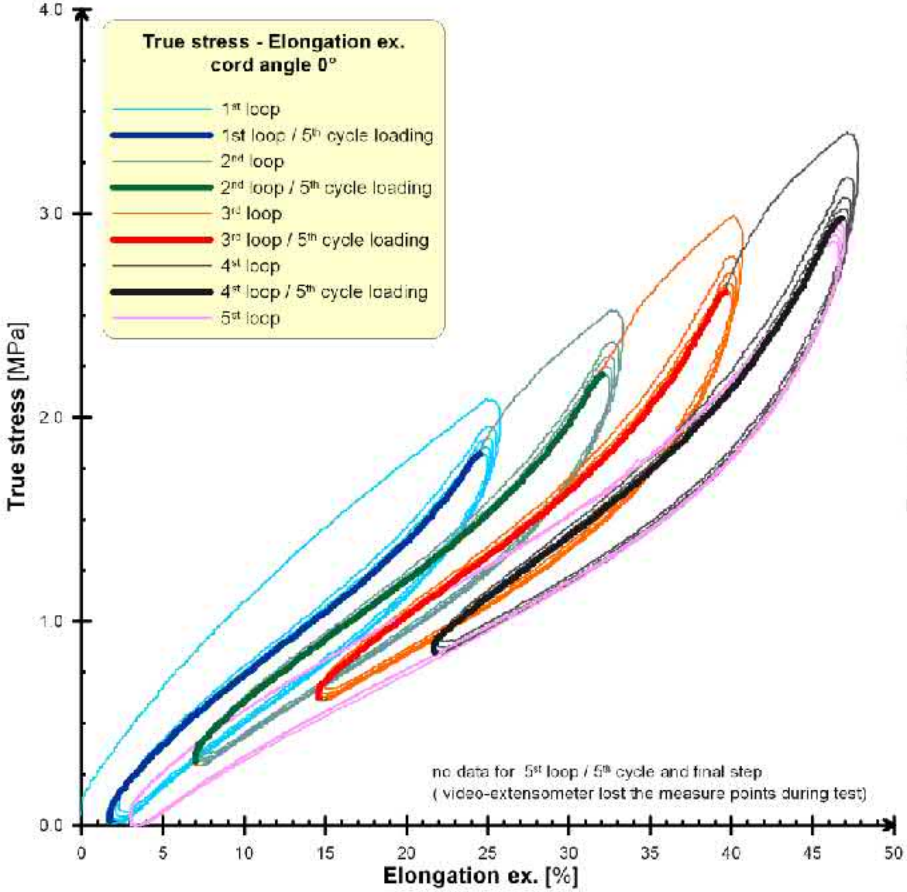
True stress - Elongation ex.
cord angle 0°
1st loop
1st loop / 5th cycle loading
2nd loop
2nd loop / 5th cycle loading
3rd loop
3rd loop / 5th cycle loading
4st loop
4st loop / 5th cycle loading
5st loop
no data for 5st loop / 5th cycle and final step
(video-extensometer lost the measure points during test)
True stress [MPa]
Elongation ex. [%]
0.0
1.0
2.0
3.0
4.0
0
5
10
15
20
25
30
35
40
45
50

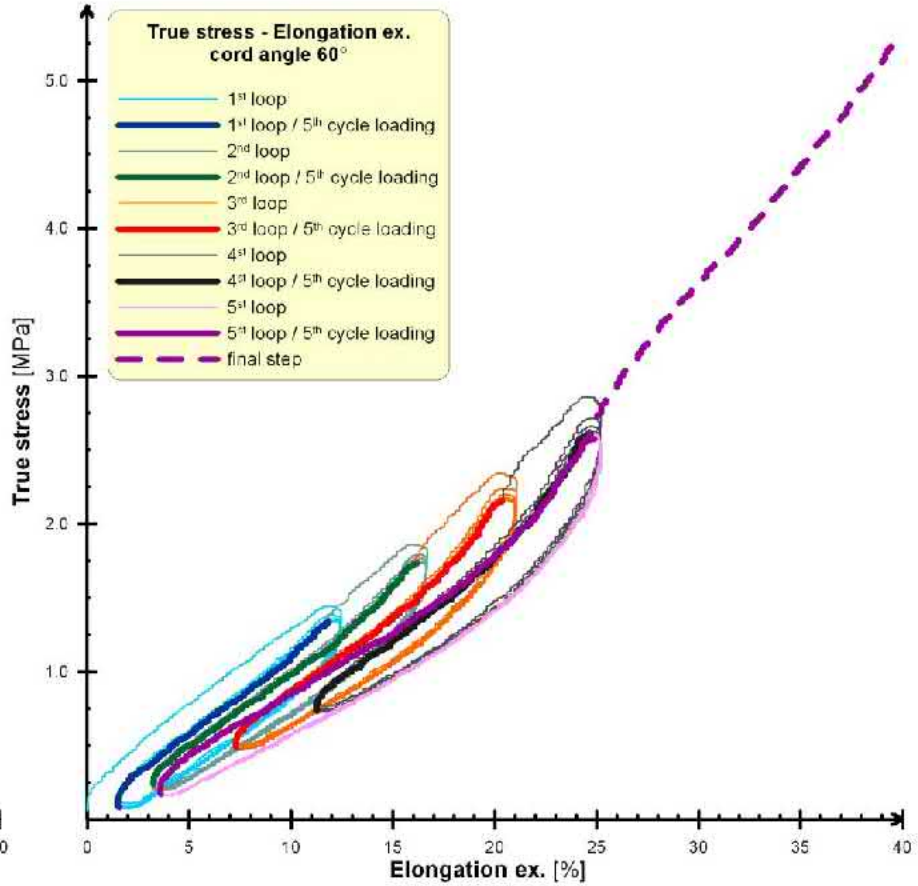
True stress - Elongation ex.
cord angle 60°
1st loop
1st loop / 5th cycle loading
2nd loop
2nd loop / 5th cycle loading
3rd loop
3rd loop / 5th cycle loading
4st loop
4st loop / 5th cycle loading
5st loop
5st loop / 5th cycle loading
final step
True stress [MPa]
Elongation ex. [%]
1.0
2.0
3.0
4.0
5.0
0
5
10
15
20
25
30
35
40

Comparison of the fifth cycles

The dependences of fifth cycle of every cycle loop are important for compare between cord angles.

For cord angles 0 and 45° the comparisons of the fifth cycles are given on the figure on the left as dependences of tensile force on displacement between clamps of test machine; on the right as dependences of true stress on elongation ex. The approximately the dependences for cord angle 0° can be used as input material parameters of elastomer matrix.

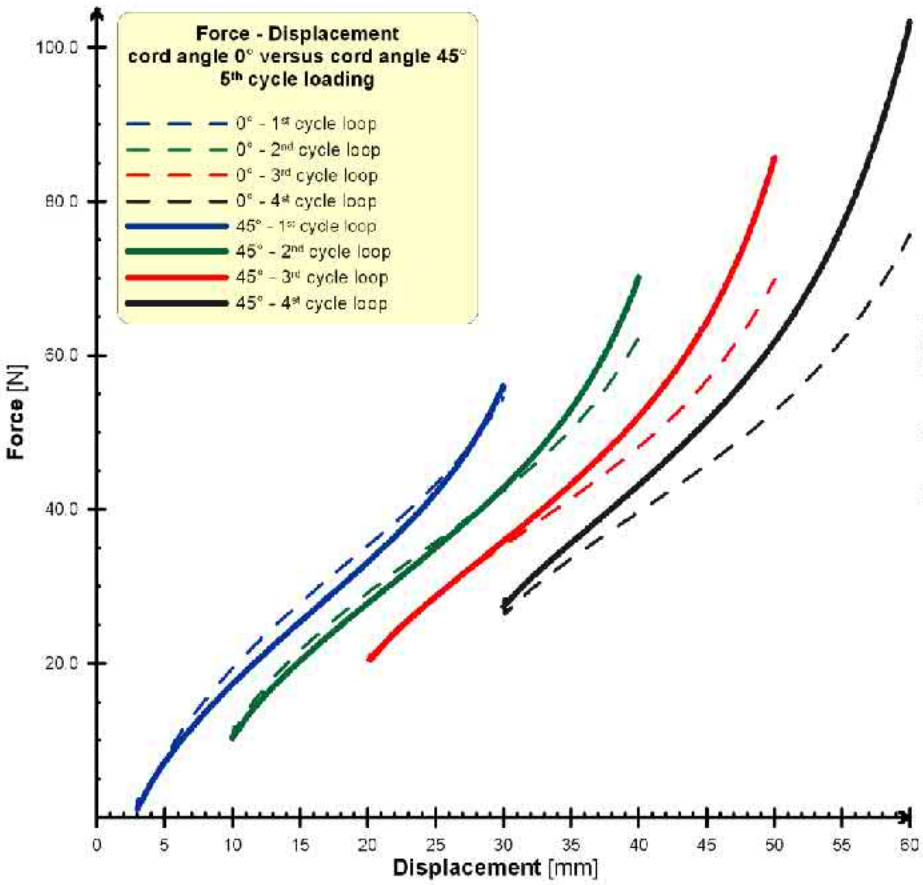

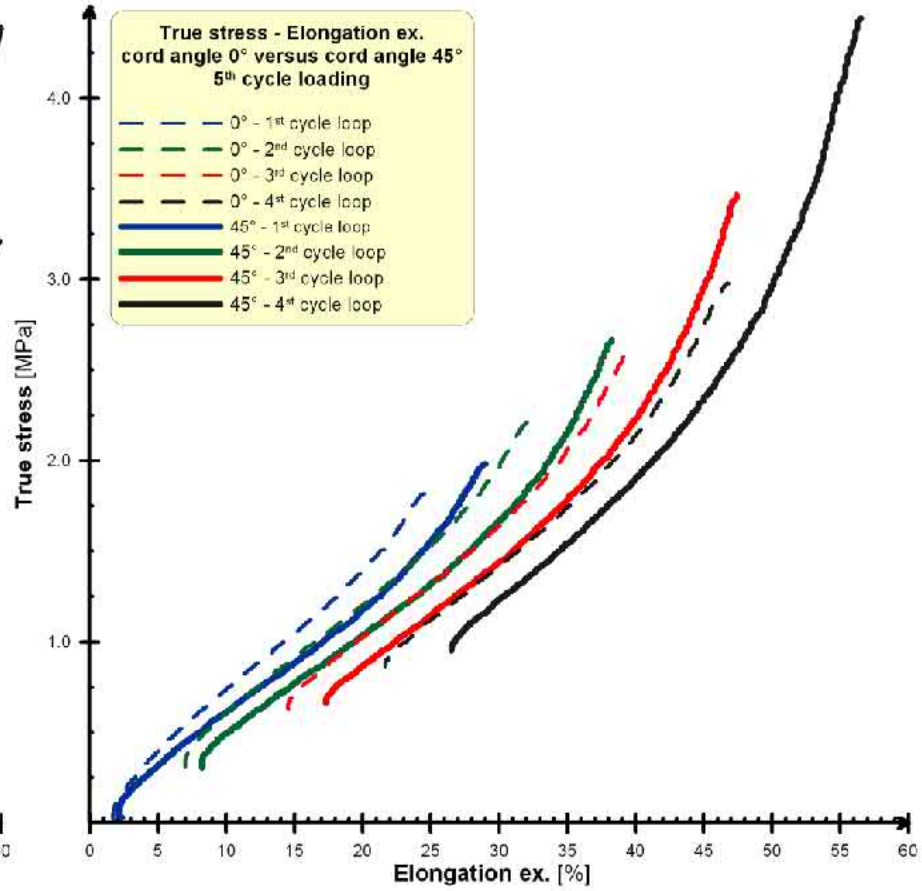

In this study, the methods with five cycle loops for different elongation with five cycles in every cycle loop have been designed with following finding:

- The fifth cycles in every cycle loops can be considered as stable cycle.
- The values of true stress for cord angle 45° are approximately 20÷25 % higher than values for cord angle 0°.
- Suggestion for second way of method: unloading for next cycle loop only to maximum elongation from previous cycle loop.

The part deals with design of methods for static experiment and dynamic experiment as low-cyclic tensile tests of polymer reinforcements for composites with using temperature chamber. For textile materials, DIN 53835-13* standard is defined and according to mentioned standard the conditions are takes into consideration during the first 5 cycles.

* DIN 53835-13, Testing of textiles; determination of the elastic behaviour of textile fabrics by a single application of tensile load between constant extension limits. 1983

.

The loading speeds are set to 250 mm/min for cycles and 50 mm/min for a pre-test (preload) by force value 2 N.
The test consisted of ten cycles; every cycle is defined as loading to certain percent of elongation with pause 5 sec (measurement with stress relaxation).
The loading speed of 150 mm/min (as the second method) was used to compare the results with loading speed of 250 mm/min.
Special jaws for textile materials were used. The initial length between the jaws was 250 mm.
The measured length (i.e. the distance between points for the video-extensometer) was approximately 150 mm.

The first tests for polyester were done upon selected positive temperatures (25 and 80 °C)

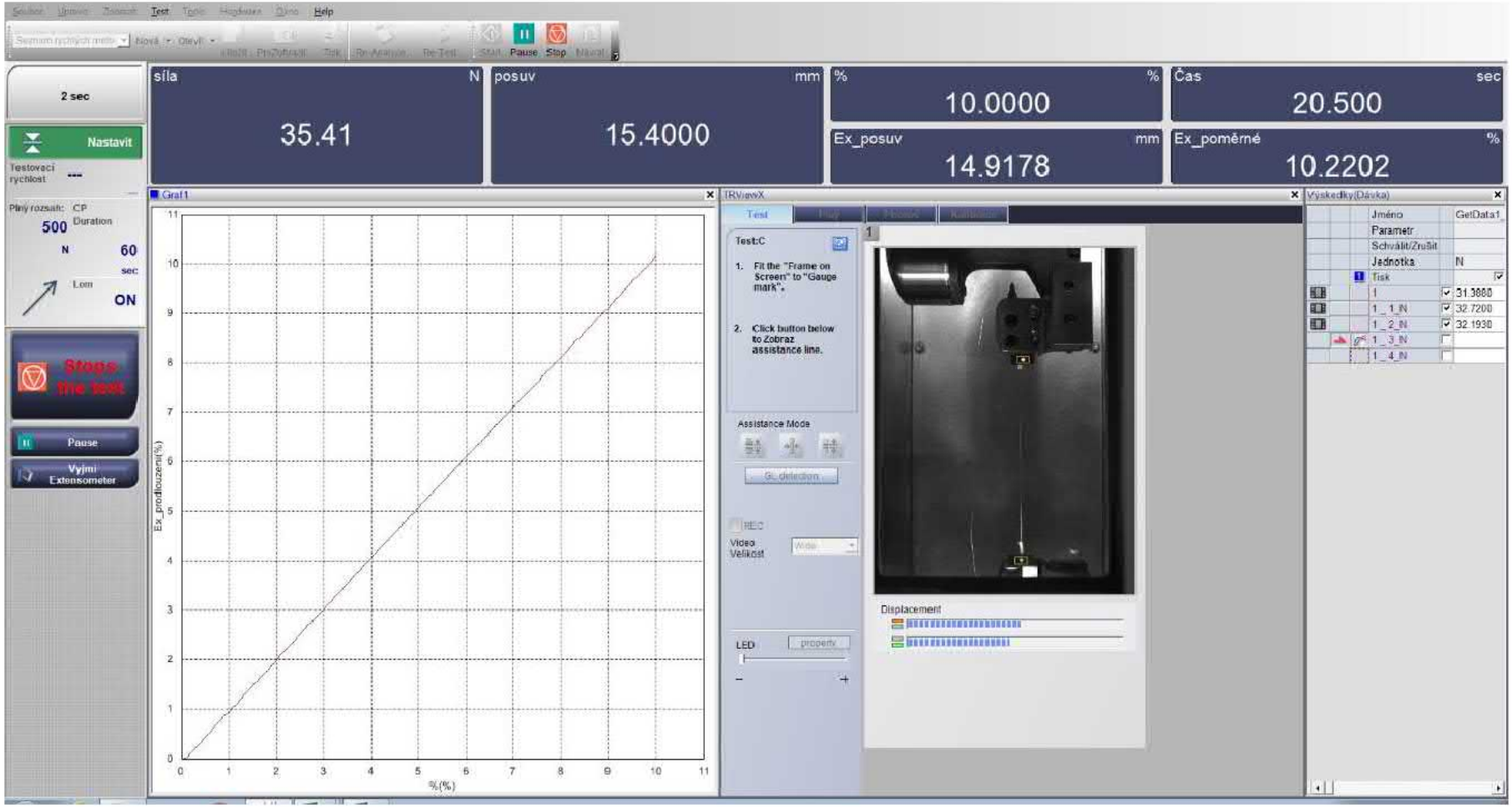

Testing with temperature chamber

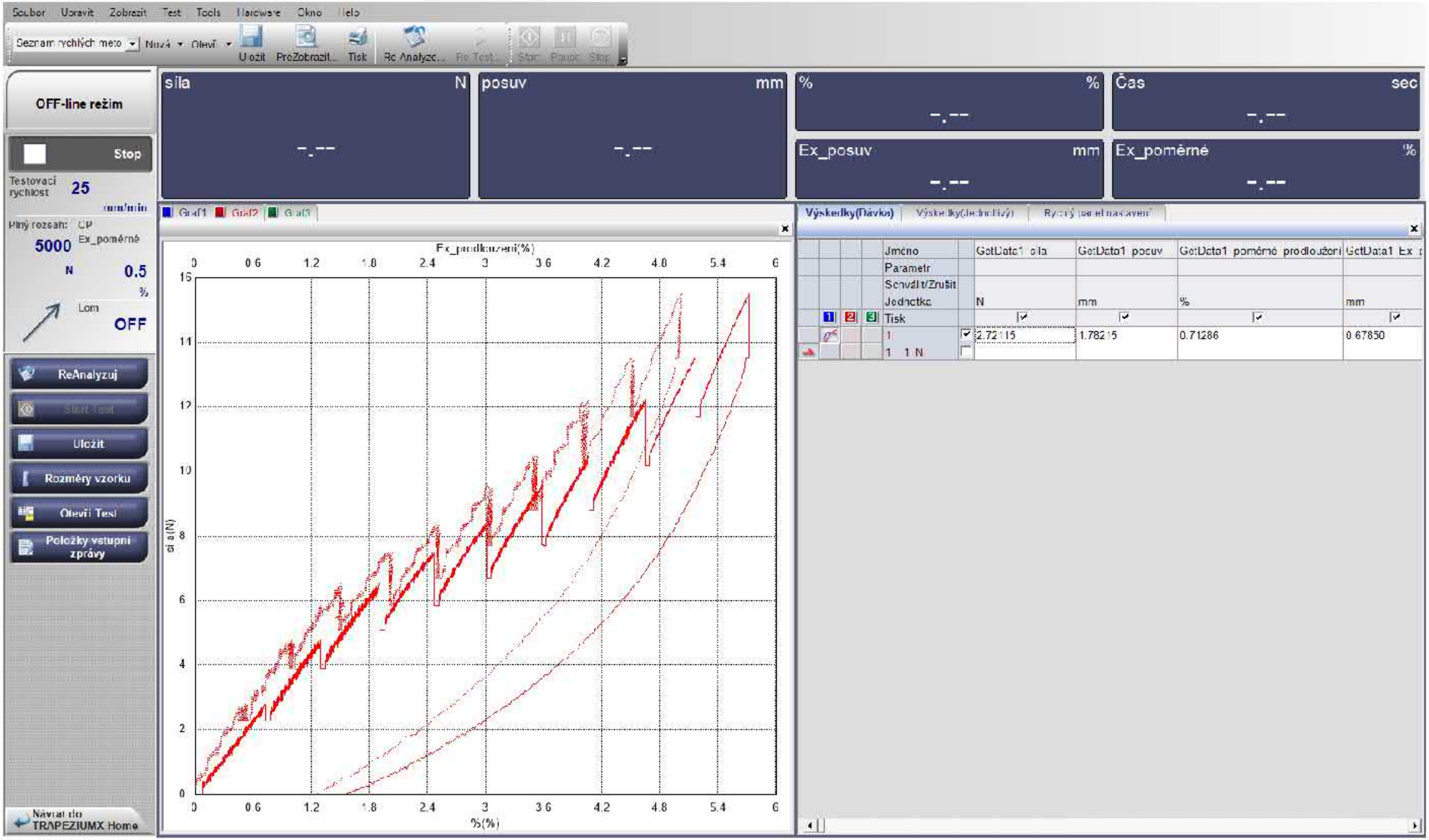

Dependences of force on deformation (elongation)

The results will be use in computational modeling as inputs for calculations in relation to the material characteristics and parameters.
The next research area of author will be focused on the specific testing of polymers upon cyclic multi-axis (biaxial) temperature loading with special testing equipment called Arcan test (see figure) with temperature chamber allows the tests from -70 to + 180 °C and from +20 to + 80 °C it is possible change humidity from 30 to 95 %.

Arcan test

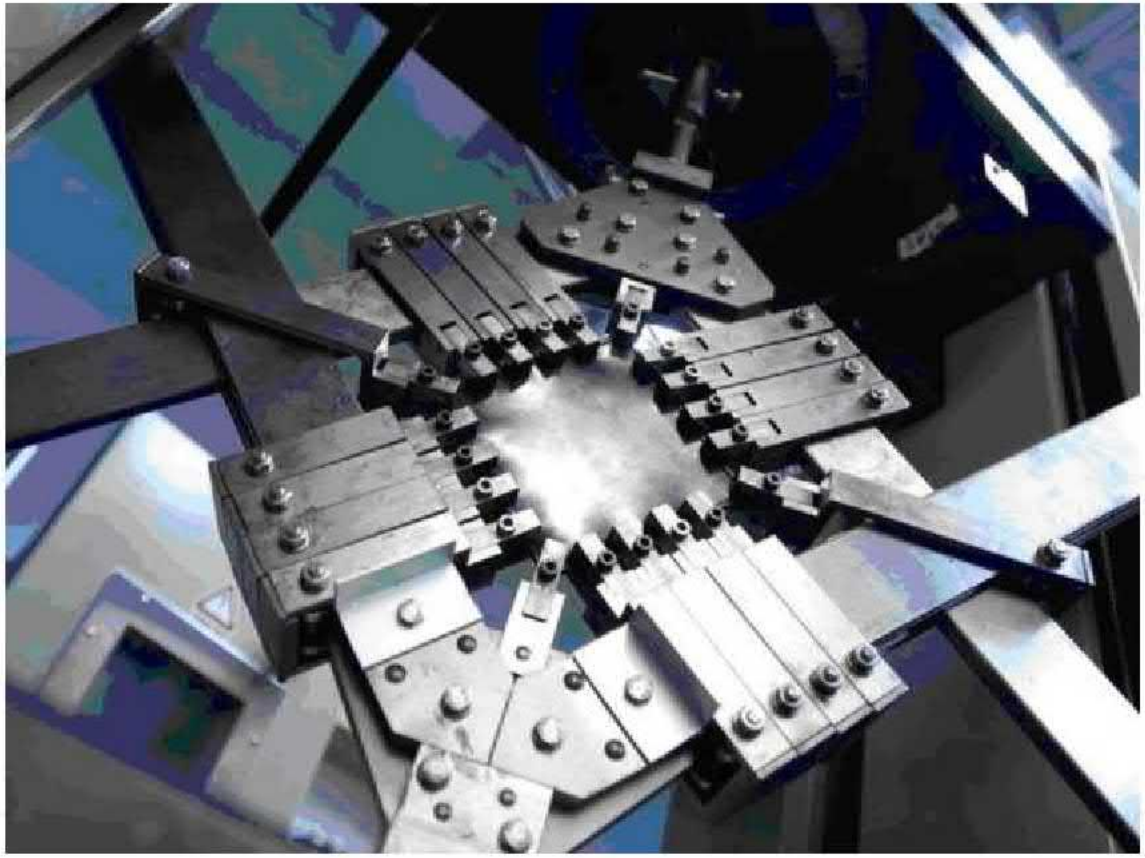

A stretch frame used for equi-biaxial loading of rubber specimens.

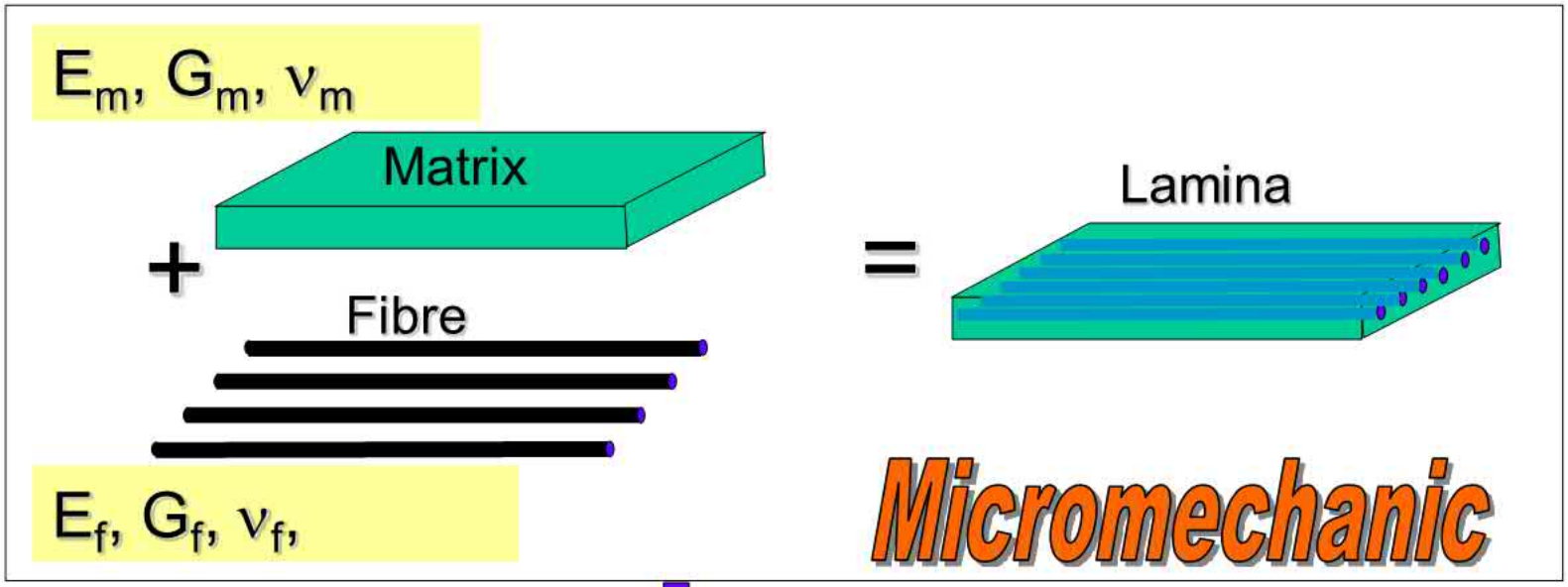

homogenization

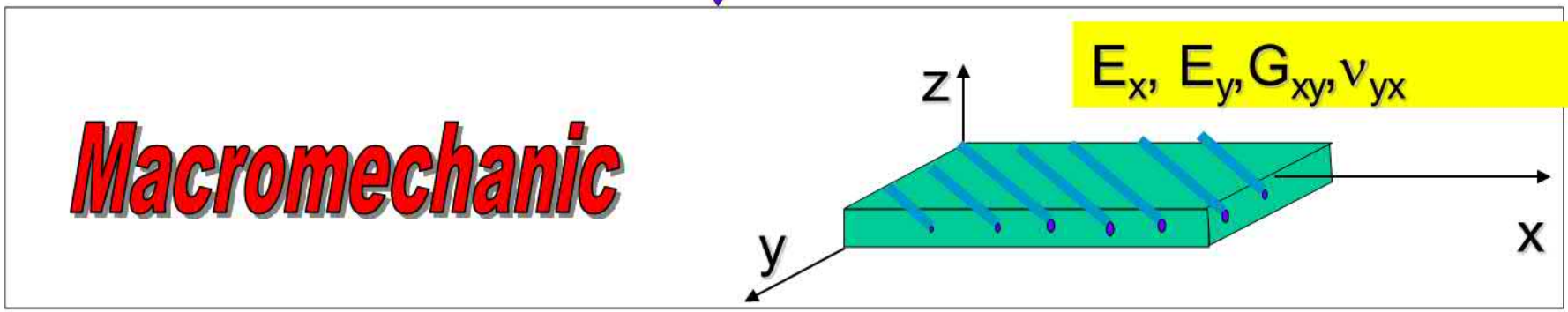

$$\varepsilon_{celk=compozite} = \varepsilon_{c=cord} = \varepsilon_{r=matrix}$$

$$\Downarrow$$

$$\sigma = f_c \cdot \sigma_c + (1 - f_r) \cdot \sigma_r = \varepsilon \cdot \left[f_c \cdot E_c + (1 - f_c) \cdot E_r \right]$$

$$\Downarrow$$

$$E_1 = E_c \cdot f_c + E_r \cdot (1 - f_c)$$

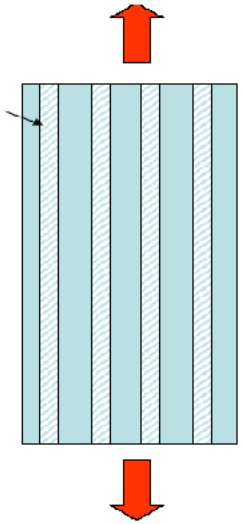

$$\delta_{celk=composite} = \delta_{c=cord} + \delta_{r=matrix}$$

$$\Downarrow$$

$$\varepsilon = f_c \cdot \varepsilon_c + (1 - f_c) \cdot \varepsilon_r = \sigma \cdot \left[f_c \cdot \frac{1}{E_c} + (1 - f_c) \cdot \frac{1}{E_r} \right]$$

$$\Downarrow$$

$$\frac{1}{E_2} = \frac{f_c}{E_c} + \frac{(1 - f_c)}{E_r} \Rightarrow E_2 = \frac{E_c E_r}{f_C E_r + (1 - f_C) \cdot E_c}$$

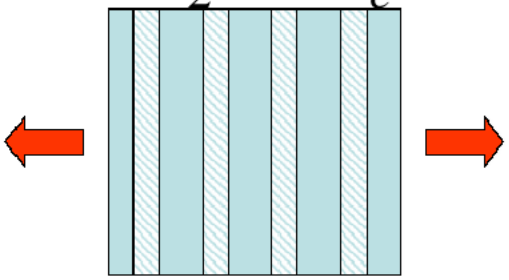

Jednosměrový kompozit (jednovložkový)

$$E_1 = E_c \cdot f_c + E_r \cdot (1 - f_c)$$

$$\nu_{12} = \nu_c \cdot f_c + \nu_r \cdot (1 - f_c)$$

$$E_2 = \frac{E_r \cdot \left[E_c \cdot (1+\zeta_1 \cdot f_c) + \zeta_1 \cdot E_r \cdot (1 - f_c) \right]}{E_c \cdot (1 - f_c) + \zeta_1 \cdot E_r \cdot (1 + f_c / \zeta_1)} \Rightarrow \text{pro Ec} \to \infty \quad \text{Er plyne:} \quad E_2 = \frac{E_r \cdot (1 + 2 \cdot f_c)}{(1 - f_c)}$$

$$G_{12} = \frac{G_r \cdot \left[G_c \cdot (1+\zeta_2 \cdot f_c) + \zeta_2 \cdot G_r \cdot (1 - f_c) \right]}{G_c \cdot (1 - f_c) + \zeta_2 \cdot G_r \cdot (1 + f_c / \zeta_2)} \Rightarrow \text{pro Ec} \to \infty \quad \text{Er plyne:} \quad G_{12} = \frac{G_r \cdot \left[G_c + G_r + f_c \cdot (G_c - G_r) \right]}{G_c + G_r - f_c \cdot (G_c - G_r)}$$

$$\nu_{21} = \nu_{12} \cdot \frac{E_2}{E_1}$$

$$f_c = \pi R^2 \cdot n / t$$

One-layer

$$\begin{pmatrix}\sigma_x\\ \sigma_y\\ \tau_{xy}\end{pmatrix}=\begin{pmatrix}Q_{11} & Q_{12} & 0\\ Q_{12} & Q_{22} & 0\\ 0 & 0 & S_{66}\end{pmatrix}\begin{pmatrix}\varepsilon_x\\ \varepsilon_y\\ \gamma_{xy}\end{pmatrix}$$

$$\begin{pmatrix}\varepsilon_x\\ \varepsilon_y\\ \gamma_{xy}\end{pmatrix}=\begin{pmatrix}S_{11} & S_{12} & 0\\ S_{12} & S_{22} & 0\\ 0 & 0 & S_{66}\end{pmatrix}\begin{pmatrix}\sigma_x\\ \sigma_y\\ \tau_{xy}\end{pmatrix}$$

$$Q_{11}=\frac{E_L}{1-\nu_{LT}\nu_{TL}} \qquad S_{11}=\frac{1}{E_L}$$

$$Q_{22}=\frac{E_T}{1-\nu_{LT}\nu_{TL}} \qquad S_{22}=\frac{1}{E_T}$$

$$Q_{12}=\frac{\nu_{TL}E_L}{1-\nu_{LT}\nu_{TL}}=\frac{\nu_{LT}E_T}{1-\nu_{LT}\nu_{TL}} \qquad S_{12}=\frac{-\nu_{LT}}{E_L}=\frac{-\nu_{TL}}{E_T}$$

$$Q_{66}=G_{LT} \qquad S_{66}=\frac{1}{G_{LT}}$$

$$E_L=\frac{Q_{11}Q_{22}-Q_{12}^{\ 2}}{Q_{22}}=E_1$$

$$E_T=\frac{Q_{11}Q_{22}-Q_{12}^{\ 2}}{Q_{11}}=E_2$$

$$\nu_{LT}=-\frac{Q_{12}}{Q_{11}}=\nu_{12}$$

$$G_{LT}=Q_{66}=G_{12}$$

Cord angle ≠ 0

One-layer

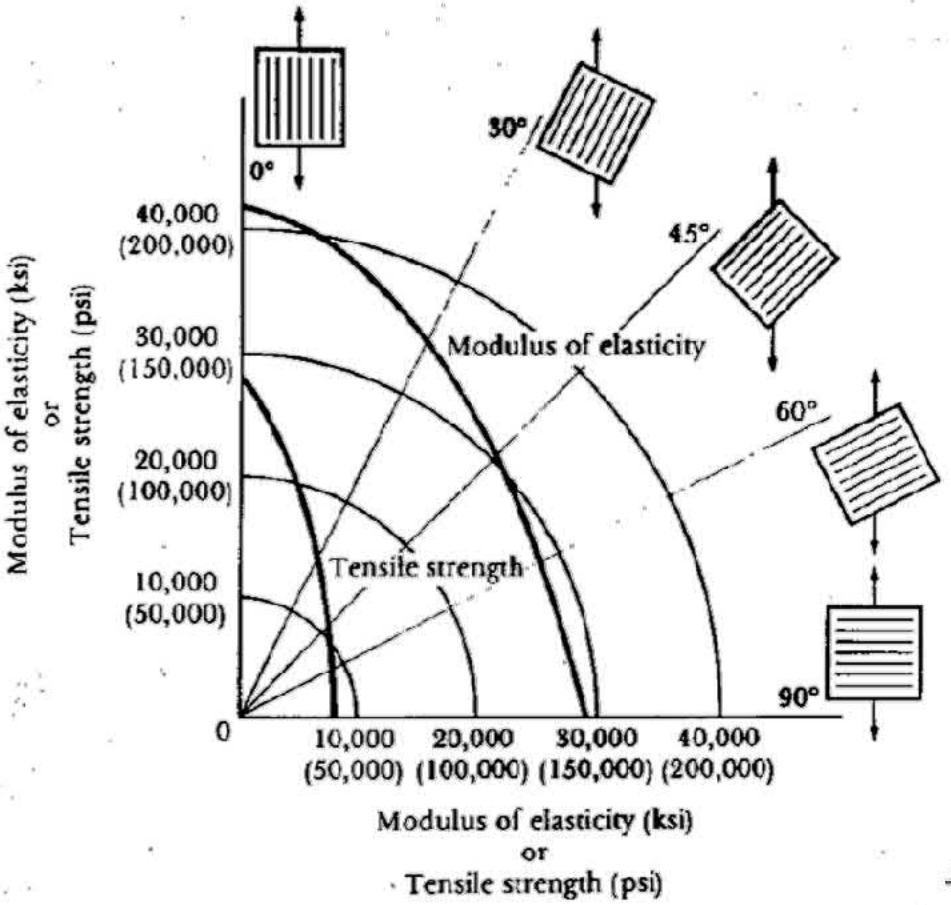

Two-layers

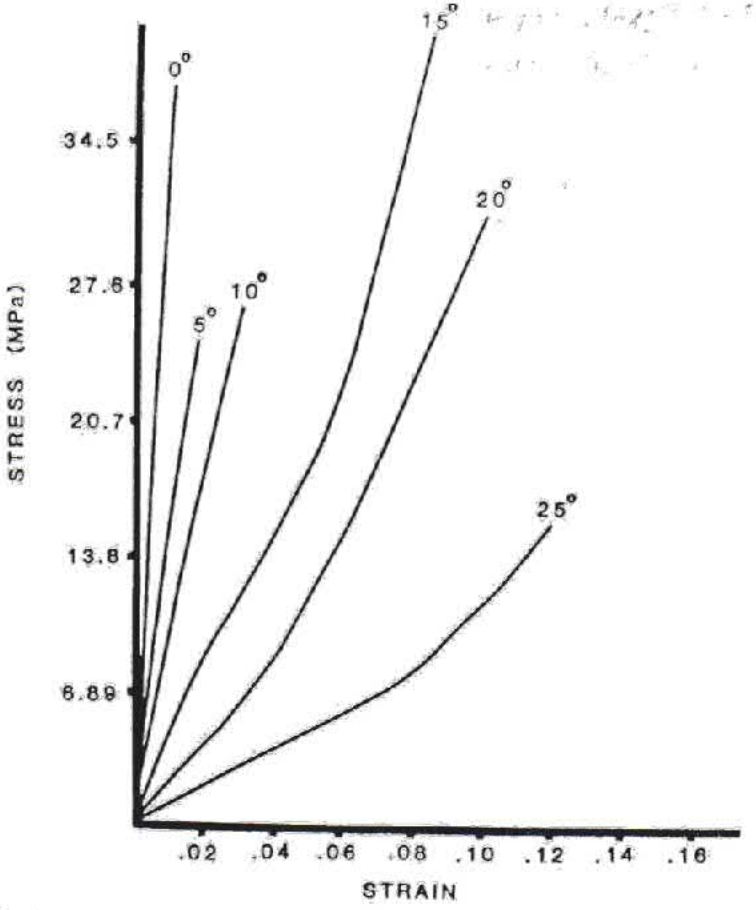

Tensile stress–strain curves for steel cord rubber 2-ply composites of varying ±θ cord angle

Cord anle ≠ 0

$$\frac{1}{E_X} = \frac{\cos^4\Theta}{E_L} + \frac{\sin^4\Theta}{E_T} + \frac{1}{4}\left(\frac{1}{G_{LT}} - \frac{2\nu_{LT}}{E_L}\right)\sin^2 2\Theta$$

$$\frac{1}{E_Y} = \frac{\sin^4\Theta}{E_L} + \frac{\cos^4\Theta}{E_T} + \frac{1}{4}\left(\frac{1}{G_{LT}} - \frac{2\nu_{LT}}{E_L}\right)\sin^2 2\Theta$$

$$\frac{\nu_{XY}}{E_X} = \frac{\nu_{LT}}{E_L} - \frac{1}{4}\left(\frac{1}{E_L} + \frac{2\nu_{LT}}{E_L} + \frac{1}{E_T} - \frac{1}{G_{LT}}\right)\sin^2 2\Theta$$

$$\frac{\nu_{YX}}{E_Y} = \frac{\nu_{TL}}{E_T} - \frac{1}{4}\left(\frac{1}{E_L} + \frac{2\nu_{LT}}{E_L} - \frac{1}{E_T} - \frac{1}{G_{LT}}\right)\sin^2 2\Theta$$

$$\frac{1}{G_{XY}} = \frac{1}{E_L} + \frac{2\nu_{LT}}{E_L} + \frac{1}{E_T} - \left(\frac{1}{E_L} + \frac{2\nu_{LT}}{E_L} + \frac{1}{E_T} - \frac{1}{G_{LT}}\right)\cos^2 2\Theta$$

Multi-layers

$$E_{\Phi(\Theta)} = E_c \cdot f_c \cdot \cos^4(\Theta) + 4 \cdot G_r \cdot (1 - f_c) - \frac{\left[E_c \cdot f_c \cdot \sin^2\Theta \cdot \cos^2\Theta + 2 \cdot G_r \cdot (1 - f_c)\right]^2}{E_c \cdot f_c \cdot \sin^4\Theta + 4 \cdot G_r \cdot (1 - f_c)}$$

$$E_{\xi(\Theta)} = E_{\Phi(\pi/2 - \Theta)}$$

$$\nu_{\Phi\xi} = \frac{E_c \cdot f_c \cdot \sin^2\Theta \cdot \cos^2\Theta + 2 \cdot G_r \cdot (1 - f_c)}{E_c \cdot f_c \cdot \sin^4\Theta + 4 \cdot G_r \cdot (1 - f_c)} \approx cotg^2(\Theta)$$

$$\nu_{\xi\Phi(\Theta)} = \nu_{\Phi\xi(\pi/2 - \Theta)} \approx tg^2(\Theta)$$

Mutti-layers versus one-layer

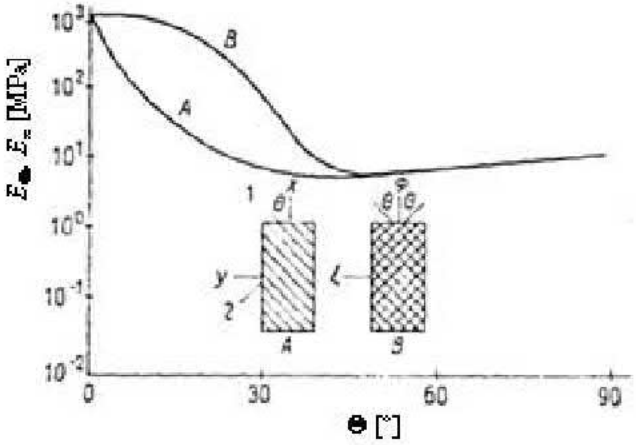

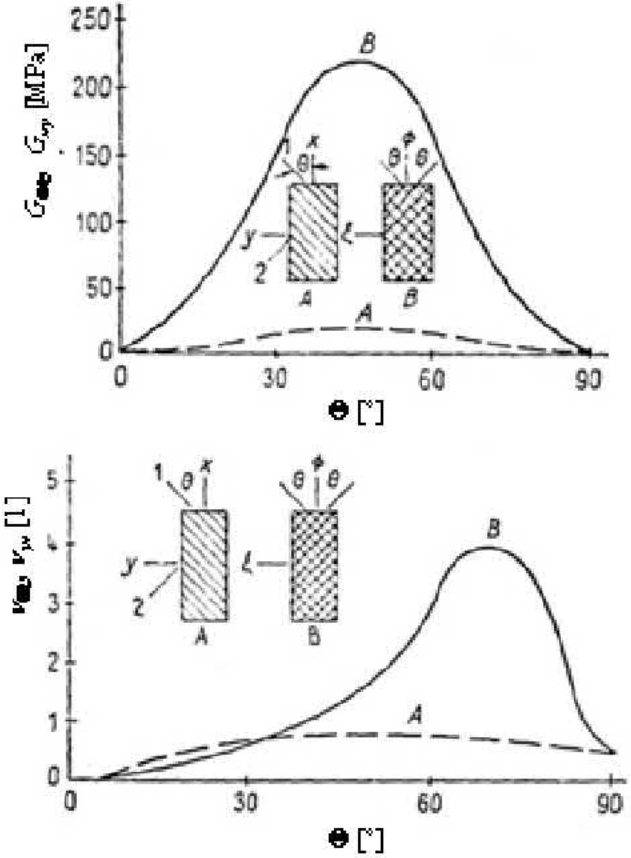

Závislosti Youngových modulů, střihových modulů a Poissonových poměrů na úhlu kordu (Nylon 94 tex/2) ⊛ pro jednovložkový (A) a čtyřvložkový (B) systém

Barbero Ever J.: Introduction to composite materials design. ISBN 978-1-4200-7915-9.

Barbero Ever J.: Finite element analysis of composite material. ISBN 978-1-4200-5433-0.

CADEC

Part 10 – CONCLUSION:

Recycling of tires, Future tire design – advantage and disadvantage

and

SEARCH STUDY ABOUT COMPUTATIONAL MODELING OF TIRE NOISE

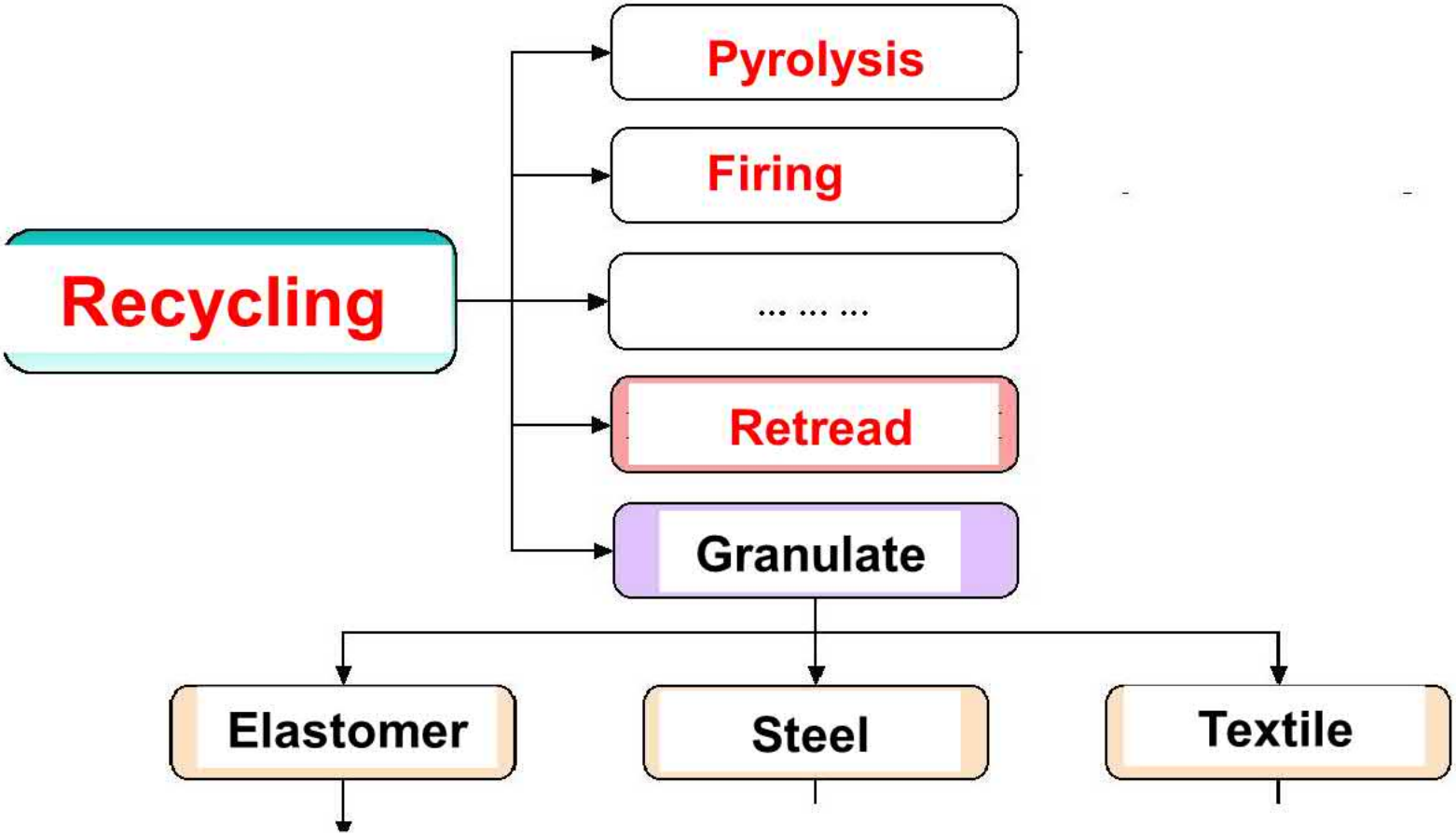

Shoe manufacturing industry
Floor material
Dampening bed
Antivibration systems
Child's playground
Roadways
Route for racehorse
PETRO-EX (liquidation oil accident - ultra-fine granulate)

advantage / disadvantage

No inflation pressure / no stability during cornering

Only for low speed

SEARCH STUDY ABOUT COMPUTATIONAL MODELING OF TIRE NOISE

1. Part – GENERAL STUDY

This search study deals with problem of tire-noise in term of computational modeling (different models, approach to models for tire-noise) and some articles deal with experiments for calculations.

The first part of search study includes list of companies concerned with tire noise, also list of books, journals, articles or presentations.

INSTITUTES, LABORATORIES concerned with study tire-noise (in term of computation or experiment with some download articles, research projects, presentations etc.):

- **Institute of Mechanics and Computational Mechanics, Leibniz University Hannover, Germany** web address http://www.ibnm.uni-hannover.de/en/institut
  contact: **M. Brinkmeier, U. Nackenhorst, J. Biermann – Institute of Modelling and Computation , Hamburg University of technology** biermann@tu-harburg.de ☺ GOOD WEBSITE
  download papers: e.g. poster Numerical simulation of tire rolling noise radiation: http://www.ibnm.uni-hannover.de/de/forschung/projekte/finite-element-algorithms/numerical-simulation-of-tire-rolling-noise-radiation
  http://www.fv-leiserverkehr.de/pdf-dokumenten/euronoise_2006/tuhh_uh_euronoise2006.pdf FEM/IFEM acoustic model

- **Transports and Environment Laboratory LTE, The French National Institute For Transport and Safety Research, INRETS, Bron, France** http://www.inrets.fr/ur/lte
  Bécot, Barreled, W. Kropp[1], **J.-F. Hamet, P. Klein, J. Périsse**
  download papers on field **Acoustique Physique**: e.g. poster On sound radiation from tyres: http://www.inrets.fr/ur/lte/publi-autresactions/lesposters/soundradiation.pdf
  http://www.inrets.fr/ur/lte/publications/publications-pdf/web-hamet/in00_674.pdf

- **Colorado Department of Transportation** http://www.dot.state.co.us
  Hanson, James (or National Center for Asphalt Technology, Auburn University, Alabama)
  download research reports: http://www.dot.state.co.us/publications/ResearchReports.htm#Noise
  http://www.pavetrack.com/documents/NCAT%20Reports/04-02%20Tire-Pavement%20Noise%20Study.pdf

- **ATS Consulting, Los Angeles, California** http://www.atsconsulting.com/profile.html
  H. Saurenman – solutions for noise and vibration
  download some articles: http://www.atsconsulting.com/hughpdfs.html http://www.atsconsulting.com/projects.html

- **List of organizations in field of tire-pavement noise – website link**
  http://www.fhwa.dot.gov/environment/noise/tp_noise.htm
  ☺ GOOD WEBSITE

- **SILENT ROADS (and IPG)** Wokshop and symposium http://www.silentroads.nl/
  M+P consulting engineers, Müller-BBM group http://mp.nl ☺ GOOD WEBSITES
  http://www.silentroads.nl/index.php?section=research&subject=**workshop2006**
  http://www.silentroads.nl/index.php?section=research&subject=**workshop2004**
  http://www.silentroads.nl/research/workshop2006/SR2006-workshop-summary.pdf **interesting**
  download presentations from SilentRoads symposium 2004
  http://www.silentroads.nl/index.php?section=general&subject=**symposium** ..... sample presentations below by Continental and Goodyear
  and very interesting presentation by
  Kuijpers – M+P noise & vibration consultants, Netherlands – Tire/road noise modelling
  (http://www.mp.nl/people/people.php?langID=1&peopleID=13, ArdKuijpers@mp.nl)
  http://www.silentroads.nl/downloads/files/Presentation_Internoise2001_Kuijpers_2000829.pdf
  presentation slides which includes list of specialists and severally models in detailed ☺ GOOD
  and http://www.silentroads.nl/downloads/files/M+P.MVW.01.8.1rev2.pdf SPERoN model ☺ GOOD
  T. Beckenbauer[2] – computational
  http://www.lfu.bayern.de/laerm/forschung_und_projekte/opa/projektbeschreibung/doc/physik_der_reifen_fahrbahn_geraeusche.pdf
  http://www.fv-leiserverkehr.de/pdf-dokumenten/euronoise_2006/Beckenbauer.pdf
  IPG Truck tires noise http://www.innovatieprogrammageluid.nl/ ☺ GOOD WEBSITE
  http://www.innovatieprogrammageluid.nl/GBpage.asp?id=927
  Graaff – tyre/road noise measurements of truck tyres
  http://www.innovatieprogrammageluid.nl/data/files/algemeen/M+P.DWW.03.7.1%20-%20Tyre%20road%20noise%20measurements%20of%20truck%20tyres.pdf
  Rooveers – literature study on the Rolling noise of truck tyres
  http://www.innovatieprogrammageluid.nl/data/files/algemeen/Literature%20study%20on%20the%20rolling%20noise.pdf
  Reeters – measurements
  http://www.innovatieprogrammageluid.nl/data/files/algemeen/M+P.DWW.03.7.2%20-%20Supplemental%20report%20I.pdf
- **CONTINENTAL AG Hannover, Germany**
  e.g. E.-U. Saemann[3] (ernst-ulrich.saemann@conti.de), **D. Zheng** (dong.zheng@conti.de), **F. Gauterin**
  Vehicle – tire – road interaction
  sample presentations:
  http://www.**silentroads**.nl/research/workshop2006/**Saemann**%20@%20WS2006.pdf h
  ttp://www.wias-berlin.de/main/events/events/herbst05/**zheng**.pdf
- **GOODYEAR Technical Center, Luxembourg**
  J. Leyssens – experiment, compute, verification FEM model **A. Pietrzyk**
  presentation: http://www.**silentroads**.nl/general/symposium/impressie/presentatieJan**Leyssens**.pdf
  project: http://www.calm-network.com/db/view.php?id=696
- **Müller-BBM group, Germany, Netherland**
  T. Beckenbauer[2]
  sample article:
  http://www.lfu.bayern.de/laerm/forschung_und_projekte/opa/projektbeschreibung/doc/physik_der_reifen_fahrbahn_geraeusche.pdf
- **Chalmers University of Technology, Department of Applied Acoustics, Sweden**
  W. Kropp[1] (wolfgang.kropp@chalmers.se) PLATE model Kropp, **K. Larsson**
  sample article: http://www.iva.se/upload/seminarier/Bullerrapport.pdf
  http://www.silentroads.nl/research/**workshop2004**/presentation%20WK%20@%20WS%20Truck%20Tyres.pdf
- **SILENCE project, AVL, Graz, Austria** "SILENCE" model http://www.avl.com

- **European LS-DYNA Conference** http://www.dynamore.de/

  Fukushima, Shimonishi – Nissan Motor Co., Japan – Tire model for dynamics
  sample articles: http://www.dynamore.de/download/af04/papers/B-I-4.pdf
  http://www.dynamore.de/download/eu03/papers/B-III/LS-DYNA_ULM_B-III-01.pdf

  Shiraishi – Sumitomo Rubber Industries, LTD., Japan – Tire model for crash simulations

- **Enterprise and Industry** http://ec.europa.eu/enterprise/automotive/projects/
  http://ec.europa.eu/enterprise/automotive/projects/report_tyre_road_noise1.pdf

- **Geschäftsstelle Leiser Verkehr, Köln** http://www.fv-leiserverkehr.de/
  http://www.fv-leiserverkehr.de/pdf-dokumenten/

BOOKS about tire-noise – e.g.:

- **Ulf Sandberg, Jerzy A.Ejsmont: Tyre/Road Noise Reference Book**: INFORMEX Sweden, ISBN Number: 91-631-2610-9, 640 page; **Tire Noise Mechanisms** ☺ **GOOD BOOK**
  http://www.informex.info/html/brochure_-_p2_semifinal_v_2002.HTM
  list of contents: http://www.road.pl/tyre-road-noise.htm

- **Tire/road contact modelling for a rolling tire**: Eindhoven University of Technology, 2006, DCT 2006.66, 55 pages, keyword: tire-road mode, contact, Abaqus
  http://alexandria.tue.nl/repository/books/626574.pdf

JOURNALS with full-text articles free download at Technische Universitat Graz – e.g.:

- **JSME** International Journal Series C Mechanical Systems, Machine Elements and Manufacturing – Publisher The Japan Society of Mechanical Engineers
  http://www.jstage.jst.go.jp http://www.jstage.jst.go.jp/browse/jsmec
  http://www.jstage.jst.go.jp/search/jsmec?dif2=and&d2=au&dp2=&dif5=and&d5=te&dp5=tire+noise&pl=20&search=Search

- **Vehicle System Dynamics** International Journal of Vehicle Mechanics and Mobility – Publisher Taylor & Francis
  http://www.informaworld.com/smpp/title~content=t713659010~db=all

- **Journal of Sound and Vibration** – website data source ScienceDirect

ALSO INFORMATION – SEARCH ENGINES – e.g.: for full-text PDF articles
http://www.pdf-search-engine.com/

also full-text articles from:
LUND University http://www.control.lth.se/publications
E.g. articles by **Svendenius**

Quartus Engineering http://www.quartus.com/resources/
by **Reid** http://www.quartus.com/resources/papers/downloads/2006-13--paper-from-conference-proceedings.pdf

IngentaConnect http://www.ingentaconnect.com/

ScienceDirect http://www.sciencedirect.com/

Keywords for searching: tire noise; fem tire; Fiala handling force model; PAC2002 Magic-formula; tire model Pacejka; Adams-tire; etc.

2. Part – COMPUTATIONAL MODELS STUDY

This part of search study describes some interesting computational models for tire-noise analyses.

LIST OF MODELS:

- **FEM/IFEM acoustic model – Hamburg University of technology + University Hannover, Germany**
  Description: Finite Element approach with Special Finite Element, stationary rolling contact by Arbitrary Lagrangian Eulerian formulation, for sound radiation analysis
  good FEM physical model ☺☺☺

- **PLATE model Kropp – Chalmers University of Technology , Sweden**
  Description: High-frequency ☺, elastic layer, orthotropic plate model, simplicity

- **SPERoN model – M+P**
  Description: hybrid model

  By Kuijpers:

  > The modelling approach used in various projects can be classified in three categories: purely statistical models, purely deterministic models and hybrid models. The purely statistical models try to relate measurement data to measured sound production. A well-known example of this approach is the work of Sandberg and Descornet [2]. Purely deterministic models try to model the physical processes involved in tyre vibration and sound radiation from the tyre. Measurement data is only used for the validation of the model. The tyre model of Kropp [3,4,5] is an influential example of this modelling approach. Lately, a combination of statistical and physical modelling is increasingly used: the hybrid modeling approach which was used by Fong [6], Hamet et al. [7], and Beckenbauer and Kuijpers [8] all these models are based on the contact force calculation method introduced by Clapp [9].

- **"SILENCE" model – SILENCE**
  Description: Inverse Boundary Element Method ☺

- **BEMSYS model – Y.H.Wijnant, University of Twente, Faculty of Engineering Technology, Department of Applied Mechanics, the Netherlands**
  Description: Boundary Element Method by program BEMSYS, for radiated sound

- **Green's Function for the Orthotropic Plate Model – INRETS-LTE**
  Description: analytical model for texture spectra

- also seaman hybrid model, analytical Kim, program MD Adams/Tire FTire, ...

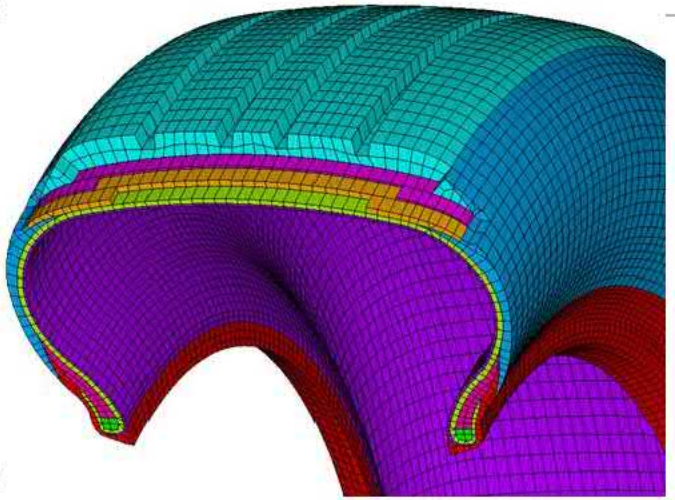

MATERIAL INPUT FOR TIRE SIMULATION

Fig. 1. Computational model of the tire casing

⇒ Introduction

Computational modeling of tires by Finite Element Method allows solving of various ways of loading. It is possible deal with static tire models if only static load should be applied (a car stands, the target is to determine deformation conditions of inflated tires loaded by the vertical force) or dynamic tire models, which will represent real states of tires during car such as tire impact on the specific barrier at a certain car speed. It is important to experimentally determine material parameters used for the description of each individual part of tire-casings [1] for computational modeling of tires, Fig. 1.

E.g. material parameters as the modulus of elasticity and Poisson ratio describe the textile fiber [2]. For the description of elastomer parts of tire-casings there are used several material models of the viscoelastic behavior of the material – constitutive models, the Mooney-Rivlin (MR) model is the most commonly used. To determine of MR material parameters, it is necessary to carry out the tensile test for elastomer samples by standard ISO 37 [3]. Next way, MR parameters can be determined on the basis of the Shore A hardness.

⇒ Determination of Mooney-Rivlin material parameters from Shore A hardness

The procedure is such that the Shore A hardness (it is expressed as A in equations) is converted to the elastic modulus E [MPa] or shear modulus G [MPa] and then MR parameters are determined from the modulus. These equations can be used conversion of the mentioned hardness. In equation (2), the elastic modulus is expressed in psi. Batterman/Köhler equation (4) is based on expression dependence between shear modulus and Shore A hardness. These equations can lead to different results of moduli for the same Shore A hardness. Mooney-Rivlin parameters are standard calculated [1].

1) Gent equation [4]

$$E = \frac{0.0981 \cdot \left(56 + 7.62336 \cdot A\right)}{0.137505 \cdot \left(254 - 2.54 \cdot A\right)}$$

2) equation [5]

$$E = \exp\left(0.0235 \cdot A - 0.6403\right)$$

3) equation [6]

$$E = 11.427 \cdot A - 0.4445 \cdot A^2 + 0.0071 \cdot A^3$$

4) Batterman/Köhler equation [7]

$$G = 0.086 \cdot 1.045^A$$

⇒ Moduli of elasticity of composite structures of tire-casings such as steel-cord belt

The moduli are determined on the basis of the statical tensile and bend tests [1] and they can be used for verification analyses between tests and computational modeling of structure parts of tire-casings. As the first method, there is used a method based on 0–8 % strain. The principle of the method lies in calculating the value of 8 % strain of the specimens. From the intersection of the dependencies of force-deformation and stress-strain from the uniaxial static tensile test, the values for applied force for given deformation and given specific strain are read and these values are inserted into Equation (5) for calculating modulus of elasticity.

$$E = \frac{\sigma}{\varepsilon} = \frac{F \cdot l}{\Delta l \cdot S} = \frac{(F_n - F_0) \cdot l}{(l_n - l_0) \cdot S}$$

where E [MPa] is the modulus of elasticity, σ [MPa] = tensile stress, ε [%] = strain, F [N] = tensile force, l [mm] = initial length of the specimen between clamps of test machine, S [mm^2] = initial cross-section area of specimen, Δl [mm] = length through which the specimen is elongated amount, Fn [N] = ending tensile force for concrete method, F_o [N] = starting tensile force for concrete method, ln [mm] = ending elongation for concrete method, l_o [mm] = starting elongation for concrete method.

Other methods are similar, but the range of values of the strain is changed for the calculation: 4–8 %, 0–10 % and 4–10 %. The last method is based on reading values of the linear part of dependence. As a sample, the calculations of moduli of elasticity are made on five specimens with a different two-layer steel-cord belt of a radial tire casing, the stress-strain dependences are in Fig. 2. The obtained values from the dependence for each method are substituted into the Equation (5) and there is calculated the modulus of elasticity – see Tab. 1.

There are differences in the methods for determination of the modulus of elasticity for each specimen. The moduli of elasticity are in the longitudinal direction of tires.

From the results, there was selected the most precise method for the determination of the modulus of elasticity, which is suitable for other specimens of steel-cord belt configurations.

Through the comparison of results of moduli of elasticity obtained by individual methods, it can be stated that the most appropriate method to calculate the modulus of elasticity of steel-cord belts is the method based on 4–8 % elongation.

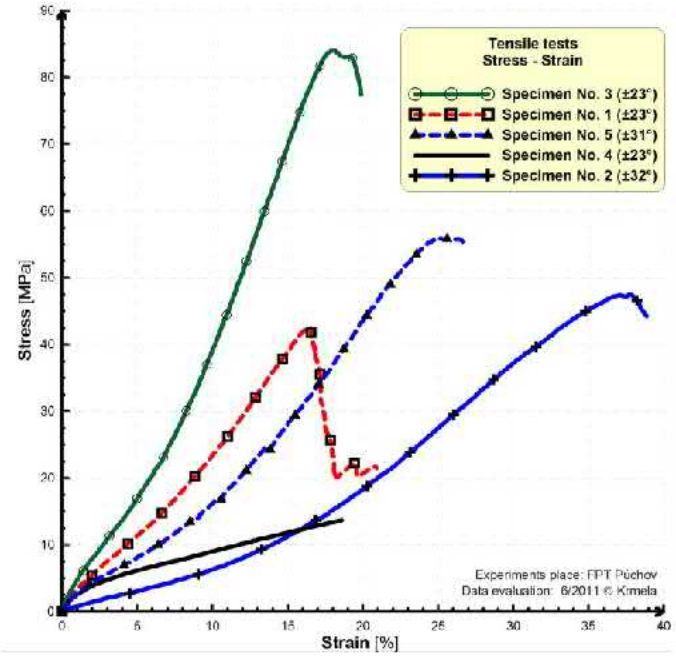

Fig. 2. Stress-strain dependences from tensile tests of specimens

Tab. 1. Moduli of elasticity for specific tire specimens

Specimen No.	Methods start–end of strain [%]	Modulus of elasticity [MPa]
1	0–8 %	225.8
	4–8 %	**218.5**
	0–10 %	223.1
	4–10 %	233.1
	linear part	265.4
2	0–8 %	55.4
	4–8 %	**53.6**
	0–10 %	58.6
	4–10 %	59.5
	linear part	200.0
3	0–8 %	357.1
	4–8 %	**380.9**
	0–10 %	380.9
	4–10 %	412.6
	linear part	1 023.1
4	0–8 %	109.2
	4–8 %	**65.5**
	0–10 %	101.3
	4–10 %	67.0
	linear part	64.0
5	0–8 %	106.7
	4–8 %	**151.7**
	0–10 %	160.7
	4–10 %	154.7
	linear part	295.2

⇒ Moduli of elasticity of tire-crown

The specimens were prepared with different width 15 and 20 mm with different directions. The static tensile tests and bend tests are performed for the specimens in agreement with the standard specifications and the aim was to obtain the modulus of elasticity for different directions of configuration of specimens. The conditions of the bend tests are: The distance between outside points was 50 mm. The loading speed was 5 mm/min. The conditions of the tensile tests are: The initial length between the clamps of the test machine is 100 mm and the loading speed is 10 mm/min. The modulus of elasticity is obtained by two elongations by 4 and 8 %.
The deformations of specimens during the bend tests are in Fig. 3 as sample and results are in Tab. 2.

Fig. 3. Specimens after bend

Tab. 2. Moduli of elasticity by the method 4–8 %

Modulus of elasticity for method 4–8 % [MPa]	Specimen width	
	15 mm	20 mm
Longitudinal	134	183
Transverse	158	173

⇒ Conclusions

The moduli of elasticity can be used for verification analyses between tests and computational modeling of structure parts of tire casings. For obtained of better results, there is necessary to deal with cyclic tensile tests of long-fiber composites with textile reinforcement. Also specific low-cyclic tensile tests of tire textile carcass are also important for obtaining material parameters too.

References

1. Krmela, J., (2017): Tire *Casings and Their Material Characteristics for Computational Modeling*. Czestochowa: Oficyna Wydawnicza Stowarzyszenia Menadżerów Jakości i Produkcji (Printing House The Managers of Quality and Production Association). ISBN 978-83-63978-62-4.
2. Krmela, J., Krmelová, V., (2018): The Material Parameters for Computational Modeling of Long-fibre Composites with Textile. *MATEC Web of Conferences* 157, 01011. DOI: 10.1051/matecconf/201815701011.
3. *ISO 37*: Rubber, vulcanized or thermoplastic - Determination of tensile stress-strain properties.
4. *Hyperelastic coefficient convertion*, (2011). Available at: https://polymerfem.com/ forum/polymerfem-downloads/general-hyperelastic-models/1237-linear-elastic-hyperelastic-coefficient-conversion
5. Reuss, B., (2011): *Convert Durometer to Young´s Modulus*. Available at: https://www.cati.com/blog/2011/07/convert-durometer-to-youngs-modulus/
6. *Mooney Rivlin Constants*, (2005). Available at: http://xansys.org/forum/viewtopic.php?p=51617&sid=609a8612c34eb2eec373756fd062aea2
7. *Constitutive Models for Rubber*, (1999). Dorfmann, A., Muhr, A. (ed.). Rotterdam: A.A.Balkema. ISBN 90-5809-113-9.

Selected and interesting results from author research work – experiments and computational modeling of composites and tyres were published in the scientific monograph "**Tyres casing and their material characteristics for computational modeling**",

which is available in selected universities and state libraries in EU states (Poland, Czech republic, Austria, Slovak republic) and states without EU (Belarus, Ukraine).

REFERENCES

1. KRMELA, J. Tire Casings and Their Material Characteristics for Computational Modeling. Scientific monograph. Czestochowa, Poland, 2017. ISBN 978-83-63978-62-4. http://krmela.wz.cz/kniha_obalka_en.png

2. Krmela J., Krmelová V. Tire casing and their material characteristics for computational modeling of tires, 16th International Scientific Conference Engineering for Rural Development, Jelgava, 2011, pp. 206-211, DOI: 10.22616/ERDev2017.16.N043, ISSN 1691-5976

3. Krmela J., Vančo M. Bike tire with textile reinforcement - experiment and computational modeling, Vlákna a textil (Fibres and Textiles), 21(3), 2014, pp. 31-34.

Title: Experiments and Computational Modelling of Tires : Textbooks for university students
Author: doc. Ing. Jan Krmela, Ph.D.
Book type: Textbook for university students
Edition: First, December 2020
Publisher: Jan Krmela, Zborov 32, Czech Republic

This textbook has not been checked and corrected for spelling errors.

© Jan Krmela, 2020

ISBN 978-80-270-9020-4

ISBN 978-80-270-9020-4